2014

DEVELOPMENT OF INDUSTRY ORIENTED CFD CODE FOR ANALYSIS / DESIGN OF FACE VENTILATION SYSTEMS

Todor P. Petrov
University of Kentucky, petrov.tp@gmail.com

STUDENT AGREEMENT:

I represent that my thesis or dissertation and abstract are my original work. Proper attribution has been given to all outside sources. I understand that I am solely responsible for obtaining any needed copyright permissions. I have obtained needed written permission statement(s) from the owner(s) of each third-party copyrighted matter to be included in my work, allowing electronic distribution (if such use is not permitted by the fair use doctrine) which will be submitted to UKnowledge as Additional File.

I hereby grant to The University of Kentucky and its agents the irrevocable, non-exclusive, and royalty-free license to archive and make accessible my work in whole or in part in all forms of media, now or hereafter known. I agree that the document mentioned above may be made available immediately for worldwide access unless an embargo applies.

I retain all other ownership rights to the copyright of my work. I also retain the right to use in future works (such as articles or books) all or part of my work. I understand that I am free to register the copyright to my work.

REVIEW, APPROVAL AND ACCEPTANCE

The document mentioned above has been reviewed and accepted by the student's advisor, on behalf of the advisory committee, and by the Director of Graduate Studies (DGS), on behalf of the program; we verify that this is the final, approved version of the student's thesis including all changes required by the advisory committee. The undersigned agree to abide by the statements above.

Todor P. Petrov, Student

Dr. Andrzej M. Wala, Major Professor

Dr. Thomas Novak, Director of Graduate Studies

DEVELOPMENT OF INDUSTRY ORIENTED CFD CODE FOR ANALYSIS / DESIGN OF FACE VENTILATION SYSTEMS

DISSERTATION

A dissertation submitted in partial fulfillment of the
requirements for the degree of Doctor of Philosophy in the
College of Engineering at the
University of Kentucky

By

Todor Petrov

Lexington, Kentucky

Director: Dr. Andrzej M. Wala, Professor of Mining Engineering

Lexington, Kentucky

2014

ABSTRACT OF DISERTATION

DEVELOPMENT OF INDUSTRY ORIENTED CFD CODE FOR ANALYSIS / DESIGN OF FACE VENTILATION SYSTEMS

Two of the main safety and health issues recognized during deep cut coal mining are methane and dust hazards. Advances in continuous miner technology have improved safety and productivity. However, these advances have created some environmental problems, notably more dust and methane being generated at the face during coal extraction.

Results of studies performed in the last three decades concerning the face ventilation for deep cut mining showed very complicated airflow behavior. The specifics of flow patterns developed by the face ventilation systems presents significant challenge for analytical description even for equipment-free entry. Fortunately, there are methods, such as numerical simulations that could be used to provide an engineering solution to the problem. Computational Fluid Dynamics (CFD) codes have been successfully applied during the last decade using the power of Supercomputers. Although significant progress has been made, a benchmark industry oriented CFD code dedicated to face ventilation is still not available.

The goal of this project is to provide the mining industry a software for CFD analysis and design of face ventilation systems. A commercial CFD system SC/Tetra Thermofluid Analysis System with Unstructured Mesh Generator, copyright © Cradle Co, was selected for a development platform. A number of CFD models were developed for the needs of this study including methane release, dust generation, 3D models of commonly used continuous mining machines, scrubbers and water spray systems. The developed models and the used CFD code were successfully validated in the part for methane dilution, using available data from small scale and full scale experiments. The developed models for simulation of dust control systems need to be validated in the future. The developed code automates all necessary steps needed for simulation of face

ventilation systems, starting with the construction of a 3D model, generation of the computational mesh, solving and monitoring the calculations, to postprocessing and graphical representation of the obtained results. This code shall allow mining engineers to design better and safer face ventilation systems while providing the Mine Safety and Health Administration (MSHA) a tool to check and approve the industry' proposed ventilation plans.

KEYWORDS: face ventilation, CFD simulation, methane dilution, dust control, coal miners safety.

Todor P. Petrov

_____

Student's Signature

9/18/2014

_____

Date

DEVELOPMENT OF INDUSTRY ORIENTED CFD CODE FOR ANALYSIS / DESIGN OF FACE VENTILATION SYSTEMS

By

Todor Petrov

Dr. Andrzej M. Wala
_____
Director of Dissertation

Dr. Thomas Novak
_____
Director of Graduate Studies

9/18/2014
_____

ACKNOWLEDGMENTS

This study was supported by the National Institute of Occupational Safety and Health (NIOSH), under Grant # 200-2009-30678. The authors would like to express their gratitude to the Joy Global, Inc for providing CAD data of the continuous miners needed to build some of the CFD models. Special thanks also extended to Dr. Gerrit Goodman, NIOSH PRL; Chris Pritchard, Ventilation Team Leader, Spokane Mining Research Division, NIOSH; Jay Colinet, Senior Scientist, NIOSH; John A. Organiscak, Senior Research Engineer, NIOSH; and Timothy W. Beck, NIOSH PRL for their professional advices during the project.

.

TABLE OF CONTENTS

LIST OF TABLES

LIST OF FIGURES

Chapter 1

INTRODUCTION

1.1 Overview

This work demonstrates a methodology for development of an industry oriented CFD code for analysis and design of face ventilation systems. The developed Face Ventilation Simulator (FVS) code supports three dimensional CFD analysis of flow behavior, methane dilution and dust control of face ventilation systems. This involves model development of key elements of the face ventilation systems, procedure for assembly of these elements into a prime CFD model, a scenario-oriented computational mesh generation algorithm, automation of solving and monitoring, and post processing of the simulation results. A commercial CFD software SC/Tetra thermofluid analysis system with unstructured mesh generator, copyright © Cradle Co., has been selected for a development platform. The development started with building a library of 3D models of face ventilation systems using typical cut scenarios approved by MSHA. A series of preliminary CFD simulations were performed to determine the capabilities of SC/Tetra. A number of CM models were created using 3D CAD[1] drawings provided by JoyGlobal, including technical information for their spray systems and machine-mounted scrubber configurations. A CFD code validation study was performed using available data from experimental studies in small scale and full scale physical models conducted at the University of Kentucky and at the National Institute of Occupational Safety and Health (NIOSH) Pittsburgh Research Laboratory (PRL). The study covered: CFD code validation for flow against tests data obtained by Particle Image Velocimetry (PIV) measurements using 1:15 scaled physical model; CFD code validation for flow and methane gas distribution using data of full scale tests for equipment free face area and with CM in place.

The FVS[2] code includes Visual Basic (VBS) Scripts, Visual Basic for Application (VBA) modules and C language user functions supported by Cradle CFD. The developed code uses Microsoft Component Object Model to communicate with the Cradle CFD software. A number of models were developed for the needs of the FVS, including, methane release, dust model, scrubber and water spray systems.

Primarily, a procedure for creating a CFD model of a face ventilation system, to simulate a user defined scenario was developed. This procedure involves input of CAD data for a face ventilation system geometry, to place the equipment and to produce a CFD model that is ready for use. Usually, a new model of a face ventilation system starts from a sketch. This sketch is transformed to 3D CAD model following an easy to follow

[1] Computer Aided Design
[2] Face Ventilation Simulator

procedure of eight steps. A VBS guides the user through the process of region recognition such as inlets, outlet, walls, curtain and face. Thus, the risk of human errors such as misspellings or missing a region is minimized. A predefined library of continuous miner models is available for use during the model assembly. A VBS code automatically runs a scenario-oriented mesh generation procedure by calculating the prime mesh settings for the analysis. Constructed this way, the model is available for mesh adaptation analysis. This is espetialy important because, the selection of a proper mesh for use in analysis is one of the first considerations when simulating flow. It is clear, that the solution will be specific for every particular face ventilation scenario defined by the user. If the generated mesh does not comply to the specifics of the CFD analysis, the simulation cannot be performed using the best possible conditions. Mesh adaptation analysis is a proven way to automate the mesh generation process for achieving accurate simulation results (Cradle, 2009).

Second, a VBS code that automatically generates analysis settings for the simulation, was developed. Three general types of CFD analysis are supported:

- Flow Behavior Analysis
- Methane Dilution Analysis
- Dust Control Analysis

The FVS is designed to perform 3D steady state analysis (SSA) of face ventilation system for flow, methane and SF6 tracer gas distribution, including the effect of the scrubber, along with time dependent analysis (TDA) for simulating the effect of water spray systems and the scrubber on methane/SF6 gas distribution and respirable dust using the particle tracking method. Built-in SC/Tetra sub-models, such as the particle break-up method and the Arbitrary Lagrangian Eulerian (ALE) method are switched on to simulate water spray droplets interaction into the air and analyze the flow around the cutting head of a CM. A library of analysis condition template files corresponding to the described CFD analysis is developed. A VBS uses input parameters, such as intake flow rate, scrubber flow rate, methane inflow, spray system configuration, and generates code for condition file corresponding to the required CFD analysis. Methane liberation model uses porous media volume attached to the face. Spray system setup can vary depending on the equipment characteristics. A commonly used setup of 60 spray nozzles in total is provided with options to switch on and off selected spray groups (panels). The dust control setup requires user input for the perent scrubber efficiency. the dust generation model implements a Lognormal distribution of the dust particles size. The attributes of the simulated dust particles correspond to published laboratory data for coal dust and silica content. The dust particles generation points cover the area around the continuous miner cutting head. A dust generation model was developed in C++ user functions for SC/Tetra. Run time control of the scrubber dust removal efficiency is performed by another C language user function. This function counts the particles passed through the simulated scrubbing filter region, reads its attributes, and passes only percentage of them,

corresponding to the specified scrubber efficiency. Both, the spray and the dust model used particle tracking method in their realization.

Third, a VB script code was developed to run the simulation and perform automatic monitoring of the calculation process. The script initiates a two stage solving procedure using the data prepared during the previously described steps to establish automatic monitoring on a set of runtime variables for convergence and stability. The code performs runtime interrupt checks by evaluating the data bias of flow velocity values and gas concentrations in preset check points, which are typically positioned adjacent to the face. If the interrupt criteria is met, the calculation will be interrupted and the results will be saved. Otherwise the calculation will continue until reaching the default final cycle given by default and the program will initiate mesh adaptation analysis. This procedure automatically generates adapted mesh for the analysis by reconfiguring the existing one using the last saved results. After re-meshing, the simulation is restarted to improve the prediction. The run time monitoring remains intact and the new results are saved. No further actions for refinement of the solution were designed.

Fourth, a VB application code was developed to automate the post-processing of the simulation results using Cradle SC/Tetra post-processor. A three-button dialog window guides the user through the process of report generation. The "Generate Animations" button automatically opens the Cradle SCTpost application, loads the simulation results, and produces a series of animation files. The code uses the powerful graphical Cradle SCTpost engine to produce animated presentation of the simulated results. This includes:

- Static plan and isometric views including vector maps, contour maps, and 3D gas concentration isosurfaces
- Moving vector maps
- Moving contour maps for gas concentration, with plan views and 3D isometric views.

The animation preview can be interactively controlled by the user. No spatial CFD skills are required to follow the animated preview scenario.

The "Generate Report" button automatically creates graphical results of the performed simulation. The code automatically opens the SCTpost application and sends automation instructions to it. The graphical output is specific to the analysis type and follows predesigned templates dedicated to different simulation scenarios.

The "Generate Cradle Viewer File" button automatically creates a 3D interactive presentation file for Cradle Viewer. The Cradle Viewer is a small stand alone application that allows interactively preview of the simulation results, including zooming and 3D

rotation. The generator also uses scenario-oriented templates to create the Cradle Viewer file according the analysis type.

The use of template files adds flexibility to the application of FVS. The post-processing output can be improved rapidly without needing to write code and re-compile the application.

1.2 Background

One of the earliest applications of CFD for face ventilation analysis supported by field study is reported by Sullivan and Heerder (1993). In this study, the continuous miner was modeled in one cutting position. Drum rotation, a machine mounted scrubber, and methane emission rate were included in the input data. Each of the modeled ventilation scenarios was compared with measurements in underground continuous miner sections. Another study (Moloney et al., 1997 and 1999) showed the increasingly important role of CFD as a design tool in face ventilation. In this research, the flow patterns produced by a set of auxiliary tubing ventilation configurations was simulated using k-e RNG model. The simulation results were correlated with small scale and full scale gallery tests. In other research (Wala et al., 1997) CFD was successfully applied to study the flow across the main airways of a mine ventilation system, particularly investigating the flow through the transition zone between the upcast shaft and main fan. The simulation results were validated with field data. The developed CFD model was recommended as a useful tool for predicting the effect of changes in ductwork configurations on energy losses.

During experimental study (Wala et al. 2000-2004, Turner et al., 2002) different face ventilation arrangements have been investigated using 1:15 scaled and full scale physical models. The scaled model is equipped with Particle Image Velocimetry (PIV) measurement system. The PIV system consist of a dual head Nd:YAG laser, one megapixels CCD camera connected to a PC card frame grabber, and a timing control block to synchronize the triggers of the laser heads with the CCD camera. The flow is seeded with 1 mm size tracer particles. The laser optics creates a light sheet and illumines the tracer particles in a desired plan. The CCD camera captures 50 image pairs at a rate of 10 Hz, storing them onto the PC memory. This image pairs are analysed with PIV software to determine velocity vectors. The processing software applying fast Fourier transformations and cross-correlation methods to produce a resulting set of velocity vectors. The result is a time averaged planar velocity vector map similar to the vector fields obtained by CFD simulations. That makes PIV systems invaluable tool for CFD code validation. During comprehensive CFD code validation study (Wala et al., 2000 - 2001) observed early airflow separation in some of the tested face ventilation system during the experimental period of the project. In 2002, the results obtained on the scaled model were confirmed by full scale tests conducted at the NIOSH PRL (Wala et al., 2004-2005). In 2003, an experimental and CFD simulation study dedicated to effect of

machine mounted scrubbers on face ventilation during deep cut mining was performed (Wala et al., 2004). Different scrubber to face ventilation airflow ratios were tested. Later on, benchmark experiments for CFD code validation were conducted at the NIOSH PRL (Wala et.al. 2006, 2008). As a result, FLUENT CFD code was successfully validated data for flow and methane using experimental results for equipment free entry and with CM in place equipped with a machine mounted scrubber. Three commercial CFD software packages which were available at that time (Wala et al., 2001 - 2008) have been tested as follows: CFD-2000; CFX; and FLUENT. The earliest simulation results using CFD 2000 showed different flow patterns than the observed during the experiments. The most promising results were achieved with FLUENT using HP Superdome Complex at University of Kentucky. The study showed, that in addition to the needs of establishing a greed independent solution, the proper choice of CFD code may have crucial impact on the accuracy of the solution. In 2009 Dr. George Huang at Wright State University, Dayton OH, being project consultant and participant in the performed CFD validation study at the University of Kentucky, recommended a new CFD software - SC/Tetra Thermofluid Analysis System with Unstructured Mesh Generator, ©Cradle Co. A comparison of SC/Tetra with 10 popular commercial CFD software is shown on Figure 1.1.

SC/Tetra has a version for the Microsoft Windows OS. One of the features of SC/Tetra is low memory consumption, about 2 MB memory is required for every 10,000 mesh. Previously performed simulations of face ventilation systems have included about 2 million generated mesh elements. Important characteristics of SC/Tetra related to the current project are:

- SC/Tetra system provides an "all in one" package of applications embracing User friendly geometry import and program creation, a pre-processor with a powerful mesher that includes automatic mesh refinement, a powerful Solver, and a state of the art Postprocessor.
- Useful tools for automation of user's actions such as executable command history files supported by the SCTPre-processor, application of templates for visualization of the results supported by CTPost-processor, called Status files.
- User defined functions are supported by the SCTSolver utilizing Visual C++ giving access to SC/Tetra internal methods and variables.
- Visual Basic interface utilizing Microsoft COM (Component Object Model) and WSH (Windows Scripting Host) automation technologies.
- SCTJob application enables to set a series of jobs, for meshing and solving models, to be executed consecutively.
- CradleViewer application enables the user to preview formatted post-processor results using a very simple interface. This is a portable standalone 32 bits application (about 6 MB).

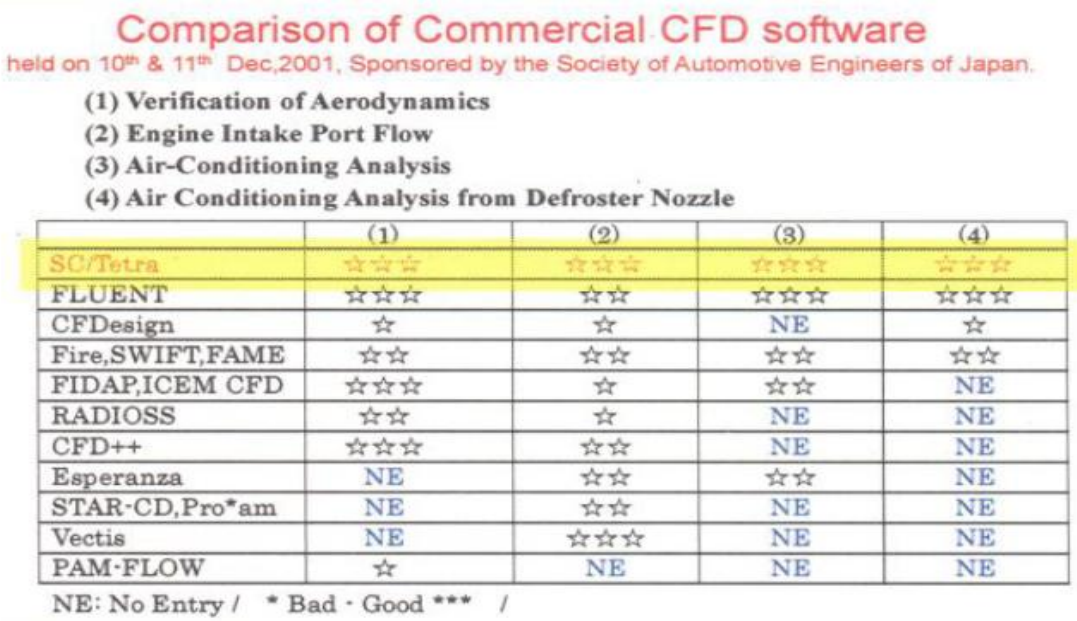

Comparison of Commercial CFD software

held on 10th & 11th Dec,2001, Sponsored by the Society of Automotive Engineers of Japan.

(1) Verification of Aerodynamics
(2) Engine Intake Port Flow
(3) Air-Conditioning Analysis
(4) Air Conditioning Analysis from Defroster Nozzle

	(1)	(2)	(3)	(4)
SC/Tetra	☆☆☆	☆☆☆	☆☆☆	☆☆☆
FLUENT	☆☆☆	☆☆	☆☆☆	☆☆☆
CFDesign	☆	☆	NE	☆
Fire,SWIFT,FAME	☆☆	☆☆	☆☆	☆☆
FIDAP,ICEM CFD	☆☆☆	☆	☆☆	NE
RADIOSS	☆☆	☆	NE	NE
CFD++	☆☆☆	☆☆	NE	NE
Esperanza	NE	☆☆	☆☆	NE
STAR-CD,Pro*am	NE	☆☆	NE	NE
Vectis	NE	☆☆☆	NE	NE
PAM-FLOW	☆	NE	NE	NE

NE: No Entry / * Bad · Good *** /

Figure 1.1 Comparison of Commercial CFD software (Huang and Welsh, 2010)

The experience obtained during the application of CFD for mine ventilation showed the potential of this approach to design more economical and safer systems. However, spatial attention should be paid to the development of the numerical model and the engineering interpretation of the simulation results. Any incorrect specification of the boundary conditions or improper computational mesh (grid) may lead to misleading results. Consequently, validation against mining related test data retains its significance in the transfer of the CFD code for design of mine ventilation system. Results of the studies performed by Wala et al. (2000-2008) were used to validate the developed models and the Cradle CFD code.

1.3 Motivation and Objectives

A number of safety and health issues related to methane dilution, dust control, and system ability to conduct air from the last open crosscut to the face need to be considered in the design of a face ventilation system. In many circumstances, environmental conditions cannot be accurately measured. Factors like system geometry, variety of equipment operating in the confined space of the face area, airflow separation phenomenon - typical for the line brattice systems, and flow recirculation caused by the machine-mounted scrubbers and water sprays make every face ventilation system unique. Experimental approaches using full scale models have been successfully used to test different face ventilation arrangements and study new equipment. However, due to the number of factors which are of concern in face ventilation system analysis makes anexperimental approach too costly and time consuming. Small scale models may be

used to test design options for better understanding of a system behaviour, accident reconstruction and validation of numerical models. Scale modeling is based on scaling laws that assume the scaled model will behave in a predicted way if the associated analytical description is correct (Saito et al., 2010). However, each scale model has limitations associated with the physical implementation of the scaling laws or makes assumptions for relaxation of its analytical description. For instance, a scaled model of a face ventilation system could be set to represent flow velocities or pressure distribution, but not both simultaneously. Another challenges related to small scale physical simulation of a machine mounted scrubber includes the scrubber discharge effect and water sprays. Physical realization of small scale water spray model, if feasible, would present significant technical difficulties. For example, the spray nozzles which are currently available for mining application used high-pressure systems. They typicaly, operate at 45 - 70 PSI to generate micron size water droplets moving with velocities of tenths meters per second. Fortunately, numerical approaches could be used to provide engineering solution to the problem for the face ventilation system analysis and design. In the last decade Computational Fluid Dynamics (CFD) code have been successfully applied for simulation of face ventilation systems using the power of Supercomputers. Although significant progress has been made, a benchmark industry oriented CFD code dedicated to face ventilation is still not available. The main goal of this work is to develop an industry oriented CFD code that provides tools for analysis/design of face ventilation system. The features of FVS software will support CFD analysis of face ventilation systems for flow behavior, methane dilution and dust control in coal mines utilizing continuous mining technology.

Chapter 2

LITERATURE REVIEW

"Face ventilation by line brattice is unusual in that the system does not develop the normal flow patterns of slots or jets discharging in free air. The confining influence caused by the proximity of roof, ribs, floor, and face alter conditions to the extent that flow patterns and mixing appear unique to the system" - James V. Luxner

2.1 Aspects of Face Ventilation

Face ventilation methods can be classified into two general groups: the tubing face ventilation method and line brattice face ventilation method. This review is focuses on line brattice face ventilation systems operating blowing to or exhaust from the face and their application in coal mines utilizing continuous mining technology in room and pillar sections. Each system, whether blowing or exhaust, has its own benefits and limitations and can also be affected by the use of machine mounted scrubber and spray system. Blowing face ventilation systems are usually preferred over exhausting face ventilation system due to better methane control. Exhaust face ventilation system are generally preferred over blowing face ventilation system for dust control because the dust is removed from the face before it passes over the machine operator's location. However, for a given set-back distance, airflow quantities reaching the face are less and face methane concentration higher.

Delivering the neccessary air quantity required to ventilate the immediate face zone is recognized as one of the major ventilation problem in coal mines using room and pillar method with CM. The immediate face zone is a location were mining takes place and methane and dust are generated, usually 1.2-2.4 m (4-8 ft) outby the face. Research showed that the method of ventilation is one of the primary factors determining the effectiveness of face ventilation with line brattice. It is assumed that a blowing curtain, as opposed to an exhaust curtain, generally achieves greater penetration distance and is more effective in delivering more intake air to the face area. In practice, however, both systems suffer from one significant disadvantage - early airflow separation. Due to this phenomenon, the line brattice do not deliver sufficient amounts of air to the immediate face zone. As a result methane emissions may be inadequately diluted and excessive concentrations may develop. One of the earliest research results on airflow separation has been reported by Luxner, (1969), see Figure 2.1. In an experimental mine at Bruceton, Pa., Luxner performed series of investigations of airflow using smoke to visualize the flow patterns, and measuring methane distribution developed by various line-brattice systems. According to Luxner's study, the average immediate face area ventilating efficiency for the studied blowing systems was aproximately 54 percent, that of all exhaust systems was about 11 percent. The immediate face area ventilating efficiency is a

measure of methane dilution ability for a given method of ventilation. It should not be confused with line brattice system efficiency that refers to the ability of a system to conduct air from the last open crosscut to the face (Luxner 1965). Luxner found, that exhaust line brattice systems with a curtain set-back distance to the face which exceeds 5 feet can be considered as a poor ventilating arrangements. The set-back distance is the maximum distance that the inby end of the ventilation control device (tubing, line brattice/curtain, etc.) can be installed from the area of deepest point of mining penetration (Shultz et. al. 2010). Luxner stated five factors that affect the ability of line-brattice systems to provide adequate face ventilation:

1. Method of ventilation employed
2. Tight rib distance
3. Set-back distance
4. Volume of air delivered by the line brattice
5. Volume of methane released in the face area

Later on, studies conducted by number of authors (Gillies, 1982; Taylor and Goodman, 1997; Taylor, and Zimmer, 2001) showed flow patterns that differ from Luxner's observations and the latest experimental results, see Figure 2.2. The flow separation phenomenon, as previously observed by Luxner, has been confirmed using small scale and full scale physical models, and numerical simulations by Wala et. al. (2001 and 2003), see Figure 2.3 and Figure 2.4. Because the velocities of secondary airstream are lower than that of the primary one, methane released at the immediate face zone is ventilated in reduced air volumes. In addition, the recirculation (swirling) action of secondary airstream continuously re-contaminates the face area (Luxner 1969, Wala et. al 2001) . This is valid for both, methane and dust contaminants.

The latest tests conducted at the NIOSH ventilation test gallery, using 2D and 3D ultrasonic anemometers, proved the complexity of airflow at the face area (Hall et al. 2007). Data analysis showed, that airflow the readings behind the curtain differed by less than 3.5%, while the differences at the face were greater. Behind the curtain, the average vertical angle of flow above or below the horizontal plane was no greater than 3 degrees with standard deviation less than 2 degrees. However, at the face, the average angle varied from 3 to 8 degrees with standard deviation from 8 to 24 degrees.

Significant efforts have been made by NIOSH and other researchers (Gillies, 1982; Volkwein et al., 1985, 1989 ;Taylor et al., 1996; Goodman, et al. 1995, 2000, 2006; Red and Taylor, 2010; Taylor and Karacan, 2010; Organiscak and Beck, 2010; Listak et al., 2010; Schultz et al., 2010) and its predecessor, the U.S. Bureau of Mines (Foster-Miller, Contract Report, 1988), to move more air closer to the face.

Designed primarily for dust control water sprays and scrubbers has also be used to reduce methane levels by increasing the amount of intake air that reaches the face.

Application of the different types of auxiliary air-moving devices, like mechanical fans, spray fans, water sprays, and even a dust scrubber were counted as an air-movers.

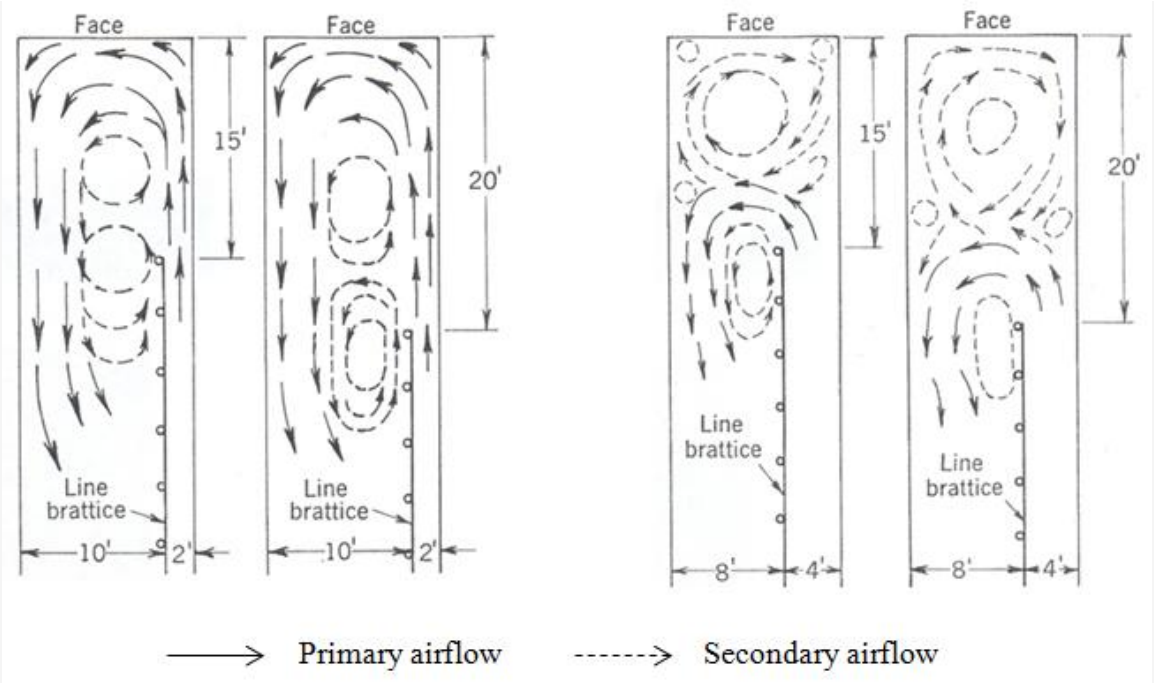

Figure 2.1. Flow patterns independent of the intake flow rate, developed by blowing curtain installed 0.6 m (2 ft) and 0.6 m (4 ft) from the rib. Luxner Research Study (1969), U.S.B.M., RI #7223

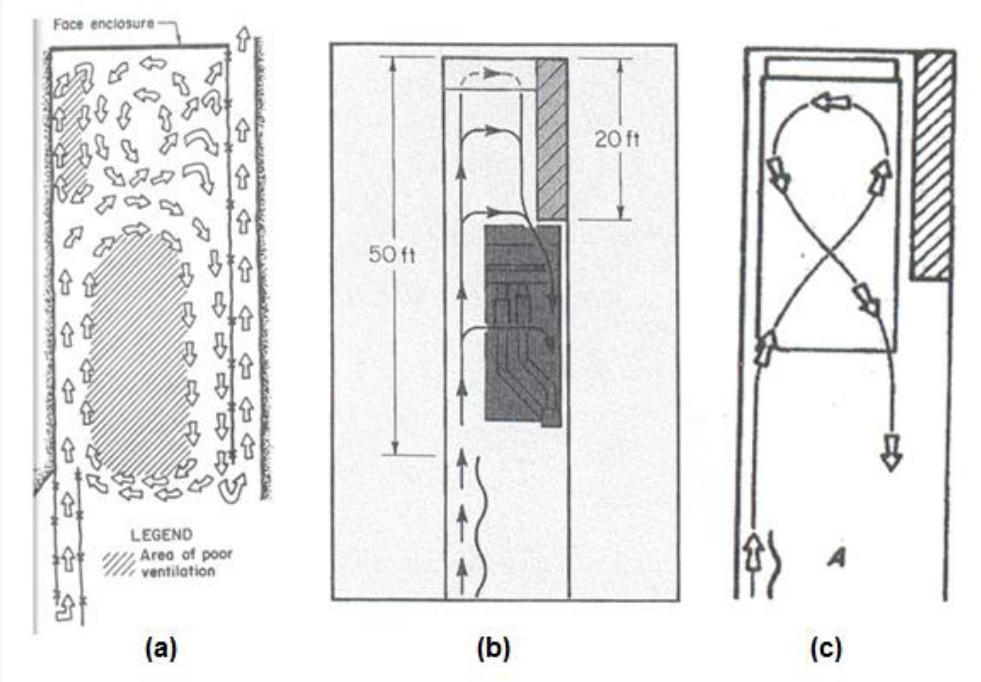

Figure 2.2. Flow patterns shown by different authors, (a) Taylor and Goodman (1992), (b) Taylor (2000), (c) Taylor and Zimmer (2001)

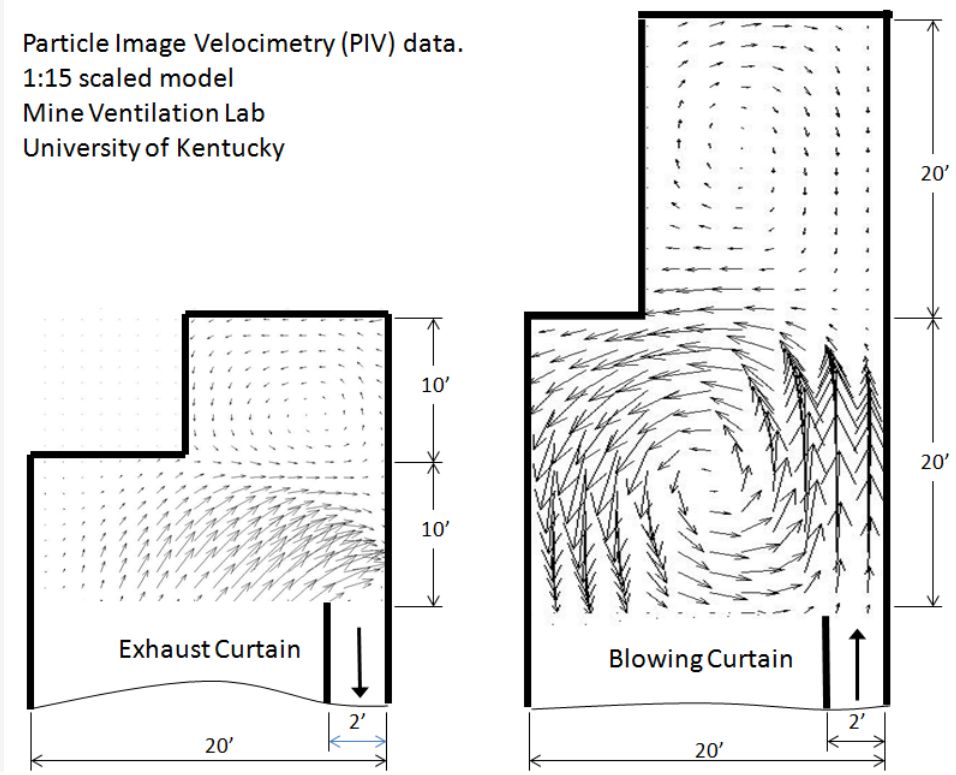

Figure 2.3. Particle Image Velocimetry (PIV) data of flow patterns developed by exhaust curtain, and blowing curtain face ventilation system (after Wala et. al 2001, 2003).

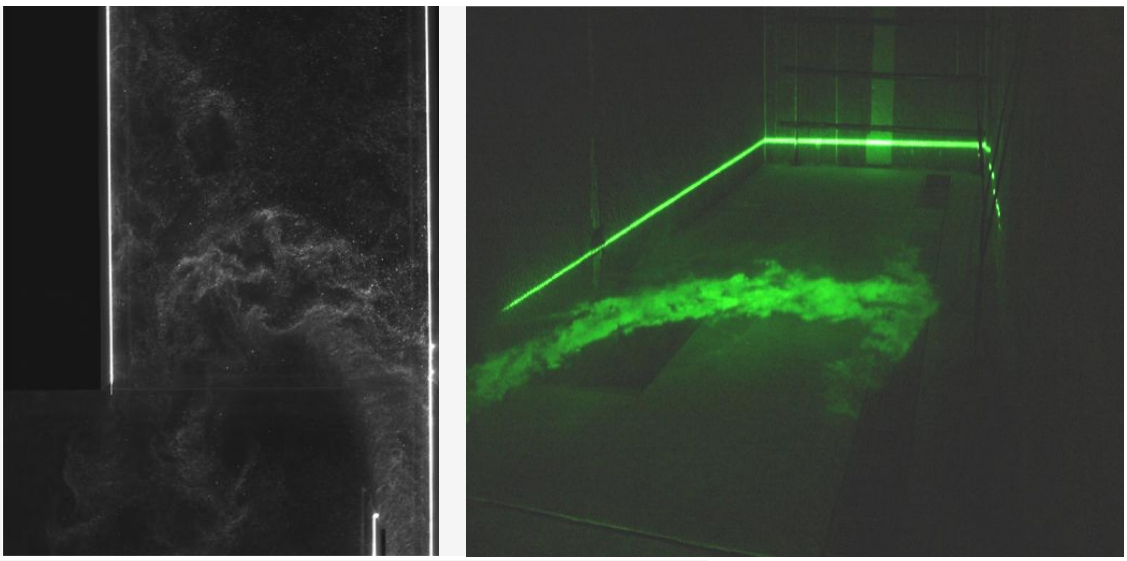

(a) (b)

Figure 2.4. CCD camera images, (a) Test on 1:15 scaled physical model, Mine Ventilation Laboratory, University of Kentucky, (b) Full scale test, NIOSH Research Laboratory, Pittsburgh, PA (after Wala et. al 2001).

Over many years, different arrangements of all these air-moving devices were analyzed and tested in the laboratories and in the mines with a limited success. Forcing the scrubber flow rate to values close to the intake flow rate caused serious recirculation in the system with negative consequences on the methane dilution at the face and dust rollback to the miner's operator location (Volkwein at al. 1989; Thimons at al., 1998; Goodman at al., 2001). The water jet spray systems showed similar effects (Volkwein at al., 1988; Tylor and Zimmer, 2000).

Airflow reaching the face is the only adequate control that can reduce face methane concentration. Generally, the quantity of air reaching the face decreases as tubing or curtain set-back distance increases. Methane concentration at the face change quickly due to changes in airflow. Currently, there are no anemometers approved for underground use that can accurately measure airflow velocities between the mouth of the curtain and the face. Airflow measurement made at the inby end of the tubing or curtains are usually the only measurement available for estimating face airflow. Hand held anemometers cannot be used under unsupported roof. However, past studies have shown that the air quantities measured at the inby end of the line curtain are not good estimates of how much air actually reaches the face (Luxner, 1969; Thimons et al., 1999; Wala et al., 2001-2008, Hall et al., 2007). The fact that methane ignitions continue to occur at the mining face indicates that monitoring with machine-mounted methane sensors does not always indicate the presence of high methane concentration (Hall et al., 2007).

Many of the methane ignitions in bituminous coal mines could be attributed to poor face ventilation (Luxner, 1969). Methane ignitions caused by cutting picks during mining operation remain a hazard in worldwide coal mining (Courtney 1990; Cook, 2001; Taylor and Karacan, 2010). Ignitions could also be reduced by cooling the rock surface with water directed from a nozzle mounted directly behind the bit (Courtney 1990) or so called "Wet Head"" technology. The wet head continuous miner cutterhead incorporates a fine spray behind each cutting bit of the cutter drums to reduce the potential for frictional ignitions and to reduce respirable dust level. There are mixed results from the study as to the effectiveness of the wet head system to reduce respirable dust. A South African study showed 60 to 65% reduction in respirable dust at the continuous miner operator location (Belle and Clapham, 2002). However, several US studies could not prove a significant difference in dust reduction when testing wet head versus standard machine mounted sprays (Fields et al., 2005; Chugh et al., 2006; Goodman et al., 2006). From visual observation and interviews with the mine personnel in the U.S. there were very favorable responses to wet head use (Listak et al., 2010). The miner operator on the wet head machine maintained a large setback distance, claimed that dust conditions were improved by this action. All operators found that the wet head system greatly increased visibility while mining. Also, the dust cloud created at the miner's boom while loading shuttle cars was eliminated. However, according the recent

evaluation of the wet head to reduce respirable dust, most improvements were small and some shifts showed the wet head concentration higher (Listak et al., 2010).

Although significant progress has been made to improve face ventilation applying machine-mounted scrubbers and water sprays, coal workers' pneumoconiosis has increased during the last decade (NIOSH - CWXSP program 2008), see Figure 2.5. Coal miners overexposure to respirable coal and crystalline silica (or quartz) dust cause pneumoconiosis which are debilitating and potentially fatal respiratory lung diseases.

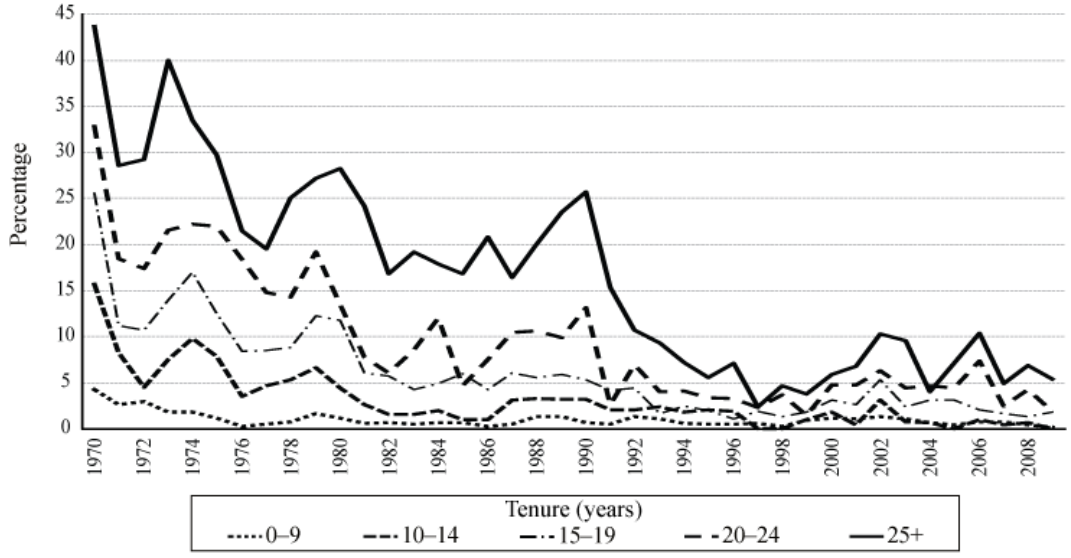

ILO - International Labour Organization

Source: Coal workers' pneumoconiosis data from NIOSH Coal Workers' X-ray Surveillance Program (CWXSP).

Figure 2.5. Percentage of examined underground miners with coal workers' pneumoconiosis by tenure in mining, 1970-2008 (NIOSH, 2008).

Results from surveillance examination, conducted from 2005 to 2009, of 6373 working U.S. coal miners demonstrated geographically clustering of regions with high rate of coal workers pneumoconiosis (Wang et al., 2013; Watzman 2013). Observed coal workers pneumoconiosis prevalence was significantly higher than predicted in MSHA districts 4-7, and significantly lower than predicted in other regions (1.6% v/s 3.6%) (Suarthana et al., 2011; Watzman, 2013). Dust level at the location of miner operator is affected by many variables. According to data supplied by MSHA, over 3100 samples were collected at the continuous mining machine operator in 1988. Nearly 60 percent of the samples contained more than 5 percent respirable silica dust while 40 percent of these contained silica concentration in excess of 100 μg/m^3. Half the respirable silica generated in the underground coal mines has a size between 1.0 and 3.5 microns (Goodman et al., 2000). In-mine survey of blowing ventilation section conducted by MSHA, Pittsburgh Safety and Health Technology Center, Dust Division, Field Group

found inadequate intake line curtain air qualities to be the primary reason for continuous miner operators being overexposed. Another observation was that continuous miner operators at some of the surveyed operations were not working in their proper work positions, the inby end of the line curtain. Instead, they were working on the return side of the curtain causing them to be overexposed (Schultz et. al., 2010). Other research results (Steiner et al., 1998) indicated that operators tend to place themselves in one particular spot for the entire mining sequence unless there are unusual tasks that need to be performed. It was found that operators prefer a zone with an area of 2.1 m (7 ft) by 2.4 m (8 ft), located at the right rear corner of the machine when they were legally required to do so. However, survey findings (Schultz et. al., 2010) showed that a continuous miner operator on blowing ventilation sections could be exposed to excessive dust concentration despite being in the proper work location and following the ventilation plan. Therefore, exhaust face ventilation has become the recommendation as a more effective method for lowering the dust exposure of the operators of the remotely controlled continuous miner machines. Research for the exhaust face ventilation showed that the lowest dust level position of the miner's operator is on the off-curtain side of the entry, parallel to the inlet end of the exhaust curtain (Goodman and Listak, 1999; Organiscak and Beck, 2010). Other research focused on the joint performance on machine-mounted scrubber and external water sprays confirmed that water sprays setup has a significant impact on dust distribution around the mining machine for both blowing and exhaust face ventilation (Goodman, 2000; Goodman et. al., 2006; Organiscak and Beck, 2010). The efficiency of scrubber system typicaly range from 58 percent to 95 percent dust removal (Colinet & Flesh, 2002). The use of scrubber creates recirculation near the working face and recirculation of contaminated scrubber exhaust air over the continuous miner operator proper work position. The scrubber discharged air can still contain a significant amount of respirable dust (Schultz et al., 2010). Therefore it is recommended to take measurements at the operator location and in the return to determine whether one dust control system is more effective than the other (Listak et al., 2010).

In summary, the ventilation control devices used in the last 30 years, lead to improvement in methane dilution, and dust reduction at the face area, but introduce a number of negative effects such as:

- recirculation;
- lack of reversibility (for split ventilation);
- expected maintenance and downtime;
- increased noise level at the face area;
- increased water demand; and
- increased power demand for ventilation.

The analysis of various studies completed to date indicate that to solve these problems requires a different approach to face ventilation design. An approach that will

allow a ventilation specialist to simulate the effect of machine mounted scrubber and sprays and design their performances according the specifics of the face ventilation system for better methane dilution and dust control efficiency.

2.2 Requirements to Face Ventilation Design

A modern face ventilation system design has to provide solution for both, maximize the effectiveness of the system in terms of safety by methane dilution and to ensure healthy level of dust exposure at the operators position during the extended-cut mining. Literature sources that provide theoretical description with analytical or empirical equations suitable for face ventilation system design, particularly for line brattice ventilation systems are very limited (Voronina et al., 1962; Kirkpatrick and Kenyon, 1994). Ventilation requirements in U.S.A. are specified by the Code of Federal Regulations, title 30 CFR. A minimum of 3000 cfm must reach each working face and this quantity must be measured "... at or near the end of the line curtain, ventilation tubing, or other ventilation control device." (30 CFR §75:325 (a) (1)). For faces with exhaust ventilation, the mean entry air velocity must be measured "... at or near the inby end of the line curtain, ventilation tubing, or other ventilation control device." (30 CFR §75:326). As long as the methane concentrations does not exceed 1 percent, it is assumed that a sufficient air quantity is reaching the face. Whenever methane readings are one percent or higher mining must stop until concentrations are reduced below one percent.

A newly exposed coal surface will emit methane at a rate that decays with time. McPherson, (1993) stated the following factors to the rate of gas emission into the mine ventilation system.

- initial gas content of the coal
- degree of prior degassing by methane drainage or mine workings
- method of mining
- thickness of the worked seam and proximity of other seams
- coal production rate
- panel width (of longwalls) and depth below surface
- conveyor speeds
- the natural permeability of the strata and, in particular, the dynamic variations in permeability caused by mining
- fragmentation of the coal

In room and pillar workings, gas will be produced from faces, rib-sides and the pillars of the seam being worked. Peaks of gas emission will occur at the faces of the rooms due to the high rate of fragmentation caused by mechanized coal mining (McPherson, 1993). Usually, a methane emission rate is given by methane desorption curve plotted against time and could be obtained by in-mine methane inflow measurements or predicted by analytical, empirical or numerical methods.

The methane emission rate is a dimensionless ratio of the volume of gas emitted after time to the total volume of gas in a spherical and porous particle with single sized and non-connecting capillaries. A practical approximation for methane emission rate less than 0.25 is given by McPherson (1993), see Equation [2.1]

$$\frac{q(t)}{q_{max}} \approx \frac{12}{d}\sqrt{\frac{Dt}{\pi}} \qquad [2.1]$$

where

$q(t)$ is volume of gas (m^3) emitted after time t (s)
q_{max} is total volume of gas in particle
D is coefficient of diffusion (m^2/s)
d is equivalent diameter (m) of particle (= 6 x volume/surface area)

The Equation [2.1] implies that during the early stage of desorption the emission rate is proportional to the square root of time (McPherson, 1993). The major problem associated with this equation is the variability of the coefficient of diffusion D during the degassing process. A further weakness is that the Equation [2.1] was derived in assumption on uniformly sized capillaries (McPherson, 1993). The considerable number of variables that affect the rate of methane emission and their non-linear interaction renders it difficult to apply analytical means to the problem of predicting methane emissions. For this reason, empirical and numerical models are utilized for prediction of methane emission rate of developing mining (Creedy et al., 1988; Lunarzewski, 1998, Karacan and Schatzel, 2008). The predicted methane inflow is needed as an input data for the face ventilation design and is one of the boundary conditions required for the CFD simulation of face ventilation. Modeling the methane flow into the coal seam is outside the scope of this project.

Scrubber air quantity is a key operating parameter that must be known when designing a ventilation plan. Typically, intakes to the scrubbers are located as close to the face as possible. To minimize recirculation, adequate intake air must be maintained behind the curtain. A conventional suggestion is the minimum amount of intake air at the end of the line curtain should be equal to or greater than the measured air quantity of the scrubber. However, the use of scrubber could significantly impact the line curtain air quantities, due to the change in localized air pressures near the face and the effect of the scrubber exhaust (Schultz et al., 2010). Tests using scrubbers with both blowing and exhausting ventilation showed, that the scrubber exhaust flow interferes with the movement of the intake air toward the face (Kissel and Bielicki, 1975; Taylor, 1996).

With blowing ventilation using scrubbers, the minimum air quantity of intake air required behind the line curtain is based on the scrubber air quantity. Currently MSHA policy on blowing ventilation systems when utilizing scrubbers is to have a minimum line curtain air quantity equal to the measured scrubber air capacity with an upper limit of 20

percent or +0.5 m^3/s (1,000 cfm). Filed investigations indicated that when the line curtain air quantity is less than the measured scrubber airflow, recirculation of air from the scrubber exhaust can occur into the intake air of the line curtain (Schultz et al., 2010). When using a dust scrubber, the mouth of the exhaust curtain must be positioned outby the exhaust of the scrubber. Extensive research done by NIOSH, its predecessor, the U.S. Bureau of Mines and other authors showed clearly the scrubber alone does not create adequate ventilation in the immediate cutting zone of the miner (Volkwein and Wellman, 1989; Taylor and Zimmer, 2001; Goodman et al., 2001, Wala et al., 2003 - 2008). Previous research by the former U.S. Bureau of Mines and others had shown that scrubber effectiveness is improved when high pressure water sprays are utilized. Research work has shown that water sprays alone improved effectiveness of the scrubber by a factor of 2 to 3 (Volkwein and Wellman, 1989).

An example spray system used on a continuous miner consists of 60 hollow cone nozzles type HC-2 or BD-2, working at operating pressure of 483 kPa (70 psi), with water consumption of 2.6 liters/min (0.7 gpm) per nozzle.

Most exhaust ventilation sections use sprays but not scrubbers. Sprays with a scrubber are used together on most sections that have blowing ventilation (Taylor and Zimmer, 2001). Research showed that ventilation improved most when the spray system was directed toward the return side of the face (Volkwein and Wellman, 1989; Chilton et al, 2006). Sprays angled 30 degrees toward the return side of the face created a spray pattern that interfered less with face airflow pattern than the top straight spray. This resulted in lower face methane levels.

When sprays are used with blowing face ventilation and a scrubber, the water sprays influence airflow primarily within 0.9 m to 1.2 m (3 to 4 ft) of the face. Although they can have significant on redistributing the gas at the immediate face zone, the sprays have little effect on moving methane out of this area. Attention should be paid with the design of a spray system due to the turbulent flow developed by the sprays can create excessive dust rollback. In some situations the use of particular water spray system can cause the dust to bypass the scrubber inlets, thus reducing the scrubber collection efficiency (Taylor and Zimmer, 2001).

In summary, the best design for a particular face ventilation system is one that provides the adequate airflow quantity with consistent flow patterns (intake to return) at the immediate face area.

2.3 Discussion about CFD Analysis

By definition CFD - Computational Fluid Dynamics is a simulation technique to understand fluid dynamic phenomena applying mathematics, computer science, physics and chemistry. The "state of the art" of CFD technology today is definitely better than experts' guess and it can be used to indicate trends. In order to be applied in quantitative

design some CFD satisfaction guarantee must be given going through a process of testing, adaptation and validation, see Figure 2.6 (Huang and Welsh, 2010)

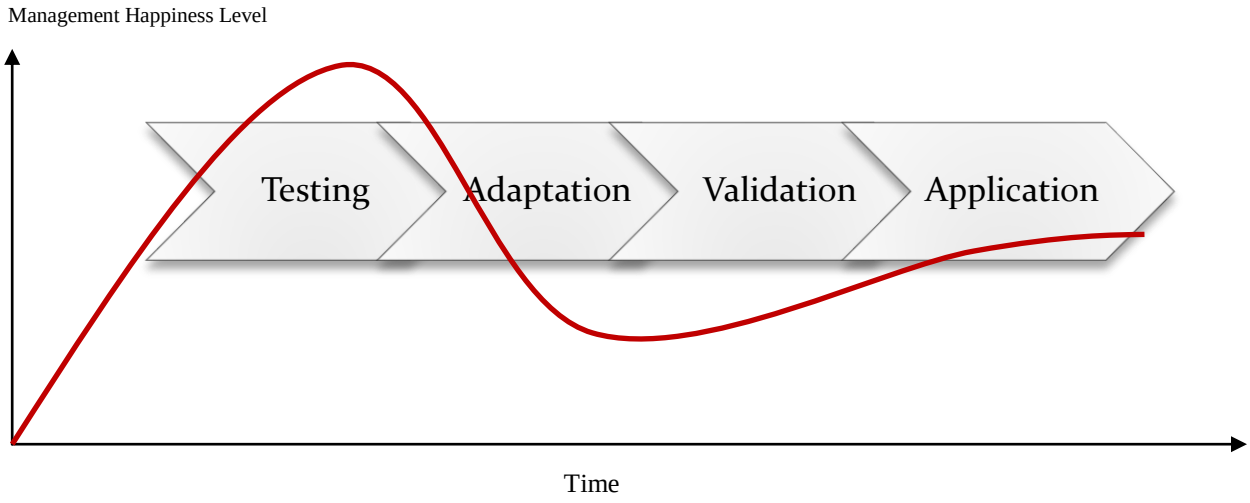

Figure 2.6. CFD Satisfaction Guarantee (Huang & Welsh, 2010).

CFD and its application is a rapidly developing discipline due to the continuous improvement of the commercial software and the growth of computer power. CFD is already widely used in different industries and its application is set to spread. With help of CFD it is possible to get increased insights about the phenomena in the domain of interest and answering of "what if" questions. The face area during the extended cut mining is the domain of this project.

There are several approaches to modeling turbulence phenomena. The first one is Direct Numerical Simulations (DNS) of turbulent flows. Currently DNS is not feasible today for practical application. It requires huge meshes and tiny time-steps to embrace all time and space scales of turbulence. Assuming that the trend of computer speed is historically increased by a factor of 10 every seven years and, assuming that the same trend continues to hold, it will take 50 years until DNS of complete solution for simple industrial flows are possible (Jimenez, 2004).

Fortunately, other methods for CFD simulations are available. The known methods for solving practical fluid flow problems could be divided on three main groups:

1. Reynolds-Averaged Navier Stokes (RANS) methods
2. Large Eddy Simulations (LES)
3. Hybrid methods (combination of LES and RANS)

The classical scheme for computing turbulent flows is to solve the Reynolds-averaged Navier-Stokes (RANS) (Jimenez, 2004). RANS have many different forms: Eddy Viscosity k-ε and k-ω models; Linear and Non-Linear Turbulence Models; High and Low-Reynolds-Number versions; one equation models (k) and others (Cradle,

2009). RANS models are using an approach of time-averaging of governing equations to introduce a turbulent viscosity to deal with Reynolds Stress.

In the domain of interest - extended-cut face ventilation systems, turbulent flows take place and separation phenomena are important. For instance, the Reynolds Number determined for the intake jet developed by a blowing line brattice is greater than sixty thousand ($Re > 60{,}000$) indicated fully developed turbulence. On the other hand, flow measurement results point that at the immediate face zone turbulence becomes less likely if the setback distance increases beyond 6 m (20 ft) and airflow separation take place. The situation becomes significantly more complicated when the scrubber and water sprays are operational. Therefore a careful selection of a turbulence model is needed and a special treatment of the boundary conditions is required to distinguish the zones with low Reynolds Number.

Face ventilation by line brattice provides a lot of cases not appreciable by time-averaged characteristics. For instance, the intake jet flow when blowing line brattice is applied or the effect of a scrubber discharge are two of the representatives, mainly due to an unsteadiness of a turbulent flow. Of course, unsteady RANS methods are available so that the various problems induced by the unsteadiness of turbulence can be evaluated properly. However, these phenomena are not necessarily caused by only a pure unsteadiness of turbulence but closely related to the essence of turbulent phenomenon, such as airflow separation, that is organized by various sizes of turbulence eddies generated by a cascade process of turbulence (Cradle, 2009). Therefore, a method completely different from RANS is needed.

One of the candidates for truly predicting turbulent flows is Large Eddy Simulation, referred as LES. The general idea of LES comes from the fact that the isotropic inertial range is more or less universal, and can be parameterized only by the energy transfer rate. If this rate is used to model the effect of the inertial range it should be possible to avoid not only the dissipation scales, but all those which are approximately isotropic and in equilibrium (Jimenez, 2004). The concept of LES is explicitly to resolve large scale eddies, but represent the effect of smaller eddies using sub-grid scale closure. LES models use spatial filtering of governing equations (Cradle, 2009). Attention must be paid for the use of LES, setting up the initial conditions, the limitations related with the method, and the interpretation of the results, mainly due to the fact that all the quantities such as velocity and pressure obtained from LES are instantaneous values (Cradle, 2009). Therefore, in order to know some averaged characteristics, the averaging method should be applied using the obtained time series. According the literature, at least a few ten thousand ore more time steps may be necessary for averaging with high accuracy (Sagaut, 2002).

In summary, there always exist advantages and disadvantages in either RANS or LES. As for the mesh size, RANS can be reached at stable computation no matter how rough the mesh size is or how large the aspect ratio is. Thanks to the available highly-

accurate methods for evaluating boundary conditions such as low-Reynolds Number adaptive wall function are prepared for in RANS, wall-turbulent flows can be predicted with high accuracy. On the other hand, in the region away from a wall, stable computation via LES can be carried out due to the relatively small aspect ratio of mesh geometry. Therefore, if RANS is applied to the region near the wall while LES away from the wall, the method will be of great help to the practical applications. The Detached Eddy Simulation (DES) approach for turbulence models can be applied to distinguish the situations between RANS and LES and combine the advantages of both methods in a dedicated model.

Another important issue concerning face ventilation CFD analysis is the method for simulation of water sprays and dust distribution. When sprays and/or dust particles are modeled, the assumption that the particles does not influence the flow could not be made. Sprays could be modeled in two different ways: first: the Eulerian method, where the droplets flow is modeled as a continuum, and second: the Lagrangian method (or particle tracking method), where the trajectories of the droplets/particles or clusters of particles are tracked through the domain using Lagrangian equations of conservation. In this approach, the presence of particles/droplets in the flow is modeling by introducing a fraction and additional source terms in the equations for the continuous fluid phase. These terms account for the exchange of mass, momentum, energy and turbulence between the particles and the fluid (Rutherford, 1989). The Lagrangian model is the most widely used approach for particle tracking and has the advantage of being computationally cheaper than the Eulerian method for a large range of particle sizes (Gant 2006, Walmsley, 2000).

The following steps are typical for a CFD modeling process and analysis:

- Recognize the simulation domain
- Build the geometry
- Define volume and surface regions
- Introduce boundary and initial conditions
- Apply conservation laws
- Meshing / Grid Generation
- Solve the algebraic equations
- Post-process the results
- Engineering analysis

For the current project, to get efficiency in the face ventilation design a set of CFD analysis need to be designed to forecast the performance of the modeled face area ventilating systems. It requires modeling of mining equipment, and simulate different cut scenarios corresponding to a given mining sequence. And the last but not least, the

appropriate CFD code have to provide a platform for development and automation of the simulation process so that the final product can feat to the Mine Ventilation Specialist's needs.

2.4 Basic Equations and Methods

Basic equations used in SC/Tetra Cradle CFD (Cradle, 2009) with application for the development of FVS are briefly described in this section. In this project the incompressible flows is of interest. In general, the incompressible CFD models required following set of properties, variables and equations, as described in Table 2-1.

Table 2-1. General CFD variables and equation needed for modeling of incompressible flows

Properties	Density	ρ
	Viscosity	μ
	Specific heat (optional)	C_p
	Heat conductivity (optional)	k
Variables	Velocity	$U, V, and\ W$
	Pressure	P
	Temperature (optional)	T
Equations	Conservation of mass	1 equation
	Conservation of momentum	3 equations
	Conservation of energy	1 equation (decoupled)
	Turbulence	2 equations
	Mass transport of species	Can be solved with additional species conservation equations w/ and w/o chemical reactions.

For incompressible flows, the relative pressure difference should be used to calculate pressure field. Therefore, at least one reference point where $P = 0$ should be defined in the simulated domain.

2.4.1 *Mass Conservation Equation*

Increase in mass within control volume V = mass of fluid flowing into control surface S, see Equation 2.1.

$$\frac{d}{dt}\int_V \rho dV = -\int_S \rho u_i n_i dS \qquad [2.1]$$

where,

V is a control volume
ρ is the density of the fluid
S is the control surface
u_i is the velocity of the fluid in the direction i.
n_i is the direction cosine of a normal line drawn on S toward the exterior of the surface.

Applying Gauss's integration theorem the following equation is obtained for the mass conservation:

$$\frac{\partial \rho}{\partial t} + \frac{\partial}{\partial x_i}\rho u_i = 0 \qquad [2.2]$$

For incompressible fluids the change in its density is extremely small, so the density can be treated as constant and the mass conservation is simplified to the following equation.

$$\frac{\partial u_i}{\partial x_i} = 0 \qquad [2.3]$$

2.4.2 *Momentum Conservation Equation*

Increase in momentum in control volume V = momentum flowing into control surface S + stress acting on S + external forces acting on the fluid within V, see Equation 2.4.

$$\frac{d}{dt}\int_V \rho u_i dV = -\int_S \rho u_i u_j n_j dS + \int_S \sigma_{ij} n_j dS + \int_V \rho g_i \, dV \qquad [2.4]$$

where,

$-\int_S \rho u_i u_j n_j dS$ is the momentum introduced by the mass flowing into the control surface S

σ_{ij} is the Stress Tensor. For an incompressible fluid $\sigma_{ij} = -p\delta_{ij} + 2\mu e_{ij}$
where, p is the static pressure. If the fluid is stationary $e_{ij} = 0$. If the stress in the fluid in motion correspond to the strain velocity (Newtonian fluids), $e_{ij} = \frac{1}{2}\left(\frac{\partial u_i}{\partial x_j} + \frac{\partial u_j}{\partial x_i}\right)$.

$\int_S \sigma_{ij} n_j dS$ is the stress acting on S

$\int_V \rho g_i \, dV$ is the sum of the external forces acting on the fluid moving in the control volume

Applying Gauss's integration theorem the following equation is normally used to express the momentum conservation, see Equation 2.5:

$$\frac{\partial \rho u_i}{\partial t} + \frac{\partial u_j(\rho u_i)}{\partial x_j} = \frac{\partial \sigma_{ij}}{\partial x_j} + \rho g_i \qquad [2.5]$$

For incompressible fluids the equation for conservation of momentum becomes Equation 2.6:

$$\frac{\partial \rho_0 u_i}{\partial t} + \frac{\partial u_j \rho_0 u_i}{\partial x_j} = -\frac{\partial p}{\partial x_i} + \frac{\partial}{\partial x_j}\mu\left(\frac{\partial u_i}{\partial x_j} + \frac{\partial u_j}{\partial x_i}\right) - \rho_0 g_i \beta (T - T_0) \quad [2.6]$$

where,
β is the coefficient of volume expansion
$T = T_0 + T'$ is the temperature changes
T_0 and ρ_0 - fixed temperature and density

2.4.3 *Equation for Conservation of Diffusive Species*

The equation of conservation of diffusive species represents the balance of the flux of diffusive species in a control volume. Increase in diffusive species within control volume V = - diffusive species flowing into control surface S per unit time - the mass transfer of diffusive species transported due to the concentration gradient on front and back of the control surface S + generation of diffusive species in control surface S, see Equation 2.7.

$$\frac{d}{dt}\int_V \rho C dV = -\int_S \rho C u_j n_j dS - \int_S \rho F_j n_j dS + \int_V \rho \dot{d}\, dS \quad [2.7]$$

where,

C is the concentration of the diffusive species
$F_j = -D_m \frac{\partial C}{\partial x_j}$ is the diffusion flux (proportional to the gradient of concentration of diffusive species at a given point (Fick's law))
D_m is the mass diffusivity coefficient
$\dot{d}$ is the source term of diffusive species, [l/s]

Applying Gauss's integration theorem the basic equation for diffusive species becomes Equation 2.8:

$$\frac{\partial \rho C}{\partial t} + \frac{\partial u_j \rho C}{\partial x_j} = \frac{\partial}{\partial x_j}\rho D_m \frac{\partial C}{\partial x_j} + \rho \dot{d} \quad [2.8]$$

2.4.4 *Arbitrary Lagrangian Eulerian (ALE) Method*

ALE method can be used to analyze flow around an object with movements more complex than rotation. This method involves moving the mesh, and adding factors to the equations for the fixed coordinate system to factor in the movement of the mesh. ALE mass conservation equation for incompressible fluids is given by Equation 2.9.

$$\frac{\partial(u_i - v_i)}{\partial x_i} = 0 \qquad [2.9]$$

ALE momentum conservation equation for incompressible fluids is given by Equation 3.10.

$$\frac{\partial \rho_0 u_i}{\partial t} + \frac{\partial (u_j - v_j)\rho_0 u_i}{\partial x_j} = -\frac{\partial p}{\partial x_i} + \frac{\partial}{\partial x_j}\mu\left(\frac{\partial u_i}{\partial x_j}\right) - \rho_0 g_i \beta (T - T_0) \qquad [2.10]$$

where,
v_j is the speed of movement of the mesh

2.4.5 *Particle Tracking Method*

SC/Tetra offers well developed model for particle tracking including sub-models to account for the effects such as turbulent dispersion, wall interaction, particle coalescence and breakup (Cradle, 2009). This approach requires time dependent CFD analysis (TDA) of the simulated domain. The motion of particles that exists in fluid is driven by the flow. SC/Tetra can also simulate the interaction between particles and fluid. If a particle moves, the fluid near-by is influenced. In SC/Tetra a particle is assumed sphere negligibly small compared to the volume of fluid in a control volume.

The drag force (F_f) from fluid is given by the Equation 2.11.

$$F_f = C_D \, \frac{1}{2} \rho {u_r}^2 A_p \qquad [2.11]$$

Where,
C_D is drag coefficient,
ρ is density of fluid,
$u_r = |u_f - u_p|$ is relative velocity of fluid and particles
u_f is fluid velocity,
u_p is particle velocity, and
A_p is projected area of the particle.

The drag coefficient (C_D) between particles and the air is modeled as a function of particle Reynolds number (Re_p), see Equations 2.12 and 2.13.

$$C_D = \frac{24}{Re_p}\left(1 + 0.1255\left(Re_p\right)^{0.72}\right) \quad for\ Re_p \leq 1000 \qquad [2.12]$$

$$C_D = 0.44 \quad for\ Re_p > 1000 \qquad [2.13]$$

$$Re_p = \frac{\rho d_p u_r}{\mu_f}$$

Where,
ρ is fluid density,
d_p is particle diameter,
u_r is relative velocity of fluid and particles
μ_f is dynamic viscosity of fluid.

When using the particle tracking method, a representative number of droplets should be generated in order to always have a drop present in an inlet cell of the mesh. The required number of the particles (generation frequency) to meet this requirement could be determined by Equation 2.14.

$$f = \frac{u_{d,max}}{s_z} \quad [2.14]$$

where,
$u_{d,max}$ is the maximum droplet (axial) velocity, and
s_z is the cell (octant) size.

Once particle is ejected from computational domain through its boundaries, it automatically disappears. Interaction between the particles and the wall surfaces is controlled by a repulsion coefficient. Repulsion coefficient range from 0 to 1, assigned to the wall surfaces. Repulsion coefficient equal to 0 denotes particle adheres (sticks) to the wall after a collision. If the coefficient is equal to 1, the particle is elastically bounced. Repulsion coefficient between 0 and 1 represents a weaker reflection. SC/Tetra regards a repulsion coeficient as the attribute only of a particle.

Simulation of too many particles may be impossible due to computational cost. In such case, a cluster (flock) of particles can be represent by one particle, assuming that all particles in the group move the same path. This is controlled by the user defined effective number that denotes how many particles are effectively represented by one particle in the computational domain. If the effective number is set to 0, a particle is regarded as being passive, i.e., the particle is affected by the drag force, but has no effect on the fluid.

- In summary, the following inputs are required for particle tracking:
- Initial particle location, [m]
- Initial particle velocity, [m/s]
- Density of particle, kg/m^3
- Diameter of particle, [m]
- Drag coefficient of particle - specified either arbitrary or by formula
- Repulsion coefficient of particle

- Effective number of particle

2.5 Boundary Conditions

2.5.1 *Flux Boundary Conditions*

Transfer of physical variables, such as mass, momentum, energy and concentration, caused by the flow is referred as advection. Denoting $\emptyset$ as any one of the physical variables, the amount of inflow at Flux boundary by advection is expressed by Equation 2.15:

$$-\int_S \emptyset u_j n_j dS \qquad [2.15]$$

where,
u_j is the velocity of control surface (boundary surface)
n_j is the direction cosine of normal of control surface, outward positive

As shown in the equation, the normal velocity $u_j n_j$ and the value of $\emptyset$ must be given of the boundary to define flux condition. For the purpose of the current study It can be done by setting up the inlet and the outflow.

- INLET
  - Velocity normal to the inlet face, or
  - Velocity components, U, V and W to the inlet face, or
  - Mass flow rate, and
- OUTFLOW
  - Fixed static pressure $P = 0$

For steady-state computation, initial conditions affect the rate of convergence, but not the final solution. One can than stabilize convergence using under-relaxation factor ($\alpha < 1$), see Equation 2.16.

$$\emptyset_{NEW} = \alpha \emptyset_{CALCULATED} + (1 - \alpha)\emptyset_{OLD} \qquad [2.16]$$

For unsteady computation (transient analysis), a time step should be selected so that the Courant number, see Equation 2.17, keeps on the order of one ($CFL \leq 1$).

$$CFL = u\frac{\Delta t}{\Delta L} \qquad [2.17]$$

where,
u is the flow velocity
Δt - the chosen time step
ΔL - the element size

2.5.2 *No-Flux Boundary Conditions*

In assumption that the boundary surface is a solid surface, no-flux boundary conditions have no direct impact on the mass conservation equation. However they have an impact on the equation for conservation of momentum, energy and diffusive species passing through the boundary surface. The types of the boundary surface should be determined in the way the stress acts.

2.5.2.1 No-Slip Walls

If the fluid is Newtonian and its flow is laminar, the stress acting to the X direction can be expressed by the Equation 2.18:

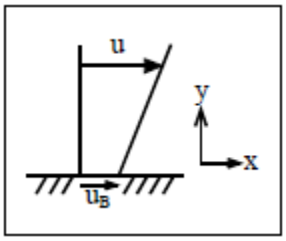

$$\sigma_{xy} = \mu \frac{\partial (u - u_B)}{\partial y} \qquad [2.18]$$

where,
u is the velocity in X direction
u_B is the velocity of boundary surface to the X direction
μ is the molecular viscosity

2.5.2.2 Log Law

If the flow is turbulent, the following velocity profile is found by experiments on turbulent boundary layers in a homogenous flow parallel to a flat plate. This profile is referred to as the Log Law, see Figure 2.8 and Equation 2.19.

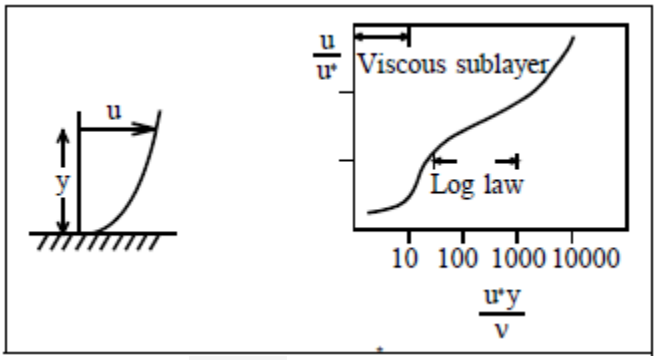

Figure 2.7. Log law

$$\frac{u}{u^*} = \frac{1}{\kappa} \ln \frac{u^* y}{\nu} + A \qquad [2.19]$$

where,

κ : Karman's constant (0.4)
A : Constant (5.5)
y : Distance from the wall surface
u : Flow velocity at position y
u^* : Friction velocity ($=\sqrt{\tau_0/\rho}$)
τ_0 : Shear stress

However, in the region of $y^+ = \frac{u^* y}{\nu} < 30$ the distribution differs from the log law and it becomes closer to the Equation 2.21.

$$\frac{u}{u^*} = \frac{u^* y}{\nu} \qquad [2.20]$$

Nearest to a wall the state of shear stress appears to be similar to a laminar flow (the shear stress is proportional to the velocity gradient), and the region is referred to as a viscous sub-layer. On the other hand, where $y^+ = \frac{u^* y}{\nu} = \frac{\rho u^*}{\mu} > 1000$ the velocity profile moves away from the Log Law equation. Accordingly, the range of applicability (effective range) of the log law is $30 < y^+ < 1000$. In addition, a more generalized wall treatment, the low-Reynolds-number adaptive wall function switches the wall boundary conditions naturally and smoothly between viscous-sublayer and log-layer in SC/Tetra WLTY command (Cradle, 2009).

Log Law for rough surface is given by the Equation 2.21.

$$\frac{u}{u^*} = \frac{1}{\kappa} \ln \frac{1}{K_s} + B \qquad [2.21]$$

where,
K_s : Equivalent roughness
B : Constant = 8.5

2.5.3 *Porous Media Model*

Porous media model is used in this project to simulate methane emission from the face. A porous media region consists of fluid and solid. The solid is called porous media material. The porosity is defined as a fraction of the volume occupied by the fluid over the total volume Modeling the complexity of porous media by treating fluid and solid region separately is impracticable from a viewpoint of computational cost. Thus, the coexistence of fluid and the solid in one element is treated and called porous media (Cradle, 2009). SC/Tetra does not consider the configuration of flow path in porous media in calculation. An external force is applied in opposite direction of flow in order to produce pressure loss. The following Equation 2.22 describes porosity ε and pressure loss term F_i introduced into the momentum Equation [2.6] for the fluid part in the porous

media (Cradle, 2009-2012). When flow is solved by using porous media function, external forces per unit volume acting on the fluid are output to an L file.

$$\frac{\partial \varepsilon \rho_0 u_i}{\partial t} + \frac{\partial u_j \rho_0 u_i}{\partial x_j} = -\frac{\partial p}{\partial x_i} + \frac{\partial}{\partial x_j}\mu\left(\frac{\partial u_i}{\partial x_j} + \frac{\partial u_j}{\partial x_i}\right) - \rho_0 g_i \beta (T - T_0) + \mathrm{F_i} \qquad [2.22]$$

where,
ε denotes porosity
$\mathrm{F_i}$ is pressure loss per unit length in the x_i direction.

A method to calculate the pressure loss depends on porous media models.

Because the entire cross section is not completely covered with the porous media material information to evaluate area ratio is also needed. The area ratio means the ratio of the area of the porous media material to the entire cross section. If the material is isotropic, the area ratio is assumed to be equal to 1 and independent of the directionality. If the material is anisotropic, the area ratios in mutually orthogonal three directions must be specified. SC/Tetra provides some isotropic and anisotropic porous media models (Cradle, 2009-2012)

The heat transfer from the porous media material to the fluid is not considered in this project.

2.5.4 *Computational Mesh Generation*

The procedure of discretization the domain into many small volumes of certain shape such as rectangular, tetrahedron, pyramid, prism, hexahedron to represent the variation of physical quantities in space and time is called Meshing. The Meshing or grid generation use to be one of the most sophisticated and time consuming part of CFD modeling process before intelligent methods for automatic mesh generation to be developed and its application is set to spread. (CRADLE, 2009). There are two general mesh types:

- Structured mesh
- Unstructured Mesh

Any of the mesh types posses it own characteristics and features such as the mesh generation toughness, computation speed, stability, ease of use, geometry precision, local refinement ability and the coupling with Final Element Analysis (FEA) methodology. The unstructured mesh posses the excellence of the last three features, namely exact geometry representation, flexible local refinement ability and straightforward coupling with FEA, which makes it the preferred mesh type, regardless of the difficulties associated with its mathematical description and generation (Huang & Welsh, 2010).

What kind of mesh to use for analysis is one of the first considerations when analyzing flow. Developing an effective mesh requires a certain degree of experience, and this in turn is closely related to having a clear understanding of the problem in hand. In comparison to a tetrahedral mesh, using a hybrid mesh including prism element at the wall boundary is known to provide higher accuracy in the analysis of turbulence. The prism layer is basically inserted into a no-slip wall. As a rule, it is not necessary to insert prisms into discontinuous surfaces or mirror planes. When creating a mesh containing prisms, the main problem is deciding on the size of the tetra mesh and the thickness of the prism layer. It is important to exercise care in selecting these values as they will have a direct impact on the efficiency, stability and accuracy of a computation. Roughly speaking, if the thickness of one prism layer is less than about 1/4 of the size of the adjoining tetrahedral elements, computation will become unstable. To conduct an analysis of turbulence accurately, the thickness of the first prism layer y, see Equation 3.23, must be set so as the value of y^+, see Equation 3.24 be in the effective range of the log-law. When the wall is smooth, the value of y^+ must be within the range of 50 - 150 for accurate flow analysis. When deciding the thickness y of the prism layer, it is possible to decide the values of ρ, μ, and y^+ before an analysis, but is not possible to determine the values of u^* with good accuracy. However, as the value of friction velocity u^* can be estimated at around 5% of main stream velocity U, see Equation 2.25, this value is used when determining prism thickness.

$$y = \mu y^+ / \rho u^*, \text{ [m]} \qquad [2.23]$$

$$y^+ = \frac{\rho u^*}{\mu} \quad \text{or set a design value.} \qquad [2.24]$$

$$u^* = 0.05U, \text{ [m/s]} \qquad [2.25]$$

$$U = \sqrt{2\Delta P/\rho} \text{ or known, [m/s]} \qquad [2.26]$$

However, setting prism thickness in this way may not always produce a suitable mesh. If the size of the volume in which flow is to be analyzed is several tens of meters, these settings are likely to produce a larger than expected total number of elements, and in the case of volumes with a small diameters (for example 50 mm), the mesh resulting from the above settings is likely to be too coarse. In such cases, the number of meshes can be controlled by adjusting the design value of y^+. As y is proportional to y^+, increasing the design value of y^+ makes the prism layer thicker, and reducing it makes the prism layer thinner. In some cases, the value of y^+ may fall outside the effective range. When y^+ is too small one possible solution is to use a low-Reynolds-number turbulence model. If y^+ is too large, the basic solution is to make the mesh finer, but if this is not possible, it is important to recognize that the analysis is not being performed

under the best possible conditions. Using wall functions can save time and mesh points because the sublayer region can be bypassed ($y^+ > 30\ for\ 1^{st}\ grid\ point$). Because for the current study the separation is important, integrating the domain to the wall is possible by using a low-Reynolds number model, but make sure you have sufficient points to cover the boundary layers ($y^+ < 1\ for\ 1^{st}\ grid\ point$).

A sufficient number of prism layers near a wall are needed in all cases to ensure numerical accuracy. Two to three layers are enough when using standard wall functions. Up to 30 layers could be needed when using low-Reynolds Number models. Need far greater mesh density to resolve the complexities of flow separation (Huang & Welsh, 2010). If the form of the model is simple, and if 4 or more layers are successfully inserted, using resulting mesh in computation presents no further problems. The way to avoid divergence is to reduce the number of layers.

Chapter 3

PARAMETRIC STUDY OF AIRFLOW SEPARATION PHENOMENON IN LINE BRATTICE FACE VENTILATION SYSTEMS

Evidence provided from previews studies (Luxner, 1965, Gillies, 1982, Taylor and Goodman 1992, Taylor 2000, Taylor and Zimmer 2001, Wala et al. 2000 to 2008) clearly show that the geometry of the entry is a critical factor for the flow separation at the face area. Using smoke for flow visualisation,Luxner (1969) observed flow patterns that changed with the curtain tight-rib distance, independent of the intake volume of air delivered by the line brattice. Owing to its ability to deliver more of the intake air to the immediate face zone this study was focused on the blowing curtain face ventilation systems. Analyzing the flow behavior at the face area ventilated by blowing curtain, the observed flow patterns were categorized and divided into three categories (Petrov, Wala and Huang, 2013):

A) Flow Penetration;

B) Flow Separation; and

C) Unsteady flow.

Observed categories of flow behavior regardless of inflow rate for different geometry of blowing curtain face ventilation systems are shown in Table 3-1.

Table 3-1. Observed categories of flow behavior for different geometry of blowing curtain face ventilation system, regardless the intake flow rate

Curtain tight-rib distance,	Entry width					
	3.7 m (12 ft)	4 m (13 ft)	4.3 m (14 ft)	4.6 m (15 ft)	4.9 m (16 ft)	6.1 m (20 ft)
0.3 m (1 ft)	**A**	**A**	**A**	**A**	**A**	**A**
0.6 m (2 ft)	**B**	**B**	**B**	**C**	**A**	**A**
0.9 m (3 ft)	**B**	**B**	**B**	**B**	**B**	**B**
1.2 m (4ft)	**B**	**B**	**B**	**B**	**B**	**B**

Surprisingly, the air streams showed little response to the changes of wall roughness. The effect of changes in the air viscosity to the flow patterns was not taken into account in the previews sudies, but the viscosity participated in the wall boundary conditions and into the stress tensor of Navier–Stokes momentum conservation equations. Therefore, the air viscosity cannot be eliminated from the research by default. The observed independence of the flow patterns from the intake air quantity also need to be generally proven and supported by theoretical explanation.

Analysis of variance (ANOVA) method (Box et al, 1978) was used to perform a parametric study for the flow behavior of the blowing curtain face ventilation systems. Seven parameters were included in this study:

(i) inflow rate, Q_{in}

(ii) width of the entry, w

(iii) curtain tight-rib distance, d'

(iv) height of the entry, h

(v) curtain setback distance, s

(vi) wall roughness, r

(vii) air viscosity, μ

The technique of ANOVA was used to determine the impact of the selected seven parameters to the primary air stream's separation distance from the curtain discharge X_{sep} and the air quantity delivered to the face Q_f. The sensitivity of X_{sep} and Q_f to the variance of the listed parameters were analyzed, using data by series of CFD simulations particularly designed for this study. The theory of design and analysis of experiments (Montgomery, 2009) required parametric matrix of 2^7 for the needs of this study. Therefore 128 simulations were performed, using validated CFD code. Details about the CFD code validation are given in Chapter 4. The obtained results were introduced into a Matlab program to implement the ANOVA technique, see Appendix. To test the ability of a model to accurately predict the response parameter value a diagnostic check was performed using Normal plot of residuals, see Figure 3.1. The performed diagnostic check indicates the model appears reasonably appropriate for the conducted analysis.

Analysis of variance was conducted under the null hypothesis H0: the modification has made no difference. If the H0 is rejected, the alternative hypothesis H1: a statistically significant difference has occurred. The levels of confidence to reject H0 hypothesis were accepted as given in Table 3-2. The significance of the individual parameter effect was first measured by running one way ANOVA tests for X_{sep} and Q_f , see Table 3-3 and 3-4 respectively. Then the model was modified based on the rejected terms (Prob.F$\geq$0.20) and the sensitivity of X_{sep} and Q_f to the variance of the remained parameters and associated interactions was measured using four way ANOVA test, see Table 3-5 and 3-6.

Table 3-2. Levels of confidence to reject H0 hyphothesis

Probability (Prob.F) intervals	Significance levels of skepticism
0.01 or less	Fairly Confident
0.05	Somewhat Confident
0.10	Somewhat Suspicious
0.20 or greater	Suspicious

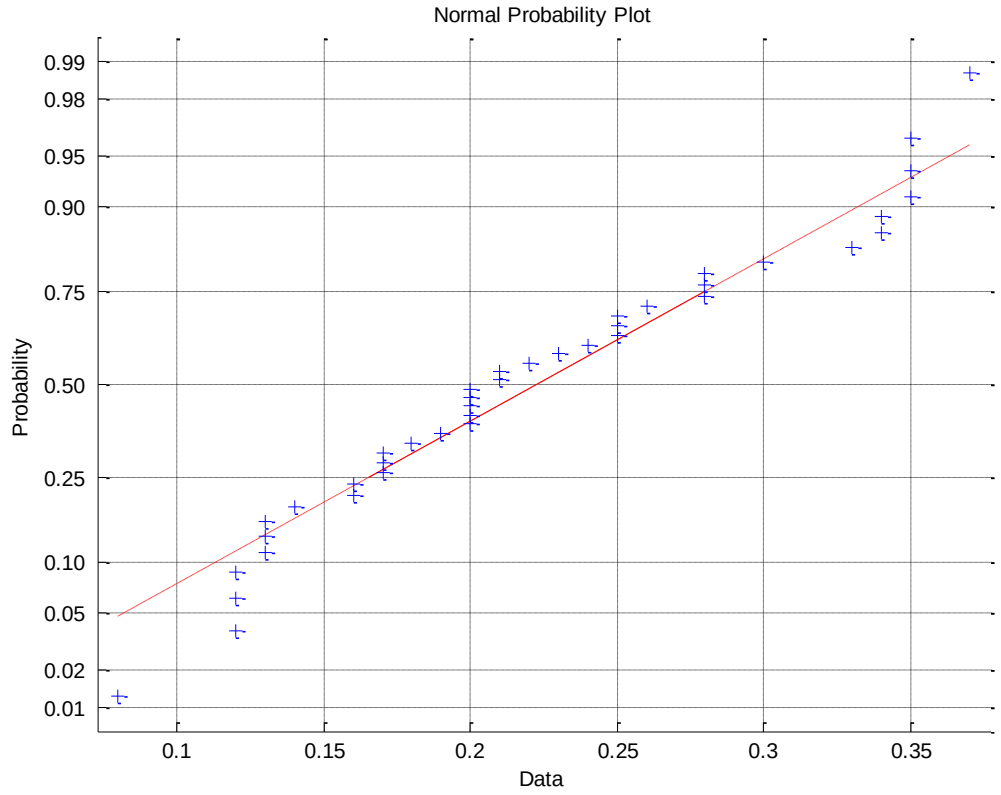

Figure 3.1. ANOVA model diagnostic check

Table 3-3. One way ANOVA test results for Q_f

Analysis of Variance

Source	Sum Sq.	d.f.	Mean Sq.	F	Prob>F
w	0.12066	1	0.12066	21.14	0
d	0.31106	1	0.31106	54.49	0
Q	0.00002	1	0.00002	0	0.9535
wall	0.0291	1	0.0291	5.1	0.0258
viscosity	0.01598	1	0.01598	2.8	0.097
h	0.01182	1	0.01182	2.07	0.1528
setback	1.33866	1	1.33866	234.5	0
Error	0.68504	120	0.00571		
Total	2.51234	127			

Constrained (Type III) sums of squares.

Table 3-4. One way ANOVA test results for X_{sep}

Analysis of Variance

Source	Sum Sq.	d.f.	Mean Sq.	F	Prob>F
w	0.183	1	0.183	7.83	0.006
d	12.2389	1	12.2389	523.77	0
Q	0.0001	1	0.0001	0	0.954
wall	0.2048	1	0.2048	8.76	0.0037
viscosity	0.0435	1	0.0435	1.86	0.1749
h	0.0018	1	0.0018	0.08	0.7818
setback	1.4323	1	1.4323	61.29	0
Error	2.804	120	0.0234		
Total	16.9084	127			

Constrained (Type III) sums of squares.

Table 3-5. Four way ANOVA test results for Q_f

Analysis of Variance

Source	Sum Sq.	d.f.	Mean Sq.	F	Prob>F
w	0.12066	1	0.12066	37.86	0
d	0.31106	1	0.31106	97.6	0
setback	1.33866	1	1.33866	420.01	0
wall	0.0291	1	0.0291	9.13	0.0031
w*d	0.00219	1	0.00219	0.69	0.4084
w*setback	0.04241	1	0.04241	13.31	0.0004
w*wall	0.00829	1	0.00829	2.6	0.1096
d*setback	0.15332	1	0.15332	48.11	0
d*wall	0.06616	1	0.06616	20.76	0
setback*wall	0.00144	1	0.00144	0.45	0.5022
w*d*setback	0.01069	1	0.01069	3.36	0.0696
w*d*wall	0.00513	1	0.00513	1.61	0.2074
w*setback*wall	0.03094	1	0.03094	9.71	0.0023
d*setback*wall	0.00119	1	0.00119	0.37	0.5427
w*d*setback*wall	0.03413	1	0.03413	10.71	0.0014
Error	0.35696	112	0.00319		
Total	2.51234	127			

Constrained (Type III) sums of squares.

Table 3-6. Four way ANOVA test results for X_{sep}

Analysis of Variance

Source	Sum Sq.	d.f.	Mean Sq.	F	Prob>F
w	0.183	1	0.183	12.77	0.0005
d	12.2389	1	12.2389	854.03	0
setback	1.4323	1	1.4323	99.94	0
wall	0.2048	1	0.2048	14.29	0.0003
w*d	0.003	1	0.003	0.21	0.648
w*setback	0	1	0	0	0.9647
w*wall	0.0578	1	0.0578	4.03	0.047
d*setback	0.4371	1	0.4371	30.5	0
d*wall	0.2869	1	0.2869	20.02	0
setback*wall	0.1213	1	0.1213	8.46	0.0044
w*d*setback	0.0465	1	0.0465	3.25	0.0743
w*d*wall	0.0282	1	0.0282	1.97	0.1634
w*setback*wall	0.0694	1	0.0694	4.84	0.0298
d*setback*wall	0.12	1	0.12	8.38	0.0046
w*d*setback*wall	0.0741	1	0.0741	5.17	0.0249
Error	1.6051	112	0.0143		
Total	16.9084	127			

Constrained (Type III) sums of squares.

The results of the analysis of variance supports the following conclusions:

1. The inflow rate Q_{in} (Prob.F>0.95), the air viscosity and the height of the entry are not significant for the variation of Q_f and X_{sep}.
2. It is fairly confident (Prob.F<0.006) that the variations of Q_f and X_{sep} are caused by the impact of three significant parameters, namely tight-rib distance d', width of the entry w and curtain setback distance, s.
3. It is confident (Prob.F<0.03) that the wall roughness plays role for the flow penetration scenarios.
4. In this case it is fairly confident (Prob.F <0.002) that the associated parameter interaction is of type w*d'*s*r.

Performed Analysis of covariance showed that the sought relationships $Q_f(d')$, $Q_f(w)$ and $Q_f(s)$ are expected to be non-linear.

The performed analysis confirmed that, the changes in the intake air quantity have no significant impact on the flow patterns and the amount of air delicered to the immediate face zone. For better understanding of the flow separation phenomenon, pressure forces need to be considered. As it can be seen on Figure 3.2, changes in the inflow rate caused change in the static pressure distribution. As the flow rate increases positive static pressure builds up in the confined space between the face and the primary

air-stream, see Figure 3.2. The intake flow separates relatively at the same location, regardless of the intake air quantity delivered behind the curtain.

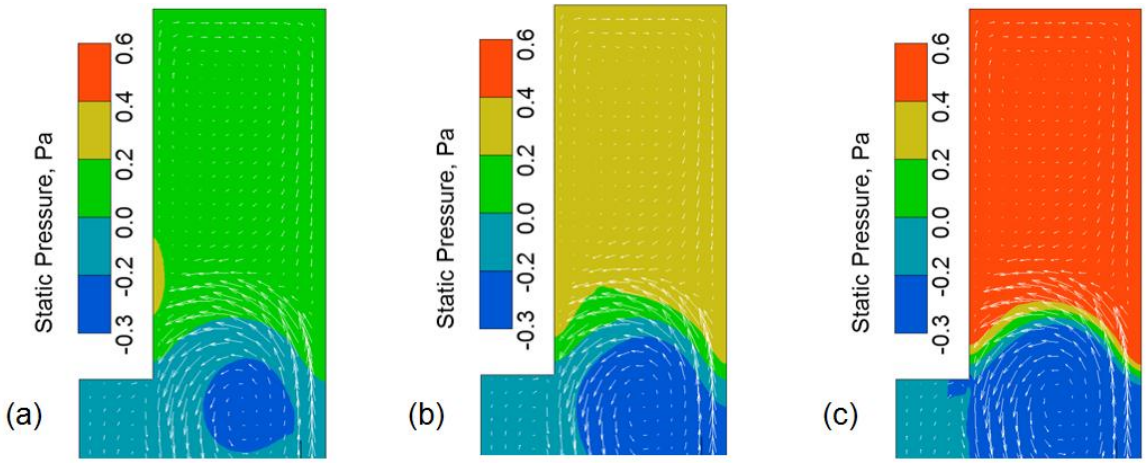

Figure 3.2. Static pressure distribution for three different inflow rates, (a) Qin=1.3 m^3/s (2700 cfm), b) Qin=1.7 m^3/s (3500 cfm), c) Qin=2.6 m^3/s (5500 cfm)

To obtain the relationship between the geometry of the face area and the dynamic parameters, a scaling analysis using the law approach method (Emory et al., 2009) were performed. Heuristic arguments to obtain the functional relationship among dimensionless quantities (known as pi-numbers) based on physical insight are described below.

Accordingly the performed analysis, flow separation occurs when the parameters tight-rib distance d' and width of the entry w (=d+d') exceed a certain value, see Figure 3.3.

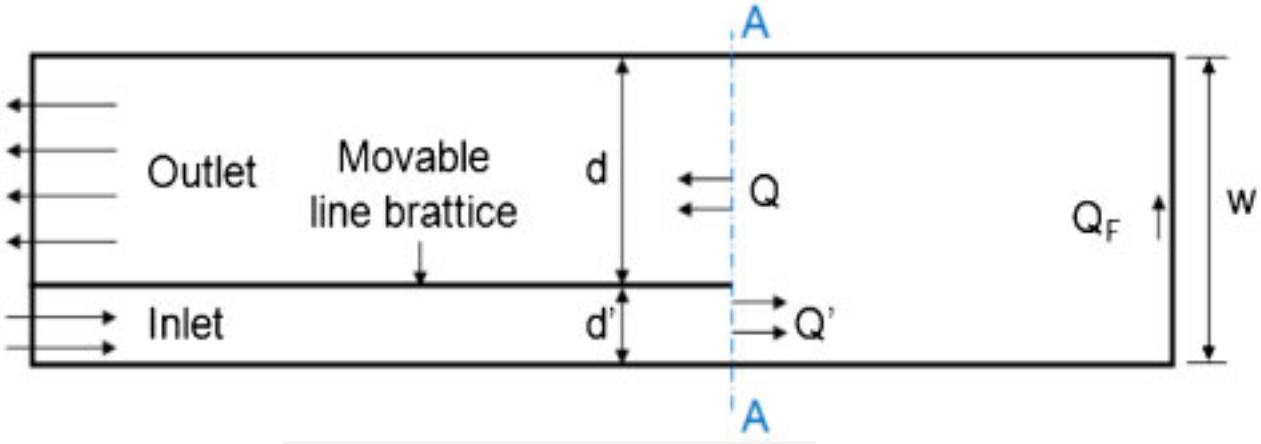

Figure 3.3. Simplified face area with blowing curtain

The flow behavior in the studied face area is governed by the laws of mass conservation and momentum conservation. The Reynolds numbers determined for the

intake jet Re' were > 60 000 which indicates developed turbulence conditions. Inertia and pressure forces in the motion of air are dominant compared with the forces of internal friction (viscous term).

When airflow separation takes place the air quantity delivered to the face Q_f is less than the inflow quantity Q'.

$$Q_f < Q' \tag{3.1}$$

The return airflow rate (Q) balances (2) the intake jet flow rate (Q') in the cross section marked with A-A, see Figue 3.3.

$$Q = Q' \tag{3.2}$$

Reynolds numbers for the intake jet can be determined by formula (3).

$$Re = \frac{\rho u D}{\mu} \tag{3.3}$$

where ρ is the air density, u is the air velocity, μ is kinematic air viscosity, and D is the equivalent diameter of the mine opening given by Equation 3.4.

$$D = \frac{4S}{Per} \tag{3.4}$$

where, S denotes cross section area of the opening, and Per is the perimeter of the opening.

Taking into account the similarity of the airflow into the face areas in different scales and adopting scaling analysis as a tool for better understanding of the observed phenomena we obtain the first pi-number, see Equation 3.7.

$$\frac{Re}{Re'} = \frac{\rho u D / \mu}{\rho' u' D' / \mu'} \tag{3.5}$$

but $\rho = \rho';\ \mu = \mu';$ and $h = h'$, then substituting D we obtain

$$\frac{Re}{Re'} = \frac{uSPer'}{u'S'Per} = \frac{\mathrm{Q}Per'}{Q'Per} \tag{3.6}$$

but Q = Q', so

$$\frac{Re}{Re'} = \frac{Per'}{Per} = \frac{d'+h}{d+h} \qquad [3.7]$$

Relationship (3.7) shows that for the studied face area the Reynolds pi-numbers does not depend of the air quantities.

Following the outcomes of the study, it is assumed that not the intake air quantity, but the kinetic energy of the intake stream is a key parameter for the observed airflow behavior. Furthermore, the kinetic energy of the intake air-stream K' will always be greater than the kinetic energy of the return air-stream K. Air-stream kinetic energy is described by Equation 3.8.

$$K = \rho \frac{u^2}{2} \qquad [3.8]$$

Where u is the air-stream velocity; and ρ, the air density.

Scaling the kinetic energies of the return air-stream to the intake air-stream in the cross section A-A, see Figure 3.3, another important dimensionless pi-number is obtained, see Equation 3.9.

$$\frac{K}{K'} = \left(\frac{u}{u'}\right)^2 = \left(\frac{d'}{d}\right)^2 \qquad [3.9]$$

This pi-number reveals, that kinetic energy ratio depends of reciprocal ratio of the distances (widths) on square.

Using the experimental data an empirical criterion has been found (Equation 3.10), called Jet Separation Ratio (JSR). The JSR criterion is to distinguish the flow separation cases (scenarios) from the cases where no flow separation occurs.

$$\left.\begin{array}{c} IF \\ \text{JSR} = \left(\dfrac{tight\ rib\ distance}{width\ of\ the\ entry - tight\ rib\ distance}\right)^2 > 0.02 \\ \\ Flow\ separation \\ will\ take\ place \\ regardless\ of\ the \\ intake\ air\ quantity \end{array}\right\} \qquad [3.10]$$

Scenarios close to the threshold such as the 4.6 m (15 ft) entry width and 0.6 m (2 ft) curtain tide-rib distance showed unstable behavior of the wall-jet. Unfortunately for

the practically used face ventilation system setups with entry width in range 12 ft to 20 ft and curtain tight rib distance ranged from 3 to 4 ft, flow separation takes place.

The JSR ratio was derived based on blowing curtain systems, but the result is valid also for exhaust curtain systems. In blowing curtain d' < d and the JSR is always less than 1. In exhaust curtain, d' > d and the JSR >1. The jet separation criterion remains the same. This means, that the exhaust curtain systems always developed flow separation, as observed in practice.

Result of the performed parametric analysis lead to better understanding of flow behavior developed by the line brattice face ventilation systems. This strengthen the belief, that the key for improvement of face ventilation is in preventing the flow separation. The current technologies for face ventilation improvement, include powerful scrubber and spray system with 40 to 60 spray nozzles with water flow rate about 2.5 liters/min per nozzle. Originally designed for dust removal, the machine mounted scrubbers and sprays are also acting as air moving devices. Both systems are concentrated mainly in the immediate face area, trying to overcome the flow separation and bring more air to the face but also creating significant air recirculation at the face area.

To prevent the flow separation phenomenon in blowing curtain face ventilation systems, a passive regulator in shape of airfoil positioned at the curtain discharge was proposed (Petrov and Wala, 2014). The proposed "Wing Regulator (WR)" was design with shelter space for protection of the remote CM operator from the dust, while no obstruction his visibility to the CM and communication with the shuttle car operator. Results of the performed filed tests showed, that the WR prevents the flow separation overcoming 13.7 m (45 ft) curtain set back distance to the face for acceptable pressure losses. Measurements in equipment free entry showed 4 to 5 times more air at the immediate face area. Field test for the effect of the wing regulator on methane dilution and respirable dust control during typical cut showed about two times decrease in methane concentration at the face and respirable dust accumulation at the CM operator compared to similar cut without WR. CFD simulation results, indicated that decreasing the scrubber performance has positive effect on dust control. Best results were achieved for scrubber to face ventilation ratio about 0.6. The test results obtained so far are encouraging, but complete feasibility study and MSHA approval is needed to make this technology available to the industry.

Future research is needed to optimize the scrubber performance and spray system to benefit the effect of the WR for improvement of both, methane dilution and dust control. The proposed WR is a subject of international IPT - U.S. patent pending.

Chapter 4

MODEL DEVELOPMENT

For the needs of the project 6 generic CFD models were developed as follows:

1. Equipment-free face ventilation system model.
2. Methane release models, including model of full scale NIOSH Research Gallery manifold equipment and additionally developed porous media model.
3. Continuous miner (CM) models, which involves models of mockup CM used in small scale and full scale experiments at the Mine Ventilation Lab, University of Kentucky and NIOSH Research Gallery and also models of commonly used JOY CM.
4. Water spray model, including full cone and hollow cone spray nozzles.
5. Dust generation model, with ability to simulate respirable coal and silica dust.
6. Scrubber model, with ability to simulate given flow rate and dust removal efficiency.

Generally, the models discussed in this work are incompressible models. Series of preliminary simulation based on small scale and full scale experimental studies published by other authors, including Wala et al. (2000 - 2008); Chilton et al., (2006); and Organiscak and Beck (2010) were conducted to test the performance of the available in SC/Tetra turbulence models. In result, the RNG k-EPS (Renormalization Group Method) performed better and was selected for further use. Later on, field test measurements confirmed the applicability of the selected turbulence model.

For convenience, herein and after, some default values needed for description of the discussed CFD analysis will be assumed. By default, RNG k-EPS is the implemented turbulence model. The default number of calculation cycles was set to 700. The default convergence thresholds were set to 10^{-4} average residuals for calculation of velocities, pressure, turbulent energy and turbulent dissipation rate. For methane concentrations, the convergence threshold was set to 10^{-5} average residuals.

All the developed models, except the dust model, were successfully validated against experimental data for flow and methane. Details about the model development are discussed in this chapter.

4.1 Equipment-Free Face Ventilation Systems Model

The equipment-free entry face ventilation system model is the initial element of the developed Face Ventilation Simulator (FVS). This model outlines the framework of computational domain for more complicated scenarios involving equipment.

A simple model geometry of an equipment free line brattice face ventilation system consists of five surface regions and a volume region of air, see Figure 4.1. The surface regions are named as follows: inlet; outlet; walls; face; and curtain. The detailed model description is given in Table 4-1.

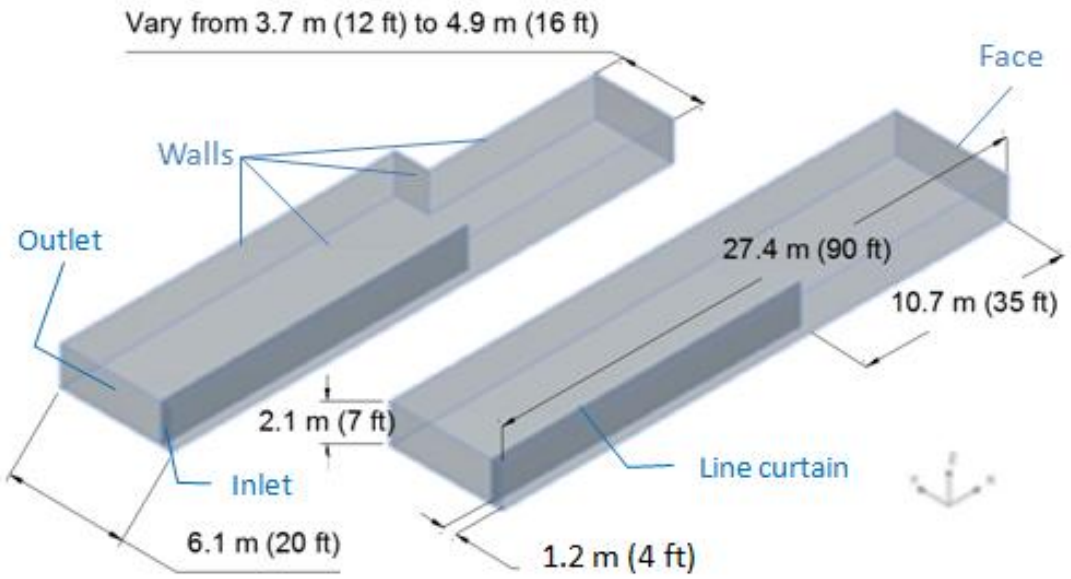

(a) Box-cut (b) Sump-cut

Figure 4.1. Example model geometry of an equipment-free face ventilation system.

Although the geometry of the system may vary, the above defined regions will retain their identification names. If is needed, the "walls" region could be divided to ribs, floor and roof region. Parametric study of line brattice face ventilation systems flow behavior (Petrov, Wala and Huang, 2013), showed five important outcomes:

1) Proved that the flow patterns developed by line brattice face ventilation systems are independent of the intake flow rate.

2) Two parameters govern the occurrence of early flow separation, namely width of the entry and the curtain tight rib distance.

3) Curtain setback affects the air quantity reached the immediate face zone

4) Roughness of the wall has no significant effect to the changes of flow patterns.

5) Height of the entry is not significant for the variations of flow separation distance and the air quantity reached the immediate face zone.

Following the parametric study results, it was assumed same wall conditions to the ribs, floor and roof of the simulated domain. However this model simplification may not fit to some user defined scenarios, such as flow penetration studies using different types of ventilation controls. To meet the requirements of such cases, wall roughness may

need to be assigned for accuracy of the simulation results. Example simulation result is shown on Figure 4-2.

Table 4-1. Description of a Flow Behavior Analysis using Equipment Free Line brattice Face Ventilation System Model

Analysis Types	
Flow (turbulent flow)	
Material Properties	
Air incompressible (standard conditions at 20 ^{o}C)	
Boundary Conditions	
inlet:	Fixed flow
outlet:	Fixed static pressure (0.0 Pa)
walls:	Stationary wall (log-law)
face:	Stationary wall (log-law)
curtain:	Panel, stationary wall (log-law)
Analysis Conditions	
Type of flow:	3-dimensional incompressible turbulent flow
Time dependency of simulation:	Steady State Analysis (SSA)
Turbulence model:	RNG k-EPS model
Convergence threshold:	Default
Equation to be Solved	
Momentum equation	
Mass conservation equation	
k-EPS equations	

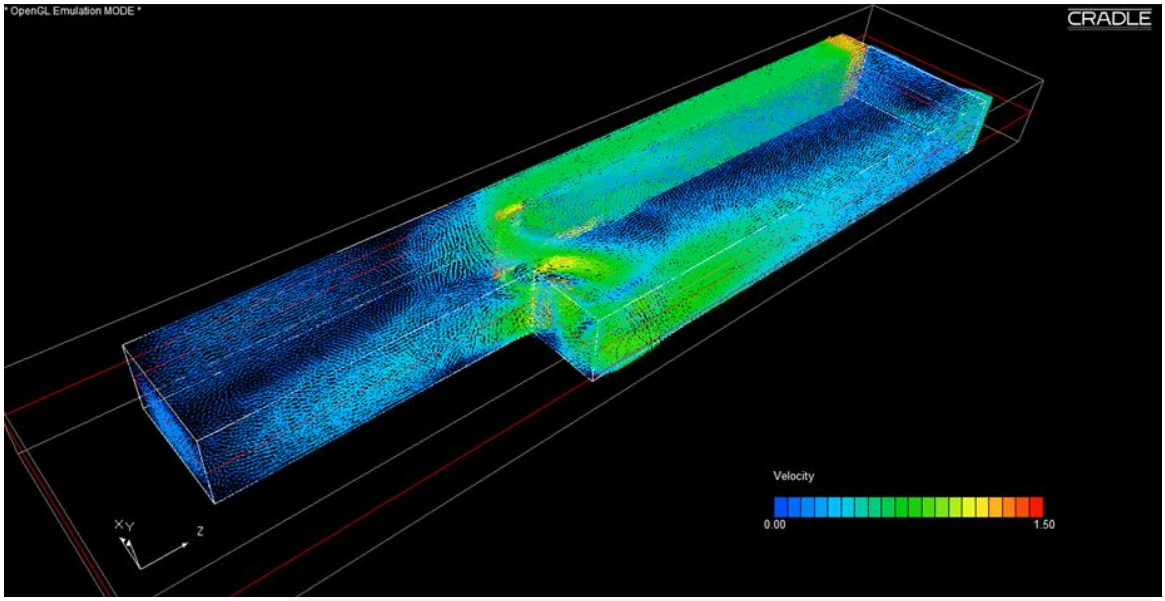

Figure 4.2. Blowing curtain face ventilation system. Box cut scenario, 4 ft curtain tight rib distance, entry width 20 ft, 12 ft wide box cut, entry height 7 ft, 35 ft setback, 7280 cfm inflow rate

A detailed 3D view of flow separation patterns are shown on Figure 4.4.

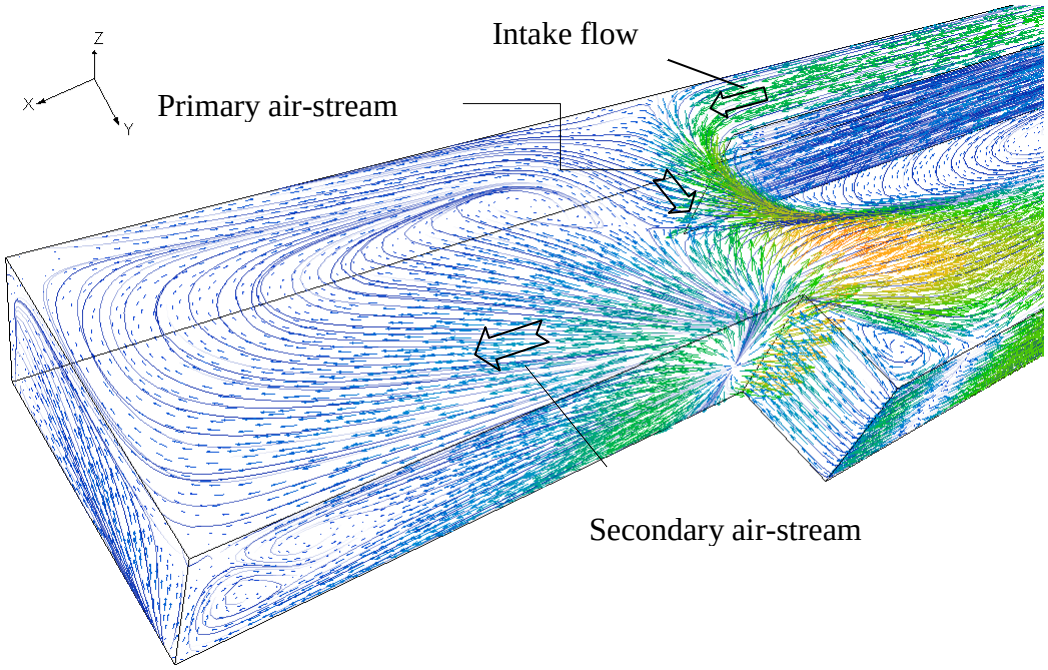

Figure 4.3. Flow separation airflow patterns. Simulation results for blowing curtain face ventilation system, box cut scenario with 35 ft setback

Because heat exchange, change in water content of the air due to evaporation and condensation are not simulated, the input for the intake air quantities must be normalized to standard conditions for air incompressible at 20 ^{o}C with density 1.206 kg/m^{3}.

This simplification allowed to skip the Energy conservation equation in the model and also the additional data needed to set up the thermal and material properties of the wall surfaces and volume regions related to the mining entry and the simulated equipment. For models with CM in place the benefit of this simplification can be expressed in millions of mesh elements and hours of computational time.

4.1.1 *CFD code validation for flow using PIV data*

To validate the mode and the SC/Tetra code, experimental data obtained by Particle Image Velocimetry (PIV) measurements on 1:15 scaled model located at the Mine Ventilation Lab, University of Kentucky was used (Wala et al., 2000 and 2001). Number of scenarios were simulated for different system geometry and intake air flow rates for both, blowing and exhaust curtain. Selected examples of the performed validation study are depicted on Figure 4.5 for blowing curtain, and figure 4.6 for exhaust curtain. The simulated results were in agreement with the experimental results.

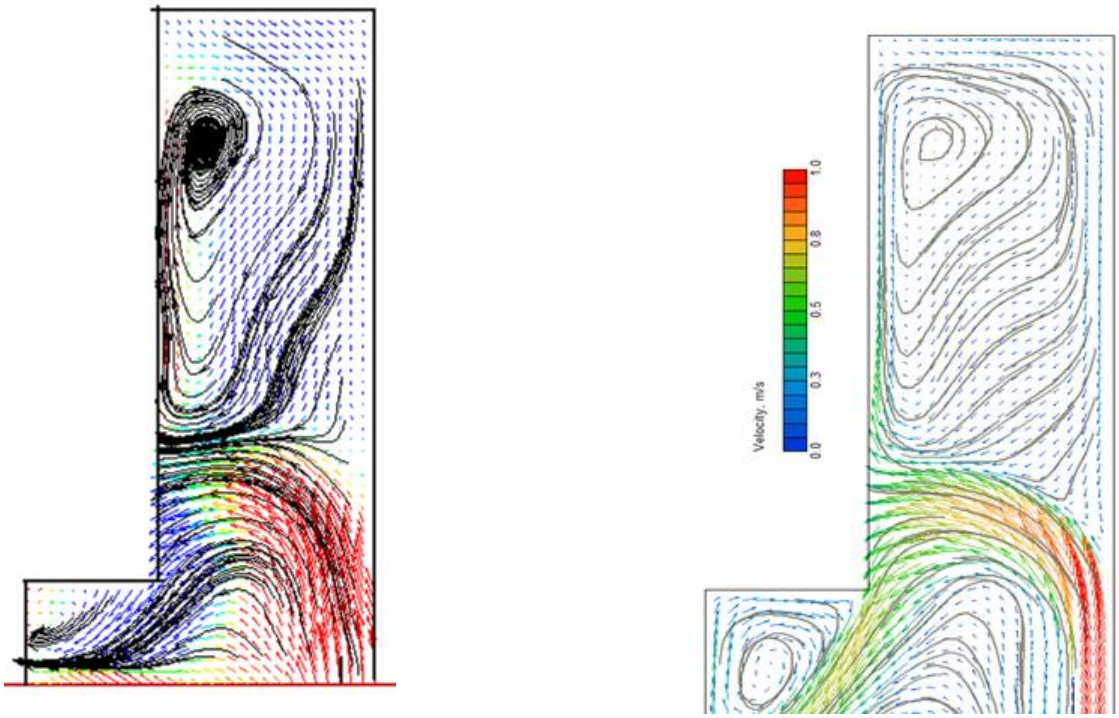

(a) (b)

Figure 4.4. Blowing curtain face ventilation system. Comparison between PIV data and simulation results, (a) PIV data for 1ft curtain tight rib distance, (b) corresponded simulation results

PIV data Simulation Results

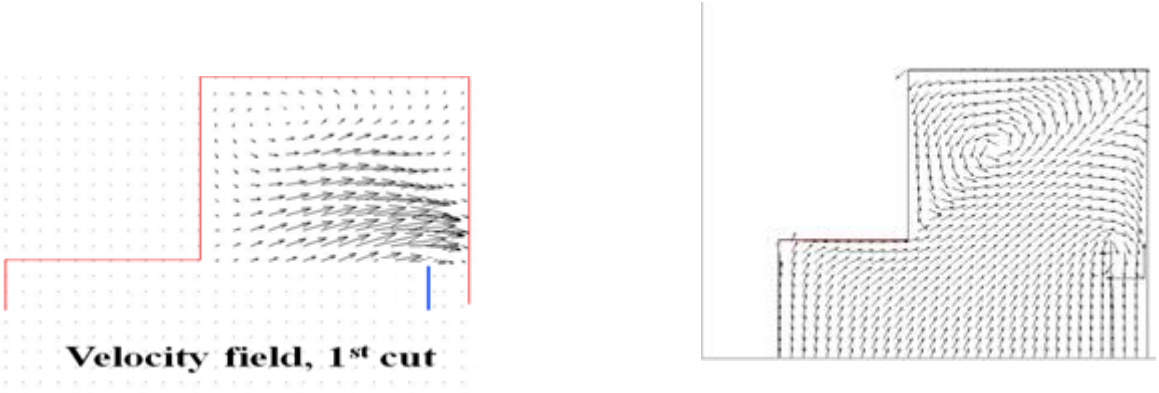

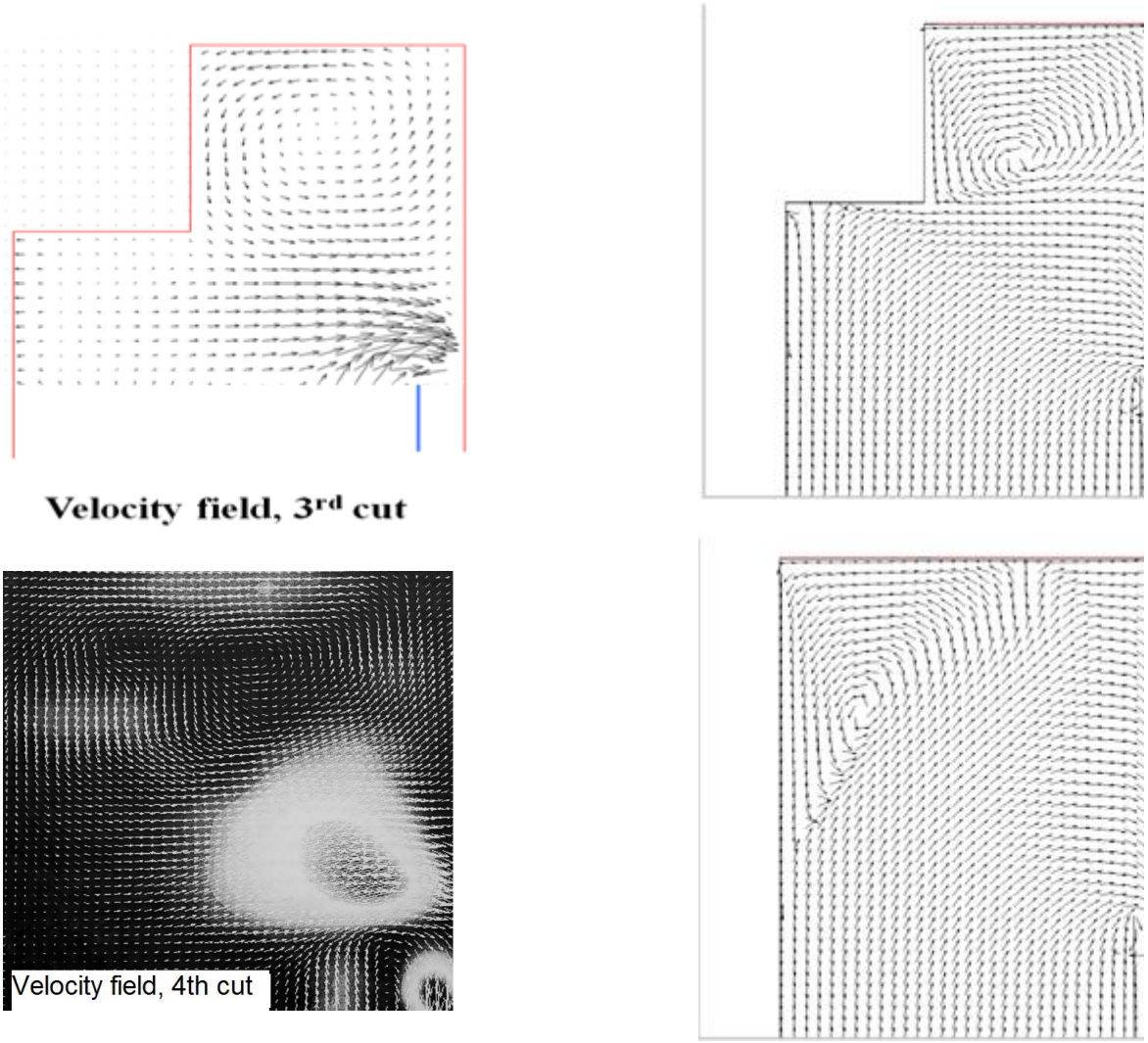

Figure 4.5. Exhaust curtain face ventilation system. Comparison between PIV data (left column) and simulation results (right column)

4.2 Methane Release Model

4.2.1 *Model of laboratory setup*

The first methane release model, built for needs of this project, followed a mining related benchmark experimental study performed at the NIOSH Pittsburgh Research Lab (PRL) under guidance of University of Kentucky (Wala et al., 2006). Results of this study were used for CFD code validation. In the lab setup, the methane was introduced at the face using four perforated manifold tubes positioned parallel to the face one under another. In the model, the surface of the tubes was registered as an inlet (CH4_inlet). To simulate methane distribution in the entry, simple diffusion model was applied. This required to add additional equation for conservation of diffusive species (Equation 3.8) to the system of equations to be solved. The other flux and non-flux boundary conditions

remained the same as in the previously developed and validated model of equipment free entry. The model description is summarized in Table 4-2.

Table 4-2. Description of Gas Control Analysis using manifold tubes methane release model

Analysis Types	
Flow (turbulent flow) Diffusive species (methane diffusion)	
Material Properties	
Air incompressible (standard conditions at 20 ^{o}C) Methane gas (at 20 ^{o}C)	
Boundary Conditions	
inlet:	Fixed flow
outlet:	Fixed static pressure (0.0 Pa)
CH4_inlet	Fixed flow rate
walls:	Stationary wall (log-law)
face:	Stationary wall (log-law)
curtain:	Panel, stationary wall (log-law)
Analysis Conditions	
Type of flow:	3-dimensional incompressible turbulent flow
Time dependency of simulation:	Steady State Analysis (SSA)
Turbulence model:	RNG k-EPS model
Convergence threshold:	Default
Equation to be Solved	
Momentum equation Mass conservation equation k-EPS equations Equation for conservation of diffusive species (simple diffusion)	

4.2.2 *CFD code validation for flow and methane distribution*

The developed model was validated against experiential data for equipment free entry using results of studies performed at the NIOSH PRL (Wala et al., 2006). In these studies methane was released at the face by manifold tubes and the methane concentration was measured in 108 points distributed in three levels. A box cut scenario with 35 ft setback distance, 6,000 cfm intake flow rate, and 5.7 cfm methane flow rate was selected for validation of the model. The simulated results were in agreement with the experimental data, see Figure 4.7 and 4.8. The positions of the measurement points are shown on of Figure 4.8. For better understanding of the obtained results the airflow directions are indicated on the shematic with blue arrow cursors.

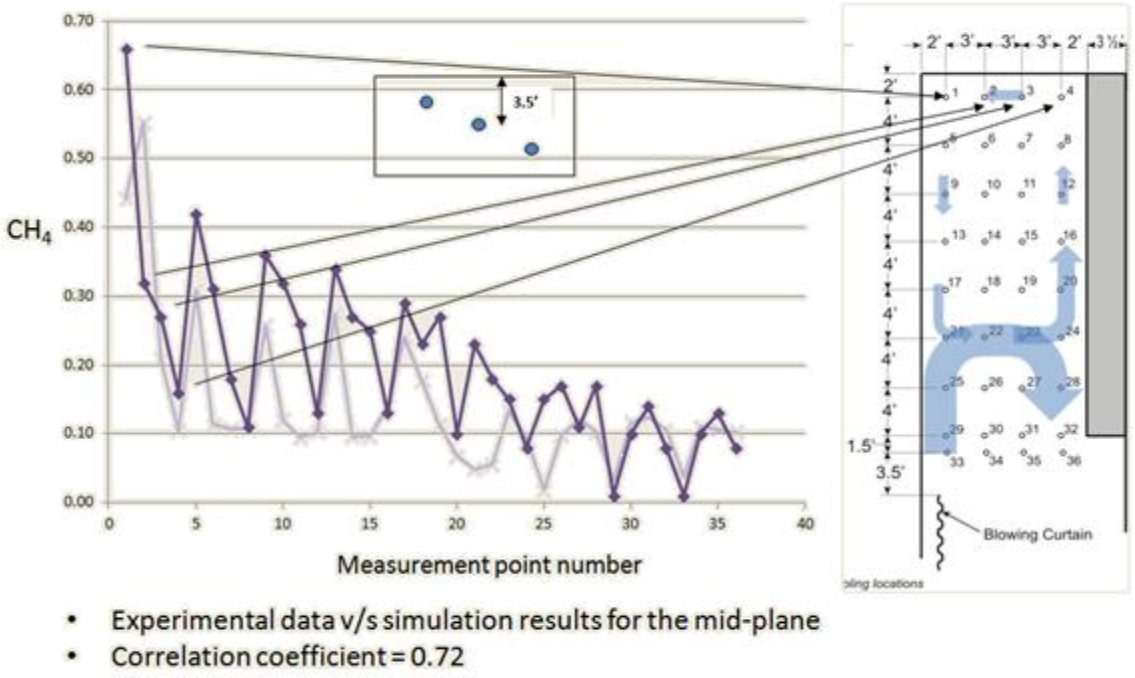

Figure 4.6. Comparison between measured (bold line) and simulated methane concentrations (pale line) at the locations of measurement points

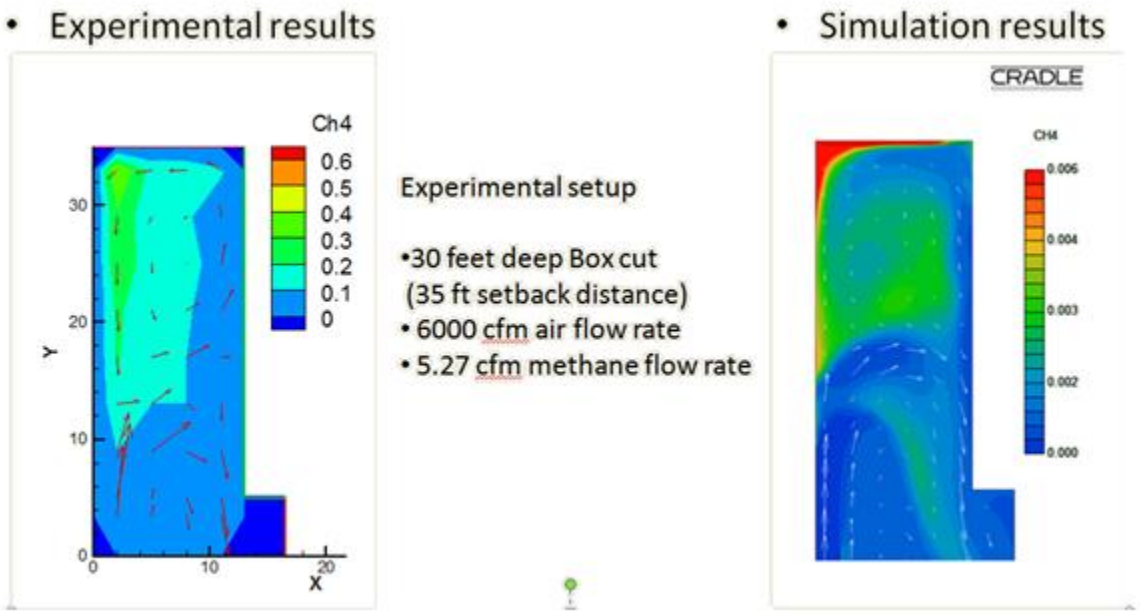

Figure 4.7. Comparison between experimental results (Wala et al., 2006) and simulation results

Due to the airflow separation, the maximum gas concentration (0.6%) developed arround the curtain side corner of the face. Lower gas concentrations were observed along the off-curtain wall of the box-cut (points 4-6-12-16-20, Figure 4.7), due to the effect of the secondary air-stream. The lowest gas concentration, were measured in the zone of the primary intake air stream (points 33 and 29, Figure 4.7). Generaly, the simulation correctly predict both, the flow behavior and the methane concentration in the studied face area.

4.2.3 *Porous media model*

For more realistic representation of methane release, the manifold tubes methane release model were replaced by porous media model. In assumption that the most significant source of methane during mining operations is the working face, a porous media volume was attached to the face surface to simulate methane release, see Figure 4.9.). If flow cannot be fully developed due to lack of length of porous media in the streamwise direction, this model is inappropriate (Cradle, 2009). A depth of about 2.1 m (7 ft) is needed to ensure numerical stability of porous media model for this application.

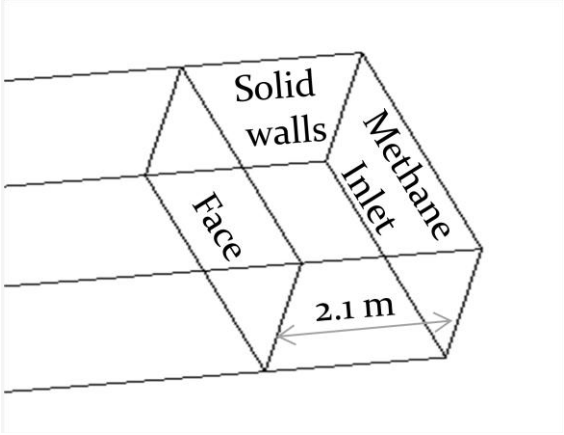

Figure 4.8. Porous media volume attached to the face

A particle type of porous media with porosity of 0.25 and diameter of particles 0.0001 m was implemented for the needs of the project. The porous media volume is surrounded by solid walls. By default, the methane flux boundary conditions are assigned to the methane inlet (region name CH4_inlet according Table 4-4) by fixed mass flow rate in kg/s. For time dependent simulations, user defined variable table describing the flow rate as a function in time could be given instead of the fixed mass flow rate. Detailed description of the model is given in Table 4-4. This model is not intended to simulate the real porosity of the coal seam around the face, but to involve the whole face area into the methane release process instead of using manifold tubes. SC/Tetra provides some other porous media models such as isotropic, anisotropic, and fin models (Cradle, 2009-2012) that could be utilized in the future if needed. These models required

additional information for their proper set up, as well as experimental and validation study which is outside the scope of this project.

Table 4-3. Description of a Gas Control Analysis using porous media methane release model

Analysis Types	
Flow (turbulent flow)	
Diffusive species (methane diffusion)	
Porous media	
Material Properties	
Air incompressible (standard conditions at 20 ^{o}C)	
Methane gas (at 20 ^{o}C)	
Boundary Conditions	
inlet:	Fixed flow rate
outlet:	Fixed static pressure (0.0 Pa)
CH4_inlet	Fixed flow rate / Variable table
walls_porous	Porous media solid walls
walls:	Stationary wall (log-law)
face:	Porous media boundary surface
curtain:	Panel, stationary wall (log-law)
Analysis Conditions	
Type of flow:	3-dimensional incompressible turbulent flow
Time dependency of simulation:	Steady State Analysis (SSA)
Turbulence model:	RNG k-EPS model
Convergence threshold:	Default
Equation to be Solved	
Momentum equation	
Mass conservation equation	
k-EPS equations	
Equation for conservation of diffusive species (simple diffusion)	
Porous media porosity and pressure loss term introduced into the momentum equation	

4.3 Continuous Miner Models

Continuous miner models consist of five general parts and two sub-models

- miner body part
- tail part
- loading pan part
- boom part
- cutting head part
- scrubber system sub-model
- spray system sub-model

The geometry of miner body is simplified shell of a CM including the basic chassis, crawler chains, and the conveyor bed. The tail and the boom of a CM model are provided in fixed positions. The effect of cutting head rotation to the flow patterns is simulated in SSA and TDA, using ALE method (see Chapter 3, 3.1.4). Scrubber effect on flow patterns and methane dilution can be simulated in both, SSA and TDA conditions. Simulations that involve sprays or/and dust used particle tracking method (see Chapter 3, 3.1.5) and required TDA. Due to the specifics of the scrubber and spray system models the description of these two models are given separately in this chapter. Six models of CM machines were developed for the needs of the different stages of this study, see Figure 4.10. The first CM model represents the wooden CM model available at the Mine Ventilation Laboratory, University of Kentucky. This model was used in Cradle CFD code validation studies for flow, against PIV data recorded on the 1:15 scale model of face ventilation system. The second CM model, called NIOSH 1, represents the full scale mockup CM model available at the NIOSH Research Gallery. The model was built for the needs of performed Cradle CFD code validation study for the effect of a machine mounted scrubber on methane dilution. The third model, called NIOSH 2, represents the full scale mockup model of CM available at the NIOSH Pittsburgh Research Lab for dust studies. The fifth model represents Joy 14CM12 continuous miner using CAD data provided by JoyGlobal. The sixth model represents Joy 14CM15 continuous miner with a new scrubber inlet. The model was built based on CAD data provided by JoyGlobal. This is one of the most commonly used continuous miners in U.S. This model was developed in variants with left-hand side and right-hand side scrubber exhaust. The model was used in variety of CFD analysis of blowing and exhaust face ventilation system. And the seventh model represents Joy 12CM30 Miner Bolter. Examples with Joy 14CM15 and 12CM30 are given in Chapter 6.

Building CM models is a time consuming job. Attention should be paid to the level of details of the model during geometry cleaning procedure to optimize the CM model for CFD analysis. In addition, multiple surface and volume recognitions are needed. Every CM model will be used in different face ventilation arrangements defined by the user. This raises three important requirements:

1) Flexible mesh settings around the continuous miner, to ensure compatibility with the particular analysis conditions.

2) CM model with properly recognized regions with consistent names for further use in code development.

3) Reusability of the developed CM models

Following this requirements will give opportunity to develop user friendly procedure for rapid incorporating a CM model into a user defined face ventilation scenario. To meet these requirements, the CM models are provided encapsulated in a cuboids volume region, called box, with material properties of air.

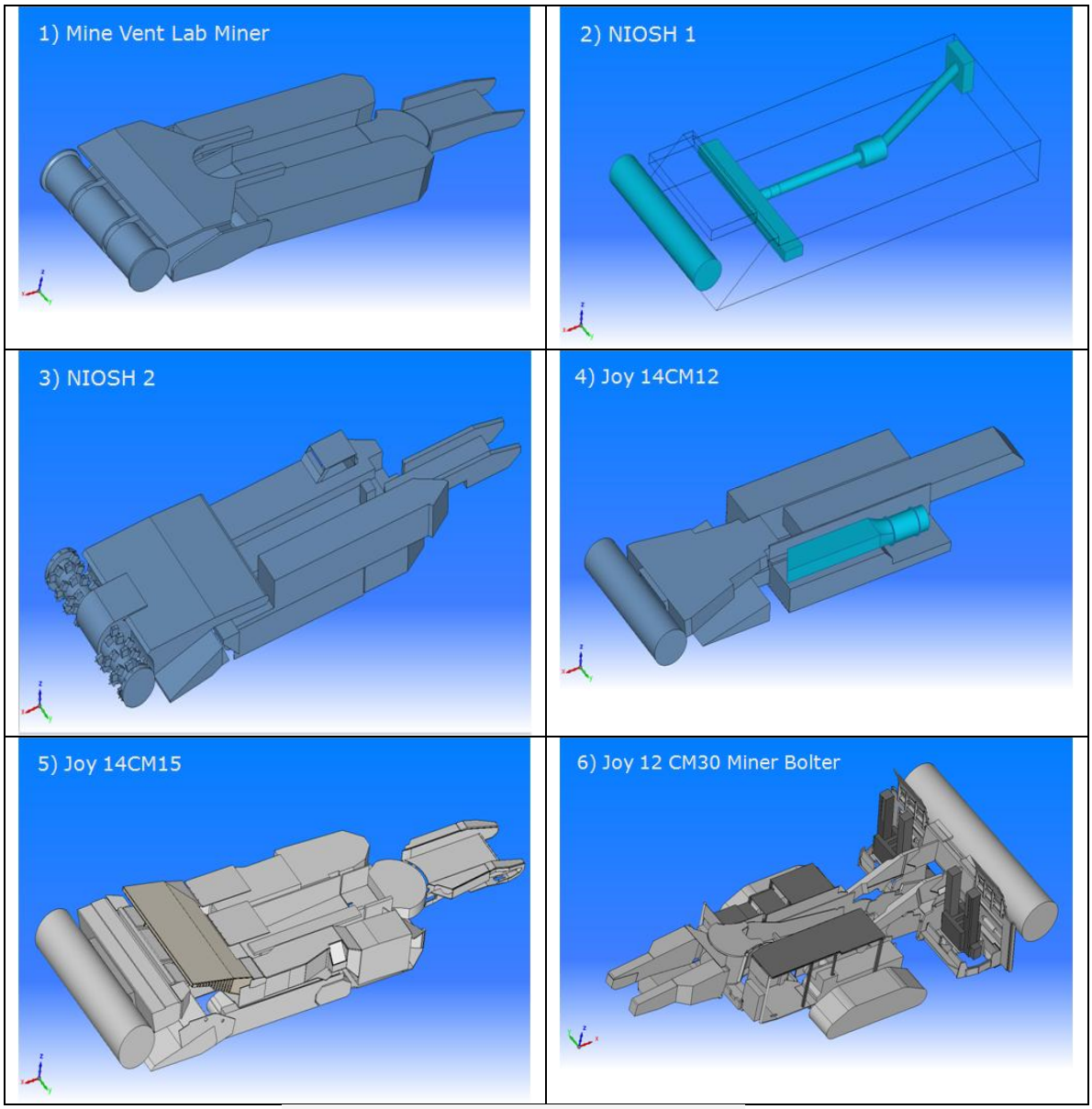

Figure 4.9. Geometry of Continuous Miner models

The CM model is provided with properly registered regions and generated octree, see Figures 4.11 and 4.12. The results are saved as Cradle .mdl and .oct files.

The ambient surface of the box volume, called envelope, is used as a interface region for embedding of the CM model into the equipment-free face ventilation system provided by the user. The bottom part of the envelope region is registered as a wall and after embedding automatically inherits the properties of the entry's walls. The embedding procedure is described in details in Chapter 5, 5.4. Rotating bits volume is used by the ALE method to simulate the effect of rotation of CM's cutting head. The drum surface rotates together with the rotating bits volume mesh. The roughness of the drum surface is

according the size of the cutting bits. This methods saves millions of mesh elements, consequently computational time, needed if geometry of the bits is included. The impact of cutting drum rotation onto the flow patterns is shown on Figure 4.13 and 4.14.

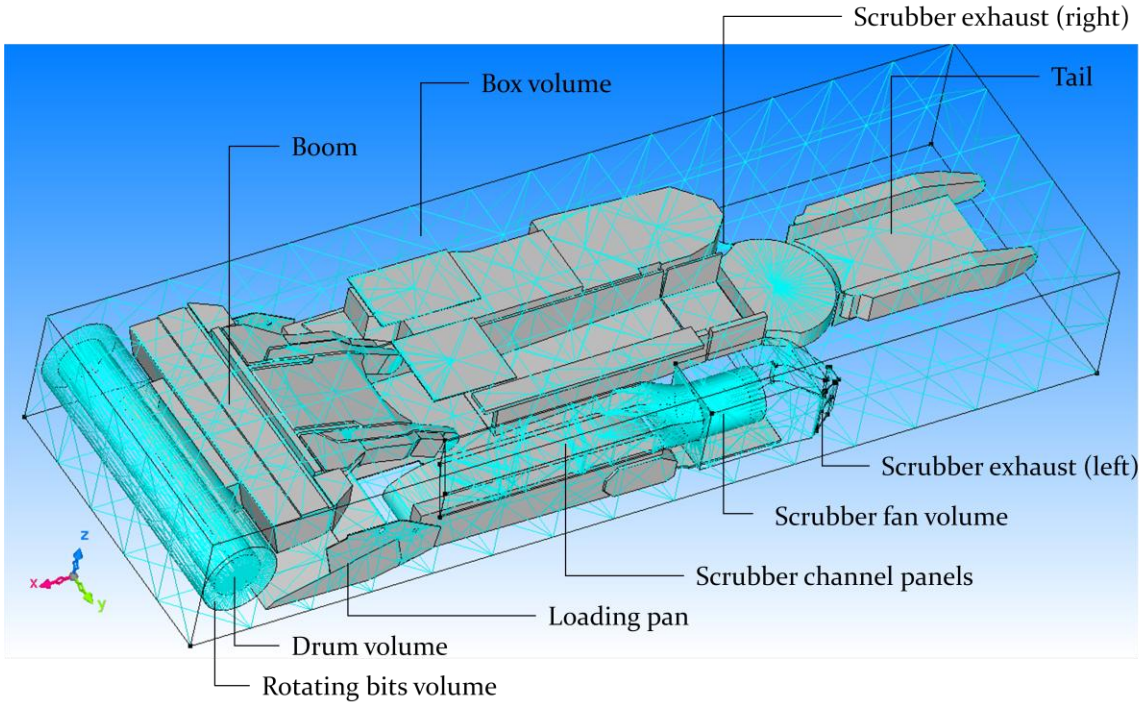

Figure 4.10. Encapsulated CM model

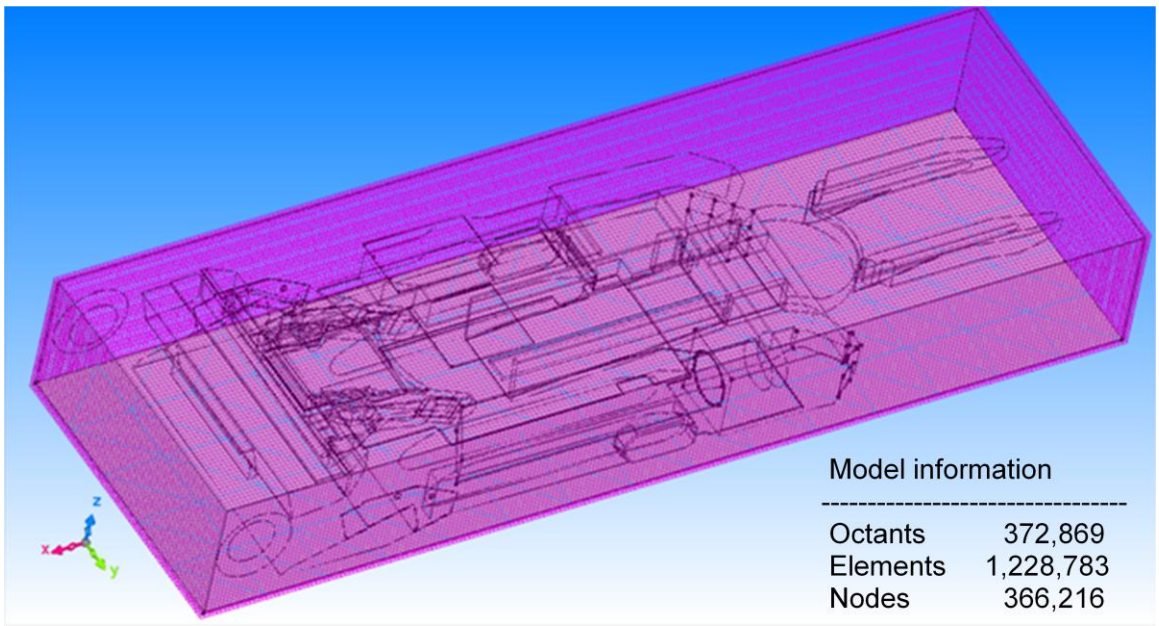

Figure 4.11. Octree of the CM model

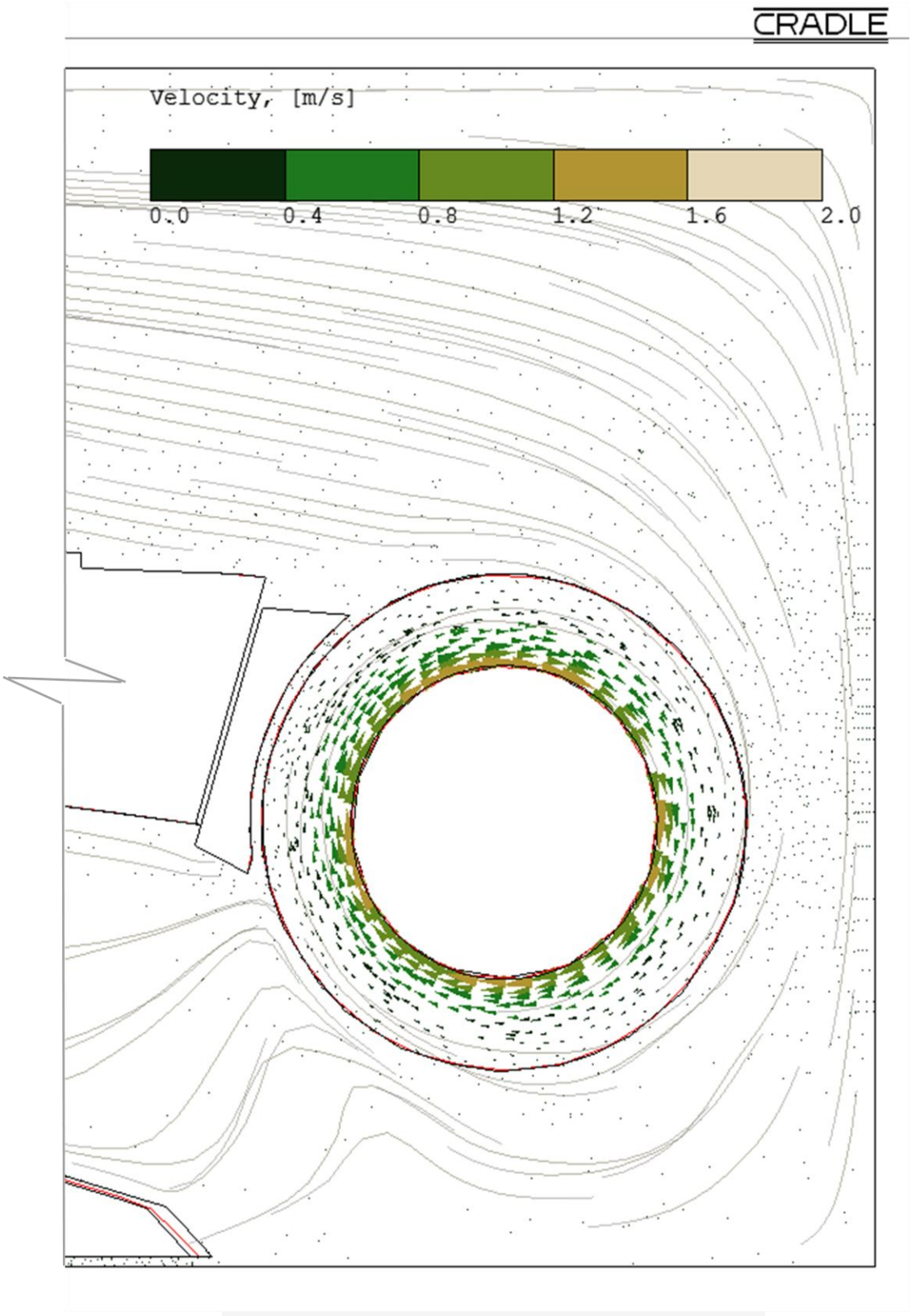

Figure 4.12. Vector field around cutting head. Simulation results.

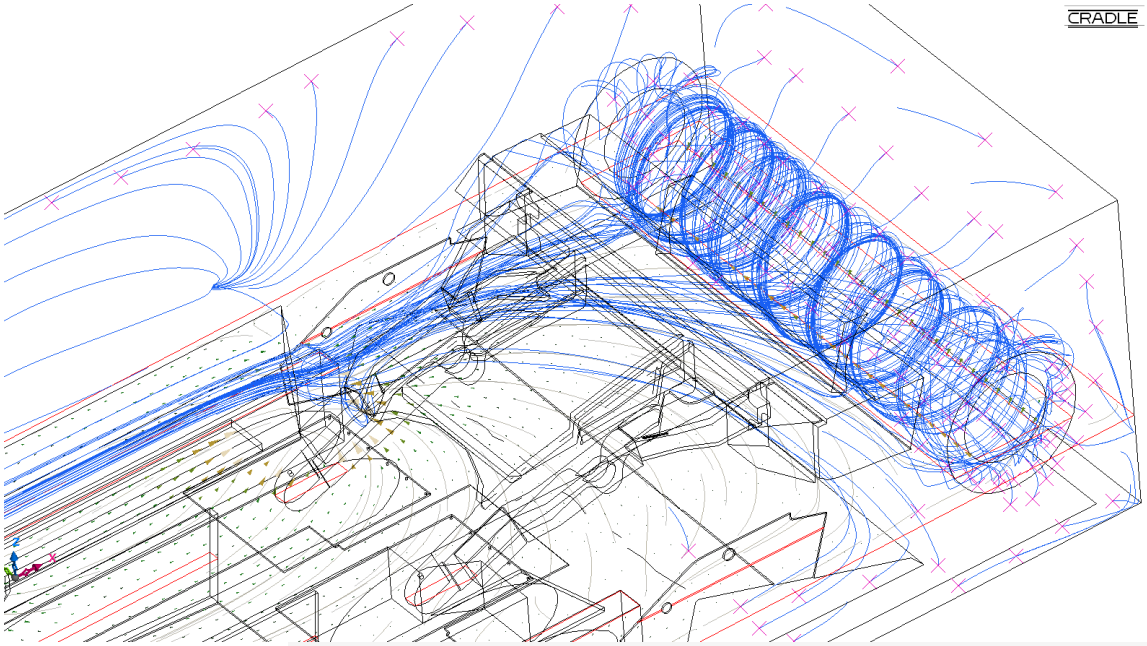

Figure 4.13. Streamlines around rotating cutting head and immediate face zone. Steady state simulation results, utilizing Joy 14CM15 model with scrubber.

4.4 Water Spray Model

Common water spray nozzle types used on a continuous miner machine are hollow cone nozzle and full cone. According information provided in mine ventilation plans, the number of nozzles used on a CM machine mounted spray system can vary from 35 to 60. The spray nozzles are groped in spray blocks of 3 to 5 nozzles in block. The blocks are mounted on various locations, such as: on top of the CM boom; under boom; at the left and right hand side of the cutting head, called end ring spray; behind the cutter motor on gathering head; throat spray; and left and right hand chassis spray. Schematic of an example CM's spray configuration is shown on Figure 4.15. Initially designed as a dust suppression system, CM's machine mounted sprays are used also as air moving devices or water fans for improvement of methane ventilation at the immediate face area. Therefore, the spray model must take into account both, the effect of spray onto the air flow patterns, respectively methane dilution, and interaction of spray droplets with dust particles. A brief discussion of methods for CFD simulation of sprays was done in Chapter 3. Particle tracking method was selected for simulation of sprays and dust particles. Cradle CFD provides a well developed sub model for particle tracking. One of the advances of particle tracking method is that the detailed modeling of the nozzle geometry, and dealing with two-phase (air-water) flow CFD simulations are not necessary. The resulting effect of a spray system is actually simulated, involving shape,

droplet size distribution, initial droplet velocities etc. In this sense, this is a "black box" kind of model. But, to build a successful model, a good understanding about the sprays' operational principles and the link between the technical data and the information required for numerical description is needed.

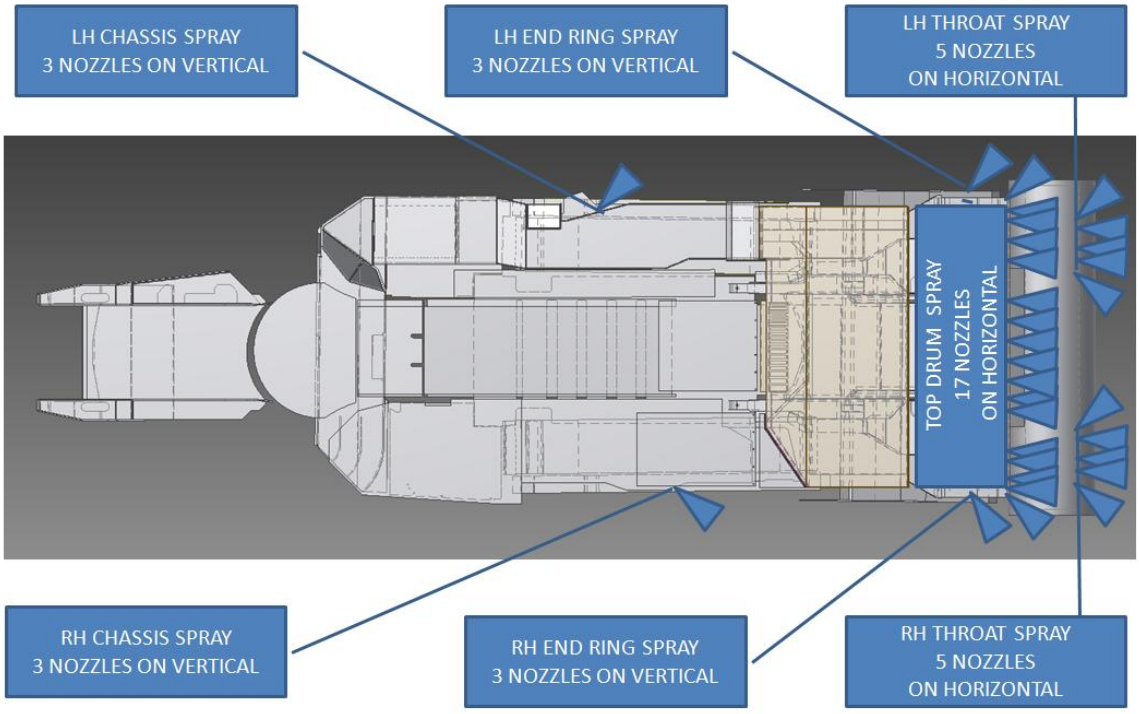

Figure 4.14. Example schematic of a CM's spray system configuration

4.5.1 *Technical characteristics of water spray nozzles*

Technical specification of a spray nozzle provided by a manufacturer usually contain information about:

- Nozzle type (shape of the spray patterns)
- Body/tip orifice size
- Rated capacity as a function of water pressure
- Spray angle as a function of water pressure

BD type in-line WhirlJet® wide angle spray nozzles of Spraying Systems Co and SH type spray nozzles by Wm Steinen Manufacturing Co, Hahn mining nozzle division are generally used in mining for dust suppression. These type of nozzles produce uniform hollow cone spray patterns with a ring shaped impact area. For example one of the commonly used type of nozzles for mining applications is BD-2. BD-2 has orifice size of 0.078 in, rated capacity 0.31 to 0.62 gallons per minutes, and spray angle 109^{o} to 90^{o} for working pressure range 20 to 80 psi respectively. SH 2 spray nozzles are direct

replacement for equivalent spraying system type BD-2 nozzles. SH 2 has orifice size of 0.078 in, rated capacity 0.28 to 0.63 gallons per minutes, and spray angle 60^o to 70^o at working pressure in range of 20 to 80 psi respectively.

Detailed information about the drops size distribution and drop velocity usually is not included into the datasheets. This information is very important input for proper modeling of a spray using particle tracking method. Research (Gemci et al., 2003; Pollock and Organiscak, 2007) showed that these two spray characteristics and the spray angle determined the spray interaction with the ambient air flow and dust collection. Using Phase Doppler Particle Analyzer for different type of spray nozzles, Pollock and Organiscak (2007) found that higher spray nozzle working pressure reduced water droplet sizes and lead to increase in droplet velocity, airflow inducement, and airborne dust capture. Spray nozzles with wider discharge angle were observed to induce more airflow, but reducing dust capture efficiency. Important conclusion of this study is that the sprays with the air moving capability showed poor dust capture efficiency, and those with poor airflow inducement demonstrated high dust capture efficiency (Pollock and Organiscak, 2007). Using the results of their study, Pollock and Organiscak (2007) developed graphical representation of the following characteristics:

- Sauter Mean Diameter (SMD) and mean droplet velocity measured around the spray centerline parallel to the nozzle axis at two different water pressures (Lower test pressure P1 = 552 kPa, and higher test pressure P2 = 172 kPa) .
- Range of water droplet SMDs for various nozzle types across the spray patterns at both P1 and P2.
- Range of mean droplet velocities for various nozzle types across the spray patterns at both P1 and P2.

Souter Mean Diameter (SMD), also denoted in literature as D_{32} is one of the mean diameters used to characterize sprays. SMD found application in research of mass transfer reactions and represents the mean diameter ratio of total droplet volume to total droplet surface area of a spray sampled, see Equation 4.1.

$$SMD = \frac{\sum N_i D_i^3}{\sum N_i D_i^2} \qquad [4.1]$$

where:

Ni is the number of drops with i^{th} size class

Di is the corresponding drops diameter

The data for the researched hollow cone nozzle showed that near the center of the generated spray patterns smaller water droplets were generated with the highest mean droplet velocities. In contrast, lower droplet velocities were measured away from nozzle centerline. Generally the research showed that there are different droplet characteristics

with regard to nozzle type. The wider angle hollow cone nozzles tend to generate smaller and slower water droplets.

The simplest approach to define a representative droplet size is the commonly used Sauter Mean Diameter (SMD. SMD measured within various spray patterns range between 50μm and 300μm and depends on the water pressure, spray nozzle, and method used to create droplets (Pollock and Organiscak, 2004). Studies of spray droplets shape (Husted, 2007) using Dantec Classic Phase Doppler Analyzer has shown that spray droplets could be treated as reasonably spherical.

4.5.2 *Numerical description of water spray systems*

The information needed to describe a spray system conditions utilizing the provided by Cradle CFD particle tracking method and spray sub model is given in Table 4-5.

Table 4-4. Data needed to describe a spray system conditions using Cradle CFD particle tracking method

<u>General data needed for the spray block.</u>
Material properties of the spray fluid: water
Spray droplet diameter
Initial axial spray droplet velocity
Mass flow rate per nozzle
Number of droplets generated per unit time per spray block
Internal angle of the spray cone
External angle of the spray cone
Orifice size
<u>Data needed for every single nozzle</u>
3D coordinates of the spray nozzle
Spray direction vector
Start time of droplets generation
End time of droplets generation

The required data can be specified combining three sources of information:

1) Information provided by the designed or approved mine face ventilation plan.
2) Spray manufacturer data sheets.
3) Research results available for the particular spray nozzles.

An example part of a condition S-file with numerical description of a spray block with 5 nozzles is shown in Table 4-6. In this example the nozzle type for all five water sprays is a hollow cone nozzle with orifice size 1.98 mm, 68^o spray angle, ring shaped impact area with 1^o offset (67^o internal cone), 15 m/s initial droplet velocity, 75 microns spray droplet diameter, 2.1 liters/min water flow rate (per nozzle), 5,000 water droplets are to be generated every second. The first nozzle of the block is rotated on 45^o right hand

side. The others are pointed straight parallel to X direction, or toward the face. The spray will start generate droplets at time 0 (at the beginning of simulation) and will end after 60 seconds simulation time. This way allowed to keep the model simple and clear, but it has an important disadvantage.

Table 4-5. Example part of condition S-file with coded spray data

```
SPRY
  1
              67              68          0.00198
              15           -0.26   -5000
             998           75e-006               0
    0     1     1
            4180              20
         0.00015           0.001          0.0728
          14.227           0.387           1.182
               1               1               0
               0               0               0
               0              60               0
          14.227            0.45           1.182
               1               0               0
               0               0               0
               0              60               0
          14.227           0.583           1.182
               1               0               0
               0               0               0
               0              60               0
          14.227           0.716           1.182
               1               0               0
               0               0               0
               0              60               0
          14.227           0.849           1.182
               1               0               0
               0               0               0
               0              60               0
/
```

A full description of a spray system with 60 spray nozzles in a condition S file is given in the Appendix.

The droplet size is fixed to a constant diameter. The real spray consist of drops with various size distribution. For example, an 81^{o} hollow cone nozzle at 172 kPa water pressure generates droplets with SMD size distribution ranged from 40 to 90 microns with average centerline SMD about 60 microns (Pollock and Organiscak, 2007). Study showed, that the airflow developed around large water droplet prevents coal dust particles from contacting the droplet but the dust particles, however, easily impact a smaller droplet (Schowengerdt and Brown, 1976). The optimum water droplet size (Cheng, 1973)

was estimated on 150μm for 1μm particle size irrespective of droplet velocity. Due to the importance of droplets size for the spray interaction with the ambient airflow and dust collection, this model needs further improvement. One way to make the model more realistic is to simulate break-up and coalescence effect in droplet interaction with the ambient airflow and with each other. This will produce variety of droplet sizes into the spray flow according the simulated conditions. Such a sub model is supported by Cradle CFD but requires solving of an additional temperature equation and needs input data about surface tension coefficient and viscosity of the spray fluid (water in our case).

Other way to simulate droplet size distribution is to develop a C++ user function that controls in run time the spray droplet generation according to a given statistical distribution, representative for the simulated spray system. This way gives opportunity for more complicated simulations, including moving sprays.

When using the particle tracking method, a representative number of particles representing droplets should be generated in order to always have a particle present in an inlet cell of the mesh.

For steady state simulations and time dependent simulations in which the CM is given in fixed position, the first described model extended with brake-up model was preferred.

4.5.3 *CFD code validation of the spray model for flow and methane distribution.*

To validate the spray model ability to predict the effect of a machine-mounted spray system on methane dilution at the face area data from a full scale research conducted by NIOSH (Chilton et al., 2006) were used. The experiment simulates mining entry that is 16.5ft wide by 7ft high with a blowing line brattice constructed 2ft from the left rib. with 35ft setback and a continuous miner located at the center of the 13ft wide box-cut. Methane concentrations were measured at 15 locations positioned 17in from the roof, see Figure 4.16. A scenario with 2.8 m^3/s (6,000 cfm) intake air, a methane flow rate of 0.015 m^3/s (32 cfm), and four straight low pressure sprays was chosen for this validation study (Fig. 4.17). The spray nozzles, model 3/8-BD-3 hollow cone, were positioned on the boom approximately 41in back from the face. The given average water flow rate for a spray nozzle is 0.7gal/min at water pressure 70psig (low-pressure). Detached Eddy Simulation (DES) turbulence model was applied in this simulation.

A comparison between the experimental data and the simulation result for methane concentration are shown on Figure 4.18 and Figure 4.19. The simulation results were in agreement with the experimental data. The validation study showed that the developed spray model could be successfully used in CFD simulations of face ventilation scenarios.

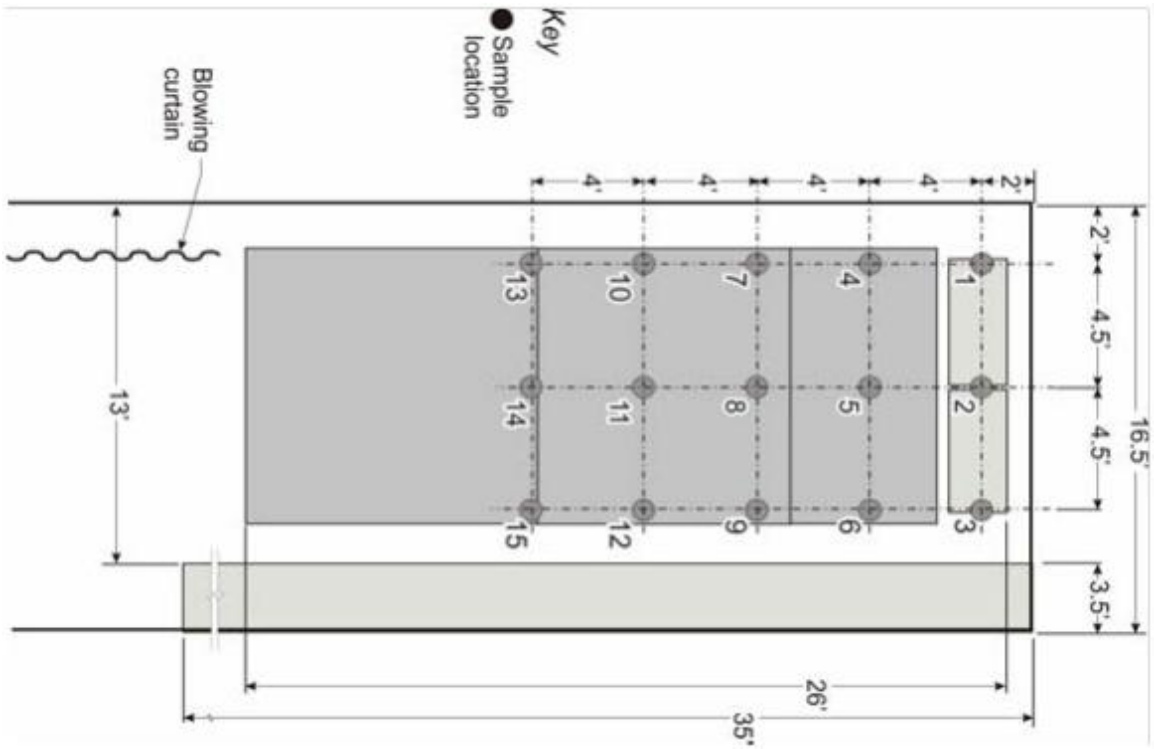

Figure 4.15. Methane sampling location above model mining machine, as published by Chilton et. al., (2006)

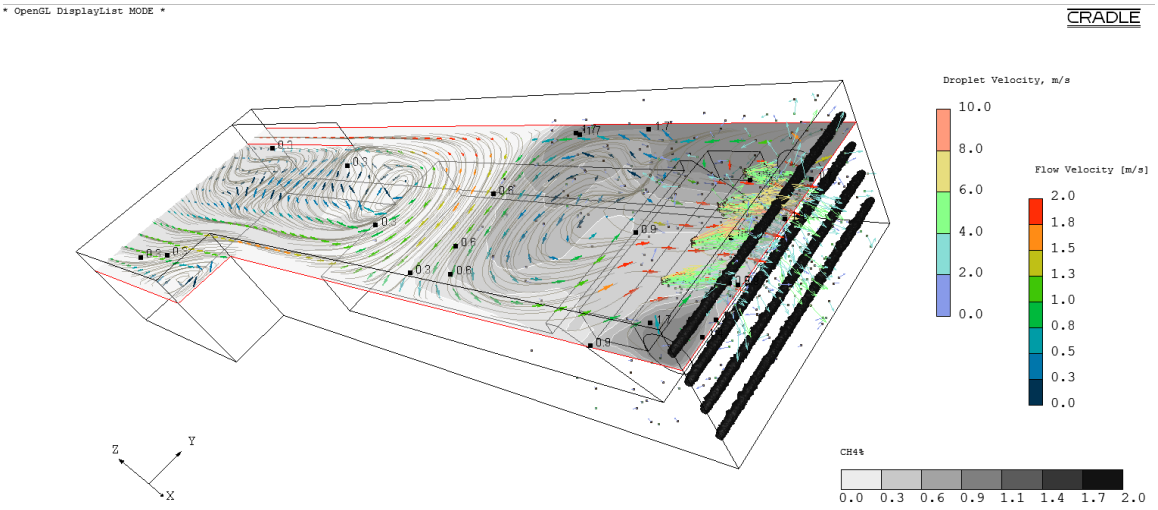

Figure 4.16. CFD simulation results for 6,000 cfm intake air, 32 cfm methane inflow and four straight low (70 psig) pressure sprays

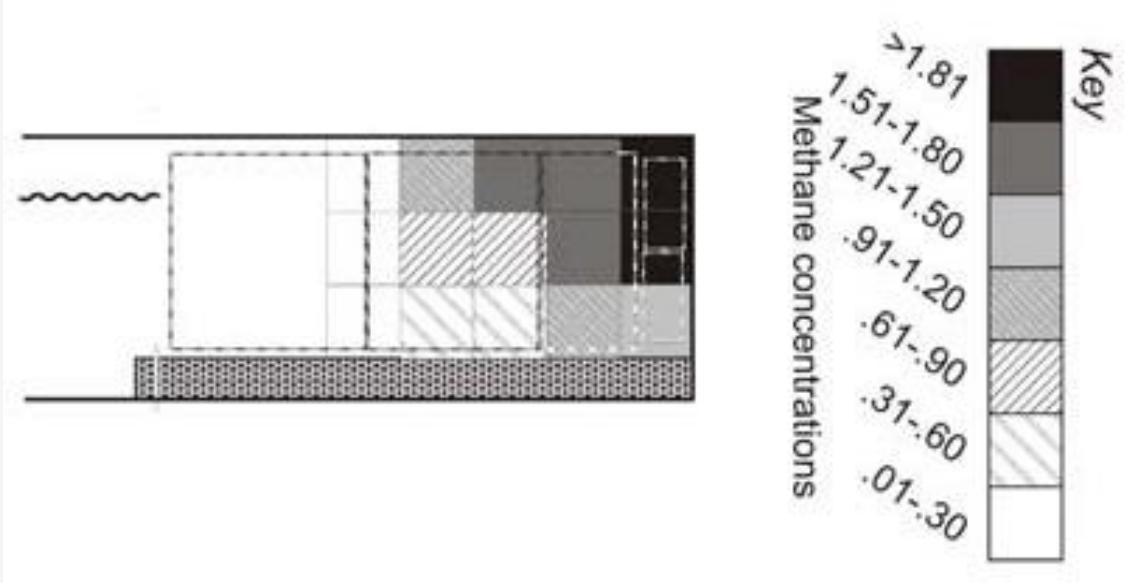

a) NIOSH experimental data, after Chilton et. al. 2006

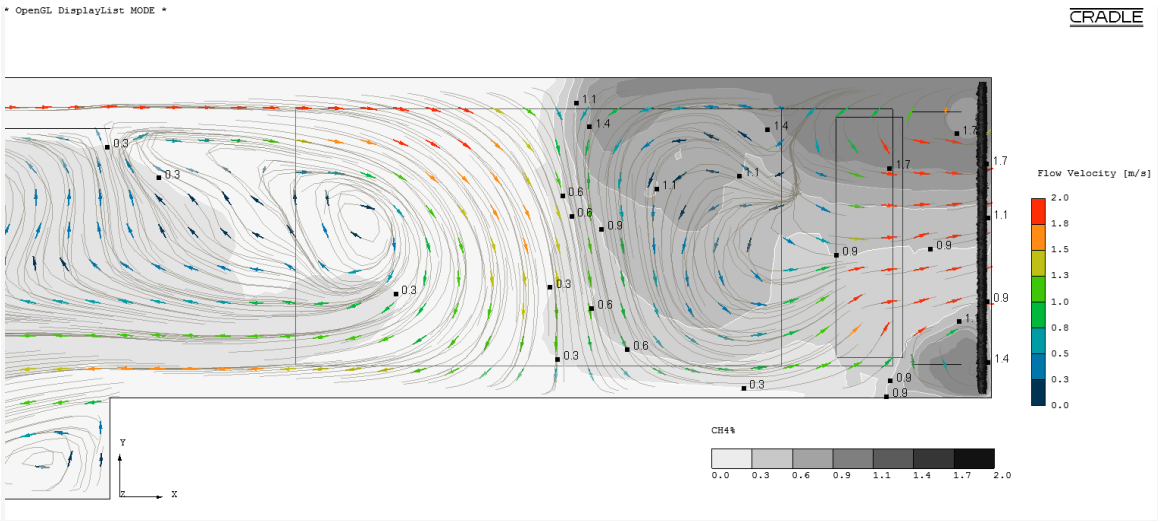

b) CFD simulation results

Figure 4.17. Comparison between (a) experimental data and (b) the CFD simulation results

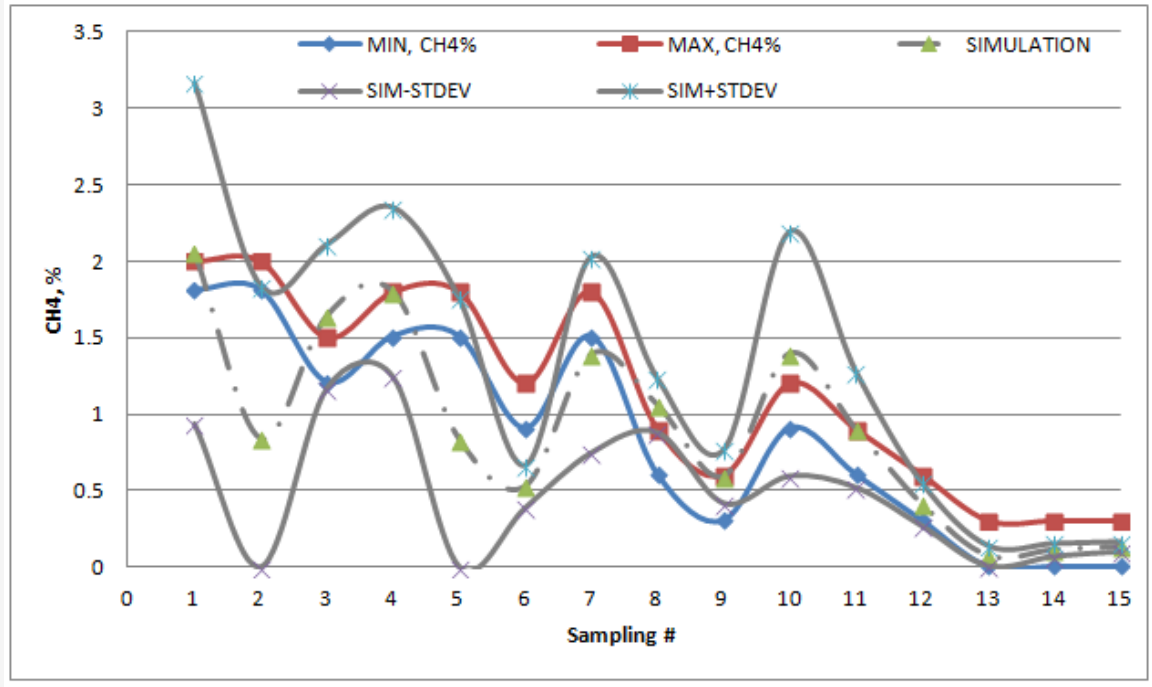

Figure 4.18. Comparison of the CFD simulation results for methane concentration at the sampling locations with the experimental data

4.5 Dust Generation Model and Particle Tracking

Simulation of the dust distribution uses built-in Cradle CFD particle tracking method. The dust generation model was built in following assumptions:

- The dust generation during mining operation, utilizing CM machine, takes place mostly at the at the working face.
- Loading and unloading operations at the CM's loading pan, and from the CM's conveyor to the shuttle car are secondary sources of dust, but the coals at those places are already wet due to the water sprays and produced significantly less dust compared to the cutting operation.
- Dust particles are generated at the ambient surface of the cutting head. This is a cylindrical surface with radius measured from the center of the CM's cutting head to the top of the cutting bits.
- The dust coming with the intake air, from mine sections outside of the computational domain, can be simulated at the inlet region of the domain as an additional boundary condition.

Particle tracking approach for dust simulation requires time dependent analysis conditions. The following information is needed to set up the boundary conditions for simulations involving dust particle tracking:

- Dust generation surface region or an array with 3D coordinates of dust generation points
- Dust mass inflow rate
- Initial particle velocities
- Number of particles to be generated
- Effective number of particles
- Density of the simulated dust particles
- Equation for calculation the drag coefficient of the particles
- Repulsion coefficient assigned to the boundary wall surfaces
- Dust particle size distribution

The dust generation surface region was assumed to be the outer ambient surface of the cutting head. Assigning this surface region as a dust generation region is the most direct way to setup this boundary condition. More advanced approach is to develop a C++ user function that uses Monte Carlo algorithm to generate 3D coordinates of dust generation points. In general case, the coordinates of the dust generation points can follow a surface in vicinity of the face region or a cylindrical segment representing a contact volume of the cutting bits with the coal seam. Trial simulations were performed to explore both ways. Results of the trial simulations are shown in Chapter 6.

Dust mass inflow rate, is required input for dust generation model. Example for an indicative value could be found in a full scale test study performed by Organiscak and Beck (2010) at the NIOSH PRL. In this study coal dust with mass flow rate of 25 g/min (0.9 oz/min) was introduced at the face in front of the CM's drum to simulate dust generation during coal cutting.

Initial particle velocities could be determined following the assumption that the dust particles are generated at the ambient surface of the cutting drum and their initial velocities matched the rotation speed of the drum. For instance if we assume that the dust will be generated around a cutting drum with diameter of 1.11 m (44 in) rotating with 50 rpm (0.83 revolution per second), the calculated initial particle velocity will be 2.9 m/s directed tangentially. In the next computational cycles the generated particle will interact with the flow and other particles changing its velocity and trajectory according to the particle tracking method coupled with the implemented turbulence model.

Number of dust particles to be generated could be determined using an estimation of representative number of particles to ensure a particle present in an inlet cell of the computational mesh. For instance if the base octant size of the computational mesh is 0.05 m and the initial velocity of the particles is 2.9 m/s, the estimated generation frequency will be 58 s^{-1}. This is counted for a representative number of particles that needs to be created in a particular dust generation point per unit time. Usually, a set of generation points are created every calculation cycle to simulate dust generation.

Effective number represents the number of particles effectively simulated by one particle. Simulation of as many particles as in the real dust generation process may be not

feasible or computationally costly. Using this number a cluster or flock of particles can be represent by one particle. By default, the effective number is set to 1.

Particle's density is the density of the material from which the particle is composed. If focus on respirable dust particles, a solid spherical shape composed of homogeneous material can be assumed. Therefore, the data about the bulk density, typical for the coal being mined, could be used for particle density. In case of spherical particles, the drag coefficient between particles and the air is modeled as a function of particle Reynolds number as given in Equation 3.12. For simulation of dust particles with more complicated shape different approach is required, including corrections in the equations for calculation of particle drag coefficient.

Repulsion coefficient is an attribute of the wall regions that controls the behavior of the particles that collide with the region's surface. As briefly discussed in Chapter 3 the repulsion coefficient accepts values in range from 0 to 1. Assuming that entries' wall surfaces are wet, the dust particles touching a wall could be treated as adhering to its surface and will be removed from the system. In this case the repulsion coefficient will be set to zero. In real mining condition, the particle repulsion may vary at the face, ribs, roof, and floor. Including, having different values within the zones that belongs to the same region. Additional research is needed in this direction to properly calibrate this attribute for the different wall regions.

Dust particle size distribution is a very important input for the model. The representative size distribution of the respirable bituminous coal dust (Dick et.al., 1996) shows a bimodal distribution (0.6-1.2 μm) with a significant fraction below 1 μm, see Figure 4.20. The study was dedicated to distinction of coal dust particles from liquid droplets. The authors found, that the second mode of the distribution (at 1.2 μm) is due to liquid droplets recognized by the equipment as dust particles. (Dick et.al., 1996) also measured high sphericity index (greater than 93%) of the low coal fraction using optical detector DAWN-A. Therefore it was considered to treat the respirable dust particles in the model as spherical particles with a unimodal size distribution. To simulate the size distribution of respirable coal dust a theoretical lognormal statistical distribution was used. This distribution is widely applied in the description of natural phenomena including particle size distribution of aerosols (Cooper 1982, Raabe 1971). The lognormal distribution is a continuous probability distribution of a random variable whose logarithm is normally distributed. A random variable which is log-normally distributed takes only positive real values. Given a random variable Z drawn from the normal distribution with 0 mean and 1 standard deviation, then the variable X has a lognormal distribution with parameters μ and σ, see Equation 4.2. A lognormal distribution with mean *m* and variance *v* has parameters μ and σ, see Equation 4.3 and 4.4. An example histogram of a generated lognormal distribution for particle size in range of 0.1 to 5 microns , mean size m = 0.68 microns, and variance v = 0.14 is depicted on Figure 4.21.

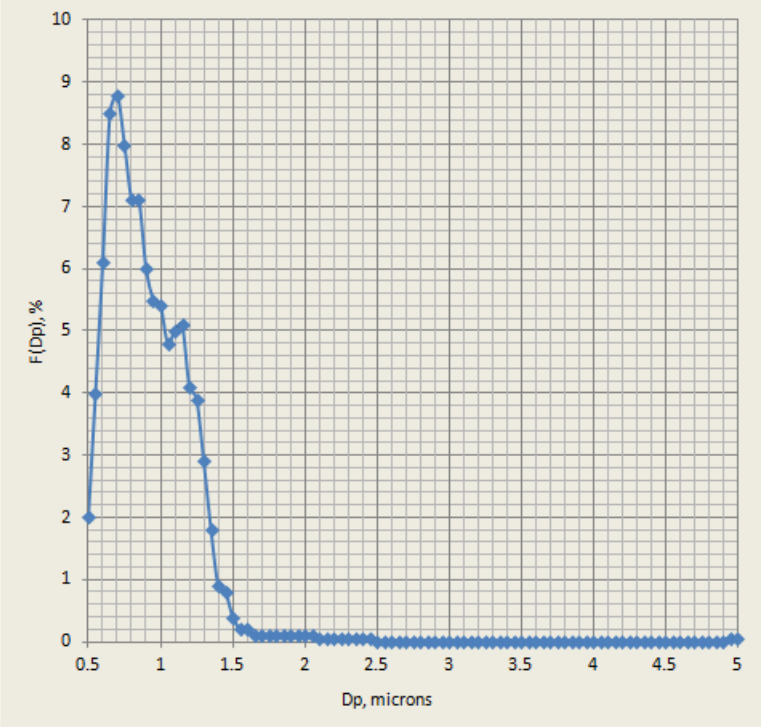

Figure 4.19. Size distribution of bituminous coal dust, after Dick et al. (2011)

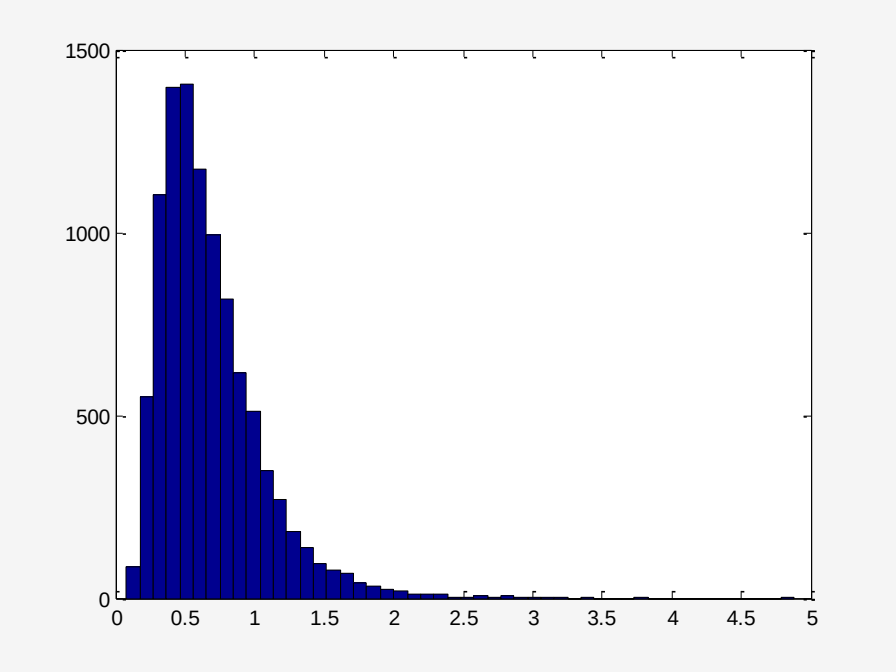

Figure 4.20. Generated lognormal particle size distribution histogram using Matlab

$$X = \exp(\mu + \sigma Z) \quad [4.2]$$

$$\mu = \log\left(\frac{m^2}{\sqrt{v + m^2}}\right) \quad [4.3]$$

$$\sigma = \sqrt{log\left(1 + \frac{v}{m^2}\right)} \quad [4.4]$$

The Matlab code for generation of this histogram is listed in the Appendix.

Example input data needed for simulation of coal dust particles are summarized in Table 4-7

Table 4-6. Example input data for simulation coal dust particles

Property	**Value**
Particle material	Coal
Shape	Spherical
Bulk density	800 kg/m^3
Mean particle size (m)	0.6 μm
Particle size range	0 - 5 μm
Variance (v)	0.14 μm
Specific heat	0.00138 J/kg.K
Initial temperature	20 ^{o}C
Viscosity	0.0005 Pa.s
Surface tension coefficient	0.02 N/m

The described information is coded to the Attribution of Particles C function. The function reads the required input data from a predefined condition file (S-file). The user can change the data about the density, the distribution parameters, and the initial temperature. The dust is generated around the cutting head of the continuous miner using Particle Start Points C function. The function generates random coordinates of release point belonging to the release surface and returns number of start points, i.e. particles with the described attributes.

In order to simulate dust monitoring stations, a set of control surfaces are needed. First, control surfaces for airflow rate; and second, control surfaces for particle count. Cylindrical surfaces with height and diameter of 0.31 m (12 inches) established at the location of the operator and other areas of interest serves as dust monitoring stations. The operator station is usually located at the expected position of the operators head. The first role of the control surfaces is to count the number of particles passing through it. Then, because the particles with different mass and size are involved in the simulation, additional two counters were defined using the same surfaces to record the mass of the particles and classify their size. The application of this model was presented in 2012

SME Annual Meeting, Seattle, WA and during the 2014 NIOSH Ventilation Capacity Building BAA Meeting, Salt Lake City, Utah.

4.6 Scrubber Model

Scrubber model developed for flow and gas distribution simulations and the enhancement of the model for dust control analysis will be discussed. The model was developed to simulate CM's machine mounted scrubbers, but could also be applied for simulation the effect of stand-alone scrubber units on the flow, methane dilution or dust control analysis.

4.7.1 *Scrubber model for flow and gas distribution simulations*

Generally the scrubber model consists of five elements: Scrubber fan; filter element; scrubber channels; scrubber inlet; and scrubber outlet. Geometry of the scrubber fan, channels, inlet and outlet configuration follow the specifications provided by the manufacturer. The filter element is treated as a "black box". The machine mounted scrubbers used on CMs affects the flow and dust distribution, but the methane passes freely through it. The scrubber model implemented for the needs of gas distribution analysis does not include a filter element and its resistance is therefore not simulated. For Steady State Analysis, the scrubber fan flow rate can be given by a constant flow implementing the available in Cradle CFD fan-source model. For Time Dependent Analysis a function of scrubber flow rate v/s time could be applied. This flow rate time function can simulate the decrease in scrubber performance due to the filter clogging. Due to the assumed simplifications, the only input data needed for this model is the scrubber flow rate (Q_S). Model geometry of two different machine mounted scrubber systems are shown on Figure 4.22.

4.7.2 *Enhancement of the scrubber model for dust control simulations*

Run time control of the scrubber dust removal efficiency is performed by C++ user function. The list of an example function is given in Appendix. This function counts the particles passed through the simulated scrubbing filter region, reads its attributes, and passes only percentage of them, corresponding to the specified scrubber efficiency. This is done by monitoring the particle passed through a control region established at the inlet of the filter volume. The filter volume is a special region with no mesh, zero region. The particles passed through it being automatically removed from the domain. The code reads the number of particles passed through the filter inlet before their removal. The filter outlet region regenerates the flow rate as specified for the scrubber fan, and creates filtered set of particles with number equal to the specified percentage corresponding to the scrubber dust removal efficiency. The "passed through" particle size distribution is controlled by the code. It could be assumed the same as the initial dust particle

distribution, or according the characteristics of the equipment given by the manufacturer, or by test data.

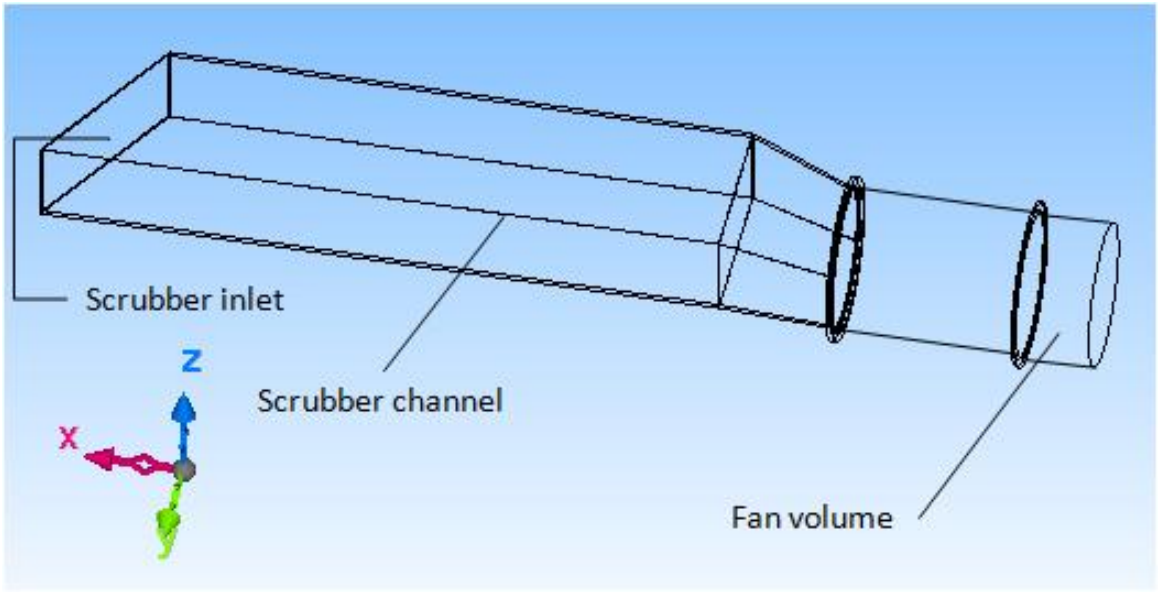

(a)

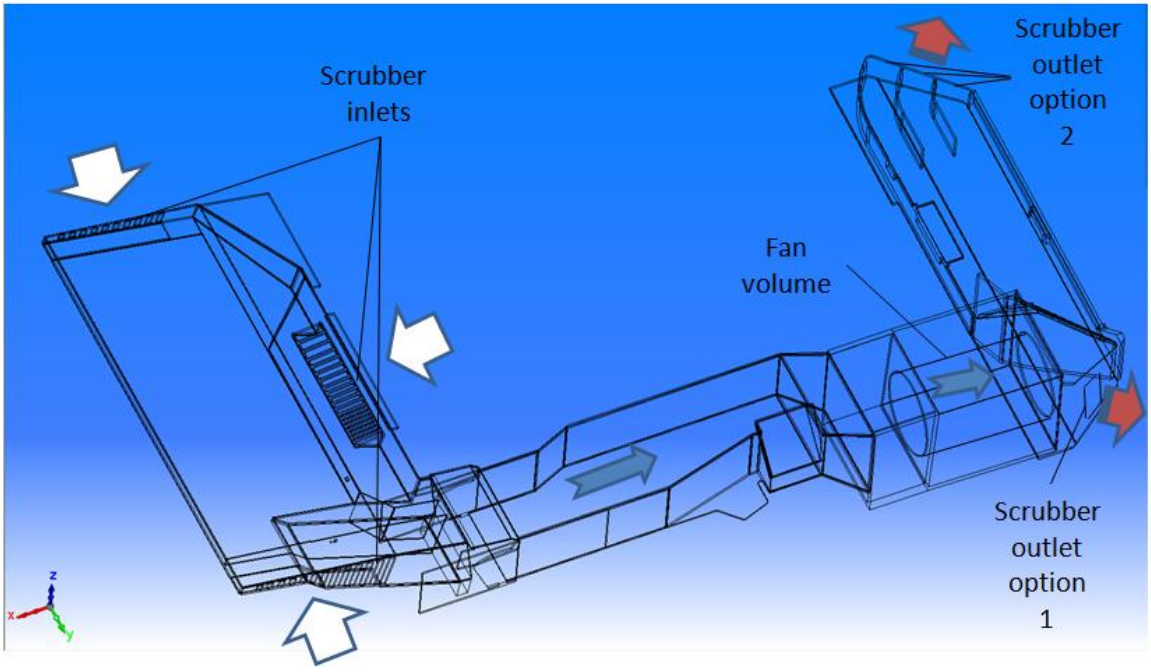

(b)

Figure 4.21. Schematics of scrubber models geometry, (a) Scrubber model for left hand side machine mounted application, (b) Scrubber model with three inlets, and two optional outlets

To illustrate the performance of the developed C++ code, a trial simulation results of scrubber with specified dust removal efficiency of 85% is depicted on Figure 4.23. The data used for this simulation are shown in Table 4-8.

Table 4-7. Particle data input for the performed trial simulation of scrubber performance for dust control analysis

Property	Value
Particle material	Coal
Shape factor	1 (spherical)
Bulk density	833 kg/m^3
Particle size range	0 - 5 μm

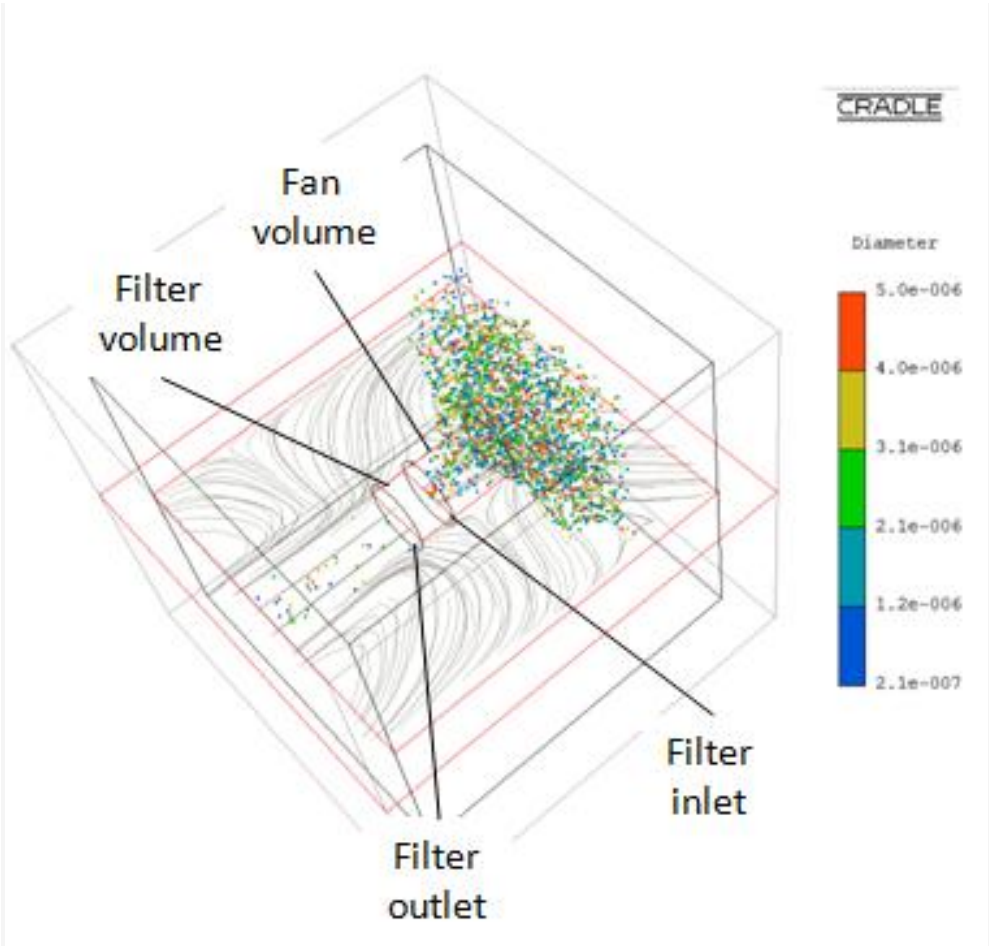

Figure 4.22. Trial simulation results of scrubber with 85% dust removal efficiency

The dust control analysis uses particle tracking method and therefore requires time dependent analysis. Details about the performed analysis are given in Table 4-9.

Table 4-8. Description of a dust control analysis using Scrubber model	
Analysis Types	
Flow (turbulent flow)	
Particle tracking	
Material Properties	
Air incompressible (standard conditions at 20 ^{o}C)	
Coal dust	
Boundary Conditions	
inlet:	Fixed flow rate
outlet:	Fixed static pressure (0.0 Pa)
fan (scrubber):	Source conditions, fan model, fixed flow rate
scrub_in (filter inlet):	-
scrub_out (filter outlet):	-
walls:	Stationary wall (log-law)
walls_scrubber:	Stationary wall (log-law)
Analysis Conditions	
Type of flow:	3-dimensional incompressible turbulent flow
Time dependency of simulation:	Time Dependent Analysis (TDA)
Turbulence model:	Detached Eddy Simulation (DES) w/ RNG k-EPS
Convergence threshold:	Default
Equation to be Solved	
Momentum equation	
Mass conservation equation	
k-EPS equations	
Particle tracking equations	
Spatial Directions	
Developed user functions:	
C++ user functions dynamic link library:	sctusr_Dx64.dll
- Attribution of particles:	usr_pcle1; use_pcle1
- Particle start points:	usr_pcl_typ11
- Information of particle pass:	usr_pclget10; use_pclget10;

4.7.3 *CFD code validation of the scrubber model for flow and methane distribution*

Validation study of the developed scrubber model and the Cradle CFD code was performed using airflow and methane measurements collected during benchmark experiments conducted at the NIOSH-PRL Research Gallery with a continuous miner and

machine mounted scrubber in place (Wala et al., 2008). Four scenarios were validated as follows:

Scenario 1) Scrubber off, intake flow Q_{in} = 4,000 cfm

Scenario 2) Scrubber flow Q_s = 4,000 cfm, intake flow Q_{in} = 4,000 cfm,

Scenario 3) Scrubber off, intake flow Q_{in} = 6,000 cfm

Scenario 4) Scrubber flow Q_s = 4,000 cfm, intake flow Q_{in} = 6,000 cfm, Q_s/Q_{in} = 0.66

Table 4-9. Description of a Gas Control Analysis using manifold tubes methane release model, NIOSH 1 CM model w/ scrubber

Analysis Types	
Flow (turbulent flow)	
Diffusive species (methane diffusion)	
Material Properties	
Air incompressible (standard conditions at 20 ^{o}C)	
Methane gas (at 20 ^{o}C)	
Boundary Conditions	
inlet:	Fixed flow rate
outlet:	Fixed static pressure (0.0 Pa)
CH4_inlet	Fixed flow rate
walls:	Stationary wall (log-law)
face:	Stationary wall (log-law)
miner_walls:	Stationary wall (log-law)
scrubber_walls:	Stationary wall (log-law)
curtain:	Panel, stationary wall (log-law)
fan (scrubber)	Source conditions, fan model, fixed flow rate
Analysis Conditions	
Type of flow:	3-dimensional incompressible turbulent flow
Time dependency of simulation:	Steady State Analysis (SSA)
Turbulence model:	RNG k-EPS model
Convergence threshold:	Default
Equation to be Solved	
Momentum equation	
Mass conservation equation	
k-EPS equations	
Equation for conservation of diffusive species (simple diffusion)	

Simulation results for Scenario 2 are shown on Figure 4.24. The figure shows methane concentration at three horizontal levels - above the continuous miner, in the middle plane of the face area, and below the miner As it can be seen on the figure, the methane gas concentration patterns differ significantly at the different horizontal levels

around the CM. The red color code represents methane gas concentration of 0.5%. This is the maximum gas concentration measured during the experimental study. In this scenario the curtain side of the immediate face area showed lowest gas concentrations, while the highest methane concentrations were observed at the off-curtain side of the face area.

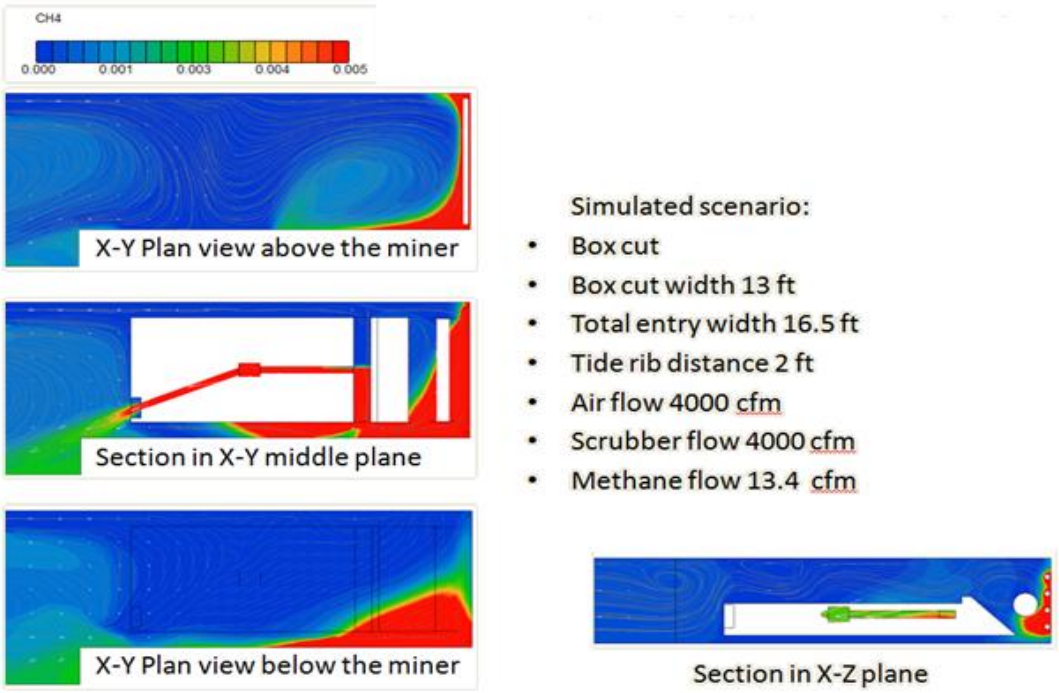

Figure 4.23. Simulated methane concentration at different plan levels for Scenario 2.

Comparison between the measured methane concentration and the simulation data for scenario 2 are shown on Figure 2.25. There are some discrepancies between the simulation esults and the experimental data in the zone of measurement points 17 to 30. The analysis of the data indicates that the measurements in these locations should be considered compromised. It was assumed that, due to the airflow separation took place exactly in this zone, very low methane concentrations are expected, although, additional tests are recommended to prove this assumption. The other possible reason for the observed discrepancy is that the position of the CM miner in the model does not match the position of the CM during the experiment. To show the role of the continuous miner position in this scenario, three additional CFD analysis were performed using the validated code, see Figure 4.26. Three dimensional isosurface of methane concentration equal to 1% combined with contour plot of the methane concentration at the middle plan of the computational domain, were used to visualize the methane distribution. The

performed analysis showed that an angle of rotation of the CM equal to 1.5 deg, while all the other analysis conditions were retained, affects significantly the methane distribution.

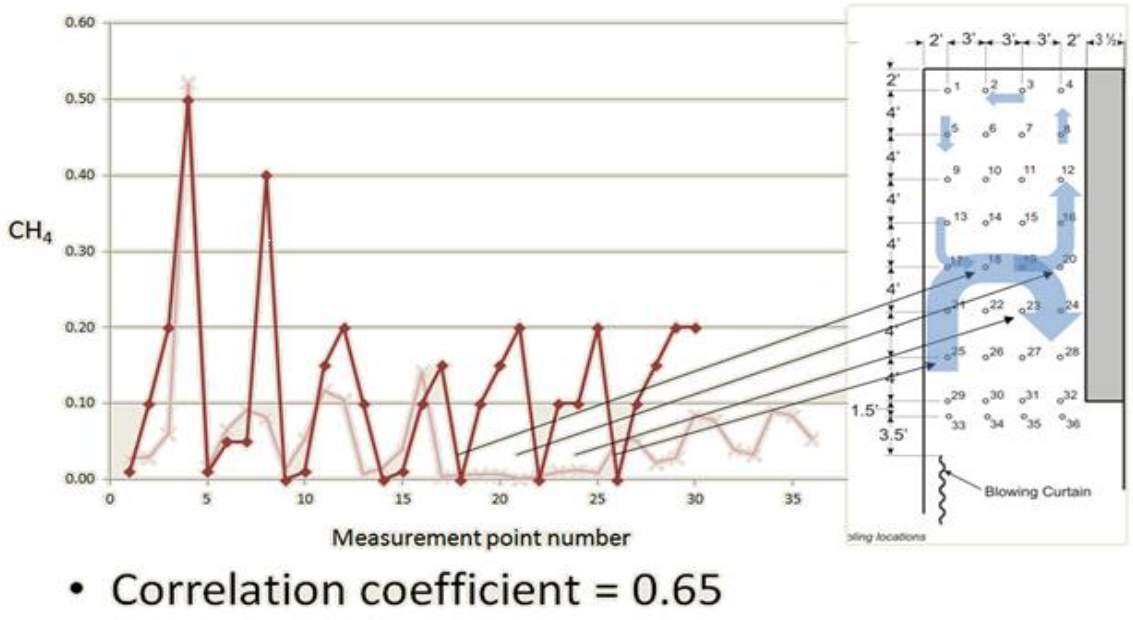

Figure 4.24. Comparison between the measured methane concentration and the simulation data

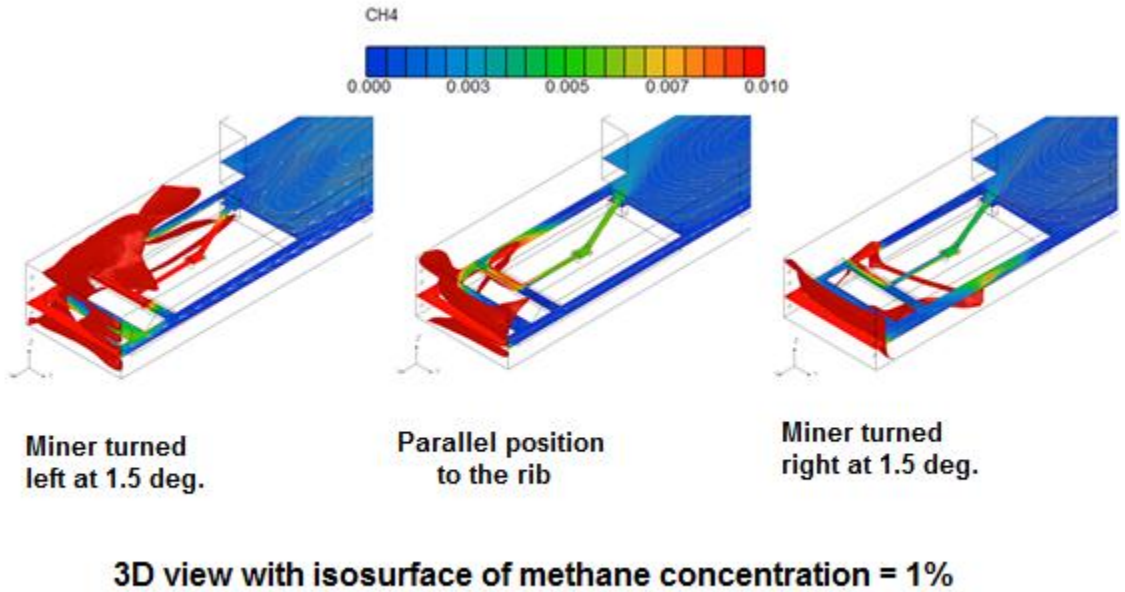

Figure 4.25. CFD analysis for three different positions of the CM

Chapter 5

FACE VENTILATION SIMULATOR CODE DEVELOPMENT

5.1 General Concept of Face Ventilation Simulator (FVS)

The general concept of the FVS is to automate the procedure for CFD simulation of user defined face ventilation scenarios using Cradle © CFD software as a development platform, see Figure 5.1. The CFD software is called SC/Tetra Thermofluid Analysis System with Unstructured Mesh Generator. To automate the CFD simulation proces, FVS uses Microsoft COM (Component Object Model) to communicate with Cradle CFD software. This involve Visual Basic (VB) interface and built-in mechanism to incorporate Visual C language user defined functions to handle the SC/Tetra functions as methods and variables.

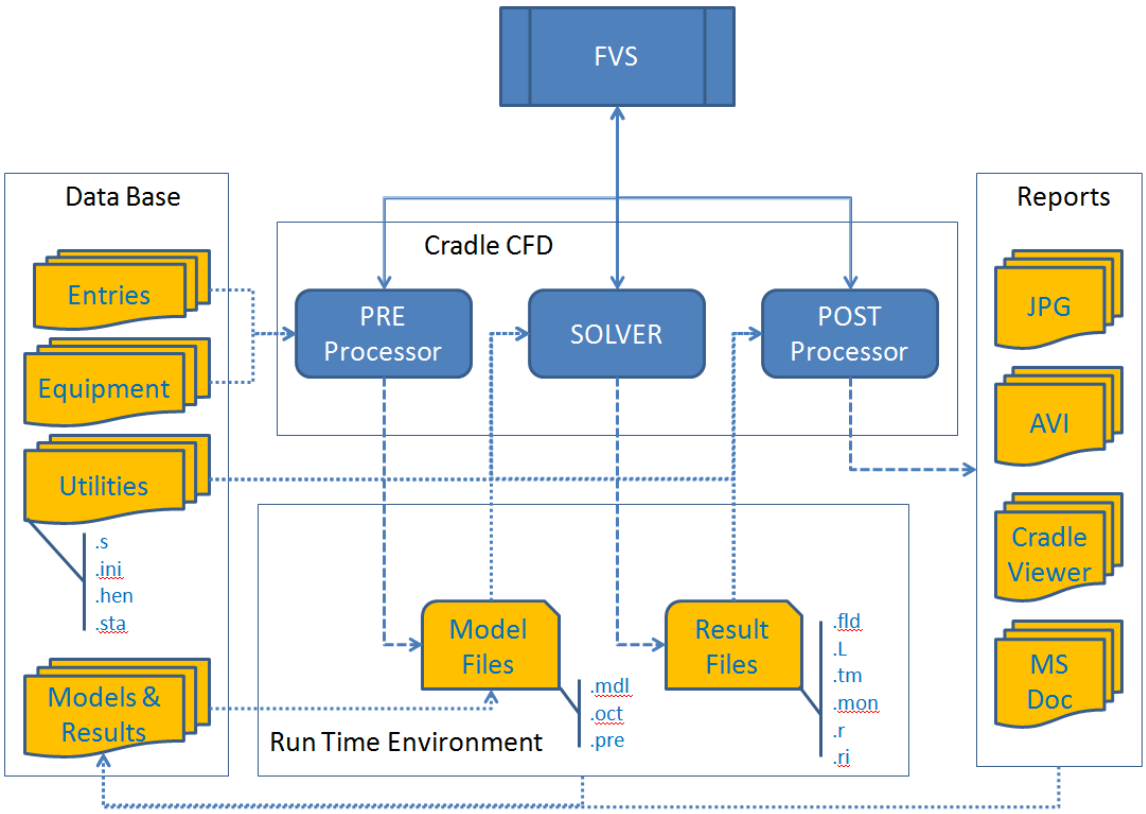

Figure 5.1. General concept of the Face Ventilation Simulator (FVS)

The FVS code was developed to encapsulate the CFD specifics for background execution and expose the potential user only the technical information usually required for face ventilation design. An attempt was made to develop an industry oriented platform for design and analysis of face ventilation systems dedicated to the needs of the mining engineers.

5.2 Scope of the CFD Analysis

The FVS was designed to provide CFD analysis of the airflow behavior, methane dilution analysis and dust control analysis of a user defined face ventilation system. This includes CFD analysis of face ventilation for equipment free entries and with continuous miner (CM) in place. The included CM models support machine mounted scrubbers and spray system simulations. The effect of cutting drum rotation on the flow patterns and consequently on the diffusive species (CH_4 or SF_6) or dust particle distribution is included.

5.3 Model Assumptions and Specification of the CFD Analysis Conditions

The performed analysis of the flow behaviour in the face area (Petrov, Wala and Huang, 2013) firmly proved that the inertia and pressure forces are dominant compared with the forces of internal friction (viscous term). The flow behavior in the studied face area is governed by the laws of mass conservation and momentum conservation. The Reynolds numbers determined for the intake air-stream, usually is greater than 60,000 indicated fully developed turbulence. Therefore, the conditions under which, the CFD analysis of face ventilation systems will be performed are assumed as follows.:

- Three-dimensional (3D) incompressible turbulent flow .
- Material properties: Air incompressible (standard condition at 20 ^{o}C)
- Time dependency of simulation: SSA[3] or TDA[4]
- Turbulence models: RNG k-EPS (Renormalization Group Method).
- Non-flux boundary conditions: Stationary no slip wall; Log-law
- Flux-boundary conditions: Velocity inlet; Fixed static pressure (0.0 Pa) outlet
- Mesh generation:
  - automatic;
  - base octant size - depends on the average intake air velocity;
  - number of prism layers = 5 .
- Equation to be solved:
  - momentum conservation equation;
  - mass conservation equation;
  - k-EPS equations.

[3] Steady State Analysis
[4] Time Dependent Analysis

- Solver settings:
    - double precision solver
    - relaxation factor = 0.6 for velocities and pressure;
    - exchange coefficient set to turbulent flow;
    - accuracy of the time derivative terms set to second-order implicit scheme.
- Convergence criteria: 10E-4 average residuals.

5.4 Problem Setup and Methodology

Realization of the features mentioned above involves steady state and time dependent CFD analysis with incorporation of equation for conservation of diffusive species, ALE method, porous media model, and particle tracking method together with the turbulence model equations. The general input data flow diagram is shown on Figure 5.2. Models of line curtains, tubing and scrubber channels used panel boundary conditions with properties of log-wall. The log-wall boundary conditions were used also to model the surfaces of the entries' ribs, floor and roof. The surface of the face is a special treatment. The face is represented as a log-wall in scenarios for flow behavior analysis, and dust control analysis. For methane dilution analysis, the methane liberation is simulated from the face using porous media model. An exception was made, for the CFD code validation of NIOSH lab scenario, where the methane was released using perforated manifold tubes. In this case, the manifold tubes' surfaces were assigned for methane inlet and the face was modeled as a log-wall surface region. Results of the performed parametric study of flow patterns developed by line brattice face ventilation systems showed low sensitivity of the flow behavior to changes of the wall roughness. These findings allowed to assume smooth log-wall boundary conditions in CFD analysis of face ventilation systems. This assumption was proved valid by the performed CFD code validation study. Nevertheless, there is an option to assign roughness to walls of the modeled face area. This option could be important when non-traditional ventilation controls to extend the flow penetration depth of the intake air stream are simulated.

Models of fans, such as scrubber fans, were built using source boundary conditions assigned to volumes and surfaces with cylindrical geometry. Such a model requires recognition of the source volume region, flow direction, fixed flow, data for time dependent flow curve, or fan characteristics. The metodology of the FVS is ilustrated on Figure 5.3. Every step of the methodology is discussed in details in the next paragraphs.

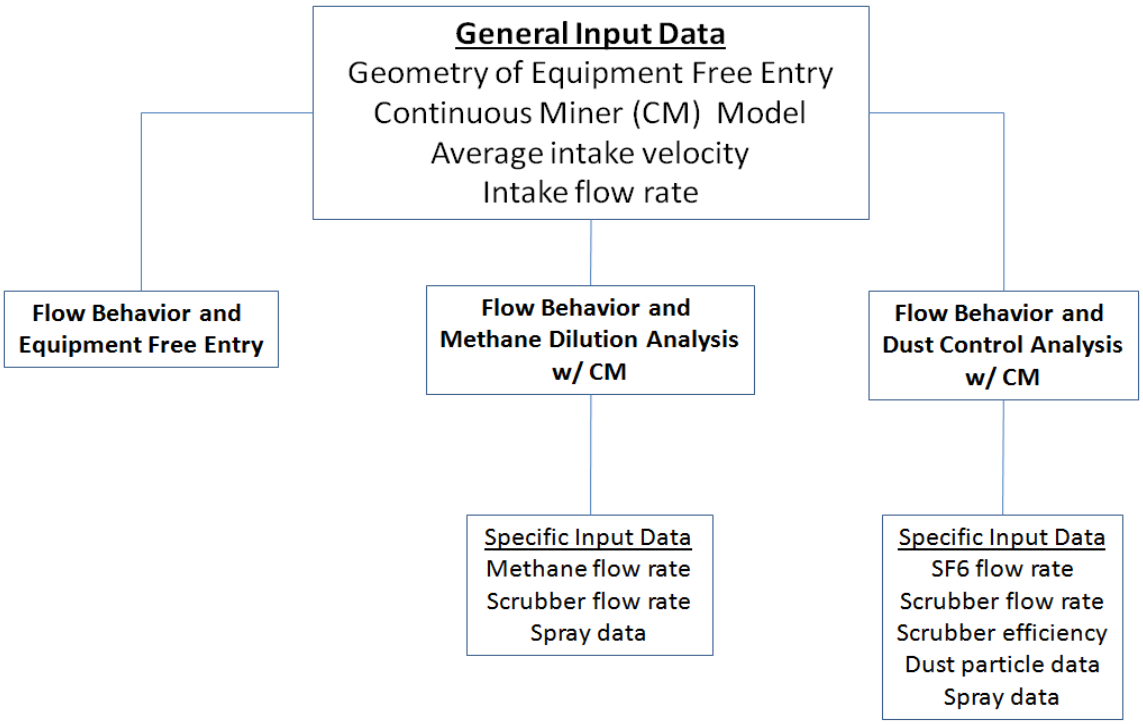

Figure 5.2. Flow chart of the general input data required by the FVS

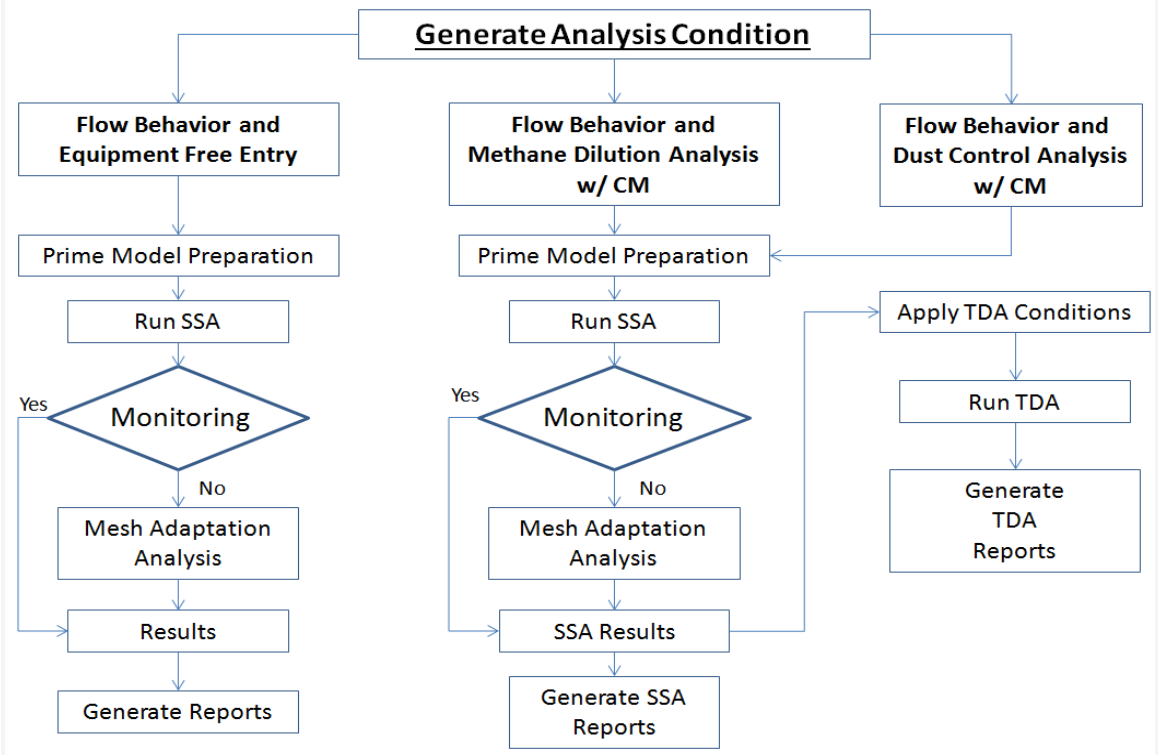

Figure 5.3. FVS methodology flow chart

5.5 Procedure for Building 3D CFD Model of a Face Ventilation System

Preparing the geometry of the system for simulation is the initial step of CFD analysis. The geometry required by the Face Ventilation Simulator is a face ventilation scenario, usually a single cut out of the cutting sequence proposed in the Ventilation Plan, see Figure 5.4 and 5.5. To construct a model for CFD simulation of a face ventilation scenario a user defined geometry of the entry and ready to use model of a continuous miner (CM) is needed. For convenience of the user, a library of CAD templates with geometry of entries corresponding to typical cut sequences was developed.

The procedure for creating a domain for CFD simulation of a face ventilation scenario consists of eight steps. Every step of this procedure will be discussed using an example cut sequence.

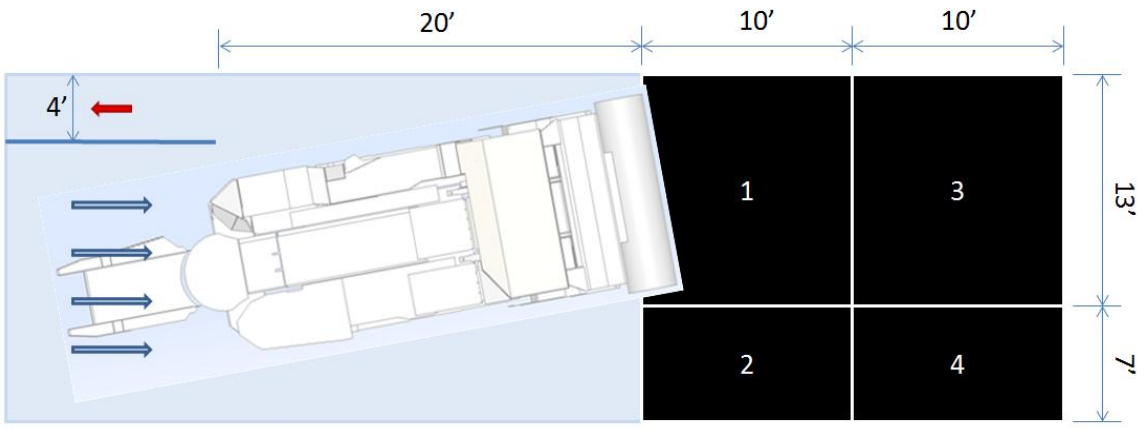

(a)

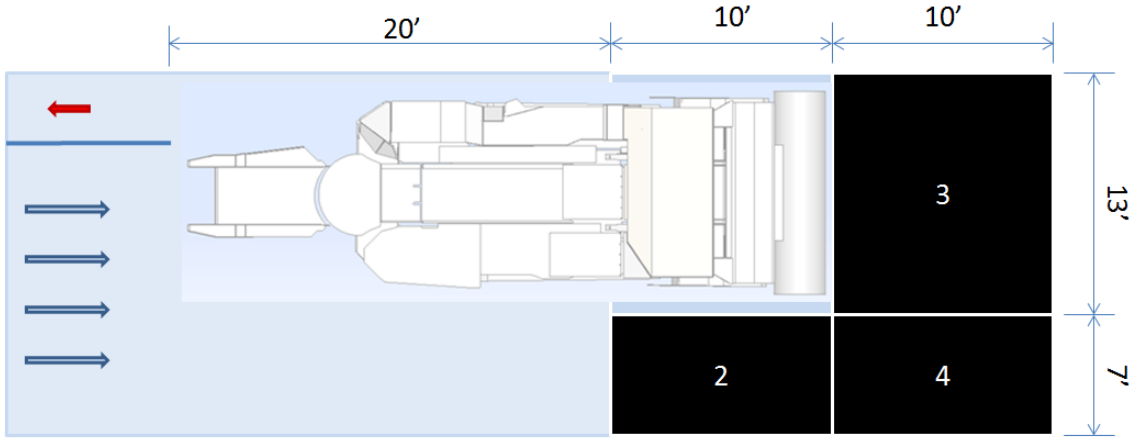

(b)

Figure 5.4. Exhaust curtain system example for extended cut: (a) Begining of the first cut; (b) End of the first cut.

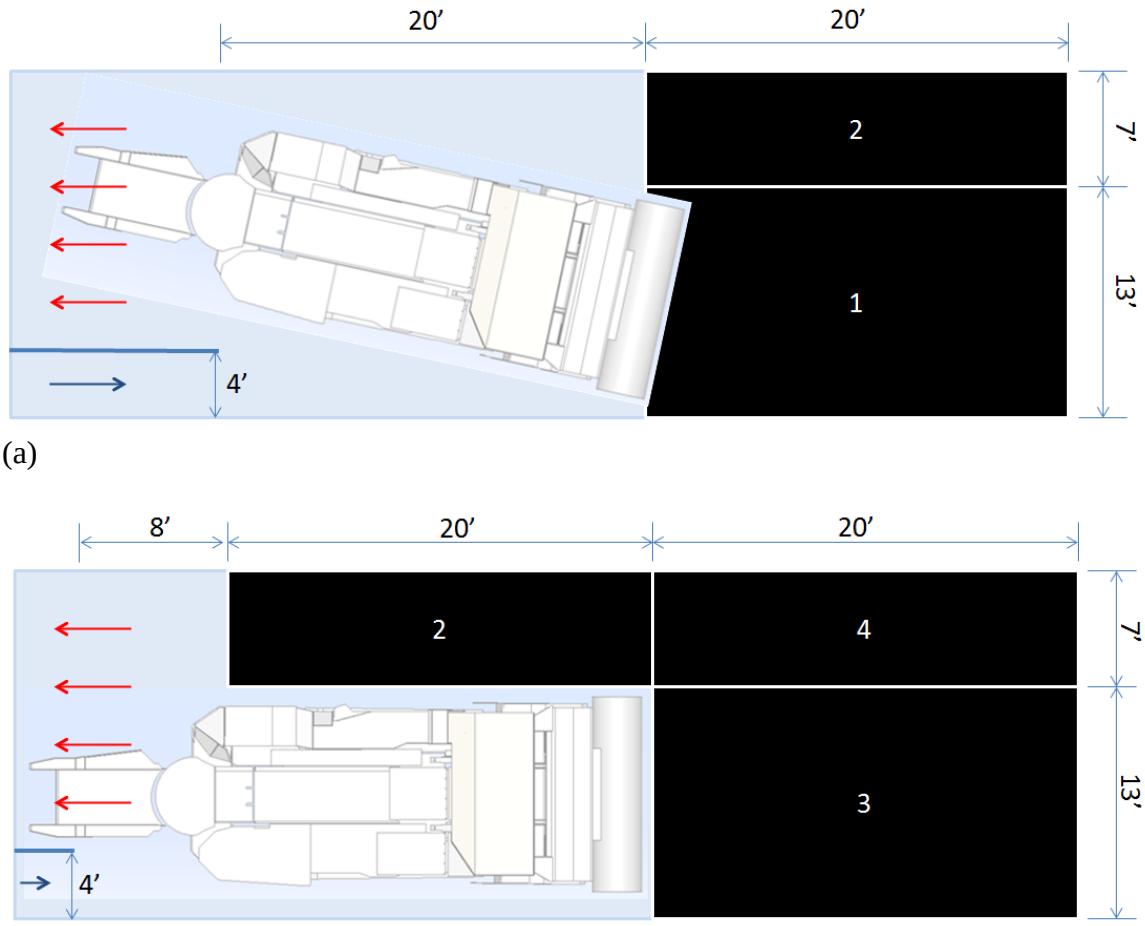

Figure 5.5. Blowing curtain system example for extended cut: (a) Begining of the first cut; (b) End of the first cut.

5.4.1 *Step 1. Create a 3D CAD model for equipment-free entry*

Let create a domain for CFD simulation of blowing curtain face ventilation system with a CM at the end of the 3rd cut based on the sketch shown on Figure 5.6. Using a CAD software the sketch is transformed to 3D model with the required height, which is 7 ft for this particular case (Fig. 5.7). To simulate methane emission out of the face, an additional cuboid attached to the face surface is needed to simulate porous media If flow cannot be fully developed due to lack of length of porous media in the streamwise direction, this model is inappropriate (SC/Tetra Solver manual). Simulation tests showed that, depth of 7 ft is needed to ensure numerical stability of porous media model for this application. When the geometry is done it must be saved as a Parasolid X_T or STEP file.

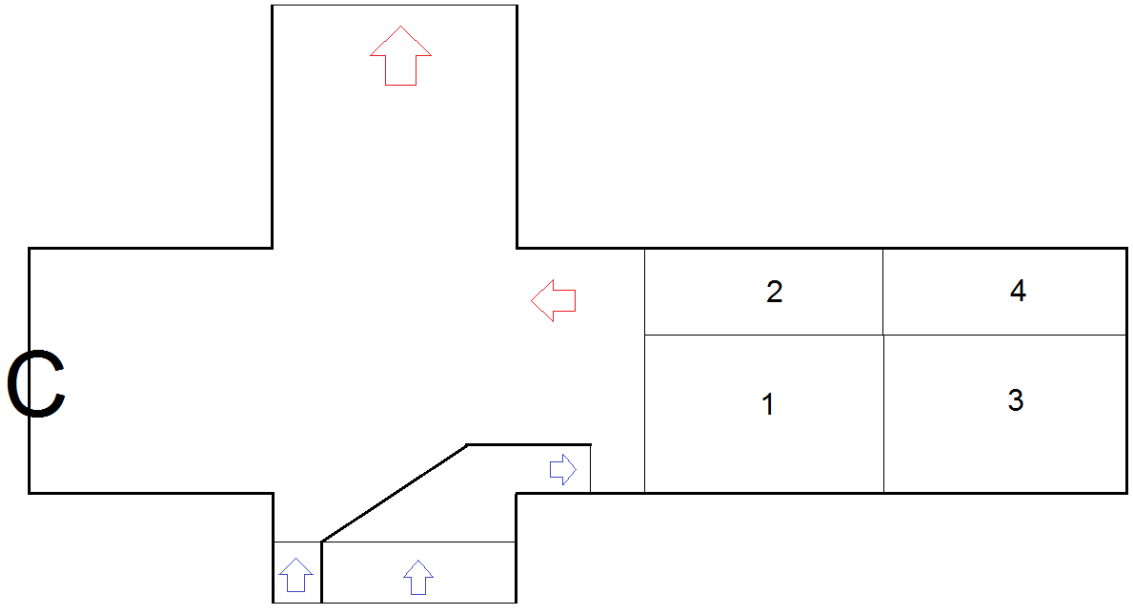

Figure 5.6. Sketch of a typical cut sequence for CM with blowing curtain face ventilation system

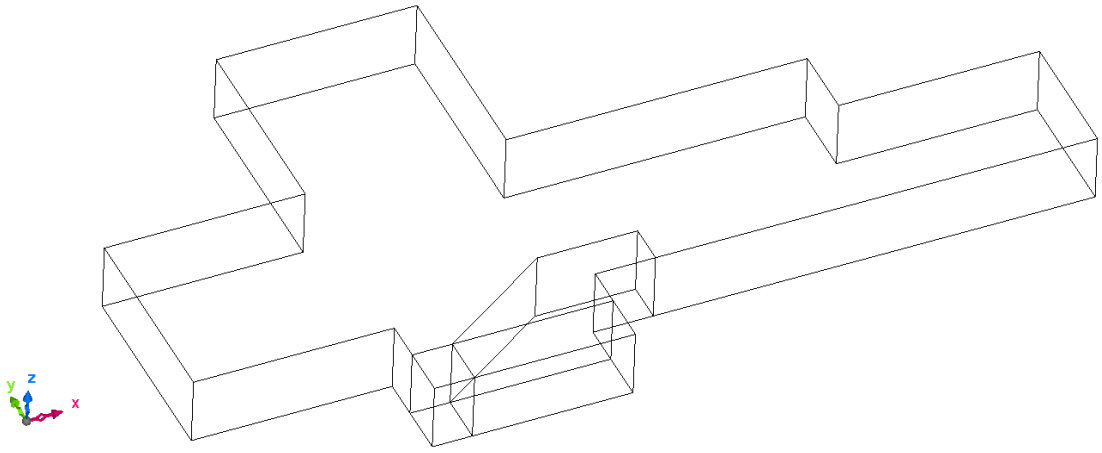

Figure 5.7. 3D CAD model of the equipment free entry at the end of the 3rd cut.

5.4.2 *Step 2. Import the model to SCT Preprocessor*

To import a CAD model to SC/Tetra, a user needs to lunch SCT Preprocessor and import previously prepared CAD data (X_T or STEP file). It could be done by using drag-and-drop. The Preprocessor will automatically enter Prime mode and display the imported geometry. In this step the height of the entry can be altered if needed, using scaling command as shown on Figure 5.8.

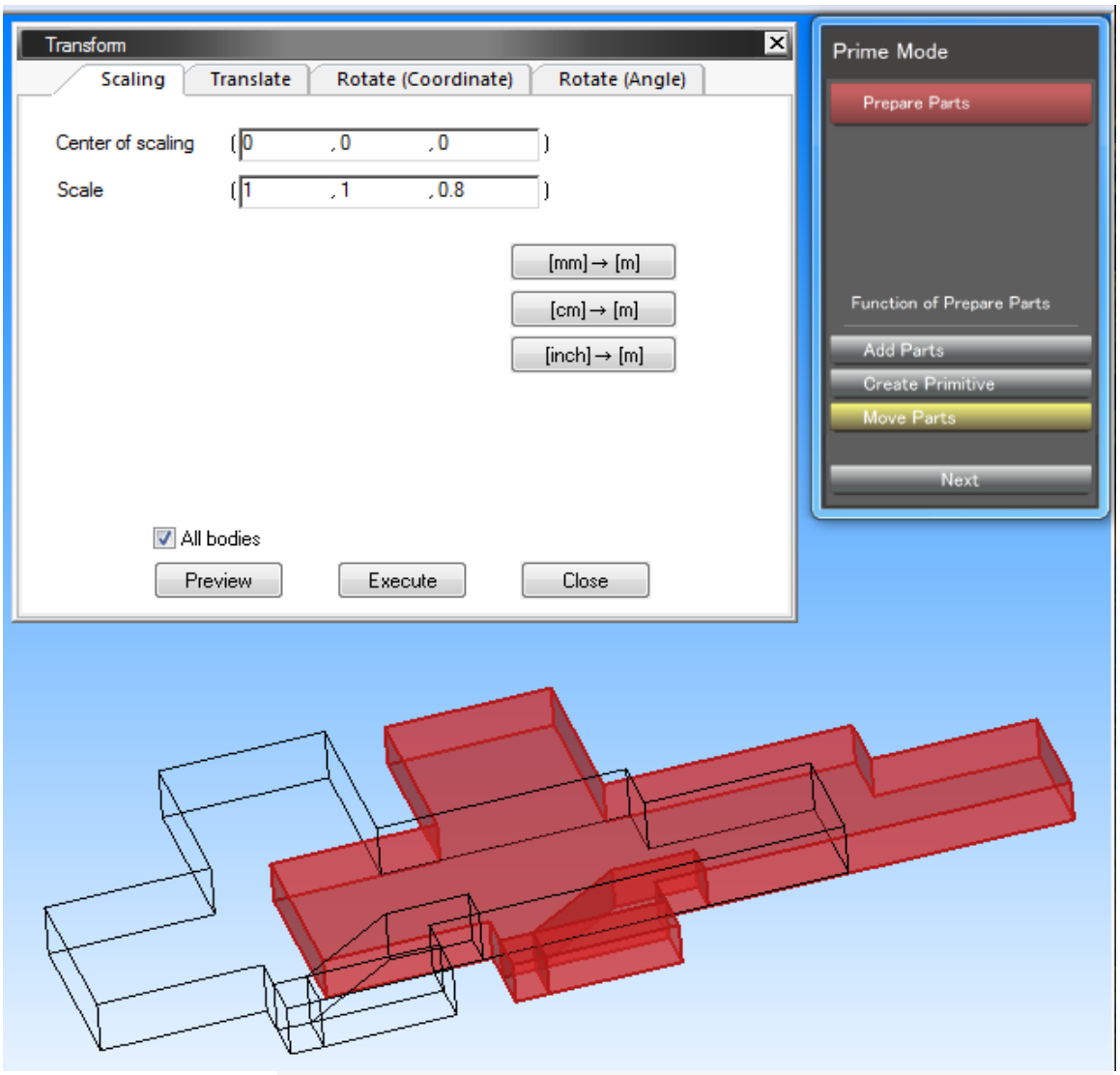

Figure 5.8. SC/Tetra Prime mode. Using of Transform tool to scale height of the entry with factor of 0.8

5.4.3 *Step 3. Set the location of a continuous miner*

A cuboid volume called MinerBox have been designed to set the location of a CM into the user defined model of equipment free entry. For this purpose a CAD file named MinerBox.x_t needs to be added to the existing Prime model. The file location is \FVS\Replace&Remesh_Models\MinerBox.x_t. This file should be added to the previously reated SCT Prime model by using "Add Parts" button or drag-and-drop (Fig. 5.9). It is important to note that MinerBox position and size should not be altered! The FVS uses the origin and the coordinate system of this particular MinerBox volume to automatically set variety of analysis conditions concerning scrubber and water sprays settings, cutting drum rotation, dust particles generation and others. Therefore, the user defined model of equipment-free entry should be adjusted in respect to the MinerBox volume.

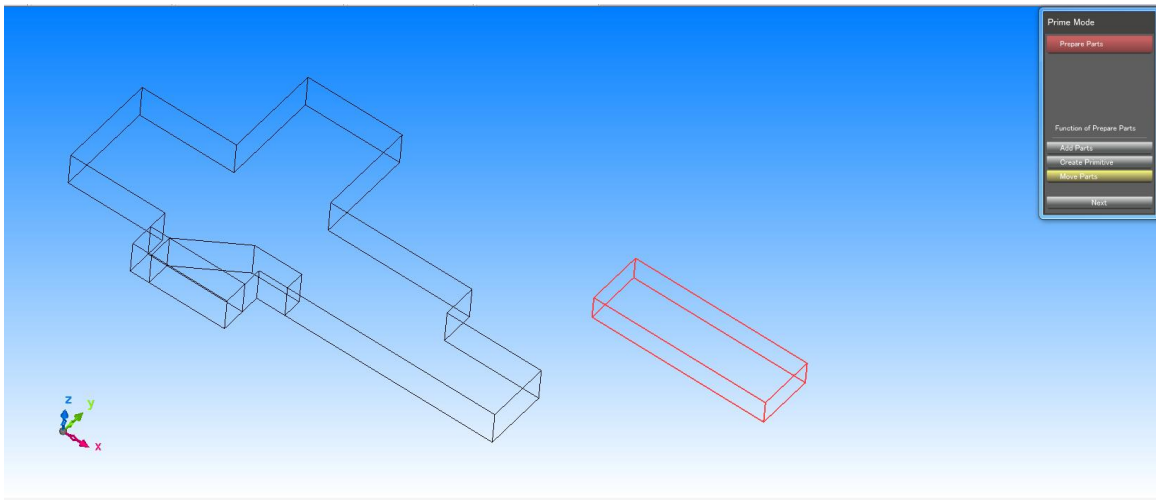

Figure 5.9. The MinerBox volume part just added to the existing model

5.4.4 *Step 4. Adjust the position of the entry in respect to the MinerBox*

In general case, the geometry will needs of adjustments. In this particular example, we need the MinerBox to appear at the end of the 3rd cut. To adjust the entry to the MinerBox, use "Move parts" button on the Prime Mode menu and adjust the entry to the desired position using translate comman. In some cases rotation of the entry may aply. It is important to mate the floor of the entry with the floor of the MinerBox at Z=0. Make sure the adjustment has made in both, X-Y and X-Z plan (Figure 5.10). This step prepared the user defined geometry for transformation to prime CFD model.

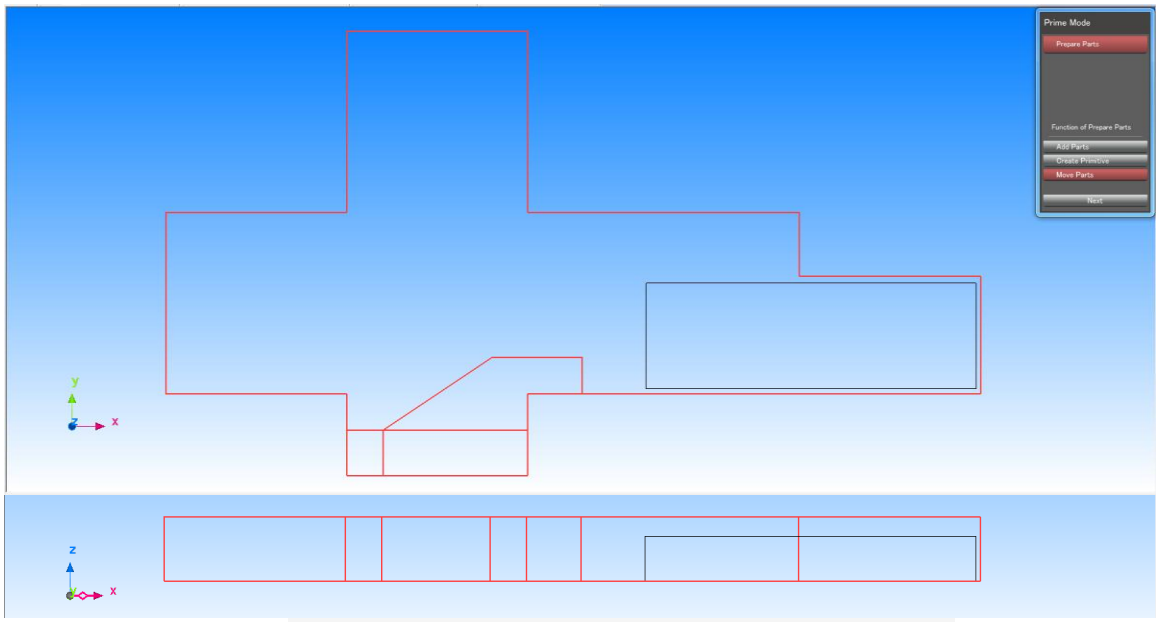

Figure 5.10. Result of the adjustment using translation command

5.4.5 *Step5. Create prime CFD model*

After finishing with the adjustment, the user needs to press "Next" button of the Prime Mode menu and run closed volume recognition procedure (Fig. 5.1). The process takes seconds. To continue, the user needs to close the check status window and press the "Create MDL" button. The result is shown on Figure 5.12. Then, the user needs to close the "Create MDL" window, press "Next" button from the Prime Mode menu and select "Move to Model Mode" . Here the user needs to confirm the folder and file name of the just created model and save it. This folder will become the working folder for the simulation process. Following the described procedure minimizes the risk of problems at this prime stage of preprocessing by keeping the model simple and the processing time short. The most-complicated part of the assembly - continuous miner model is provided ready to use and will replace the MinerBox volume as described in 5.4.7 (Step 7).

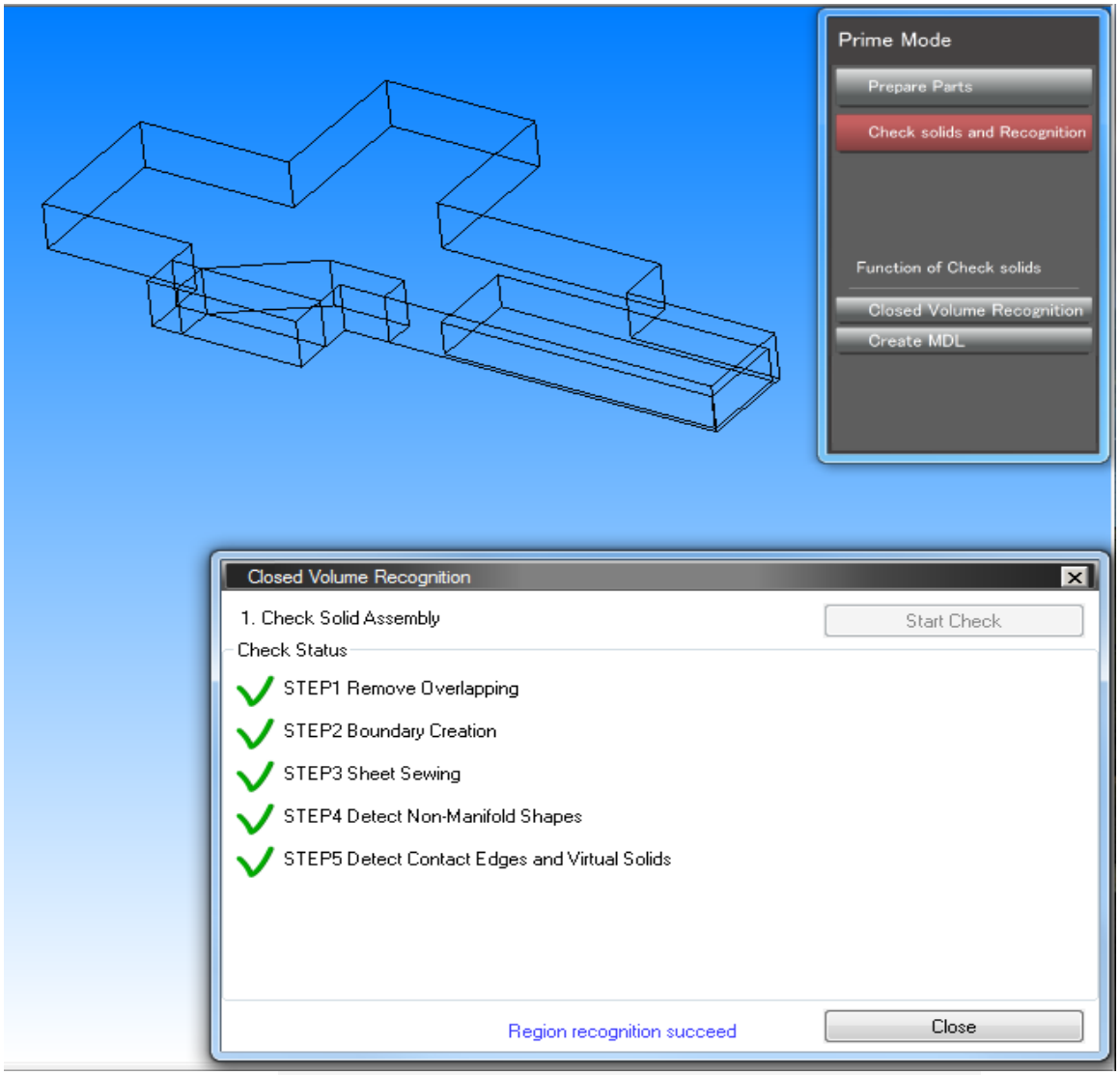

Figure 5.11. Closed volume recognition, SCT Prime preview window

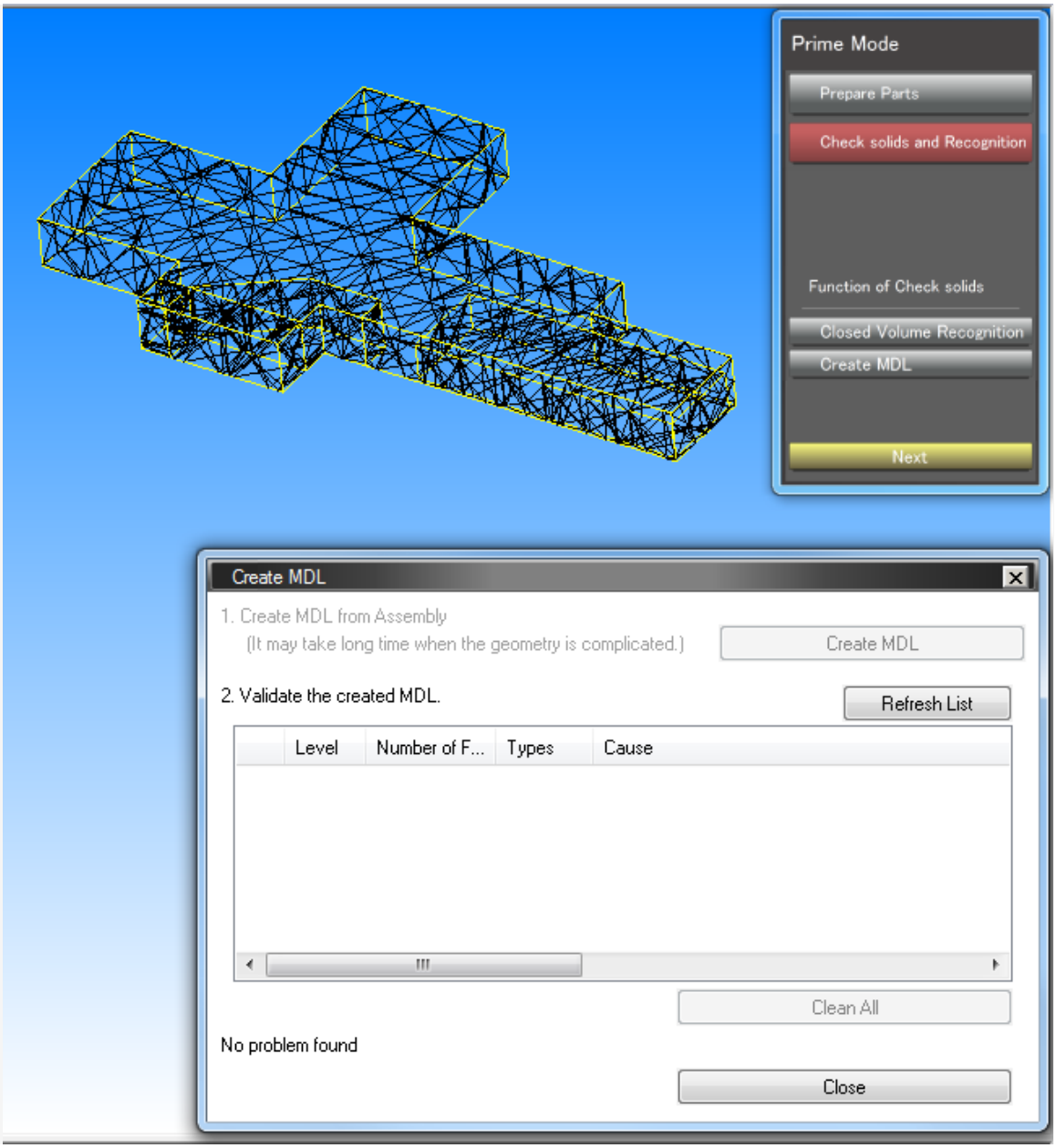

Figure 5.12. Result of the create MDL procedure, SCT Prime preview window

5.4.6 *Step 6. Register regions to model*

In the previews step, a prime model was created and saved, but the model does not contain information about registered regions. In this step the following regions will be registered:

- Surface Regions: walls; face; curtain; inlet; inlet2; outlet; envelop
- Volume Regions: box

A VB script code RegisterRegions.vbs (see Appendix) for SCT Preprocessor is to assist the user to register the regions following an interactive automated process (Fig. 5.13).

Since the location of each region may vary by data user actions are required. However, the names of the regions will remain the same regardless of their geometry and location. Table 5-1 describes the user input. The interactive process takes about five minutes and eliminates the risk of typos or omissions in the regions names. The user will be prompted which region to mark. At the end of registration, the file will be automatically saved as a new one with a keyword "Prime" added to its original name.

Table 5-1. User input data for the register region procedure

Description	Variable	Example value
Path to Working Folder	**path**	"C:\FVS\TestProject\Prime"
Model (MDL) file name	**model**	"3rdCut"

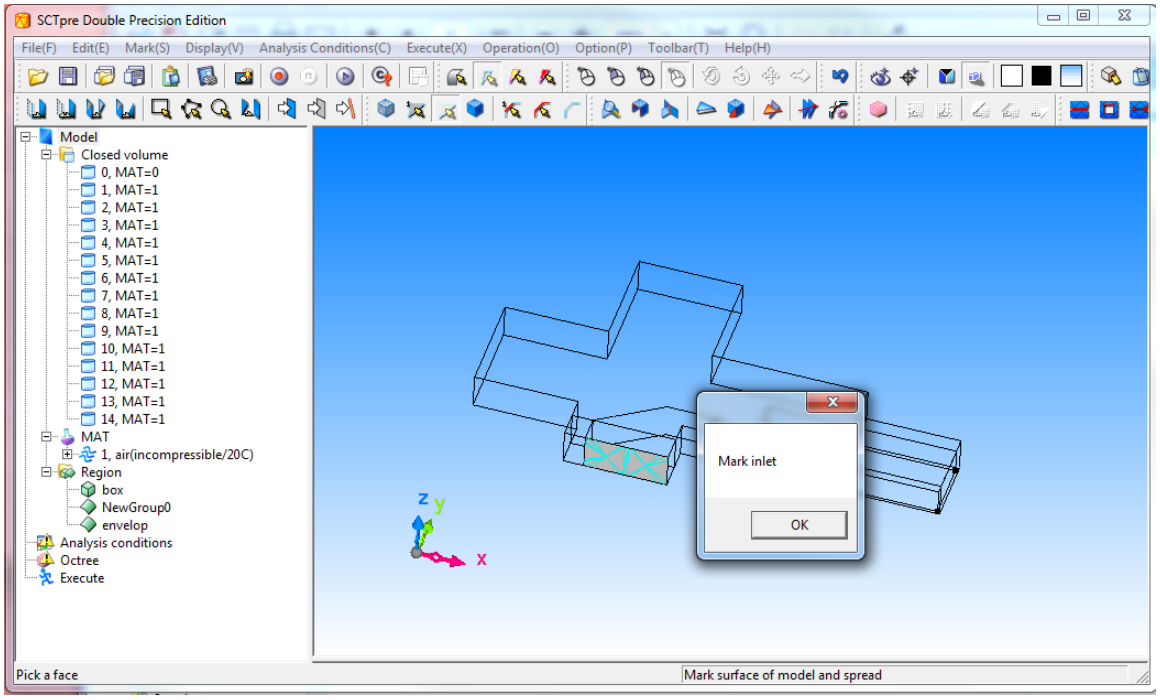

Figure 5.13. Automation of region registration process.

5.4.7 *Step 7. Mesh the prime model*

In the previews steps, closed volumes and registered regions had been appropriately set and the model had been saved as "3rdCutPrime.mdl". A VB script called MeshPrime listed in Appendix was developed to automates the mesh process of the prime model. The user input needed for this step is described in Table 5-2.

When creating a mesh containing prisms, the main problem is deciding on the size of the tetra mesh and the thickness of the prism layer. It is important to exercise care in selecting these values as they will have a direct impact on the efficiency, stability and accuracy of a computation.

The initial parameters needed for this MeshPrime VB script , such as friction velocity u*, thickness of the first prism layer y, and minimum octant size were determined according the recommended best practice using and Equations 3.23 to 3.26. For this particular example, the main stream velocity U was set to 1.5 m/s (around 300 ft/min) which corresponds to the average velocity of the intake air behind the curtain. The y^+ design value is set to 100. The density and viscosity of the air were set to their standard values, $\rho = 1.2\ kg/s$ and $\mu = 1.8e-5\frac{kg}{m.s}$. Then applying Equations 3.23 to 3.26 we obtain $y = 0.02\ m$ for the thickness of the first prism layer and $MinOctSize = 3y =$ 0.06 m. The number of prism layers on walls and face was set to 5, and 2 on the curtain. The assigned numbers of prism layers are based on the results from the performed CFD validation study. Note, that these settings are valid only for the prime mesh, before including the continuous miner model and taking into account the impact of the scrubber performance on the flow. Results of this step are four saved files as follows:

- Octree (3rdCutPrime.oct)
- Surface mesh (3rdCutPrime_meshsurf.mdl)
- Volume mesh (3rdCutPrime_tetra.pre)
- Prism layers (3rdCutPrime.pre)

These files are needed for the next step - continuous miner model insertion.

Table 5-2. User input data for the register region procedure

Description	Variable	Example value
Path to Working Folder	**path**	"C:\FVS\TestProject\Prime"
MDL file name	**model**	"3rdCutPrime"
Average intake velocity	**Uin**	1.5 m/s (300 ft/min)
Analysis type	**Analysis**	_Methane
Equipment	**Eq**	_CM_Scrubber
Flag for the air conditions	**air_cond**	"Standard" by default
Air temperature	**t_air**	Optional, for conditions other than standard.
Air density	**ro_air**	Optional, for conditions other than standard.

5.4.8 *Step 8. Analysis Settings Generation*

Three general types of FVS analysis are developed as shown in Table 5-3. The user selects which type of analysis to perform and inputs the required data. A generator of analysis conditions reads the user data and generates code for SCT S-file. A VB script code called S-Generator for methane dilution analysis is listed in Appendix. The code uses templates for three general cases: Equipment free entry; w/ CM in place (scrubber is off); and w/ CM in place and scrubber operational. The example "Scrubber.s" template is

listed in Appendix. Table 5-4 and 5-5 describes an example for user input needed for this step.

Table 5-3. General types of FVS analysis

#	Analysis Type	Time Dependency	User input
1	Flow behavior	SSA[5]	Intake Airflow Rate Scrubber Flow Rate (if present)
2	Methane Dilution	SSA TDA[6]	Intake Airflow Rate Methane Flow Rate Equipment (select from list if present) Scrubber Flow Rate (if present) Water Spray Data (if present)
3	Dust Control	TDA	Intake Airflow Rate Equipment (select from list) Scrubber Flow Rate and Efficiency Gas Flow Rate (SF6) Water Spray Data Dust Particles Data Dust Monitoring Stations Setup

Table 5-4. User input data for the S-Generator

Description	Variable	Example value
Path to Working Folder	**path**	"C:\FVS\TestProject\Prime"
MDL file name	**model**	"3rdCutPrime"
Analysis type	**Analysis**	_Methane
Equipment	**Eq**	_CM_Scrubber
Condition (S) file name	**sfile**	"3rdCutPrime_Scenario1"
Intake flow rate	**Qin**	4.25 m^3/s (9000 cfm)
Scrubber flow rate	**Qsb**	3.78 m^3/s (8000 cfm)
Methane flow rate	**Qch4**	0.0042 m^3/s (8.9 cfm)

Methane dilution analysis which included simulations of sprays as well as all the dust control analysis required time dependent analysis (TDA). They required additional user input about the spray setup and the dust particles as discussed in Chapter 4. RNG k-ε (Renormalization Group Method) is the implemented turbulence model. The default number of calculation cycles was set to 700. The default convergence thresholds were set

[5] Steady State Analysis
[6] Time Dependent Analysis

to 10^{-4} average residuals for calculation of velocities, pressure, turbulent energy and turbulent dissipation rate. For methane concentrations, the convergence threshold was set to 10^{-5} average residuals. These numbers were established during the performed CFD code validation studies.

5.6 Solving and Monitoring Automation Algorithm

To run a prepared simulation scenario no additional user input is required. A VB script called XSolverAdapt.vbs listed in Appendix runs the SCT Solver using the data generated in the previews steps. The script establish automatic run time monitoring of the calculation process by evaluation a set of runtime variables for convergence and stability. The calculations may converge far before the default end cycle if the domain mesh settings correspond to the CFD analysis conditions. As the initial mesh is likely to be coarse in some parts of the computational domain, it is assumed that the CFD analysis is not being performed under the best possible conditions.

The XSolverAdapt performs a two stage solving procedure. The main program, first initiates simulation using the initial mesh, then executes mesh adaptation analysis followed by second simulation. The program performs interrupt checks by monitoring the runtime values of the following variables:

- velocities (VELX,VELY,VELZ)";
- concentration of the simulated diffusive species (CN01) such as methane or tracer gas in a check point "A" typically positioned adjacent to the face.

For any of the monitored variables, the program evaluates the data bias for every last five cycles using their maximal values. If the following conditions are met for the last five calculation cycles, namely:

- convergence data for velocities fall below the given threshold of 2e-4, and
- the maximal velocities data bias is less than 0.01 m/s, and
- the methane concentration data bias at the check point A is less than 0.0001

then the calculations will be interrupted and the results of the last cycle will be saved as simulation results in a FLD file. Otherwise the calculations will continue until reaching steady state convergence or to the final cycle as given by default. In this case the program automatically initiates SCT Mesh Adaptation Analysis to improve the prediction. This procedure automatically generates more suitable mesh for the analysis by reconfiguring the existing one, using the simulation results saved in stage one . After re-meshing, the simulation is restarted. The automated monitoring remains intact and the new results being saved. No further actions for improvement were designed.

An example of the calculation progress using a face ventilation scenario for blowing curtain face ventilation system with Joy 14CM15 at the end of the third cut and scrubber to face ventilation ratio of 0.8 and methane gas emission simulated at the face is shown on Figure 5.12 to 5.15. The simulated flow visualized by 3D streamlines showed more developed flow patterns after mesh adaptation (Figure 5.14b) then the flow patterns simulated with the initial mesh (Figure 5.14a).

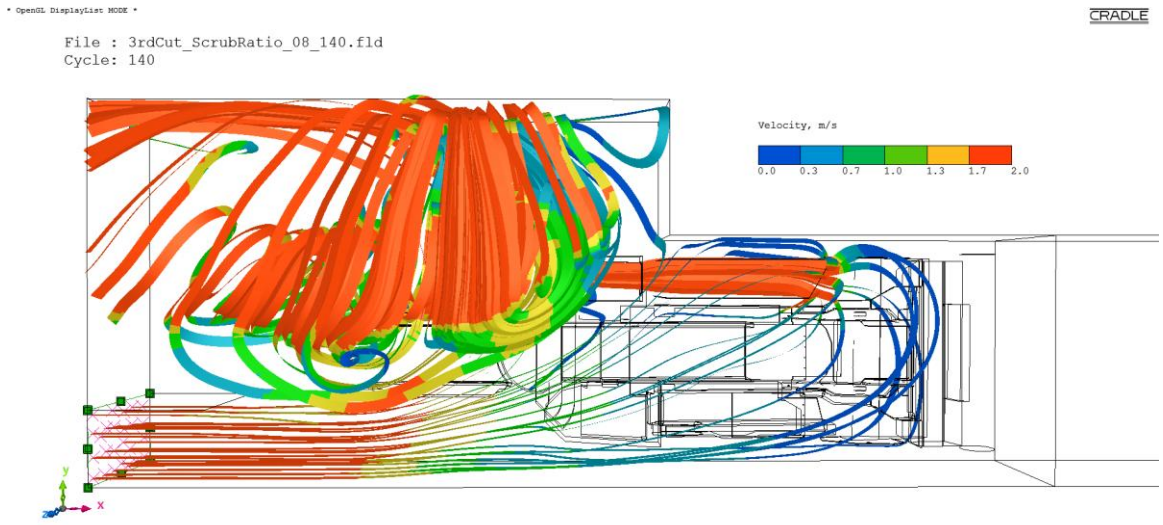

(a) First stage simulation results, using the initial mesh

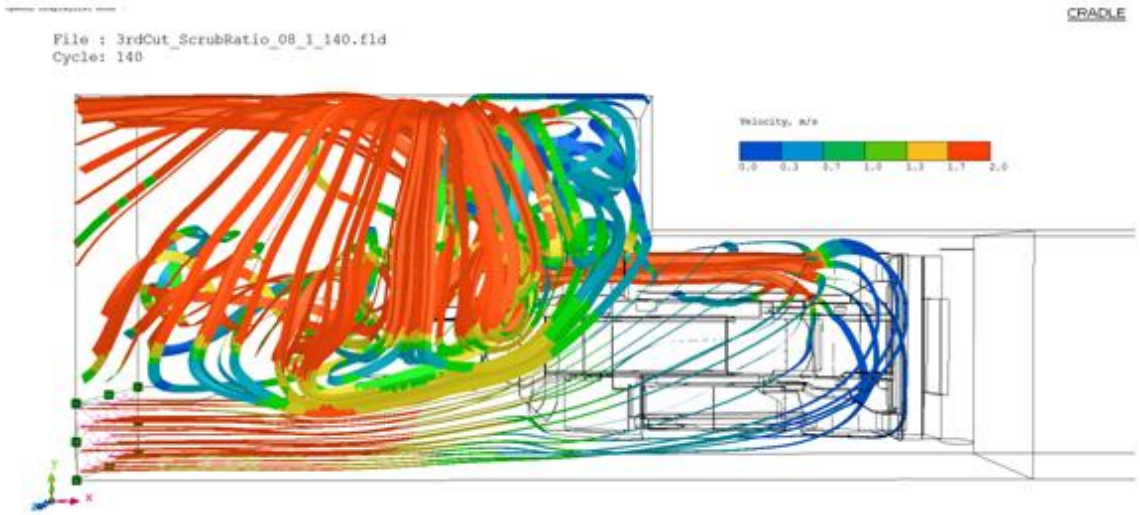

(b) Second stage simulation after mesh adaptation analysis

Figure 5.14. Simulated flow patterns results of the two stage solving process visualized by 3D streamlines

View of the SCT Solver Monitor for the methane concentration in point A (Diffusive species A) during the first stage of simulation (Figure 5.15a), and during the second stage - after mesh adaptation (Figure 5.15b) is shown below. Point A (Figure 5.16) was located above the cutting drum (1 ft below the roof) at the middle of the entry. As it can be seen on Figure 5.13b, after performing mesh adaptation analysis, the simulated methane concentration remains consistent with the advance of the calculation cycles as opposed to the first stage of the simulation (Figure 5.15a). If the mesh adaptation analysis is successful no significant changes in the simulation result will occur with the extension of the calculation cycles or with performing of next stage of mesh adaptation using more dense mesh settings. In general case the number of cycles in which the calculations

finished may differ for stage one and two. The knowledge obtained during the CFD code validation study was used to determine the suitable parameter values for the mesh adaptation analysis and to reduce the calculation steps to two in order to optimize the calculation cost.

(a) First stage of the simulation

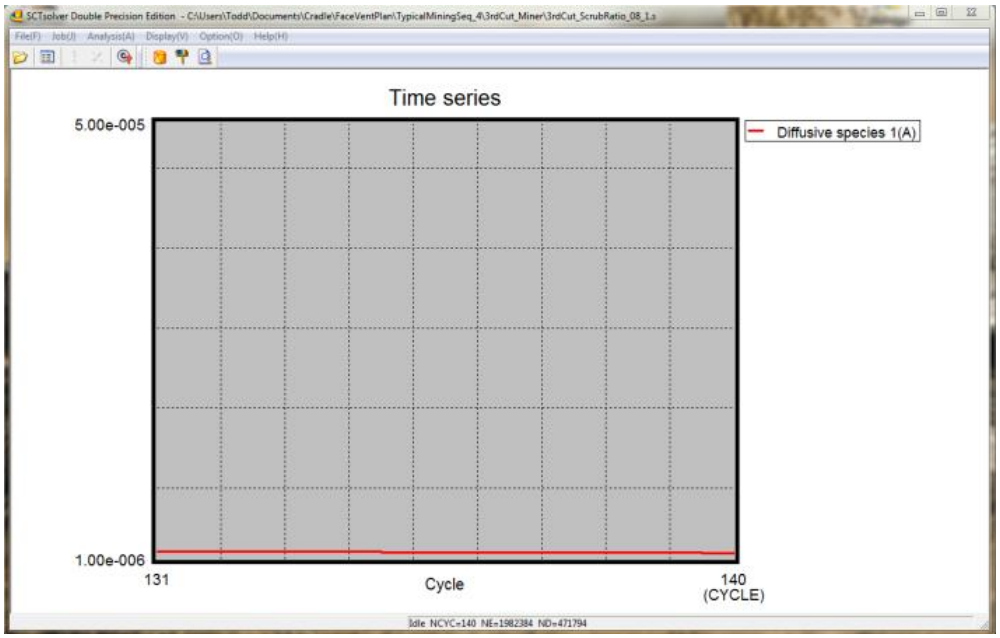

(b) Second stage of the simulation - after the mesh adaptation analysis

Figure 5.15. Views of the SCT Solver Monitor for methane concentration at point A, before (a) and after (b) mesh adaptation analysis.

The simulated methane distribution for both stages is depicted on Figure 5.16 and 5.17. The result shown on Figure. 5.17 should be accepted as a prediction of the simulated face ventilation scenario. In general case, the differences in the simulation results between the two stages could be more significant. The proposed procedure, including the previously described steps, is designed to give the best possible results on the first stage of calculations with minimum required user interactions. The second stage will be performed automatically if needed to avoid potential mesh inconsistency and for final refinement of the simulation results.

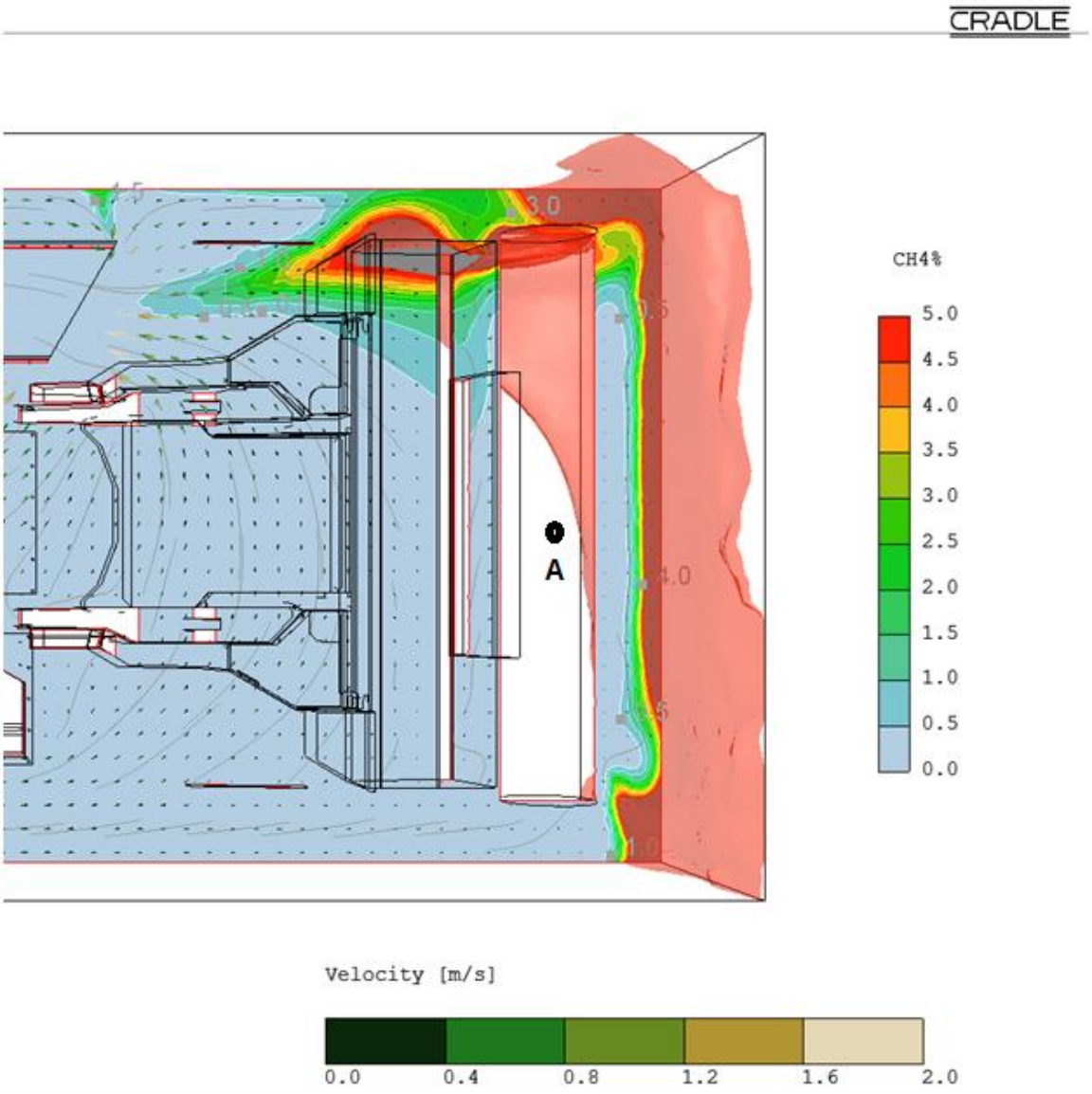

Figure 5.16. First stage simulation result for methane concentration

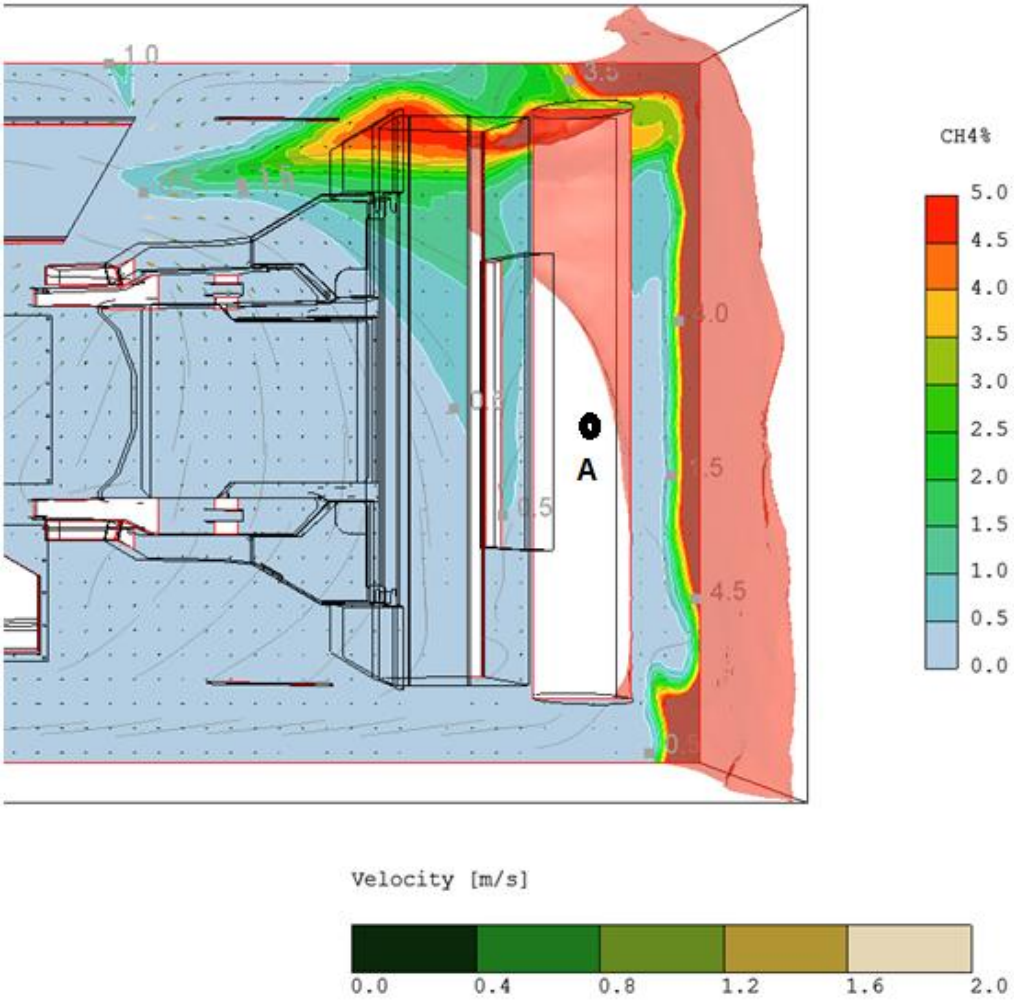

Figure 5.17. Second stage simulation result for methane concentration after mesh adaptation analysis

5.7 Post-Processing Automation Algorithm

The Face Ventilation Simulator FVS provides automation for Cradle SC/Tetra postprocessor (SCTpost). A simple dialog window (Figure 5.18) will guide the user trough the post-processing of the obtained simulation results. The "Show Animation" button automatically opens the SCTpost application, loads the simulation results stored in FLD files and runs a predesigned series of animations by programming the SCTpost. The animation shows different 3D according to the CFD analysis type (Table 3) chosen by the user. The animation sequence uses the powerful graphical capabilities of the Cradle SCTpost engine to produce suitable presentation of the simulated results. This include:

- Static plan and isometric views including vector maps, contour maps, and 3D gas concentration isosurfaces
- Moving vector maps for SSA and TDA
- Moving concentration maps, plan view and 3D isometric view.

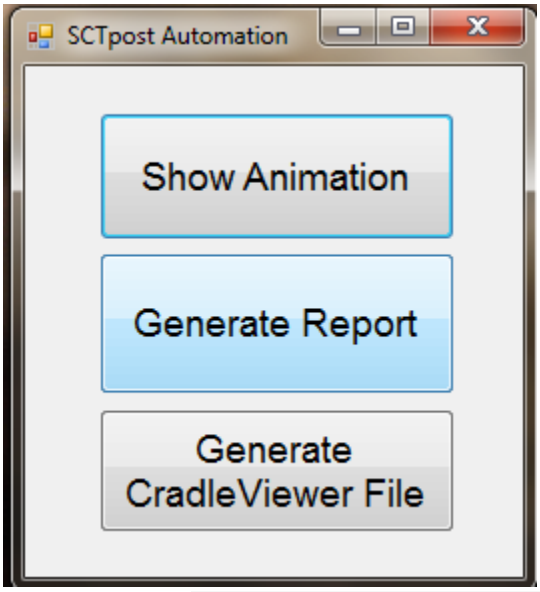

Figure 5.18. FVS dialog window for SCTpost automation.

The animation preview can be interactively controlled by the user. No spatial CFD skills are required to follow the animated preview scenario. If the user is experienced with Cradle CFD it can use the full power of the SCTpost at any point o the preview. The FVS code for SCTpost automation is listed in Appendix together with an example list of status file (STA) code used as data by the main code. Additional 17 STA template files were developed.

The "Generate Report" button creates automatically creates a Microsoft Word Document with results of the performed simulation. The code automatically opens the SCTpost application and sends automation instructions to it. The graphical output format from SCTpost is given by list of template STA files. The list is specific to the analysis type (Table 5-3) and the simulated equipment. Creating a MS Power Point presentation is another option for the report output format.

The "Generate Cradle Viewer File" button automatically creates a 3D interactive presentation file for Cradle Viewer. The Cradle Viewer is a light stand alone application that allowed a user to preview simulation result file, to switch on/off selected elements of the view, including zoom and 3D rotation. The generator also uses STA templates to create the Cradle Viewer file according the analysis type.

The use of STA template files adds flexibility to the application of FVS. The post-processing output can be improved rapidly by any advanced user of SC/Tetra without needs of writing a code and re-compile the application. The Last two options, the

generated report in MS Word format and Cradle Viewer file, gives opportunity to a ventilation specialist to analyze the simulation results without having Cradle CFD installed on his computer.

More detailed presentation of the formatted result for face ventilation system analysis and design is given in Chapter 6.

Chapter 6

EXAMPLES FOR CFD ANALYSIS OF FACE VENTILATION SYSTEMS

In the course of the development of FVS, a number of simulations were performed for CFD analysis of different face ventilation scenarios applying the created models of CM machines, scrubbers and sprays. This included:

- Steady state analysis of equipment-free face ventilation systems.
- Trial simulations of spray models using particle tracking method.
- Time dependent analysis of continuous miner spray and scrubber effect on dust concentration during deep cut ventilated by exhaust curtain.
- Steady state and time dependent analysis of methane dilution ability of blowing and exhaust face ventilation with continuous miner in place, equipped with machine mounted scrubber and spray system.
- Steady state analysis of methane dilution ability of tubing face ventilation with continuous miner bolter in place.
- Steady state and time dependent analysis of a newly developed passive regulator on methane dilution and dust control improvement at the face area ventilated with blowing curtain.

Results of the performed simulation were presented during the SME - the Society for Mining, Metallurgy, and Exploration anual meetings (2011 to 2014), NIOSH annual mine ventilation capacity building review meetings (2011-2014), Professional Engineers in Mining Seminar, Lexington, KY September 6, 2013.

Three examples CFD analysis were selected to illustrate the way of use of the developed models and FVS code for automation of SC/Tetra Cradle© CFD.

6.1. Example CFD Analysis of Methane Dilution Ability of Line Brattice Face Ventilation Systems During Deep Cut with Continuous Miner

A blowing and an exhaust curtain face ventilation system scenarios were simulated. Both scenarios are with CM positioned at the end of the 12.2 m (40 ft) box cut, See Figure 6.1. The hight of the entry is 2.13 m (7 ft). A continuous miner model of Joy Global 14CM15 with three-way inlet scrubber was used, see Figure 4.21. The input data for both scenarious were as follows:

- Tight rib distance: 1.2 m (4 ft)
- Entry width: 6.1 m (20 ft)
- Intake flow rate: 2.8 m^3/s (6000 cfm)
- Scrubber flow rate: 1.9 m3/s (4000 cfm)
- Methane flow rate: 0.0063 m^3/s (13.4 cfm)
- Spray system: see Table 6-1

Table 6-1. Spray system data

Number of spray nozzles	60
Geometry configuration	as given in Figure 4.14.
Nozzle Type (spray pattern)	SH-2 (BD-2) Hollow Cone
Water Line Pressure	783 kPa (70 psi)
Water Flow	0.00261 m^3/min (0.69 gpm)
Orifice size	1.98 mm (0.078")
Spray angle	68 deg
Mean Droplet Velocity	4.5 m/s
Droplet Souter Mean Diameter	55 microns

All the other settings of the model will automaticaly aply by the FVS code

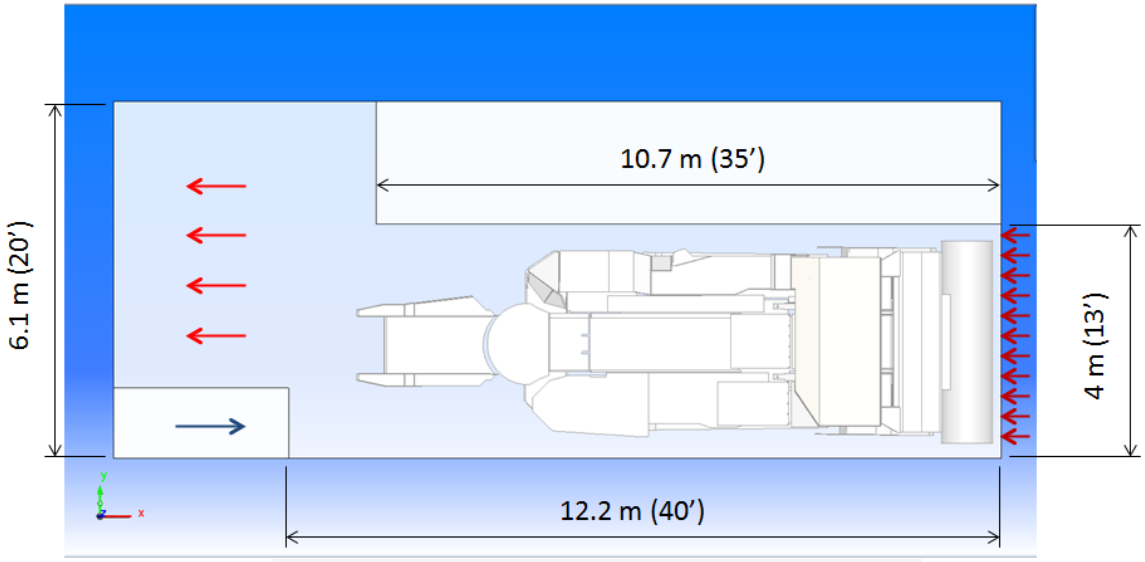

Figure 6.1. Geometry of the simulated blowing curtain system

First, steady state analysis (SSA) with simulation of the scrubber effect on the flow end methane distribution was performed for both scenarious, see Figure 6.2 and 6.3. Then time dependent analysis (TDA) with duration of 60 seconds were performed with spray system included. The results of TDA were saved in every 0.5 seccond. An avi animation file is automaticaly produced to visualize the result of TDA. Instant views of the results are shown on Figure 6.4. Generaly, the simulation showed that both system behaves similar way. The blowing curtain system shows better methane dilution efficiency compared to the exhaust curtain.

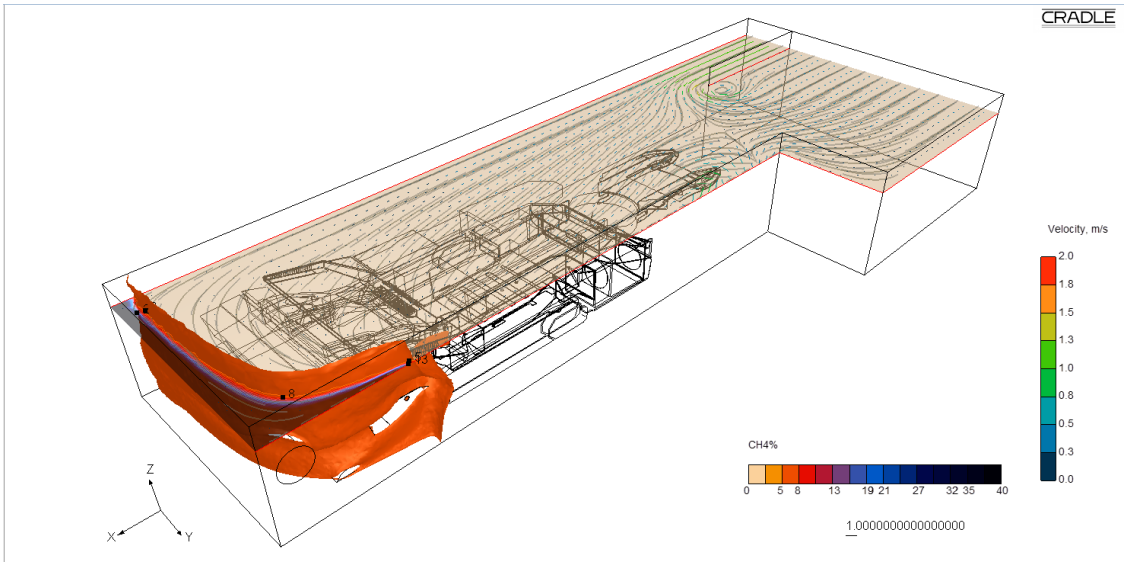

(a) Blowing curain scenario

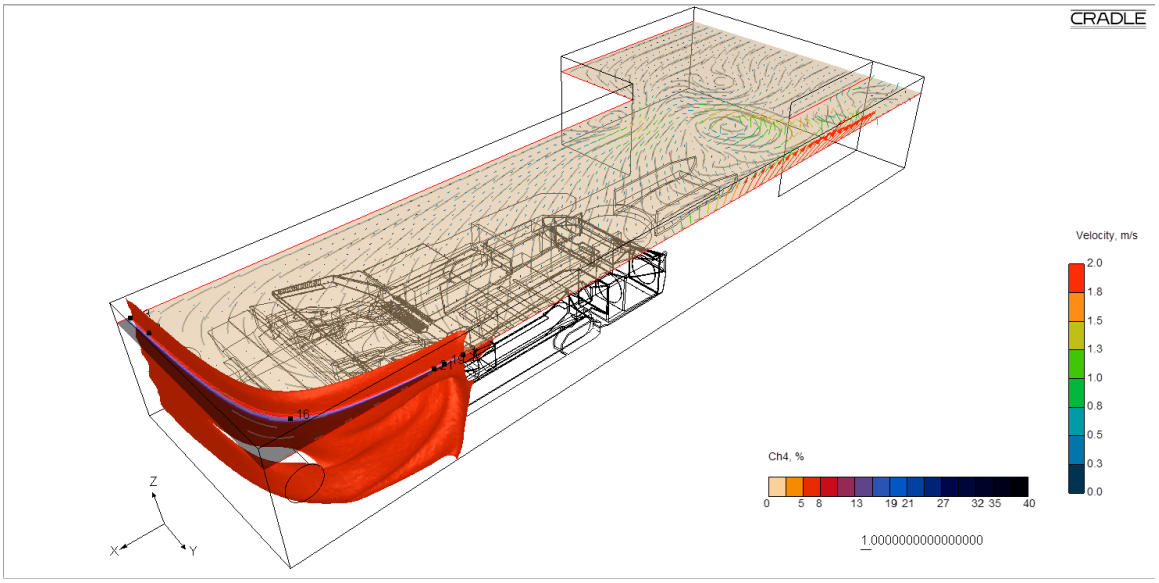

(b) Exhaus curtain scenario

Figure 6.2. Steady state simulation results for scrubber effect on methane dilution. The red collor represents methane concentration isosurface of 5%

The results shown on Figure 6.2 combined air velocity vector map with merthane concentration contour map at horizontal plan above the CM body and 3D isosurface of 5% methane.

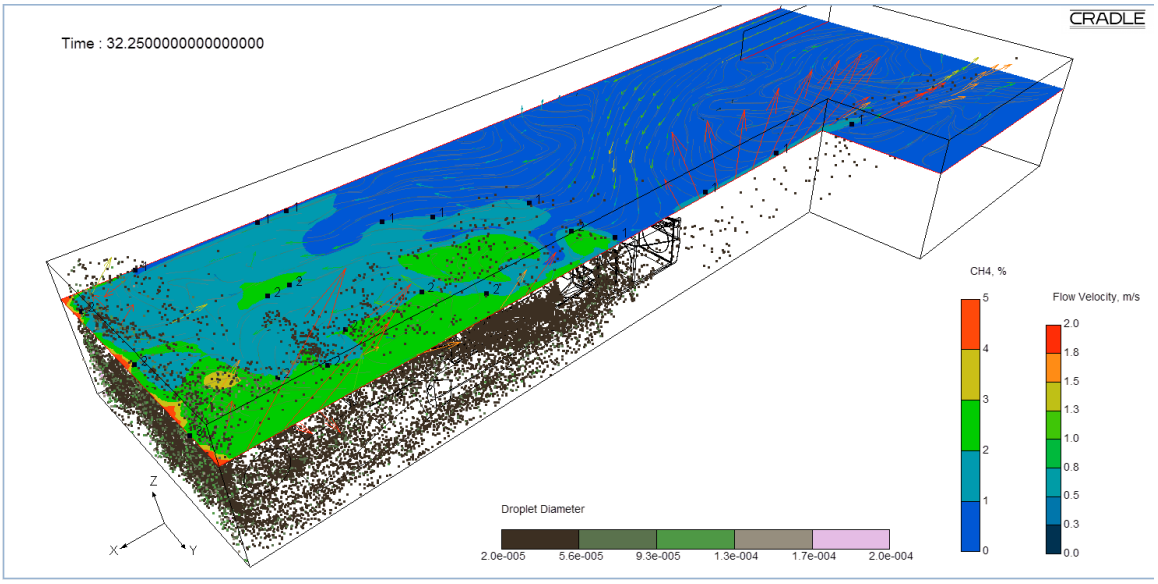

Figure 6.3. Instant view of blowing curtain time dependent simulation results, 32 seconds after spray system was turned on.

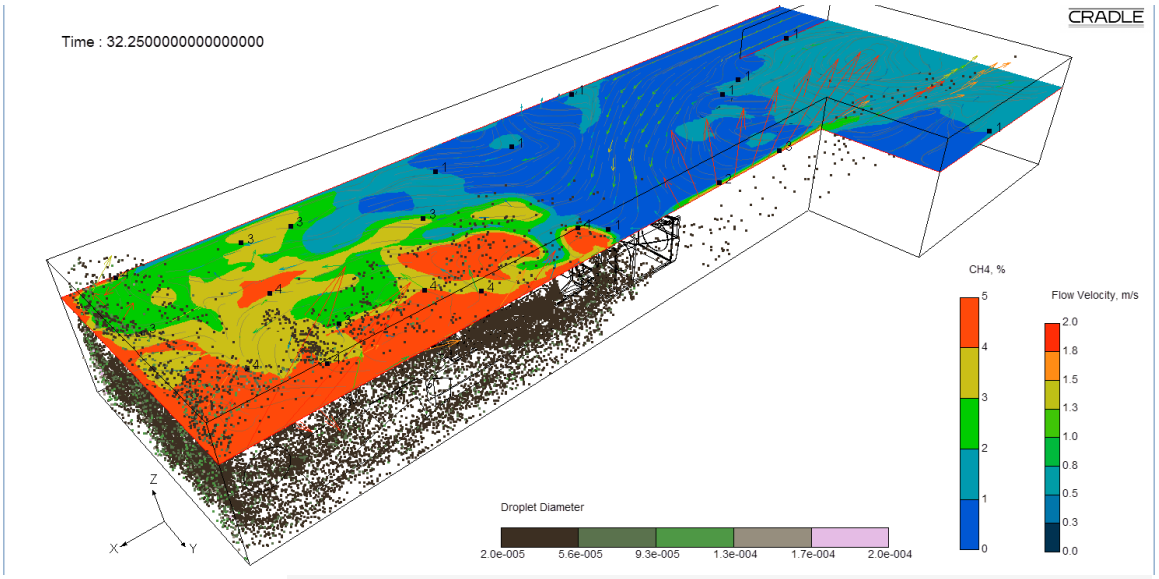

Figure 6.4. Instant view of exhaust curtain time dependent simulation results, 32 seconds after spray system was turned on.

The results shown on Figures 6.3 and 6.4 depicted air velocity vector map and methane concentration contour map at horizontal plane above the miner. The dots reprepresents water spray droplets. The different collor of the dots indicate droplet size diameter in range of 20 to 200 microns.

6.2. Example CFD Analysis of the effect of a Machine Mounted Scrubber and Spray System on Dust Concentration During Deep Cut Ventilated by Exhaust Curtain

This simulation example follows the setup of an experimental study conducted by Organiscak and Beck (2010) but with some significant differnces. The CM model, the scrubber and the spray system differ from the orignaly applied in the study. The geometry of the entry differ in the tight rib distance, that was simulated to be 1.2 m (4 ft) instead of two feet. The entry height was simulated to 2.0 m (6.5 ft). The flux boundary conditions and the location of the dust monitoring station are similar to the experimental study, see Figure 6.5.

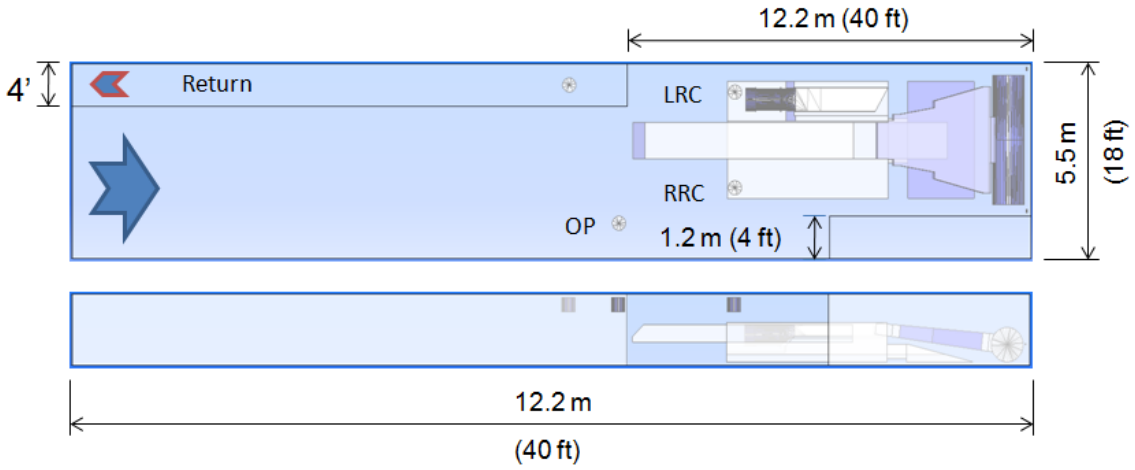

Figure 6.5. Simulation setup with displayed dust monitoring stations at the operator place (OP), at the reaturn, at the left rear corner of the CM (LRC), and at the right rear corner of the CM. (RRC).

The input data for this scenario are as follow:

- Tight rib distance: 1.2 m (4 ft)
- Entry width: 5.5 m (18 ft)
- Intake flow rate: 2.9 m^3/s (6150 cfm)
- Scrubber flow rate: 2.27 m3/s (4810 cfm)
- Dust mass flow: 0.42 g/s
- Spray system: see Table 6-2

Coal dust particles were generated along the front side of the cutting drum. Simulation result of coal dust generation without water spray is shown on Figure 6.6. The particle size distribution was simulated in the range of 1 to 5 microns. Figure 6.7 shows simulation results with water spray and dust particles droplets. For convinience, the water drops are represented in blue color, while the dust particles are in red.

Table 6-2. Spray system data

Number of spray nozzles	23
Geometry configuration	• 15 boom sprays directed at the top of the rotating drum • 3 under boom sprays directed at the loading pan • 3 sprays on each side of the cutter directed at the drum's end rings • 2 blocking sprays positioned apart on each side of the mining machine body located two feet outby the scrubber inlet and two feet above the floor.
Nozzle Type (spray pattern)	Full cone
Water Line Pressure	1,103 kPa
Water Flow	3 litres/min
Orifice size	1.98 mm (0.078")
Spray angle	77 deg
Mean Droplet Velocity	10 m/s
Droplet Souter Mean Diameter	100 microns

The effect of the scrubber on the flow was simulated. No scrubber dust removal efficiency was simulated. This simulation was performed to demonstrate the ability of the dust monitoring station model, described in Chapter 4, 4.5. The averaged respirable dust concentration and mass fraction distributions in specified locations around the continuous miner were counted using a set of monitoring stations. The dust concentration on the operator position was monitored using a cylindrical monitoring station situated on the expected location of its head. Using the results recorded at the selected dust monitoring stations, the dust concentrations at the return, at the scrubber inlet, at the operator position (OP), and at the left (LRC) and right (RRC) rear corner of the continuous miner were assessed, see Table 6-3. Using the data recorded for every time step of the simulation, the average mass fraction distribution at the selected locations were determined, see Figure 6.8. Note, that at the operator position (OP) the counted dust particles were represented by the smallest two particle size classes. At the RRC, the particle distribution accounts an additional class size from 1.7 to 2.5 μm, which is representative for this location. The particles counted at the LRC are represented by four size classes.

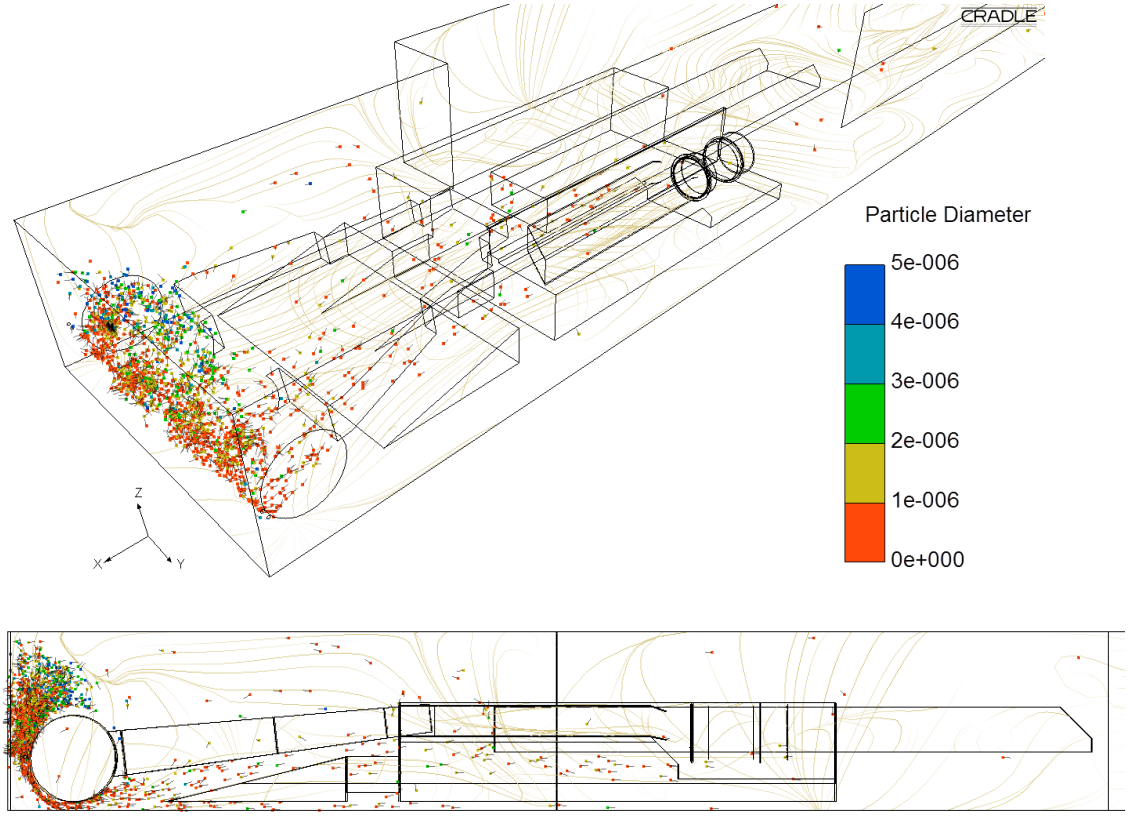

Figure 6.6. Dust particles generation without spray

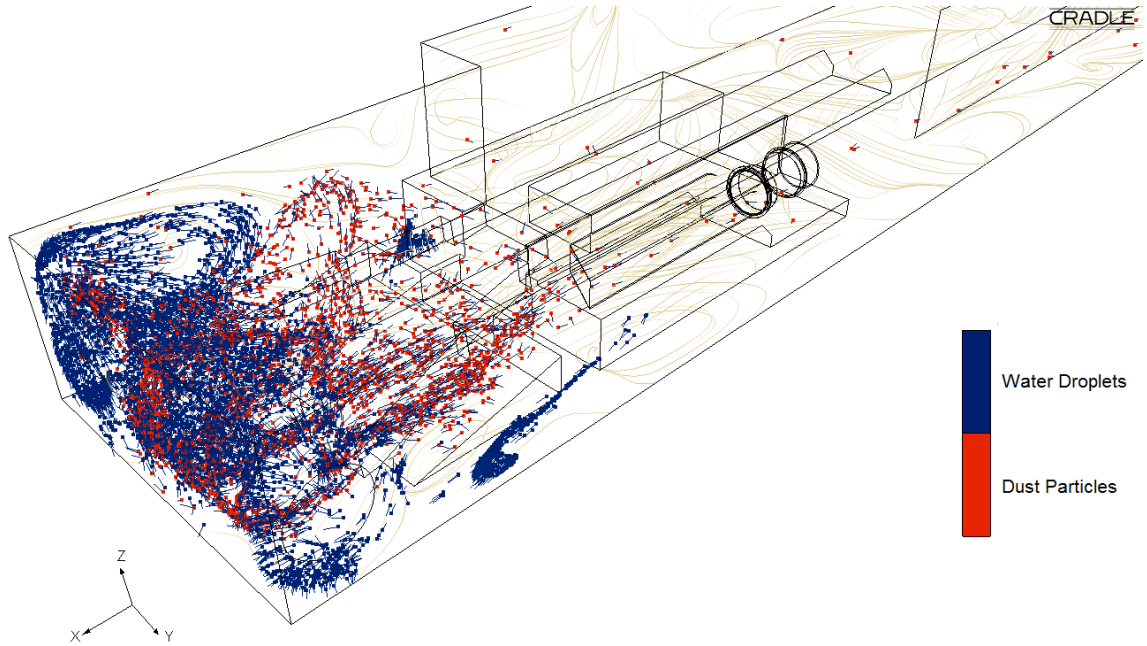

Figure 6.7. Interaction between the dust particles and spray droplets.

Table 6-3. CFD results at the dust monitoring stations

Location	Volume Flux (m^3)	Particle Mass (g)	Dust Concentration (mg/m^3)
Return	1741	22.72	13.1
Scrubber	1365	62.98	46.1
LRC	708	0.398	0.6
RRC	498	0.056	0.1
OP	630	0.035	0.1

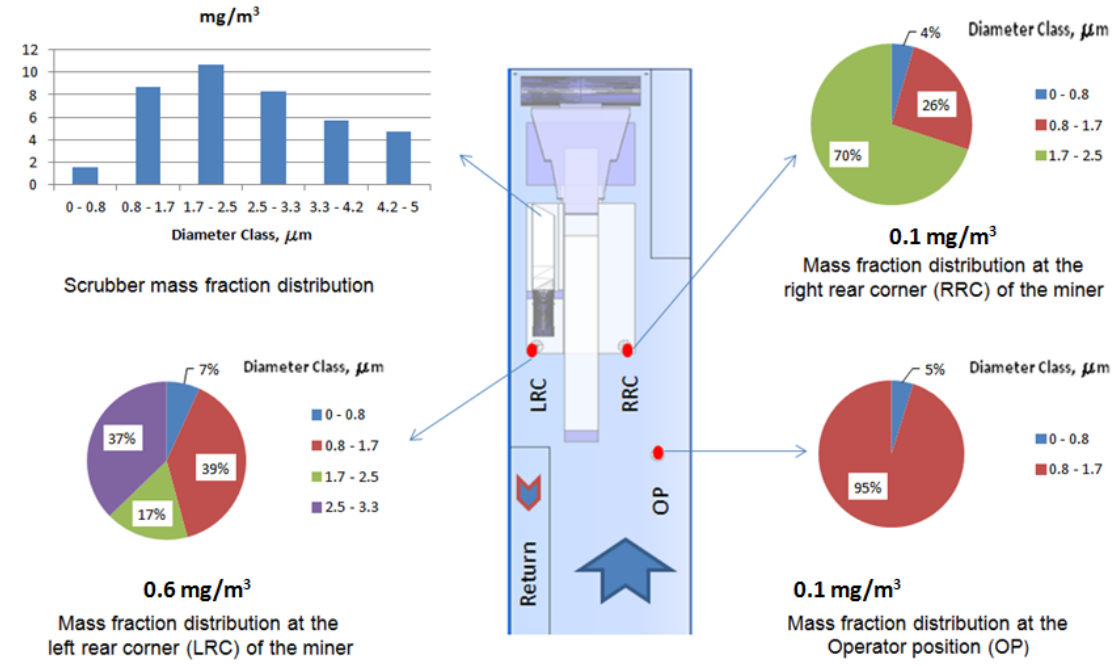

Figure 6.8. Particle mass fraction distribution analysis

At the LRC location, the size classes 0.8-1.7 μm and 2.5-3.3 μm formed 76% of the particle mass fractions. The full spectra of particle sizes are counted at the scrubber inlet. The smallest particles formed only 5% of the particle mass passed trough the scrubber while the particles with size between 1 μm and 3 μm formed about 70% of it.

The simulation showed that the most significant effect of collisions between the particles is coalescence. he lowest dust level was found at the simulated operator position on the off-curtain side of the entry, parallel to the inlet end of the exhaust curtain. The representative mass fraction of the dust captured at the operator position consist of particles with size less than 2 μm. The proposed model illustrates the benefits of using CFD for dust control analysis. This model provides a basis for further development. However, needs to be validated.

6.3. Application of CFD Analysis to Predict the Performance of a Newly Designed Device for Improvement of Face Ventilation

To prevent the airflow separation with a blowing curtain, a passive regulator that allows proper airflow into the cutting zone during deep cut mining have been proposed (Petrov and Wala. 20014). This regulator was designed to enhance the safety and health of the workers and benefit the productivity. The idea is to apply an airfoil called a Wing Regulator WR at the discharge of the blowing curtain designed to prevent airflow separation resulting in:

- Three to five times more air for methane dilution compared to the current applications of blowing curtain, thus enhancing safety.
- Shelter space for the remote miner's operator, to protect him from dust's rollback and dynamic effect of the intake jet, thus enhancing health conditions.
- Ventilating a two-pass 12 m (40 ft) extended cut, instead of four, thus enhancing safety and productivity.

CFD simulation results for equipment free entry with and without the proposed Wing regulator are shown on Figure 6.9. The simulation results shown on Figure 6.9 were confirmed by laboratory studies, using scaled physical model and by field tests in mining environment. Later on, CFD analysis was performed to study the effect of the WR on the methane dilution and dust distribution. The developed CM models were used in this study as well as the developed FVS code was utilized. Model of the WR was added for the needs of the study. First a typical cut with a CM in place was simulated with a machine mounted scrubber and spray system. Methane gas was introduced using the developed porous media model. A SSA was performed first, with scrubber turned on. The model passed mesh adaptaion analysis and the results were used as input data for TDA with spray system included. Time dependen simulations with duration of 60 secconds were performed first without the WR and then with the WR, see Figure 6.10. The simulation results showed significant improvement in methane dilution when the WR was applied.

To study the effect of the wing regulator on the dust distribution, simulations with SF6 tracer gas were performed. The visualisation of SF6 concentrations is used to indicate the potential dust rollback at the face area. A series of TDA with spray system and scrubber were performed. Results indicated, that the WR has a potential to reduce the dust concentration at the positions of the miner operator and the shuttle car operator, See Figure 6.11 (a) and (b). The results for reduced scrubber performance (Figure 6.11 (c)), suggested a need for future research of mutual effect of the WR and the machine mounted scrubber and spray system. Results of filed test cobducted durin typical mining operations showed that the application of the WR has potential to decrease the methane at the immediate face area about twice and has a potential to limit the exposure of the CM's operator to respirable dust.

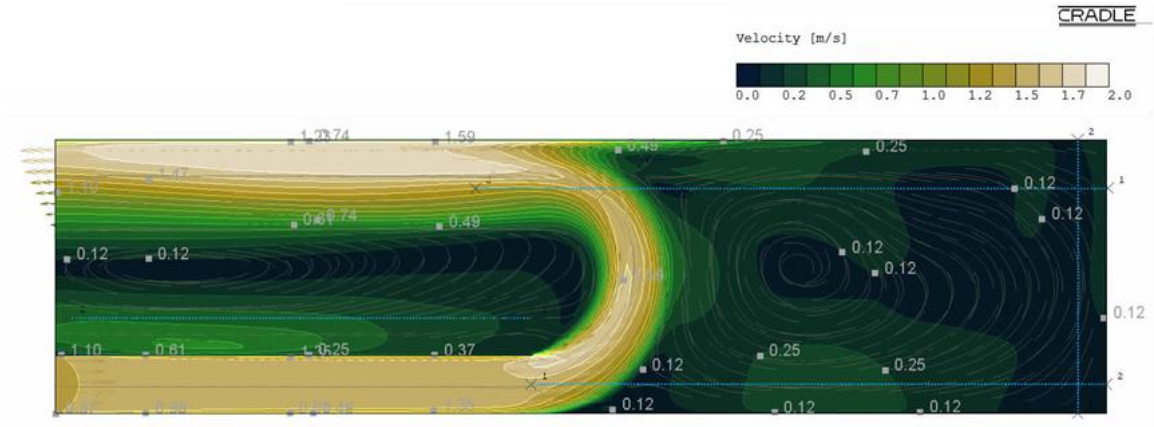

(a) Without the WR

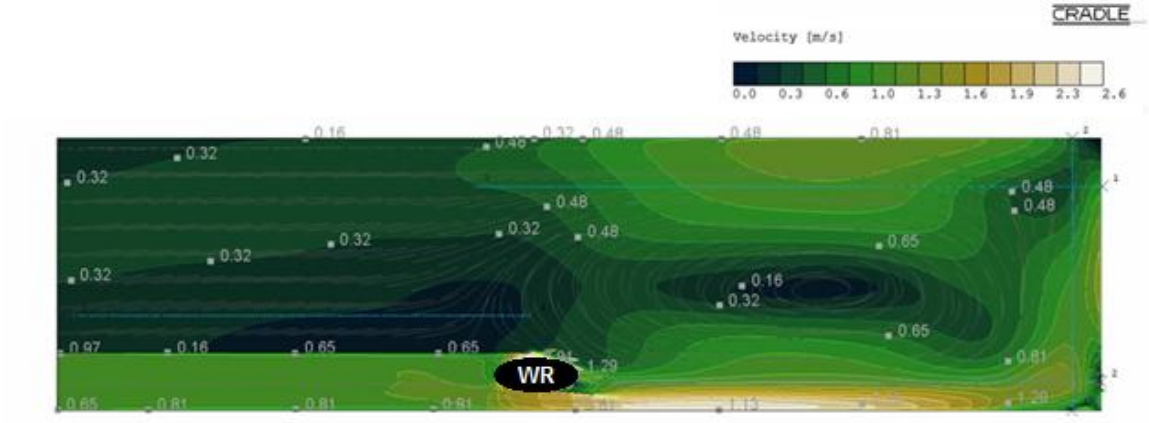

(b) With the WR

Figure 6.9. CFD simulation results for analyis the effect of the WR on the flow patterns in an equipment free entry with 4 ft tight rib distance, 7 ft height and 45 ft curtain setback distance to the face.

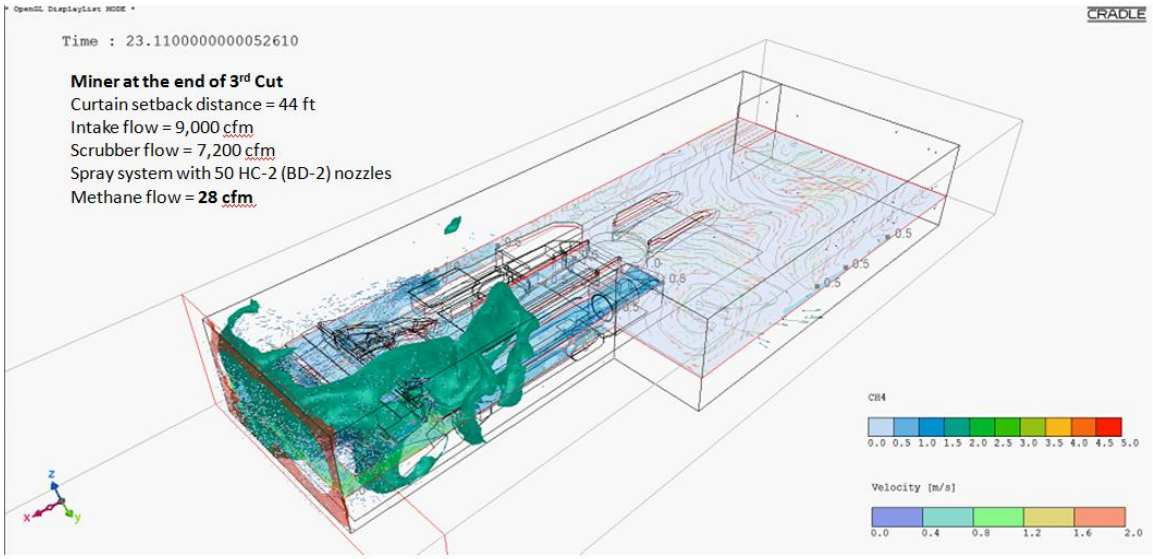

a) Without the WR

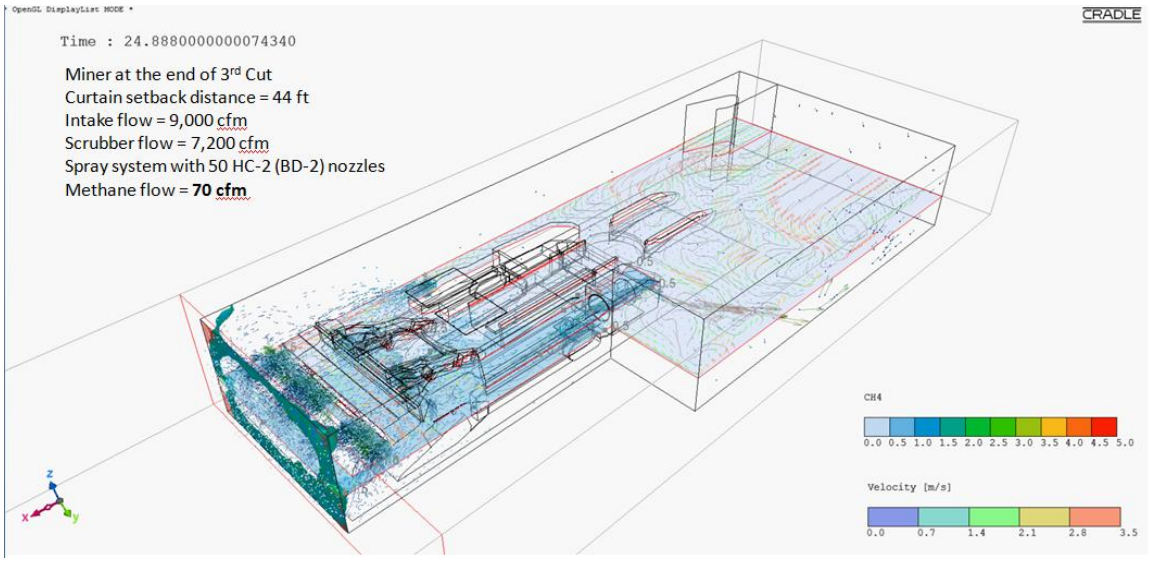

(b) With the WR

Figure 6.10. CFD results of time dependent analysis for the effect of the WR on methane dilution face area.

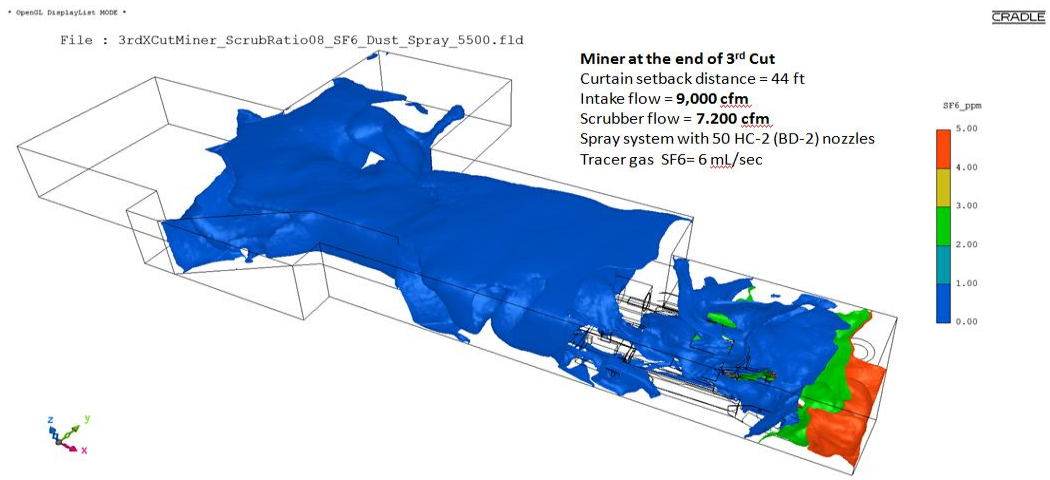

(a) Without the WR and scrubber to face ventilation ratio = 80%

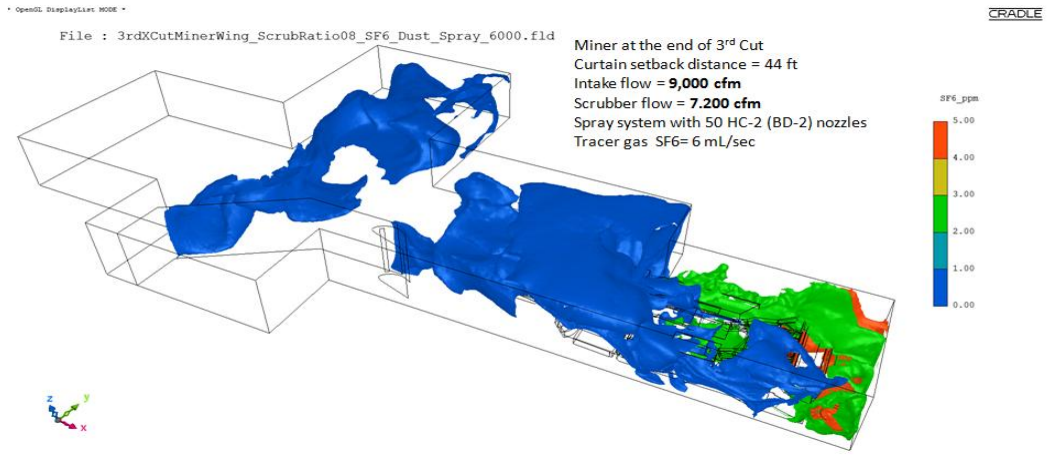

(b) With the WR and scrubber to face ventilation ratio = 80%

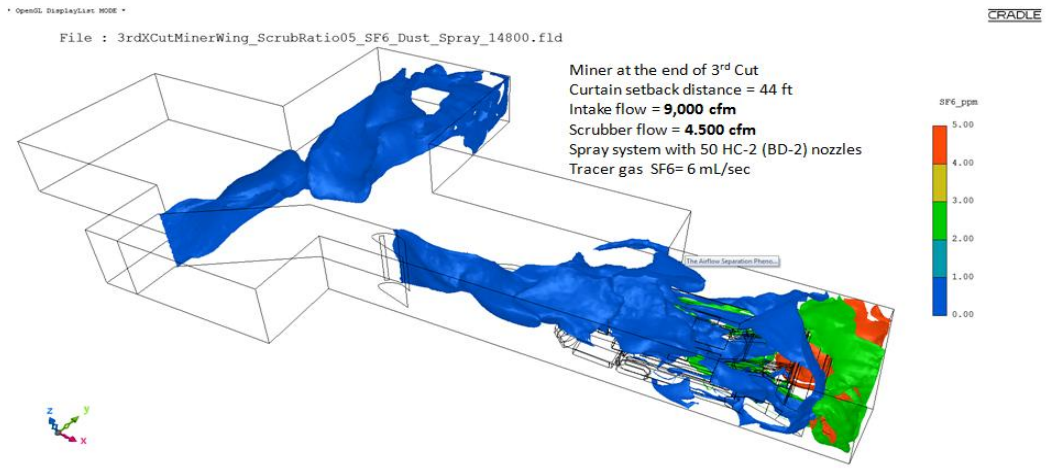

(c) With the WR and scrubber to face ventilation ratio = 50%

Figure 6.11. Simulation results with SF6 tracer gas distribution to indicate potential dust rollback with and without the WR.

Chapter 7

CONCLUSIONS AND FUTURE WORK

7.1 Conclusisons

In the course of this project, work dedicated to the completion of the following tasks was done:

A. Validation of the SC/Tetra Cradle CFD code using available data as published by Wala et al., (2000 and 2001), Turner et al., (2002), Taylor et al., (2005), Chilton et al., (2006) and Wala et al., (2006, 2007 and 2008), needed for the development of the industry oriented code for analysis and design of face ventilation systems. The Cradle CFD code was successfuly validated for flow and methane distribution using experimental data for equipment free entry face ventilation systems, with CM in place, with scrubber, and with machine mounted spray system. Eight available RANS[7] turbulence models were compared. Generally RNG k-EPS (Renormalization Group Method) performed better. Therefore, the RNG k-e turbulence model (Cradle, 2009; Frish, 1995; Kundu et al., 2002) was selected for further applications. A steady-state flow behavior was assumed for the numerical simulation for validation. A manifold tubing model was developed to simulate the methane release from the face according the experimental information. An additional equation for conservation of diffusive species (simple diffusion) was added to be solved together with the utilized RNG k-EPS turbulence model. Effect of buoyancy is included by switching on the gravity simulation. With the scrubber involved, a good similarity in methane concentrations were observed at the immediate face zone and for the all sampling locations up to 14 ft out by the face. However, discrepancy between the experimental data and the simulated results need to be noticed, especially in the sampling points located in the area spaced 16-20 feet outby the face. There are several possibilities for the observed discrepancies between the simulated results and the experimental data. One of them is that the simulation was performed under SSA conditions, while the flow during the experiment is unsteady. The analysis of flow patterns at the zone of major discrepancy (16-20 ft outby the face) indicated that this is exactly the zone of the primary airstream separation. The flow unsteadiness in this zone is additionally disturbed by the effect of the scrubber, including the recirculation caused by the scrubber exhaust jet. Unfortunately, lack of velocity measurements from experiment is reported by the authors (Wala et al., 2008) which makes the comparison with the simulation results inconclusive. For better understanding of the observed results an extended CFD simulation study was conducted to investigate the impact of the

[7] Reynolds-Averaged Navier Stokes

continuous miner position on the flow and methane dilution. Under the same analysis condition as the validation test, two more scenarios were simulated with the continuous miner turned left (toward curtain side rib) and right (toward off-curtain side rib) on 1.5 degrees in respect of its initial position - parallel to the ribs. The simulation results showed significant changes in methane distribution compared to the initial test. The differences were more significant for the scenario with continuous miner turned toward curtain side rib. For this scenario the simulation showed extended methane concentration zone above the miner spread along the off-curtain side rib. This results indicated that the simulated position of the miner may not correspond exactly with the experimental setup.

The ability of the developed spray model to predict the effect of a machine mounted spray system on methane dilution was validated using experimental data from a full scale experiment conducted by NIOSH (Chilton et al., 2006). The CFD simulations were performed on two stages. In stage one, a SSA was performed to obtain steady state results with developed flow patterns and methane concentrations. This results were used as initial conditions for the next stage that involves TDA with the spray system turned on. The simulation results for methane concentration were recorded in time series using monitoring point located at the same coordinates as the experimental sampling locations. The comparison between the experimental data and the simulation results showed good similarity in flow patterns and methane concentration.

The conducted validation study build confidence in the credibility of Cradle CFD. The knowledge obtained during the development of the CFD models needed for the validation study was used to develop a proper model generation procedure for achieving of grid independent solutions.

B. Parametric study of flow separation phenomenon in the blowing curtain face ventilation systems, which contributed to better understanding of the flow behaviour related to this systems. The analysis showed that The flow separation of the intake flow governs by two parameters, namely curtain tight-rib distance and width of the entry. The air quantity delivered by the line curtain to the face depends on the same two parameters and also on the curtain setback distance. The results of the performed analysis of variance proved that the changes of intake flow rate, the air viscosity and the height of the entry are not significant for the variations of flow separation distance and the air quantity reaching the face. The wall shear stress conditions determined by its roughness is playing role but its effect should be calculated when the primary air-stream is not separated. The research showed that, the airflow separation phenomenon cannot be prevented by increasing the inflow rate. As the flow rate increases positive static pressure builds up in the confined space between the face and the primary air-stream. The primary air-stream separates relatively at the same location, regardless of the intake flow rate. It was observed, that the primary air-stream follows static pressure intercept zone. In order to reveal the relationship between the geometry of the face area and the dynamic

parameters, a scaling analysis using the Law Approach Method (Emory et. al. 2009) was performed. Following the outcomes of the performed parametric study, not the intake air quantity, but the kinetic energy of the inflow stream is the key parameter for the observed airflow behavior. A criterion to predict flow separation called Jet Separation Ratio (JSR), based on the geometry of the face area was derived. Using the experimental and simulation data an empirical threshold value of 0.02 was determined to distinguish the flow separation cases from the flow penetration cases. According this criterion

$$\left.\begin{array}{c} IF \\ \mathrm{JSR} = \left(\frac{d'}{d}\right)^2 > 0.02 \\ \\ \textit{Flow separation will take place regardless of the intake air quantity} \end{array}\right\}$$

where: d' denotes the curtain tight-rib distance; $d = w - d'$; *and* w is the width of the entry.

Unfortunately, for all practical scenarios with line brattice hanged at distance larger than 0.9 m (3 ft) from the rib, airflow separation always take place regardless of the intake air quantity. Scenarios close to the threshold value, such as the 4.6 m (15 ft) entry width and 0.6 m (2 ft) curtain tide-rib distance, showed unsteady behavior of the primary airstream. In such cases, the wall jet will start to flip-flop between the state of flow separation and flow penetration.

The results from the performed parametric study of flow separation phenomenon can be logically extended also to the exhaust curtain face ventilation systems. The specifics is that in exhaust curtain systems the defined JSR is always greater than the threshold value and therefore, the flow separation is the only possible pattern.

C. The results of the analytical and validation studies provided valuable information concerning the parameters that driven the flow behavior in the face area ventilated by line brattice and better understanding of flow separation phenomenon. The obtained knowledge helped in shaping the general assumptions under which the numerical models to be developed, as described in Chapter 5, point 5.3.

D. A number of models for CFD analysis of face ventilation systems were developed using Cradle CFD. This includes models of methane release using porous media, dust generation and monitoring using particle tracking method, continuous miner geometry, scrubers and spray systems typicaly used in coal mining.

To improve the methane release model a particle type of porous media model was implemented to replace the manifold tubes methane release model used so far in the performed validation studies. In assumption that the most significant source of methane

during mining operations is the working face, a porous media volume was implemented for more realistic stimulation of methane release. Attention should be paid in using this model. If flow cannot be fully developed due to lack of length of porous media in the stream wise direction, this model is inappropriate (Cradle, 2009). A particle type of porous media with porosity of 0.25 and diameter of particles 0.0001 m was implemented. A depth of 2.1 m (7 ft) was found to ensure numerical stability of porous media model for this application. This model is not intended to simulate the real porosity of the coal seam around the face, but to involve the whole face area into the methane release process instead of simulating manifold tubes. This model was successfully tested in different simulation scenarios involving SSA and TDA with a continuous miner, scrubber and spray system. So far this model is implemented for face ventilation system analysis.

The roughness of the wall cannot be simulated by porous media model. Modeling the complexity of porous media by treating fluid and solid region separately is impracticable from a viewpoint of computational cost. Thus, the coexistence of fluid and the solid in one element of the computational grid is treated as porous media (Cradle, 2009). Cradle CFD does not consider the configuration of flow path in porous media in calculation. An external force is applied in opposite direction of flow in order to produce pressure loss. Therefore, the wall boundary conditions were not simulated using porous media but log law wall functions.

Because the wall functions are non-flux boundary conditions, methane release by the entry's ribs, roof and floor cannot be simulated using the wall surfaces. A practical approach to introduce the amount of the methane released by the walls into the computational domain is to modify the intake flux boundary conditions and add this amount to the intake methane concentration. Then, by performing an SSA the methane distribution will be computed according the assigned boundary conditions. This prime results will contain the methane concentrations across the entire domain in fully developed flow and can be used as initial conditions for further time dependent CFD analysis.

The use of scrubbers as air moving device to help methane dilution into the immediate face area is recognized as one of the primary ventilation controls during the extended cut sequences. For the needs of methane dilution analysis several models of scrubbers with different geometry were built and tested. For methane dilution analysis, modeling of dust filter elements and their effects on the flow and the pressure distribution inside of the scrubber is not required. In this assumptions the scrubbers model can be reasonably simplified and simulated by utilizing the provided by Cradle CFD fan source model. For this type of analysis the scrubber flow rate is the most important parameter to simulate the flow and methane distribution into the face area. The performed CFD simulation study showed that the configuration of the scrubber inlets and exhaust have significant impact on the flow patterns and accordingly on the methane distribution not only at the immediate face area but also behind the continuous miner.

Respirable dust generation model was developed and implemented for face ventilation system analysis. The dust generation surface region was assumed to be the outer ambient surface of the continuous miner's cutting head. Simulation of the dust distribution uses the built-in Cradle CFD particle tracking method. To simulate the size distribution of respirable coal dust a theoretical lognormal statistical distribution was adopted. This distribution is widely applied in the description of natural phenomena including particle size distribution of aerosols (Cooper 1982, Raabe 1971). Following the findings of a research study about the representative size distribution of the respirable bituminous coal dust (Dick et.al., 1996), the recommended settings for respirable dust generation model are: lognormal distribution for particle size in range of 0.1 to 5 microns; mean size m = 0.68 microns; and variance v = 0.14.

To simulate the dust removal efficiency of a scrubber, the previously developed scrubber model used for flow and gas control simulations was enhanced for dust control analysis. A user function for Cradle's SC/Tetra CFD writhen in C language was developed for this purpose. The function combines the dust generation model and the scrubber dust removal efficiency control. The input data required for the function are provided into the standard SC/Tetra "s" file that contains the analysis conditions. By default, the function utilizes the described above dust generation model. The required user input is the scrubber dust removal efficiency in percents. Optionally, the particle size distribution parameters of the dust particles to be generated can be altered.

To incorporate the water spray systems into the CFD analysis of face ventilation systems numerical descriptions of the commonly used on the continuous miners spray nozzles were developed. The spray model was developed in assumptions that the spray droplets influenced the flow and interact to each other. The built-in Cradle CFD spray model utilizing particle tracking method was adopted for the development. This method is recognized as the most widely used for spray modeling and has the advantage of being computationally cheaper than the Eulerian method, where the droplets flow is modeled as a continuum. Moreover, the particle tracking approach does not require exact modeling of the spray nozzle geometry, which usually is a proprietary information.

E. The developed models were implemented for steady state and time dependent CFD analysis of flow behaviour, methane dilution and dust control in face ventilation systems. Results of latest CFD simulation study of methane dilution ability of face ventilation systems performed under TDA conditions confirmed the unsteadiness of the flow in the discussed above zone (around the rear part of the continuous miner). This result suggested the future CFD simulation studies for methane dilution that involve scrubbers to be supplemented with TDA using SSA results as initial conditions. This approach is definitely more time consuming but combined with proper model development procedure concerning generation of grid independent results can ensure getting accurate CFD prediction.

F. Code was developed to automate the face ventilation simulation process using the built in Cradle CFD Microsoft COM. This involve Visual Basic (VB) interface and built-in mechanism to incorporate user defined functions written in C language to handle the SC/Tetra functions as methods and variables.

G. A passive regulator, called Wing Regulator (WR) was designed to prevent flow separation phenomenon and improve the safety and health conditions in face ventilation systems. The proposed WR is a subject of international IPT - U.S. patent pending.

7.2 Novel Contributions

In the course of the research several novel contributions were achieved regarding face ventilation system analysis, design and improvement.

- This research presents to the academia, NIOSH, MSHA, and the industry a well supported methodology to analyse and design of face ventilation systems utilizing Computational Fluid Dynamics code.
- A new comercial CFD code copyright © Cradle Co., called SC/Tetra Thermofluid Analysis System with Unstructured Mesh Generator was successfuly validated against experimental data. The credibility of the developed CFD models of face ventilation systems for flow behaviour and methane dilution analysis, that involve continuous miner machines, scrubbers, and spray systems was tested and confirmed.
- Three dimensional simulation models for time dependen analysis of face ventilation system were developed including simulation of cutting drum rotation, scrubbers, spray system, methane control and dust control simulation using particle tracking method.
- Code for automation of CFD simulations process of of face ventilation system including meshing, solving and postprocessing of the simulation results was developed using the built-in Cradle CFD Visual Basic Interface and C language User Functions.
- Parametric study of flow behavior of line brattice face ventilation systems was performed to investigate which parameters govern the airflow separation. A criterion to predict flow separation called Jet Separation Ratio (JSR), based on the geometry of the face area was derived.
- An inovative solution for improvement of blowing curtain face ventilation systems using passive regulator was proposed and succesfuly tested in mining evironment.

7.3 Future Work

The vision for future work involves three possible avenues of research.

First, further development and CFD code validation of the suggested dust control simulation model. This includes:

- Validation of the ability of the developed model to predict the dust removal efficiency of the sprays.
- Calibration the repulsion coeficcients of the surraunding walls, floor, roof, and the equipment surfaces to improve the accuracy of the prediction.
- Additional research is required to develop methodology for prediction of respirable dust concentration based on the measured cocentration of tracer gases, such as SF6, for the specific conditions of coal mine workings.
-

Second, continuation of the FVS development. This includes:

- Futher development of CFD models for time dependent analysis of methane dilution and dust control of face ventilation systems.
- Additional research and validation work is recommended for improvement of the methane release model by using porous media. Cradle CFD provides some other isotropic and anisotropic porous media models (Cradle, 2009-2014) that could be utilized in the future for improvement the accuracy of the models.
- Incorporating into the models available and newly created ventilation and dust control devices, such as aircurtains, air movers, water atomizers, spray systems, etc. trough testing and validation.

Third, research dedicated to further improvement of the face ventilation systems with use of the proposed WR trough optimisation of the scrubber performance and spray system setup.

==========

Matlab program to implement ANOVA method for face ventilation system analysis

==========

MATLAB PROGRAMM - ANOVAN k^7

```
     Qef =     [0.36  0.08     0.36     0.00     0.40     0.08
0.34     0.00     0.17     0.00     0.25     0.00     0.16
0.00     0.12     0.00     0.38     0.12     0.33     0.01
0.37     0.04     0.34     0.00     0.17     0.00     0.25
0.00     0.17     0.00     0.25     0.00     0.04     0.00
0.06     0.00     0.12     0.00     0.04     0.00     0.13
0.00     0.08     0.00     0.13     0.00     0.08     0.00
0.03     0.02     0.06     0.00     0.14     0.00     0.06
0.00     0.13     0.00     0.07     0.00     0.06     0.00
0.08     0.00     0.41     0.28     0.41     0.01     0.37
0.08     0.38     0.00     0.36     0.00     0.35     0.00
0.36     0.00     0.36     0.00     0.36     0.30     0.41
0.16     0.37     0.06     0.00     0.00     0.36     0.00
0.35     0.00     0.36     0.00     0.35     0.00     0.19
0.00     0.20     0.00     0.00     0.00     0.24     0.00
0.20     0.04     0.28     0.00     0.23     0.04     0.28
0.00     0.22     0.06     0.26     0.00     0.21     0.04
0.21     0.00     0.20     0.05     0.20     0.00     0.18
0.03    0.20    0.00];
     QefRESIDUALS =     [0.08 0.34     0.17     0.25     0.16
0.12     0.12     0.33     0.37     0.34     0.17     0.25
0.17     0.25     0.12     0.13     0.13     0.14     0.13
0.28     0.35     0.30     0.16     0.35     0.35     0.19
0.20     0.24     0.20     0.28     0.23     0.28     0.22
0.26    0.21    0.21    0.20    0.20    0.18    0.20];
     Xsep = [1.00     0.66     0.99     0.63     0.99     0.70
0.99     0.53     0.61     0.36     0.99     0.41     0.61
0.35     0.79     0.41     1.00     0.74     0.99     0.71
1.00     0.70     0.99     0.58     0.61     0.35     0.99
0.41     0.61     0.36     0.99     0.40     0.11     0.06
0.12     0.07     0.12     0.06     0.14     0.07     0.12
0.06     0.12     0.07     0.12     0.06     0.14     0.07
0.11     0.06     0.12     0.07     0.11     0.06     0.12
0.07     0.12     0.06     0.12     0.07     0.12     0.06
0.12     0.07     1.00     1.00     1.00     0.71     1.00
0.89     1.00     0.53     0.99     0.55     0.99     0.41
0.99     0.55     0.99     0.41     1.00     1.00     1.00
```

```
0.89      1.00      0.92      0.00      0.47      0.99      0.55
0.99      0.42      0.99      0.55      0.99      0.41      0.20
0.10      0.28      0.00      0.00      0.00      0.28      0.11
0.19      0.10      0.28      0.11      0.19      0.10      0.30
0.11      0.18      0.10      0.28      0.11      0.20      0.10
0.28      0.10      0.19      0.11      0.28      0.11      0.19
0.10    0.29    0.11];
     w =    [12  12  12  12  12  12  12  12  12  12  12  12
12  12  12  12  12  12  12  12  12  12  12  12  12  12
12  12  12  12  12  12  12  12  12  12  12  12  12  12
12  12  12  12  12  12  12  12  12  12  12  12  12  12
12  12  12  12  12  12  12  20  20  20  20  20  20  20  20
20  20  20  20  20  20  20  20  20  20  20  20  20  20
20  20  20  20  20  20  20  20  20  20  20  20  20  20
20  20  20  20  20  20  20  20  20  20  20  20  20  20
20  20  20  20  20  20  20  20  20  20  20];
     d =    [1   1   1   1   1   1   1   1   1   1   1   1
1   1   1   1   1   1   1   1   1   1   1   1   1   1
1   1   1   1   1   4   4   4   4   4   4   4   4   4
4   4   4   4   4   4   4   4   4   4   4   4   4   4
4   4   4   4   4   4   4   1   1   1   1   1   1   1   1
1   1   1   1   1   1   1   1   1   1   1   1   1   1
1   1   1   1   1   1   1   1   1   4   4   4   4   4   4
4   4   4   4   4   4   4   4   4   4   4   4   4   4
4   4   4   4   4   4   4   4   4   4   4];
     Q = [2700    2700      2700      2700      2700      2700
2700      2700      2700      2700      2700      2700      2700
2700      2700      2700      5500      5500      5500      5500
5500      5500      5500      5500      5500      5500      5500
5500      5500      5500      5500      5500      2700      2700
2700      2700      2700      2700      2700      2700      2700
2700      2700      2700      2700      2700      2700      2700
5500      5500      5500      5500      5500      5500      5500
5500      5500      5500      5500      5500      5500      5500
5500      5500      2700      2700      2700      2700      2700
2700      2700      2700      2700      2700      2700      2700
2700    2700    2700
     2700     5500     5500     5500     5500     5500     5500
5500      5500      5500      5500      5500      5500      5500
5500      5500      5500      2700      2700      2700      2700
2700      2700      2700      2700      2700      2700      2700
2700      2700      2700      2700      2700      5500      5500
5500      5500      5500      5500      5500      5500      5500
5500    5500    5500    5500    5500    5500    5500];
     wall =    {'Smooth' ; 'Smooth' ; 'Smooth' ; 'Smooth' ;
'Smooth' ; 'Smooth' ; 'Smooth' ; 'Smooth' ; 'Rough' ;
'Rough' ;  'Rough' ;   'Rough' ;   'Rough' ;   'Rough' ;
```

```
'Rough' ;    'Rough' ;    'Smooth' ;   'Smooth' ;   'Smooth' ;
'Smooth' ;   'Smooth' ;   'Smooth' ;   'Smooth' ;   'Smooth' ;
'Rough' ;    'Rough' ;    'Rough' ;    'Rough' ;    'Rough' ;
'Rough' ;    'Rough' ;    'Rough' ;    'Smooth' ;   'Smooth' ;
'Smooth' ;   'Smooth' ;   'Smooth' ;   'Smooth' ;   'Smooth' ;
'Smooth' ;   'Rough' ;    'Rough' ;    'Rough' ;    'Rough' ;
'Rough' ;    'Rough' ;    'Rough' ;    'Rough' ;    'Smooth' ;
'Smooth' ;   'Smooth' ;   'Smooth' ;   'Smooth' ;   'Smooth' ;
'Smooth' ;   'Smooth' ;   'Rough' ;    'Rough' ;    'Rough' ;
'Rough' ;    'Rough' ;    'Rough' ;    'Rough' ;    'Rough' ;
'Smooth' ;   'Smooth' ;   'Smooth' ;   'Smooth' ;   'Smooth' ;
'Smooth' ;   'Smooth' ;   'Smooth' ;   'Rough' ;    'Rough' ;
'Rough' ;    'Rough' ;    'Rough' ;    'Rough' ;    'Rough' ;
'Rough' ;    'Smooth' ;   'Smooth' ;   'Smooth' ;   'Smooth' ;
'Smooth' ;   'Smooth' ;   'Smooth' ;   'Smooth' ;   'Rough' ;
'Rough' ;    'Rough' ;    'Rough' ;    'Rough' ;    'Rough' ;
'Rough' ;    'Rough' ;    'Smooth' ;   'Smooth' ;   'Smooth' ;
'Smooth' ;   'Smooth' ;   'Smooth' ;   'Smooth' ;   'Smooth' ;
'Rough' ;    'Rough' ;    'Rough' ;    'Rough' ;    'Rough' ;
'Rough' ;    'Rough' ;    'Rough' ;    'Smooth' ;   'Smooth' ;
'Smooth' ;   'Smooth' ;   'Smooth' ;   'Smooth' ;   'Smooth' ;
'Smooth' ;   'Rough' ;    'Rough' ;    'Rough' ;    'Rough' ;
'Rough' ;   'Rough' ;   'Rough' ;   'Rough'};
     viscos =  {'Standard' ;     'Standard' ;     'Standard'
;      'Standard' ;      'Hi' ;   'Hi' ;   'Hi' ;   'Hi' ;
'Standard' ;     'Standard' ;     'Standard' ;     'Standard'
;       'Hi' ;    'Hi' ;    'Hi' ;    'Hi' ;    'Standard' ;
'Standard' ;      'Standard' ;      'Standard' ;      'Hi' ;
'Hi' ;   'Hi' ;   'Hi' ;   'Standard' ;      'Standard' ;
'Standard' ;      'Standard' ;      'Hi' ;   'Hi' ;   'Hi' ;
'Hi' ;   'Standard' ;      'Standard' ;      'Standard' ;
'Standard' ;     'Hi' ;   'Hi' ;   'Hi' ;   'Hi' ;   'Standard'
;     'Standard' ;     'Standard' ;     'Standard' ;     'Hi' ;
'Hi' ;   'Hi' ;   'Hi' ;   'Standard' ;      'Standard' ;
'Standard' ;      'Standard' ;      'Hi' ;   'Hi' ;   'Hi' ;
'Hi' ;   'Standard' ;      'Standard' ;      'Standard' ;
'Standard' ;     'Hi' ;   'Hi' ;   'Hi' ;   'Hi' ;   'Standard'
;     'Standard' ;     'Standard' ;     'Standard' ;     'Hi' ;
'Hi' ;   'Hi' ;   'Hi' ;   'Standard' ;      'Standard' ;
'Standard' ;      'Standard' ;      'Hi' ;   'Hi' ;   'Hi' ;
'Hi' ;   'Standard' ;      'Standard' ;      'Standard' ;
'Standard' ;     'Hi' ;   'Hi' ;   'Hi' ;   'Hi' ;   'Standard'
;     'Standard' ;     'Standard' ;     'Standard' ;     'Hi' ;
'Hi' ;   'Hi' ;   'Hi' ;   'Standard' ;      'Standard' ;
'Standard' ;      'Standard' ;      'Hi' ;   'Hi' ;   'Hi' ;
'Hi' ;   'Standard' ;      'Standard' ;      'Standard' ;
'Standard' ;     'Hi' ;   'Hi' ;   'Hi' ;   'Hi' ;   'Standard'
```

```
;    'Standard' ;    'Standard' ;    'Standard' ;    'Hi' ;
'Hi' ;   'Hi' ;   'Hi' ;   'Standard' ;      'Standard' ;
'Standard' ;     'Standard' ;     'Hi' ;   'Hi' ;   'Hi' ;
'Hi'};
     h = [1  1   2.13    2.13    1   1   2.13    2.13    1
1   2.13    2.13    1   1   2.13    2.13    1   1   2.13
2.13    1   1   2.13    2.13    1   1   2.13    2.13    1
1   2.13    2.13    1   1   2.13    2.13    1   1   2.13
2.13    1   1   2.13    2.13    1   1   2.13    2.13    1
1   2.13    2.13    1   1   2.13    2.13    1   1   2.13
2.13    1   1   2.13    2.13    1   1   2.13    2.13    1
1   2.13    2.13    1   1   2.13    2.13    1   1   2.13

     2.13    1   1   2.13    2.13    1   1   2.13    2.13
1   1   2.13    2.13    1   1   2.13    2.13    1   1
2.13    2.13    1   1   2.13    2.13    1   1   2.13
2.13    1   1   2.13    2.13    1   1   2.13    2.13    1
1   2.13    2.13    1   1   2.13    2.13    1   1   2.13
2.13];
     setback = [35   65  35  65  35  65  35  65  35  65  35
65  35  65  35  65  35  65  35  65  35  65  35  65  35  65
35  65  35  65  35  65  35  65  35  65  35  65  35  65  35
65  35  65  35  65  35  65  35  65  35  65  35  65  35  65
35  65  35  65  35  65  35  65  35  65  35  65  35  65  35
65  35  65  35  65  35  65  35  65  35  65  35  65  35  65
35  65  35  65  35  65  35  65  35  65  35  65  35  65  35
65  35  65  35  65  35  65  35  65  35  65  35  65  35  65
35  65  35  65  35  65  35  65];
     names  =  {'w';  'd';  'Q';  'wall';  'viscosity';  'h';
'setback'};
     % Design matrix is 2^k, k=7 level ANOVA
     % k=7;
     % ff2n(k)
     % ANOVA 1
     [p1  tbl1  stats1  terms1]  =  anovan(Qef,{w  d  Q  wall
viscos h setback},1,3, names)
     [p1X tbl1X stats1X terms1X] = anovan(Xsep,{w d Q wall
viscos h setback},1,3, names)
     % ANOVA 2 - more parsimonious model
     [p2  tbl2  stats2  terms2]  =  anovan(Qef,{w  d  setback
wall},  'model',  2,  'varnames',  {'w';  'd';  'setback';
'wall'})
     [p2X tbl2X stats2X terms2X] = anovan(Xsep,{w d setback
wall},  'model',  2,  'varnames',  {'w';  'd';  'setback';
'wall'})
     % ANOVA 3 - more parsimonious model
```

```
    %[p3 tbl3 stats3 terms3] = anovan(Qef,{w d setback
wall}, 'model', 3, 'varnames', {'w'; 'd'; 'setback';
'wall'})
    % ANOVA 4 - more parsimonious model
    [p4 tbl4 stats4 terms4] = anovan(Qef,{w d setback
wall}, 'model', 4, 'varnames', {'w'; 'd'; 'setback';
'wall'})
    [p4X tbl4X stats4X terms4X] = anovan(Xsep,{w d setback
wall}, 'model', 4, 'varnames', {'w'; 'd'; 'setback';
'wall'})
    % ANOVA 5 - model with random effect
    [p5 tbl5 stats5 terms5] = anovan(Qef,{wall w d
setback}, 'model', 4, 'random', 1, 'varnames',{'wall'; 'w';
'd' ;'setback' })
    figure
    bar(max(0,stats5.varest));
    set(gca, 'xtick',1:9,'xticklabel',stats5.rtnames)
    % Diagnostic check
    figure
    normplot(Qef);
    figure
    normplot(QefRESIDUALS);
    [mu,sigma,muci,sigmaci] = normfit(Qef)
    % Multicompare
    figure
    [p,t,st] = anova1(Qef,Q,'off');
    [mcc,mcm,mch,mcnms] = multcompare(st,'display','on');
    figure
    [p,t,st] = anova1(Qef,viscos,'off');
    [mcc,mcm,mch,mcnms] = multcompare(st,'display','on');
    figure
    [p,t,st] = anova1(Qef,h,'off');
    [mcc,mcm,mch,mcnms] = multcompare(st,'display','on');
    figure
    [p,t,st] = anova1(Qef,wall,'off');
    [mcc,mcm,mch,mcnms] = multcompare(st,'display','on');
    figure
    [p,t,st] = anova1(Qef,d,'off');
    [mcc,mcm,mch,mcnms] = multcompare(st,'display','on');
    figure
    [p,t,st] = anova1(Qef,w,'off');
    [mcc,mcm,mch,mcnms] = multcompare(st,'display','on');
    figure
    [p,t,st] = anova1(Qef,setback,'off');
    [mcc,mcm,mch,mcnms] = multcompare(st,'display','on');
```

```
'================================================
                                    'RegisterRegions.vbs
'================================================

        Set app = CreateObject("SCTpre_Dx64net.Application.10")
        app.Visible = true
        Set doc = app.GetDocument
        folder = path
        doc.OpenMdlFile folder & "\" & model & ".mdl", 0
        Set mdl = doc.GetModel
        mdl.RecognizeClosedVolume count
        cvcount = count-1
        mdl.RegisterVolumeRegionClosedVolume "box", cvcount, 0
        retval = mdl.RegisterSurfaceRegionSurfaceOfClosedVolume("envelop", cvcount, 1, 1, 2)
        For cv = 1 To cvcount
                mdl.SetMatOfClosedVolume cv,1
        Next
        regions = Array("inlet", "inlet2", "outlet", "walls", "face", "curtain")
        For i = 0 To 5
                MsgBox "Mark " & regions(i)
                mdl.RegisterSurfaceRegionMarkedFace regions(i), 0, 0
                mdl.UnmarkFaceAll
                app.UpdateAll
        Next
        doc.SaveMdlFile folder & model & "Prime.mdl"

'================================================
'End of script.
'================================================
```

```
'================================================
                                        'MeshPrime.vbs
'Mesh by OctSize
'================================================

Set app = CreateObject("SCTpre_Dx64net.Application.10")
app.Visible = true
Set doc = app.GetDocument

SimCase = "Miner_Gas"
folder = path
title = model

ro_air = 1.2
mu = 0.000018
y_plus = 100

if air_cond <> "Standard" then
        '-------------------------------------
        'ro_air =  UserData
        ' mu  = UserData
        '-------------------------------------
        'y_plus = ro_air *u_star/mu
end if

u_star = 0.5*Uin
y = mu*y_plus/(ro_air*u_star)
MinOctSize = 3*y
MaxOctSize = MinOctSize

sname =  folder & "\" & title & ".s"
regnname = folder & "\" & title & ".mdl"
octname = folder & "\" & title & ".oct"
surfname = folder & "\" & title & "_meshsurf.mdl"
tetraname = folder & "\" & title & "_tetra.pre"
hybridname = folder & "\" & title & ".pre"

'Convert quads to triangles
retval=doc.OpenMdlFile(regnname, 0)
Set mdl=doc.GetModel()
retval=mdl.DivideQuadIntoTria()
retval=doc.SaveMdlFile(name)

Set octp = doc.GetOctParam
octp.Clear
octp.Set "REGNMODE",1
```

```
octp.Set "REGNNAME",regnname
octp.Set "BASEMODE",2
octp.Set2 "BASESIZE",MinOctSize,MaxOctSize
octp.Set4 "BASEPOS",0,0,0,0
octp.Set "SECTTYPE",1
octp.Set "BALANCING",3
octp.Set "OCTNAME",octname
octp.Execute

Set surfp = doc.GetSurfParam
surfp.Clear
surfp.Set "REGNMODE", 0
surfp.Set "OCTMODE", 0
surfp.Set "SURFNAME",surfname
surfp.Set "OCTNAMESAVE",""
surfp.Set "SURFSMOOTH",0
surfp.Set "SURFHRLIMIT",0.05
surfp.Set "SURFSMTSTRONG",2
surfp.Set "SURFRECOVERY",2
surfp.Set "SURFISECTRETRY",0
surfp.Set2 "LENGTHPARAM",1,5
surfp.Execute

Set tetrap = doc.GetTetraParam
tetrap.Clear
tetrap.Set "SURFMODE",0
tetrap.Set "OCTMODE",0
tetrap.Set3 "SMOOTHITEM",1,0.09,2
tetrap.Set3 "SMOOTHITEM",2,0.18,2
tetrap.Set3 "SMOOTHITEM",1,0.15,2
tetrap.Set3 "SMOOTHITEM",2,0.21,2
tetrap.Set "TETRANAME",tetraname
tetrap.Set "L2D3D",3
tetrap.Set2 "HEXMESH",0,2
tetrap.Set2 "LENGTHPARAM",1,5
tetrap.Set "VMSMOOTHFIXBOUNDARY",0
tetrap.Execute


Set hybridp = doc.GetHybridParam
hybridp.Clear
hybridp.Set "TETRAMODE",0
hybridp.Set "OCTMODE", 1
hybridp.Set "OCTNAME", ""
hybridp.Set "SMODE", 1
hybridp.Set "SNAME", ""
```

```
hybridp.Set "PRISMITER",0
hybridp.Set "PRISMDEG",5
hybridp.Set "PRISMINSPRI",0.1
hybridp.Set "PRISMINSPYR",0.1
hybridp.Set "PRISMMEDGDEG01",300
hybridp.Set "PRISMMEDGDEG23",300
hybridp.Set "PRISMWALLDEG",150
hybridp.Set "PRISMHIMDFYNRRW",0
hybridp.Set "PRISMHIMDFYARND",0
hybridp.Set "PRISMHISMTH",0
hybridp.Set "PRISMTYPE",0
hybridp.Set "PRISMINSERTINSOLID",1
hybridp.Set "PRISMHISHORT",1
hybridp.Set "PRISMHISHORTRT",0.6
hybridp.Set "PRISMAVOIDCONCAVETOP",0
hybridp.Set "PRISMAVOIDCONCAVEBOTTOM",0
hybridp.Set "PRISMCONCAVEPRI",155
hybridp.Set "PRISMCONCAVEPYR",155
hybridp.Set "PRISMAVOIDTWIST",0
hybridp.Set "PRISMTWISTANGLE",13
hybridp.Set "PRISMINSSMTHPYR",1

hybridp.Set "PRISMAUTOHIFRACTION",0.3333

hybridp.Set4 "PRISMITEM","walls",5,y,1.1
hybridp.Set4 "PRISMITEM","curtain",2,y,1

Select Case SimCase
Case "EqFree_Flow"
        hybridp.Set4 "PRISMITEM","face",5,y,1.1
Case "EqFree_Gas"
'       face is ommited.
Case "Miner_Flow"
        hybridp.Set4 "PRISMITEM","face",5,y,1.1
        hybridp.Set4 "PRISMITEM","miner",2,y,1
Case "Miner_Gas"
'       face is ommited.
        hybridp.Set4 "PRISMITEM","miner",2,y,1
End Select

hybridp.Set3 "SMOOTHITEM",3,0.2,1
hybridp.Set3 "SMOOTHITEM",1,0.09,2
hybridp.Set3 "SMOOTHITEM",3,0.2,1
hybridp.Set3 "SMOOTHITEM",1,0.15,2
hybridp.Set3 "SMOOTHITEM",1,0.09,6
hybridp.Set "PRISMOOTHFIXBOUNDARY",0
```

```
hybridp.Set "HYBRIDNAME",hybridname
hybridp.Set "L2D3D",3
hybridp.Execute()

'================================================
'End of script.
'================================================
```

```
'================================================
                                    'S-Generator.vbs
'================================================

Set app = CreateObject("SCTpre_Dx64net.Application.10")
app.Visible = true
Set doc = app.GetDocument
Set scmd = doc.GetSolverCommand
SimCase = "Miner-Gas"
folder = path; title = model
Fanparam1 = -1"; Fanparam2 = 0; Fanparam3 = 0; Fanparam4 = 0
ro_air = 1.206; mu = 1.83; Cp = 1007; Tcnd = 0.0256
'SimCase << EqFree; Miner; Scrubber
SimCase = "Scrubber"
scmd.AddLine "FILS"
scmd.AddLine  "PREI " &   model & ".pre"
scmd.AddLine  "RO      model & ".r"
scmd.AddLine  "POST " & model
scmd.AddLine   "/"
scmd.ApplyLine
Select Case SimCase
Case "EqFree_Flow"
        doc.OpenSFile folder & "\" & "EqFreeFlow.s", 0
Case "EqFree_Gas"
        doc.OpenSFile folder & "\" & "EqFreeGas.s", 0
Case "Miner_Flow"
        doc.OpenSFile folder & "\" & "MinerFlow.s", 0
Case "Miner_Gas"
        doc.OpenSFile folder & "\" & "MinerGas.s", 0
End Select
if  Qsb > 0 then
        scmd.AddLine   "FANM"
        scmd.AddLine   "%CNAM Fanm_1"
        scmd.AddLine   " 4   0"
        scmd.AddLine   Fanparam1 & "  " & Fanparam2 & Fanparam3 & Fanparam4
        scmd.AddLine   Qsb
        scmd.AddLine   "fan"
        scmd.AddLine   "/"
        scmd.AddLine   "/"
        scmd.ApplyLine
end if
scmd.AddLine   "FLUX"
scmd.AddLine   "%CNAM Flux_1"
scmd.AddLine    " 0   2   0   0   1   1"
scmd.AddLine    Qin & "   0"
scmd.AddLine   "0.0001              0.0001"
```

```
scmd.AddLine   "        0"
scmd.AddLine   "inlet"
scmd.AddLine   "/""
scmd.ApplyLine
scmd.AddLine   "%CNAM Flux_2"
scmd.AddLine   "  -4   0   1   0   0   0"
scmd.AddLine   "                        0"
scmd.AddLine   "outlet"
scmd.AddLine   "/"
scmd.ApplyLine
scmd.AddLine   "%CNAM Flux_3"
scmd.AddLine   "  -1   4   0   1   0   1
scmd.AddLine   "                  -1                    0                    0    " &  Qch4
scmd.AddLine   "20"
scmd.AddLine   " 1"
scmd.AddLine   "CH4_inlet"
scmd.AddLine   "/"
scmd.AddLine   "/"
scmd.ApplyLine
scmd.AddLine   "PROP"
scmd.AddLine   "%CNAM air(incompressible /" & t_air & " C)"
scmd.AddLine   "1   1                " & ro_air & " " & mu & "  " Cp & " " & Tcnd
scmd.AddLine   "0"
scmd.AddLine   "/"
scmd.ApplyLine
doc.SaveSFile folder & "\" & sfile & ".s"
'================================================
'End of script.
'================================================


'================================================
          ' List of MinerGas.s template
          '================================================
SDAT
SC/Tetra
  10   0   0
PREI    model.pre
RI      model.r
RO      model.r
POST    model
/
  1   1   0

  1   1
AVGF
```

```
 -1   0
CHKL
      1       1       0       1       0
CYCS
    131     140
EQUA
11011
FANM
%CNAM Fanm_1
  4   0
                -1                   0                   0                   0
               3.4
fan
/
/
FLUX
%CNAM Flux_1
  0   2   0   0   1   1
              1.64   0
             0.0001              0.0001
                0
inlet
/
%CNAM Flux_2
 -4   0   1   0   0   0
                0
outlet
/
%CNAM Flux_3
 -1   4   0   1   0   1
               -1                   0                   0              0.0042
               20
                1
CH4_inlet
/
/
FOUT
USTR   1
/
GRAV
                0                   0                -9.8
GWLN
  0
INIT
TEMP
               20   1
```

```
/
PANL
curtain
scrubber
fan_wall
/
PCTY
  4
PFOC
      1
curtain
/
/
PORM
%CNAM Porm_1
  3   1   1   0   0                100
                0.25              0.0001                  1
                1650                920               0.93
  0                 0
PorM
/
/
POWT
%CNAM Powt_1
                -1                20
porm_walls
/
/
PROP
%CNAM air(incompressible/20C)
  1   1              1.206           1.83e-005              1007              0.0256   0
/
            2.4e-005                0           0.016042           0.0001027
2225              0.03281
SFOC
      1
curtain
/
/
SHEQ
  0
STBT
  1
STED
  1   1              0.0001
  2   1              0.0001
```

```
  3  1              0.0001
  4  1              0.0001
  6  1              0.0001
  7  1              0.0001
  8  1              1e-005
/
TBEC
  1  1
/
TBTY
  2
TMSR
A              14.7              2              1.8   0  -1              1   0
CN01
/
/
TRAN
  1
UNDR
  1     0.600000023841858  1
  2     0.600000023841858  1
  3     0.600000023841858  1
  4     0.600000023841858  1
  6     0.600000023841858  1
/
WL02
%CNAM Wl02_1
  0  0
%CNAM Wl02_2
  0  0
%CNAM Wl02_3
  0  0
%CNAM Wl02_4
  2  2
              -5.2              0     14.6159675629831     0.107602200742578
0.791146050667052                 0              -1              0
              0.136             0.4              8.5
/
  1
walls
/
  2
curtain
/
  3
miner
```

```
fan_wall
scrubber
/
  4
drum
/
/
WLTY
  0
WPUT
  0
ZGWV
  0
GOGO

'================================================
'End of script.
'================================================
```

```
'================================================
                                    'XSolverAdapt.vbs
'================================================

Function InterruptCheckCNX(mval, ncycf, regname)

        success = 0
        ncycback = ncycf
        val = 0.0
        val1 = 0.0
        delta = 0.0

        if job.GetGraphData_TMSR(mval, ncycf, val, regname) then
                For i = 1 To 5
                        ncycback = ncycf-i
                        if job.GetGraphData_TMSR(mval, ncycback, val1, regname)  then


                                delta = Abs((val - val1))

                                if delta < 0.0001 then

                                        success = success + 1

                                else

                                        Exit For
                                end if
                        end if
                Next

        end if

        if success > 4 then
                InterruptCheckCNX = True
        else
                InterruptCheckCNX = False
        end if

'WScript.echo(ncycf & " - " & ncycback & "  " &  mval & " = " & val & "   success = " &
success & "   delta = " & delta)

End Function
Function InterruptCheckTMSR(mval, ncycf, regname)

        success = 0
```

```
	ncycback = ncycf
	val = 0.0
	val1 = 0.0
	delta = 0.0

	if job.GetGraphData_TMSR(mval, ncycf, val, regname) then
		For i = 1 To 5
			ncycback = ncycf-i
			if job.GetGraphData_TMSR(mval, ncycback, val1, regname)  then


				delta = Abs(val - val1)

				if delta < 0.01 then

					success = success + 1

				else

					Exit For
				end if
			end if
		Next

	end if

	if success > 4 then
		InterruptCheckTMSR = True
	else
		InterruptCheckTMSR = False
	end if

'WScript.echo(ncycf & " - " & ncycback & "  " &  mval & " = " & val & "   success = " &
success & "   delta = " & delta)

End Function
Function InterruptCheckReg(mval, ncycf, regname)

	success = 0
	ncycback = ncycf
	val = 0.0
	val1 = 0.0
	delta = 0.0

	if job.GetGraphData_REGION(mval, ncycf, val, regname) then
		For i = 1 To 5
```

```
                        ncycback = ncycf-i
                        if job.GetGraphData_REGION(mval, ncycback, val1, regname)
then

                                delta = Abs(val - val1)

                                if delta < 0.01 then

                                        success = success + 1

                                else

                                        Exit For
                                end if
                        end if
                Next

        end if

        if success > 4 then
                InterruptCheckReg = True
        else
                InterruptCheckReg = False
        end if

'WScript.echo(ncycf & " - " & ncycback & "  " &  mval & " = " & val & "   success = " &
success & "   delta = " & delta)

End Function

Function InterruptCheck(mval, ncycf)

        success = 0
        ncycback = ncycf
        maxval = 0.0
        minval = 0.0
        maxval1 = 0.0
        minval1 = 0.0
        stedval = 0.0
        delta = 0.0

        if job.GetGraphData_STED(mval, ncycf, stedval) then
                if stedval < 0.0002 then
                        if job.GetGraphData_MINMAX(mval, ncycf, maxval, minval)
then
```

```
                    For i = 1 To 5
                    ncycback = ncycf-i
                    if job.GetGraphData_MINMAX(mval, ncycback , maxval1,
minval1) then

                                        delta = Abs(maxval - maxval1)

                                        if delta < 0.01 then

                                                success = success + 1

                                        else

                                                Exit For
                                        end if

                                end if

                            Next

                    end if
            end if
        end if

        if success > 4 then
                InterruptCheck = True
        else
                InterruptCheck = False
        end if

End Function

Function XSolv(s_file)

        XSolv = False
        if SolverApp.ErrorCode = 100 Or SolverApp.ErrorCode = 101 then

                Wscript.Sleep(1)

        else

                SolverApp.Execute(job)

                Do while job.GetStatusCode() < 200

                ncyc = job.GetCycle()
```

```
                if ncyc > 10 then
                        XSolv = InterruptCheck("VELX", ncyc)* _
InterruptCheck("VELY", ncyc)* _
InterruptCheck("VELZ", ncyc)* _
InterruptCheckCNX("CN01", ncyc, "A")
                        if XSolv then
                                SolverApp.Interrupt(job)
                        end if
                end if

        Wscript.Sleep(1)
Loop

end if

End Function

Sub MeshAdapt(folder, Stitle, MDLtitle, LastCyc, TargetNumOfElem, SimCase)


'================================================
'Mesh Adaptation Analysis Using Existing Result
'================================================

Set app = CreateObject("SCTpre_Dx64net.Application.10")
app.Visible = true
Set doc = app.GetDocument

CStrLastCyc = "_" & CStr(LastCyc)
regnname = folder & "\" & MDLtitle & ".mdl"
octname = folder & "\" & MDLtitle & ".oct"
surfname = folder & "\" & MDLtitle & "_meshsurf.mdl"
tetraname = folder & "\" & MDLtitle & "_tetra.pre"
hybridname = folder & "\" & MDLtitle & ".pre"
sname = folder & "\" & Stitle & ".s"
fldname = folder & "\" & Stitle & CStrLastCyc & ".fld"
roname = folder & "\" & Stitle & ".r"
logname = folder & "\" & Stitle & ".log"

'--- (1)
maxiter = 1
Set adaptivep = doc.GetAdaptiveParam
adaptivep.Clear
adaptivep.Set "exec",1
adaptivep.Set "iterMax",maxiter
```

```
'--- (2)
adaptivep.Set "lastElemNum", TargetNumOfElem
'-//-

adaptivep.Set "cof.type",1
adaptivep.Set "autoOctree",0
adaptivep.Set "mergesurfoct",0
adaptivep.Set "fromfld",1
adaptivep.Set "fromfldrestart",1

'--- Not used in this analysis.
adaptivep.Set "cond.simpl1cycl",0
adaptivep.Set "cond.cycl1",100
adaptivep.Set "cond.simpl1sted",0
adaptivep.Set "cond.sted1",0.0001
adaptivep.Set "cond.simpl2cycl",0
adaptivep.Set "cond.cycl2",100
adaptivep.Set "cond.simpl2sted",0
adaptivep.Set "cond.sted2",0.0001
'-//-

adaptivep.Set "deletefile",0
adaptivep.Set "output_alfile",0
adaptivep.Set "fname.title",MDLtitle
adaptivep.Set "fname.path",folder
adaptivep.Set "fname.log",logname
adaptivep.Set "fname.orgFld",fldname
adaptivep.Set "fname.orgRo",roname
adaptivep.Set "fname.orgMdl",regnname
adaptivep.Set "fname.orgOct",octname
adaptivep.Set "fname.orgS",sname
adaptivep.Set "fname.outSurf",surfname
adaptivep.Set "fname.outTetra",tetraname
adaptivep.Set "fname.outHybrid",hybridname
adaptivep.Set "fname.refOct",""
adaptivep.Set "l2d3d",3
adaptivep.Set "prisminsertinsolid",0

        adaptivep.Set5 "prism","walls",5,1.1,0,50
        adaptivep.Set5 "prism","curtain",5,1,0,50

'--- Region to which a prism layer is inserted.
Select Case Simcase
Case "EqFree_Flow"
        adaptivep.Set5 "prism","face",5,1.1,0,50
Case "EqFree_Gas"
```

```
        'face is ommited
Case "Miner_Flow"
        adaptivep.Set5 "prism","face",5,1.1,0,50
        adaptivep.Set5 "prism","miner",2,1,0,50
        adaptivep.Set5 "prism","drum",2,1,0,50
        adaptivep.Set5 "prism","scrubber",2,1,0,50
        adaptivep.Set5 "prism","fan_wall",2,1,0,50
Case "Miner_Gas"
'       face is omitted!
        adaptivep.Set5 "prism","miner",2,1,0,50
        adaptivep.Set5 "prism","drum",2,1,0,50
        adaptivep.Set5 "prism","scrubber",2,1,0,50
        adaptivep.Set5 "prism","fan_wall",2,1,0,50
Case Else
        adaptivep.Set5 "prism","[WALL]",5,1,0,50
End Select
'-//-

Set surfp = doc.GetSurfParam
surfp.Clear
surfp.Set "SURFSMOOTH",1
surfp.Set "SURFHRLIMIT", 0.05
surfp.Set "SURFSMTSTRONG",1

surfp.Set "SURFRECOVERY",2

Select Case SimCase
Case "Miner_Flow"
        surfp.Set "SURFISECTRETRY",1
        surfp.Set "SURFISECTNEIGHBOR", "miner"
        surfp.Set "SURFISECTNEIGHBOR", "scrubber"
        surfp.Set "SURFISECTNEIGHBOR", "fan_wall
        surfp.Set "SURFISECTNEIGHBOR", "drum"
Case "Miner_Gas"
        surfp.Set "SURFISECTRETRY",1
        surfp.Set "SURFISECTNEIGHBOR", "miner"
        surfp.Set "SURFISECTNEIGHBOR", "scrubber"
        surfp.Set "SURFISECTNEIGHBOR", "fan_wall
        surfp.Set "SURFISECTNEIGHBOR", "drum"
Case Else
        surfp.Set "SURFISECTRETRY",0
End Select

'--- Change the mesh gradually.
surfp.Set2 "LENGTHPARAM",4,5
'-//-
```

```
Set tetrap = doc.GetTetraParam
tetrap.Clear
tetrap.Set3 "SMOOTHITEM",1,0.09,2
tetrap.Set3 "SMOOTHITEM",2,0.18,2
tetrap.Set3 "SMOOTHITEM",1,0.15,2
tetrap.Set3 "SMOOTHITEM",2,0.21,2
tetrap.Set "L2D3D",3
tetrap.Set2 "HEXMESH",0,2

'--- Change the mesh gradually.
tetrap.Set2 "LENGTHPARAM",4,5
'-//-

tetrap.Set "VMSMOOTHFIXBOUNDARY",1

Set hybridp = doc.GetHybridParam
hybridp.Clear
hybridp.Set "PRISMITER",0
hybridp.Set "PRISMDEG",5
hybridp.Set "PRISMINSPRI",0.1
hybridp.Set "PRISMINSPYR",0.1
hybridp.Set "PRISMMEDGDEG01",300
hybridp.Set "PRISMMEDGDEG23",300
hybridp.Set "PRISMWALLDEG",150

'--- Restrict the thickness of prism layers at narrow spaces.
hybridp.Set "PRISMHIMDFYNRRW",1
hybridp.Set "PRISMHIMDFYARND",1
hybridp.Set "PRISMHIMDFYARNDRT", 0.5
hybridp.Set "PRISMHIMDFYNRRWRT", 0.2
'-//-

hybridp.Set "PRISMHISMTH",0
hybridp.Set "PRISMTYPE",0
hybridp.Set "PRISMINSERTINSOLID",1
hybridp.Set "PRISMHISHORT",1
hybridp.Set "PRISMHISHORTRT",0.6
hybridp.Set "PRISMAVOIDCONCAVETOP",0
hybridp.Set "PRISMAVOIDCONCAVEBOTTOM",0
hybridp.Set "PRISMCONCAVEPRI",155
hybridp.Set "PRISMCONCAVEPYR",155
hybridp.Set "PRISMAVOIDTWIST",0
hybridp.Set "PRISMTWISTANGLE",13
hybridp.Set "PRISMAVOIDTWIST",0
hybridp.Set "PRISMINSSMTHPYR",1
```

```
hybridp.Set3 "SMOOTHITEM",3,0.2,1
hybridp.Set3 "SMOOTHITEM",1,0.09,2
hybridp.Set3 "SMOOTHITEM",3,0.2,1
hybridp.Set3 "SMOOTHITEM",1,0.15,2
hybridp.Set3 "SMOOTHITEM",1,0.09,6
hybridp.Set "PRISMOOTHFIXBOUNDARY",0
hybridp.Set "L2D3D",3

'--- Specify iter=0 to prepare for the next analysis result based on the existing analysis result.
iter = 0
adaptivep.Set "iter",iter
adaptivep.Prepare()
adaptivep.SetupNextExecution()
iter = 1
adaptivep.Set "iter",iter
adaptivep.Prepare()
adaptivep.MakePreFile()
adaptivep.MakeSFile()
adaptivep.MakeSFileForGapInsertion()


Set sctsolver = CreateObject("SCTsolver_Bx64net.Application.10")
sctsolver.Visible = true
adaptivep.GetSFileNameForGapInsertion sFileName
Set job = sctsolver.CreateSolverJob(sFileName)
sctsolver.Execute(job)
Do While job.GetStatusCode() < 200
WScript.Sleep(1)
Loop
sctsolver.Quit

adaptivep.MakeRestartFile()

Set SolverApp = CreateObject("SCTsolver_Bx64net.Application.10")
SolverApp.Visible = true
adaptivep.GetSFileName sFileName
set job = SolverApp.CreateSolverJob(sFileName)
final = XSolv(sFileName)

End Sub

' MAIN PROGRAM

msg = "XSolver"
SimCase = "Miner_CH4"
```

```
TargetNumOfElem = 3000000

jobfolder = folder
jobname = sfile
MDLname = mdlfile

s_file = jobfolder &  "\" & jobname & ".s"


'Run Solver
set SolverApp = CreateObject("SCTsolver_Bx64net.Application.10")
SolverApp.Visible = True
set job = SolverApp.CreateSolverJob(s_file)

if XSolv(s_file) = False then
        msg = "Adaptaion"
        LastCyc = job.GetCycle()
        SolverApp.Quit()
        Call MeshAdapt(jobfolder, jobname, MDLname, LastCyc, TargetNumOfElem,
SimCase)
end if

WScript.echo(msg & " job completed.")
SolverApp.Quit()
WScript.Quit()
```

'==

'VBA code using Microsoft Visual Studio 2012

'==

```
       Public Class Form1

           Private Sub Start_Click(sender As Object, e As EventArgs) Handles
Start.Click

               Dim FldFile, Fld As Object
               Dim StaPath As String
               ''Dim postpid As Object
               Dim PostApp, DrawWnd, WordApp, Document As Object
               Dim ReportsPath As String
               Dim RndFileName, saveFilename As String
               Dim TmporaryBmpFile As String
               Dim GlobalW As Object
               Dim SaveBmp As Object
               'Dim SlideWidth, SlideHeight As Single
               Dim CurSlide As UShort = 0

               My.Computer.FileSystem.CurrentDirectory = folder
               FldFile = CurDir() + "\" fld + ".fld
               StaPath = CurDir() + "\STA\BMP"
               ReportsPath = CurDir() + "\Reports"


               ' Execute SCTpost.
               PostApp = CreateObject("SCTpost_Dx64net.Application.10")
               PostApp.Visible = True

               RndFileName = PostApp.GetRandomFilename()
               TmporaryBmpFile = RndFileName + ".bmp"

               ' Get the Global Window Object class.
               GlobalW = PostApp.GetGlobalWindow()
               SaveBmp = GlobalW.GetObjectSaveBitmaps()

               ' Reading the FLD file
               Fld = PostApp.CreateObjectFLD(FldFile)
               If PostApp.ErrorCode <> 0 Then MsgBox(PostApp.ErrorString,
MsgBoxStyle.MsgBoxSetForeground, "Message")

               ' Create a new WORD application
               WordApp = CreateObject("Word.Application")
               WordApp.Visible = True

               Document = WordApp.Documents.Add()


               ' Begin a loop to apply each STA file
               For Each StaFile As String In
My.Computer.FileSystem.GetFiles(StaPath, FileIO.SearchOption.SearchTopLevelOnly,
"*.*")
                   CurSlide = CurSlide + 1

                   ' Apply an STA file.
```

```
                    Fld.ApplySTA(StaFile, True)
                    DrawWnd = PostApp.GetDrawWindow()
                    DrawWnd.Redraw()

                    ' Save the figure in pts.
                    ReportsPath = CurDir() + "\Reports"
                    RndFileName = PostApp.GetRandomFilename()
                    TmporaryBmpFile = ReportsPath + "\" + RndFileName + ".bmp"
                    SaveBmp.SaveBitmap(TmporaryBmpFile)
                    ' Add a picture to the document.
                    Document.InlineShapes.AddPicture(TmporaryBmpFile)

                Next

                ' Save Word Document
                saveFilename = ReportsPath + "\Report" + ".DOCX"
                Document.SaveAs(saveFilename)
                Document = Nothing
                WordApp.Quit()
                WordApp = Nothing

                ' Delete temporary files


                'Quit SCTpost
                PostApp.Quit()
                PostApp = Nothing

            End Sub

            Private Sub Form1_Click(sender As Object, e As EventArgs) Handles
MyBase.Click

            End Sub

            Private Sub Button1_Click(sender As Object, e As EventArgs) Handles
Button1.Click
                Dim FldFile, Fld As Object
                Dim StaPath As String
                ''Dim postpid As Object
                Dim PostApp, DrawWnd As Object
                Dim ReportsPath As String
                'Dim SlideWidth, SlideHeight As Single
                Dim CurSlide As UShort = 0

                My.Computer.FileSystem.CurrentDirectory = folder
                FldFile = CurDir() + "\" fld + ".fld
                StaPath = CurDir() + "\STA\Animation"
                ReportsPath = CurDir() + "\Reports"


                ' Execute SCTpost.
                PostApp = CreateObject("SCTpost_Dx64net.Application.10")
                PostApp.Visible = True


                ' Reading the FLD file
```

```
                Fld = PostApp.CreateObjectFLD(FldFile)
                If PostApp.ErrorCode <> 0 Then MsgBox(PostApp.ErrorString,
MsgBoxStyle.MsgBoxSetForeground, "Message")


                ' Begin a loop to apply each STA file
                For Each StaFile As String In
My.Computer.FileSystem.GetFiles(StaPath, FileIO.SearchOption.SearchTopLevelOnly,
"*.*")
                    CurSlide = CurSlide + 1
                    Fld.ApplySTA(StaFile, True)
                    DrawWnd = PostApp.GetDrawWindow()
                    DrawWnd.KeyI(False, False)
                    DrawWnd.SetPerspectiveProjection()
                    DrawWnd.KeyF()
                    PostApp.AnimationStart()
                    If MsgBox("Stop animation?", MsgBoxStyle.MsgBoxSetForeground Or
MsgBoxStyle.Question Or MsgBoxStyle.YesNo, "Message") = MsgBoxResult.Yes Then
                        PostApp.AnimationStop()
                    End If
                    If MsgBox("Proceede with the next animation?",
MsgBoxStyle.MsgBoxSetForeground Or MsgBoxStyle.Question Or MsgBoxStyle.OkCancel,
"Message") = MsgBoxResult.Cancel Then
                        Exit For
                    End If
                Next


                'Quit SCTpost
                PostApp.Quit()
                PostApp = Nothing
            End Sub

            Private Sub Button2_Click(sender As Object, e As EventArgs) Handles
Button2.Click
                Dim FldFile, Fld As Object
                Dim StaPath As String
                ''Dim postpid As Object
                Dim PostApp, DrawWnd, MsgWndow As Object
                Dim ReportsPath As String
                'Dim SlideWidth, SlideHeight As Single
                Dim CurSlide As UShort = 0

                My.Computer.FileSystem.CurrentDirectory = folder
                FldFile = CurDir() + "\" fld + ".fld
                StaPath = CurDir() + "\STA\CradleViewer"
                ReportsPath = CurDir() + "\Reports"


                ' Execute SCTpost.
                PostApp = CreateObject("SCTpost_Dx64net.Application.10")
                PostApp.Visible = True


                ' Reading the FLD file
                Fld = PostApp.CreateObjectFLD(FldFile)
                If PostApp.ErrorCode <> 0 Then MsgBox(PostApp.ErrorString)
                MsgWndow = PostApp.GetMessageWindow
```

```
                ' Begin a loop to apply each STA file
                For Each StaFile As String In
My.Computer.FileSystem.GetFiles(StaPath, FileIO.SearchOption.SearchTopLevelOnly,
"*.*")
                    CurSlide = CurSlide + 1
                    Fld.ApplySTA(StaFile, True)
                    DrawWnd = PostApp.GetDrawWindow()
                    DrawWnd.KeyI(False, False)
                    DrawWnd.SetPerspectiveProjection()
                    DrawWnd.KeyF()
                    PostApp.AnimationStart()
                    Fld.SaveCradleViewer(ReportsPath + "\Ani" + CStr(CurSlide) +
".CradleViewer")
                    PostApp.AnimationStop()
                Next


                'Quit SCTpost
                PostApp.Quit()
                PostApp = Nothing

            End Sub
        End Class
```

```
'=========================================================
            ' List of the V-SurfaceMovingVectors status files (STA)code
'=========================================================

 [ENV]
   LANG_ID              = 1033
   TREE_ORDER_ID        = 0
   DEFAULT_NAME         = ""
   DEFAULT_WITHOUTPOS   = OFF
   SHORT_TITLE          = "ENV"
   LONG_TITLE           = "Option"
   DISPLAY_TITLE        = "Option"
   DISPLAY_TITLE_MODIFIED  = OFF
   COL_MATCH_MODE       = 1
   TOPPOS_MODE          = 0
   PLUSMINUS_MODE       = 0
   INTEGRATE1_CALC      = OFF
   INTEGRATE1_SAVE      = OFF
   INTEGRATE1_FN        = ""
   INTEGRATE1_USE_BEEP  = ON
   INTEGRATE1_USE_REDRAW  = ON
   INTEGRATE1_USE_STR   = ON
   INTEGRATE3_CALC      = OFF
   INTEGRATE3_SAVE      = OFF
   INTEGRATE3_FN        = ""
   INTEGRATE3_USE_BEEP  = ON
   INTEGRATE3_USE_REDRAW  = ON
   INTEGRATE3_USE_STR   = ON
   MY_ID                = 0
   PARENT_ID            = -1
   DRAWABLE             = OFF
   TEX_USE              = OFF
   TEX_TYPE             = 0
   TEX_TYPE0_X          = 1.00000000e+000
   TEX_TYPE0_Y          = 1.00000000e+000
   TEX_TYPE0_Z          = 1.00000000e+000
   TEX_TYPE1_NX         = 0.00000000e+000
   TEX_TYPE1_NY         = 0.00000000e+000
   TEX_TYPE1_NZ         = 1.00000000e+000
   TEX_TYPE1_R          = 1.00000000e+000
   TEX_TYPE1_TZ         = 1.00000000e+000
   TEX_TYPE2_NX         = 0.00000000e+000
   TEX_TYPE2_NY         = 0.00000000e+000
   TEX_TYPE2_NZ         = 1.00000000e+000
   TEX_TYPE2_S          = 1.00000000e+000
   TEX_ROTATE0_X        = 0.00000000e+000
   TEX_ROTATE0_Y        = 0.00000000e+000
```

TEX_ROTATE0_Z = 0.00000000e+000
TEX_ROTATE1_TZ = 0.00000000e+000
TEX_ROTATE1_R = 0.00000000e+000
TEX_ROTATE2_S = 0.00000000e+000
TEX_OFS0_X_X = 0.00000000e+000
TEX_OFS0_X_Y = 0.00000000e+000
TEX_OFS0_Y_X = 0.00000000e+000
TEX_OFS0_Y_Y = 0.00000000e+000
TEX_OFS0_Z_X = 0.00000000e+000
TEX_OFS0_Z_Y = 0.00000000e+000
TEX_OFS1_R_X = 0.00000000e+000
TEX_OFS1_R_Y = 0.00000000e+000
TEX_OFS1_TZ_X = 0.00000000e+000
TEX_OFS1_TZ_Y = 0.00000000e+000
TEX_OFS2_X = 0.00000000e+000
TEX_OFS2_Y = 0.00000000e+000
TEX_USECOLORKEY = OFF
TEX_COLORKEY = C16711680
TEX_UPSIDEDOWN = OFF
TEX_FILENAME = ""
ONLY_ONEVAR = ON
BILLBOARD_ENABLED = 0
RECREATE_SCALE = OFF
MSGWND_Height = -21
MSGWND_Width = 0
MSGWND_Escapement = 0
MSGWND_Orientation = 0
MSGWND_Weight = 400
MSGWND_Italic = 0
MSGWND_Underline = 0
MSGWND_StrikeOut = 0
MSGWND_CharSet = 128
MSGWND_OutPrecision = 128
MSGWND_ClipPrecision = 2
MSGWND_Quality = 1
MSGWND_PitchAndFamily = 49
MSGWND_FaceName = ",l,r ƒSƒVƒbƒN"
GUI_NEXT_TREE_MODE = 2
UNIT5_ENV_USE = 1
UNIT5_ENV_LNAM_START = 22
UNIT5_ENV_LNAM_DATA_0 = "G"
UNIT5_ENV_LNAM_DATA_1 = "DIST"
UNIT5_ENV_LNAM_DATA_2 = "PRES"
UNIT5_ENV_LNAM_DATA_3 = "TEMP"
UNIT5_ENV_LNAM_DATA_4 = "MRT"
UNIT5_ENV_LNAM_DATA_5 = "LTTP"

UNIT5_ENV_LNAM_DATA_6 = "TPOR"
UNIT5_ENV_LNAM_DATA_7 = "TSK"
UNIT5_ENV_LNAM_DATA_8 = "VEL"
UNIT5_ENV_LNAM_DATA_9 = "USTR"
UNIT5_ENV_LNAM_DATA_10 = "DENS"
UNIT5_ENV_LNAM_DATA_11 = "ENTL"
UNIT5_ENV_LNAM_DATA_12 = "TURK"
UNIT5_ENV_LNAM_DATA_13 = "TEPS"
UNIT5_ENV_LNAM_DATA_14 = "EVIS"
UNIT5_ENV_LNAM_DATA_15 = "RFV"
UNIT5_ENV_LNAM_DATA_16 = "CUR"
UNIT5_ENV_LNAM_DATA_17 = "ELPT"
UNIT5_ENV_LNAM_DATA_18 = "HUMC"
UNIT5_ENV_LNAM_DATA_19 = "HUMA"
UNIT5_ENV_LNAM_DATA_20 = "HTRC"
UNIT5_ENV_LNAM_DATA_21 = "HVEC"
UNIT5_ENV_NAME_START = 22
UNIT5_ENV_NAME_DATA_0 = "m"
UNIT5_ENV_NAME_DATA_1 = "m"
UNIT5_ENV_NAME_DATA_2 = "Pa"
UNIT5_ENV_NAME_DATA_3 = "C"
UNIT5_ENV_NAME_DATA_4 = "C"
UNIT5_ENV_NAME_DATA_5 = "C"
UNIT5_ENV_NAME_DATA_6 = "C"
UNIT5_ENV_NAME_DATA_7 = "C"
UNIT5_ENV_NAME_DATA_8 = "m/s"
UNIT5_ENV_NAME_DATA_9 = "m/s"
UNIT5_ENV_NAME_DATA_10 = "kg/m3"
UNIT5_ENV_NAME_DATA_11 = "J/kg"
UNIT5_ENV_NAME_DATA_12 = "m2/s2"
UNIT5_ENV_NAME_DATA_13 = "m2/s3"
UNIT5_ENV_NAME_DATA_14 = "Pa s"
UNIT5_ENV_NAME_DATA_15 = "W/m2"
UNIT5_ENV_NAME_DATA_16 = "A/m2"
UNIT5_ENV_NAME_DATA_17 = "V"
UNIT5_ENV_NAME_DATA_18 = "kg/(m2 s)"
UNIT5_ENV_NAME_DATA_19 = "kg/m2"
UNIT5_ENV_NAME_DATA_20 = "W/(m2 K)"
UNIT5_ENV_NAME_DATA_21 = "W/m2"
UNIT5_ENV_SCALE_START = 22
UNIT5_ENV_SCALE_DATA_0 = "1"
UNIT5_ENV_SCALE_DATA_1 = "1"
UNIT5_ENV_SCALE_DATA_2 = "1"
UNIT5_ENV_SCALE_DATA_3 = "1"
UNIT5_ENV_SCALE_DATA_4 = "1"
UNIT5_ENV_SCALE_DATA_5 = "1"

UNIT5_ENV_SCALE_DATA_6 = "1"
UNIT5_ENV_SCALE_DATA_7 = "1"
UNIT5_ENV_SCALE_DATA_8 = "1"
UNIT5_ENV_SCALE_DATA_9 = "1"
UNIT5_ENV_SCALE_DATA_10 = "1"
UNIT5_ENV_SCALE_DATA_11 = "1"
UNIT5_ENV_SCALE_DATA_12 = "1"
UNIT5_ENV_SCALE_DATA_13 = "1"
UNIT5_ENV_SCALE_DATA_14 = "1"
UNIT5_ENV_SCALE_DATA_15 = "1"
UNIT5_ENV_SCALE_DATA_16 = "1"
UNIT5_ENV_SCALE_DATA_17 = "1"
UNIT5_ENV_SCALE_DATA_18 = "1"
UNIT5_ENV_SCALE_DATA_19 = "1"
UNIT5_ENV_SCALE_DATA_20 = "1"
UNIT5_ENV_SCALE_DATA_21 = "1"
UNIT5_ENV_OFS_START = 22
UNIT5_ENV_OFS_DATA_0 = "0"
UNIT5_ENV_OFS_DATA_1 = "0"
UNIT5_ENV_OFS_DATA_2 = "0"
UNIT5_ENV_OFS_DATA_3 = "0"
UNIT5_ENV_OFS_DATA_4 = "0"
UNIT5_ENV_OFS_DATA_5 = "0"
UNIT5_ENV_OFS_DATA_6 = "0"
UNIT5_ENV_OFS_DATA_7 = "0"
UNIT5_ENV_OFS_DATA_8 = "0"
UNIT5_ENV_OFS_DATA_9 = "0"
UNIT5_ENV_OFS_DATA_10 = "0"
UNIT5_ENV_OFS_DATA_11 = "0"
UNIT5_ENV_OFS_DATA_12 = "0"
UNIT5_ENV_OFS_DATA_13 = "0"
UNIT5_ENV_OFS_DATA_14 = "0"
UNIT5_ENV_OFS_DATA_15 = "0"
UNIT5_ENV_OFS_DATA_16 = "0"
UNIT5_ENV_OFS_DATA_17 = "0"
UNIT5_ENV_OFS_DATA_18 = "0"
UNIT5_ENV_OFS_DATA_19 = "0"
UNIT5_ENV_OFS_DATA_20 = "0"
UNIT5_ENV_OFS_DATA_21 = "0"
USE_MSGWND = 1
USE_DRAWWND = 1
HASH_PARAM = 1.0000000000000000e+000
WNDSTRUCT4_NUM = 6
WNDSTRUCT4_GID_0 = 294026280
WNDSTRUCT4_GID_1 = 411547248
WNDSTRUCT4_GID_2 = 411546896

WNDSTRUCT4_GID_3 = 411547072
WNDSTRUCT4_GID_4 = 411547424
WNDSTRUCT4_GID_5 = -1
WNDSTRUCT4_AHV_0 = 2
WNDSTRUCT4_AHV_1 = 1
WNDSTRUCT4_AHV_2 = 0
WNDSTRUCT4_AHV_3 = 0
WNDSTRUCT4_AHV_4 = 0
WNDSTRUCT4_AHV_5 = -1
WNDSTRUCT4_SPL_0 = 2.5000000000000000e-001
WNDSTRUCT4_SPL_1 = 5.0000000000000000e-001
WNDSTRUCT4_SPL_2 = -1.0000000000000000e+000
WNDSTRUCT4_SPL_3 = -1.0000000000000000e+000
WNDSTRUCT4_SPL_4 = -1.0000000000000000e+000
WNDSTRUCT4_SPL_5 = -1.0000000000000000e+000
WNDSTRUCT4_RECT_0 = 0
WNDSTRUCT4_RECT_1 = 0
WNDSTRUCT4_RECT_2 = 0
WNDSTRUCT4_RECT_3 = 0
WNDSTRUCT4_RECT_4 = 0
WNDSTRUCT4_RECT_5 = 547763271234552873
WNDSTRUCT4_PT1_0 = 411547248
WNDSTRUCT4_PT1_1 = 411546896
WNDSTRUCT4_PT1_2 = -1
WNDSTRUCT4_PT1_3 = -1
WNDSTRUCT4_PT1_4 = -1
WNDSTRUCT4_PT1_5 = -1
WNDSTRUCT4_PT2_0 = 411547424
WNDSTRUCT4_PT2_1 = 411547072
WNDSTRUCT4_PT2_2 = -1
WNDSTRUCT4_PT2_3 = -1
WNDSTRUCT4_PT2_4 = -1
WNDSTRUCT4_PT2_5 = -1
WNDSTRUCT4_TIT_0 = ""
WNDSTRUCT4_TIT_1 = ""
WNDSTRUCT4_TIT_2 = "CTRLWND"
WNDSTRUCT4_TIT_3 = "FULLSURF"
WNDSTRUCT4_TIT_4 = "DRAWWND"
WNDSTRUCT4_TIT_5 = "MSGWND"
WNDSTRUCT4_CHECK = 0
WNDSTRUCT_MAINWND_SX = -8
WNDSTRUCT_MAINWND_EX = 1928
WNDSTRUCT_MAINWND_SY = -8
WNDSTRUCT_MAINWND_EY = 1048
WNDSTRUCT_MAINWND_MAX = 1
WNDSTRUCT_DLGBAR_0_MODE = 1

WNDSTRUCT_DLGBAR_0_LEFT = 189
WNDSTRUCT_DLGBAR_0_TOP = 0
WNDSTRUCT_DLGBAR_0_RIGHT = 977
WNDSTRUCT_DLGBAR_0_BOTTOM = 39
WNDSTRUCT_DLGBAR_1_MODE = 1
WNDSTRUCT_DLGBAR_1_LEFT = 976
WNDSTRUCT_DLGBAR_1_TOP = 0
WNDSTRUCT_DLGBAR_1_RIGHT = 1295
WNDSTRUCT_DLGBAR_1_BOTTOM = 39
WNDSTRUCT_DLGBAR_2_MODE = 1
WNDSTRUCT_DLGBAR_2_LEFT = -2
WNDSTRUCT_DLGBAR_2_TOP = 0
WNDSTRUCT_DLGBAR_2_RIGHT = 191
WNDSTRUCT_DLGBAR_2_BOTTOM = 39
WNDSTRUCT_DLGBAR_3_MODE = 1
WNDSTRUCT_DLGBAR_3_LEFT = 661
WNDSTRUCT_DLGBAR_3_TOP = 37
WNDSTRUCT_DLGBAR_3_RIGHT = 1078
WNDSTRUCT_DLGBAR_3_BOTTOM = 76
WNDSTRUCT_DLGBAR_4_MODE = 1
WNDSTRUCT_DLGBAR_4_LEFT = 1293
WNDSTRUCT_DLGBAR_4_TOP = 0
WNDSTRUCT_DLGBAR_4_RIGHT = 1769
WNDSTRUCT_DLGBAR_4_BOTTOM = 39
WNDSTRUCT_DLGBAR_5_MODE = 1
WNDSTRUCT_DLGBAR_5_LEFT = -2
WNDSTRUCT_DLGBAR_5_TOP = 37
WNDSTRUCT_DLGBAR_5_RIGHT = 663
WNDSTRUCT_DLGBAR_5_BOTTOM = 76
SELECTCOLOR_COLOR00   = C0
SELECTCOLOR_COLOR01   = C128
SELECTCOLOR_COLOR02   = C32768
SELECTCOLOR_COLOR03   = C32896
SELECTCOLOR_COLOR04   = C8388608
SELECTCOLOR_COLOR10   = C8388736
SELECTCOLOR_COLOR11   = C8421376
SELECTCOLOR_COLOR12   = C12632256
SELECTCOLOR_COLOR13   = C12639424
SELECTCOLOR_COLOR14   = C15780518
SELECTCOLOR_COLOR20   = C15793151
SELECTCOLOR_COLOR21   = C10789024
SELECTCOLOR_COLOR22   = C8421504
SELECTCOLOR_COLOR23   = C255
SELECTCOLOR_COLOR24   = C65280
SELECTCOLOR_COLOR30   = C65535
SELECTCOLOR_COLOR31   = C16711680

SELECTCOLOR_COLOR32 = C16711935
SELECTCOLOR_COLOR33 = C16776960
SELECTCOLOR_COLOR34 = C16777215
COL_AXIS_X = C8388863
COL_AXIS_Y = C65408
COL_AXIS_Z = C16744448
HANDLEOBJECT_CUTPLANE_AXIS_X = C8388863
HANDLEOBJECT_CUTPLANE_AXIS_HIGHLIGHT_X = C200
HANDLEOBJECT_CUTPLANE_AXIS_Y = C65408
HANDLEOBJECT_CUTPLANE_AXIS_HIGHLIGHT_Y = C51200
HANDLEOBJECT_CUTPLANE_AXIS_Z = C16744448
HANDLEOBJECT_CUTPLANE_AXIS_HIGHLIGHT_Z = C13107200
VOLUME_LIST_TREE_AUTO = 2
GL_SHINNESS2 = 1.00000000e+000
GL_PROJECTIONWIDTH = 2.9999999999999999e-001
VECTOR_BASERATE = 0.00000000e+000
VECTOR_ARROWRATE = 1.00000000e+000
USE_KUROMAKI = 0
RESET_ALLSTREAMLINE = 0
WNDMODE = 0
SHOW_PROGRESS = 0
MSG_PARAMSG = 0
COLORBAR_FIX20101207 = ON
SHOW_NEU_LOG = OFF
GL_SKIPSWAP = ON
SURFACE_FIX20111201 = ON
TREEHAND_FIX20120130 = OFF
COLORBAR_FIX20110303 = ON
PLANE_P_MODE = 2
NEW_AXIS_SIZE = 1.0000000000000000e+000
COL_ACTION_DELETE3 = 1
COL_ACTION_ARANGE3 = 1
COL_ACTION_VAR3 = ON
COL_ACTION_CYC3 = OFF
COL_ACTION_FLD3 = OFF
COL_ACTION_STA5 = OFF
COL_ACTION_PST3 = ON
COL_ACTION_OBJ13 = ON
COL_ACTION_OBJ24 = OFF
COL_MINMAX_VAR3 = ON
COL_MINMAX_CYC4 = OFF
COL_MINMAX_FLD4 = OFF
COL_MINMAX_STA3 = ON
COL_MINMAX_PST3 = ON
COL_MINMAX_OBJ13 = ON
COL_MINMAX_OBJ24 = OFF

CYC_USE_INVALID_VALUE = ON
STREAMLINE_AUTOPOS = ON
PRINT_PICKSTA = ON
PRINT_PICKJUMP = ON
COMP_AC = 4
COMP_AC2 = 1
COMP_ZMAX = 6
COMP_TYPE = 0
COMP_DISPLAY = 0
COMP_OPERATE = 1
OMITFLDANALYZE = ON
USE_DEGREE_LETTER = OFF
HIDE_TAB = ""
SURF_TREE_MODE = 1
MAT_AND_VOL_MODE = 0
PRE_TREE_MODE = 1
DEBUG_SAVE = OFF
DEBUG_USEOLDPRTGDI = OFF
DEBUG_SHOWNORMAL = OFF
DEBUG_NOTEX = OFF
DEBUG_OUTLOG = OFF
DEBUG_NOWRITE = OFF
DEBUG_WRITE_FROM_OTHERTHREAD = OFF
DEBUG_WRITE_BY_PACK = OFF
DEBUG_WRITE_MAINTHREAD = OFF
DEBUG_NODIALOG = OFF
FONT_JPN_FIX_NAME = ",l,r ƒSƒVƒbƒN"
FONT_JPN_PRO_NAME = ",l,r ,oƒSƒVƒbƒN"
FONT_ENG_FIX_NAME = "Courier New"
FONT_ENG_PRO_NAME = "Arial"
FONT_JPN_FIX_SIZE = 135
FONT_JPN_PRO_SIZE = 90
FONT_ENG_FIX_SIZE = 120
FONT_ENG_PRO_SIZE = 90
CREATE_DISKNEXTELEMINFO = OFF
SURFACEEDGE_USEV6 = ON
TREE_USE_ROOT_ICON = ON
DEFAULT_FLDOPEN_MAT_ON_CLASSTYPES = "*"
DEFAULT_FLDOPEN_MAT_OFF_CLASSTYPES = ""
DEFAULT_STAAPLY_MAT_ON_CLASSTYPES = ""
DEFAULT_STAAPLY_MAT_OFF_CLASSTYPES = ""
DEFAULT_FLDOPEN_VOL_ON_CLASSTYPES = "*"
DEFAULT_FLDOPEN_VOL_OFF_CLASSTYPES = ""
DEFAULT_STAAPLY_VOL_ON_CLASSTYPES = ""
DEFAULT_STAAPLY_VOL_OFF_CLASSTYPES = ""
GL_ANIMATION_DT2 = 50

USE_SELFSHADING = OFF
USE_GETMAXMIN = OFF
GETMAXMIN_MODE = 1
GETMAXMIN_REGISTER_POINTS = OFF
GETMAXMIN_SET_COLORBAR = ON
GETMAXMIN_DISPLAYCOORDINATES = ON
SHOW_MEMORYMAPNEXT = OFF
FONTSIZE_GLNUM = 1.00000000e+000
FONTINTERVAL_GLNUM = 10
FONTSIZE_FN = 1.00000000e+000
SAVE_MESSAGEWINDOW_TO_FILE = OFF
PATH_MESSAGEWINDOW_TO_FILE = ""
CLIPMODE2 = 2
DONT_CREATE_HASH_FOR_MOVINGOBJ2 = ON
DONT_READ_MOVINGOBJ = OFF
CUR_PRINTER = "NPI91983D (HP Color LaserJet CP4020 Series)"
PRINTING_BACKGROUND = ON
PRINTING_RESOLUTION_MODE = ON
PRINTING_LINEWIDTH_MODE = 1
TRANSPARENT_VALUE = 5.00000000e-001
TRANSPARENTMODE_LINE = 0
TRANSPARENTMODE_VECTOR = 2
TRANSPARENTMODE_POLYGON = 1
TRANSPARENTMODE_OBJECT = 0
TRANSPARENTMODE_MESH = 0
AUTORANGE = OFF
DEF_DRAW_FULLPATH_NEU = ON
REDRAW_AUTO = ON
REDRAW_LEVEL = 4
EASYANIME_MAXSTEP = 12
DETAILLOGPATH =
"C:\Users\Todd\AppData\Roaming\Cradle\SCTwin10\SCTpost_Dx64net\~$CradlePostE
rrorLog_20130614171236_12016.txt"
ROTATE_MODELCENTER = OFF
DISPLAY_MOVABLE = OFF
DISPLAY_AVTIVE = OFF
DISPLAY_OBJNAME = OFF
BACKGROUND_TYPE = ON
BACKGROUND_FILLTYPE = 0
PROJECTION_TYPE = 1
BACKGROUND_COLOR = C16777215
BACKGROUND_COLOR_TOP = C16743936
BACKGROUND_COLOR_BOTTOM = C16777215
EXIT_IMMEDIATE2 = ON
INFO_MAXTEXT3 = 10000000
BEGINNER2 = OFF

MOUSE_MODE3 = 3
MOUSE_OPERATION3 = 0
DEFAULT_USE_NAMES_START = 0
VIEW_SX = 0
VIEW_SY = 0
VIEW_EX = 0
VIEW_EY = 0
FRAME_SX = 0
FRAME_SY = 0
FRAME_EX = 0
FRAME_EY = 0
TOOLDRAW_SX = 0
TOOLDRAW_SY = 0
TOOLDRAW_POPUP = 0
TOOLDRAW_VISIBLE = 0
TOOLENVIRONMENT_SX = 0
TOOLENVIRONMENT_SY = 0
TOOLENVIRONMENT_POPUP = 0
TOOLENVIRONMENT_VISIBLE = 0
TOOLIO_SX = 0
TOOLIO_SY = 0
TOOLIO_POPUP = 0
TOOLIO_VISIBLE = 0
TOOLMOUSE_SX = 0
TOOLMOUSE_SY = 0
TOOLMOUSE_POPUP = 0
TOOLMOUSE_VISIBLE = 0
TOOLNEW_SX = 0
TOOLNEW_SY = 0
TOOLNEW_POPUP = 0
TOOLNEW_VISIBLE = 0
TOOLVIEW_SX = 0
TOOLVIEW_SY = 0
TOOLVIEW_POPUP = 0
TOOLVIEW_VISIBLE = 0
REGISTERED_POINT_NUM = 3
REGISTERED_POINT_DATA_0 = "'X' (1.0 , 0.0 , 0.0)"
REGISTERED_POINT_DATA_1 = "'Y' (0.0 , 1.0 , 0.0)"
REGISTERED_POINT_DATA_2 = "'Z' (0.0 , 0.0 , 1.0)"
REGISTERED_POINT_CURDEL = -1
SIDE_BY_SIDE_TEST = 0.0000000000000000e+000
STIPPLE_MODE = 1
STIPPLE_MANUAL_LEN = 1.0000000000000000e+000
STIPPLE_MANUAL_RATE = 5.0000000000000000e-001
STIPPLE_MANUAL_MODE = 0
SHOW_DRAWMODE = ON

USE_HINT2 = ON
CLUSTER_USE_MULTI_MESSAGEWINDOWS = OFF
CLUSTER_USE_SMALLGL_WHILE_DRAGING = ON
CLUSTER_USE_MAKING_CLUSTERINFO = OFF
USE_UNDO = ON
SEL_AWAY_COME_BOTH = 2
SPREAD_ANGLE = 1.3500999999999999e+002
SPREAD_TAJUUHEN = 0
USE_SELWHENACTIVE = ON
SHOW_DIALOG_WITH_DOUBLECLICK = ON
SET_VIEWPOINT_WITH_DOUBLECLICK = ON
READ_TEX_PER_DRAW2 = ON
USE_NAMERAKA = OFF
USE_POLDELTA = ON
USE_FASTBUFFER = ON
USE_SINGLEBUFFER = OFF
USE_BOTHBUFFER = OFF
NOUSE_DEFOBJ = OFF
FOR_QUADROBUG = OFF
FOR_COMBLACKBMPBUG = ON
USE_DIRECT = ON
USE_USEALPHABUF = ON
USE_LRGNTAB = OFF
USE_NOCLIP3 = 2
USE_AUTOROTATETRANSLATE = ON
FDLG_COMMON = ON
FDLG_FLD_SWAP = OFF
FDLG_FLD_FAZZY = ON
FDLG_FLD_KEEPPOS = OFF
FDLG_FLD_HASH = ON
FDLG_FLD_MAGIC = OFF
FDLG_HEN_RESET_ADD = 0
FDLG_INI_APPLYWINDOW_V10 = ON
FDLG_NEU_GLOBAL = OFF
FDLG_CSV_GLOBAL = OFF
FDLG_PCL_GLOBAL = ON
FDLG_TM_GLOBAL = OFF
FDLG_STA_FLD_APPLYMODE = 2
FDLG_STA_GLB_APPLYMODE = 0
FDLG_STA_APPLYWINDOW = ON
FDLG_TM_RECYCLE_CREATE = 0
WDLG_COMMON = OFF
WDLG_STA_ACTIVE_ALL = 1
TREEVISIBLEICONTYPE = 0
AUTOUPDATEFLDFILELISTTIMEELAPSE = 600000

```
[SAVEBMP]
   LANG_ID              = 1033
   TREE_ORDER_ID        = 1
   DEFAULT_NAME         = ""
   DEFAULT_WITHOUTPOS   = OFF
   SHORT_TITLE          = "SAVEBMP"
   LONG_TITLE           = "Camera"
   DISPLAY_TITLE        = "Camera"
   DISPLAY_TITLE_MODIFIED  = OFF
   COL_MATCH_MODE       = 1
   TOPPOS_MODE          = 0
   PLUSMINUS_MODE       = 0
   INTEGRATE1_CALC      = OFF
   INTEGRATE1_SAVE      = OFF
   INTEGRATE1_FN        = ""
   INTEGRATE1_USE_BEEP  = ON
   INTEGRATE1_USE_REDRAW  = ON
   INTEGRATE1_USE_STR   = ON
   INTEGRATE3_CALC      = OFF
   INTEGRATE3_SAVE      = OFF
   INTEGRATE3_FN        = ""
   INTEGRATE3_USE_BEEP  = ON
   INTEGRATE3_USE_REDRAW  = ON
   INTEGRATE3_USE_STR   = ON
   MY_ID                = 1
   PARENT_ID            = -1
   DRAWABLE             = OFF
   TEX_USE              = OFF
   TEX_TYPE             = 0
   TEX_TYPE0_X          = 1.00000000e+000
   TEX_TYPE0_Y          = 1.00000000e+000
   TEX_TYPE0_Z          = 1.00000000e+000
   TEX_TYPE1_NX         = 0.00000000e+000
   TEX_TYPE1_NY         = 0.00000000e+000
   TEX_TYPE1_NZ         = 1.00000000e+000
   TEX_TYPE1_R          = 1.00000000e+000
   TEX_TYPE1_TZ         = 1.00000000e+000
   TEX_TYPE2_NX         = 0.00000000e+000
   TEX_TYPE2_NY         = 0.00000000e+000
   TEX_TYPE2_NZ         = 1.00000000e+000
   TEX_TYPE2_S          = 1.00000000e+000
   TEX_ROTATE0_X        = 0.00000000e+000
   TEX_ROTATE0_Y        = 0.00000000e+000
   TEX_ROTATE0_Z        = 0.00000000e+000
   TEX_ROTATE1_TZ       = 0.00000000e+000
```

TEX_ROTATE1_R = 0.00000000e+000
TEX_ROTATE2_S = 0.00000000e+000
TEX_OFS0_X_X = 0.00000000e+000
TEX_OFS0_X_Y = 0.00000000e+000
TEX_OFS0_Y_X = 0.00000000e+000
TEX_OFS0_Y_Y = 0.00000000e+000
TEX_OFS0_Z_X = 0.00000000e+000
TEX_OFS0_Z_Y = 0.00000000e+000
TEX_OFS1_R_X = 0.00000000e+000
TEX_OFS1_R_Y = 0.00000000e+000
TEX_OFS1_TZ_X = 0.00000000e+000
TEX_OFS1_TZ_Y = 0.00000000e+000
TEX_OFS2_X = 0.00000000e+000
TEX_OFS2_Y = 0.00000000e+000
TEX_USECOLORKEY = OFF
TEX_COLORKEY = C16711680
TEX_UPSIDEDOWN = OFF
TEX_FILENAME = ""
ONLY_ONEVAR = ON
BILLBOARD_ENABLED = 0
BMP_FORMAT = 1
AUTO_SAVE = OFF
KEEP_ASPECT = ON
SET_WINDOWSIZE = ON
FORMAT = 1
JPEG_QUALITY = 5
USE_BEEP = ON
SIZE_X = 1434
SIZE_Y = 906
RESOLUTION = 9.6019999999999996e+001

[FLD]
LANG_ID = 1033
TREE_ORDER_ID = 2
DEFAULT_NAME = ""
DEFAULT_WITHOUTPOS = OFF
SHORT_TITLE = "FLD"
LONG_TITLE = "FLD FILE (1)"
DISPLAY_TITLE = fld_name
DISPLAY_TITLE_MODIFIED = OFF
COL_MATCH_MODE = 1
TOPPOS_MODE = 0
PLUSMINUS_MODE = 0
INTEGRATE1_CALC = OFF
INTEGRATE1_SAVE = OFF

INTEGRATE1_FN = ""
INTEGRATE1_USE_BEEP = ON
INTEGRATE1_USE_REDRAW = ON
INTEGRATE1_USE_STR = ON
INTEGRATE3_CALC = OFF
INTEGRATE3_SAVE = OFF
INTEGRATE3_FN = ""
INTEGRATE3_USE_BEEP = ON
INTEGRATE3_USE_REDRAW = ON
INTEGRATE3_USE_STR = ON
MY_ID = 2
PARENT_ID = 2
DRAWABLE = ON
TEX_USE = OFF
TEX_TYPE = 0
TEX_TYPE0_X = 1.00000000e+000
TEX_TYPE0_Y = 1.00000000e+000
TEX_TYPE0_Z = 1.00000000e+000
TEX_TYPE1_NX = 0.00000000e+000
TEX_TYPE1_NY = 0.00000000e+000
TEX_TYPE1_NZ = 1.00000000e+000
TEX_TYPE1_R = 1.00000000e+000
TEX_TYPE1_TZ = 1.00000000e+000
TEX_TYPE2_NX = 0.00000000e+000
TEX_TYPE2_NY = 0.00000000e+000
TEX_TYPE2_NZ = 1.00000000e+000
TEX_TYPE2_S = 1.00000000e+000
TEX_ROTATE0_X = 0.00000000e+000
TEX_ROTATE0_Y = 0.00000000e+000
TEX_ROTATE0_Z = 0.00000000e+000
TEX_ROTATE1_TZ = 0.00000000e+000
TEX_ROTATE1_R = 0.00000000e+000
TEX_ROTATE2_S = 0.00000000e+000
TEX_OFS0_X_X = 0.00000000e+000
TEX_OFS0_X_Y = 0.00000000e+000
TEX_OFS0_Y_X = 0.00000000e+000
TEX_OFS0_Y_Y = 0.00000000e+000
TEX_OFS0_Z_X = 0.00000000e+000
TEX_OFS0_Z_Y = 0.00000000e+000
TEX_OFS1_R_X = 0.00000000e+000
TEX_OFS1_R_Y = 0.00000000e+000
TEX_OFS1_TZ_X = 0.00000000e+000
TEX_OFS1_TZ_Y = 0.00000000e+000
TEX_OFS2_X = 0.00000000e+000
TEX_OFS2_Y = 0.00000000e+000
TEX_USECOLORKEY = OFF

TEX_COLORKEY = C16711680
TEX_UPSIDEDOWN = OFF
TEX_FILENAME = ""
MATRIX_0_0 = -0.1616975998945730
MATRIX_1_0 = 0.1616975998945730
MATRIX_2_0 = 0.0000000000000000
MATRIX_3_0 = 1.8270782278273057
MATRIX_0_1 = -0.0933561528264481
MATRIX_1_1 = -0.0933561528264481
MATRIX_2_1 = 0.1867123056528962
MATRIX_3_1 = 1.5924624958041502
MATRIX_0_2 = 0.1320255374581383
MATRIX_1_2 = 0.1320255374581383
MATRIX_2_2 = 0.1320255374581383
MATRIX_3_2 = -1.9754321042173950
MATRIX_0_3 = 0.0000000000000000
MATRIX_1_3 = 0.0000000000000000
MATRIX_2_3 = 0.0000000000000000
MATRIX_3_3 = 1.0000000000000000
DRAW_ALL = ON
DRAW_LEVEL = 0
SYNCHRONIZE = ON
ACTIVE = OFF
ROTATE_CENTER_X = 1.10000000e+001
ROTATE_CENTER_Y = 2.85750000e+000
ROTATE_CENTER_Z = 1.10500000e+000
VOL2_ISDRAW_START = 1
VOL2_ISDRAW_DATA_0 = ON
VOL2_EMTNAME_START = 1
VOL2_EMTNAME_DATA_0 = "NotRegistered"
VOL2_ORGNAME_START = 1
VOL2_ORGNAME_DATA_0 = "NotRegistered"
VOL2_CHECK = 0
MAT2_ISDRAW_START = 2
MAT2_ISDRAW_DATA_0 = ON
MAT2_ISDRAW_DATA_1 = ON
MAT2_EMTNAME_START = 2
MAT2_EMTNAME_DATA_0 = "MAT0"
MAT2_EMTNAME_DATA_1 = "MAT1"
MAT2_ORGNAME_START = 2
MAT2_ORGNAME_DATA_0 = "MAT0"
MAT2_ORGNAME_DATA_1 = "MAT1"
MAT2_CHECK = 0
ONLY_ONEVAR = OFF
BILLBOARD_ENABLED = 0
UNIT5_FLD_1ENV_2FLD = 2

```
UNIT5_FLD_USE          = 1
UNIT5_FLD_LNAM_START    = 22
UNIT5_FLD_LNAM_DATA_0   = "G"
UNIT5_FLD_LNAM_DATA_1   = "DIST"
UNIT5_FLD_LNAM_DATA_2   = "PRES"
UNIT5_FLD_LNAM_DATA_3   = "TEMP"
UNIT5_FLD_LNAM_DATA_4   = "MRT"
UNIT5_FLD_LNAM_DATA_5   = "LTTP"
UNIT5_FLD_LNAM_DATA_6   = "TPOR"
UNIT5_FLD_LNAM_DATA_7   = "TSK"
UNIT5_FLD_LNAM_DATA_8   = "VEL"
UNIT5_FLD_LNAM_DATA_9   = "USTR"
UNIT5_FLD_LNAM_DATA_10  = "DENS"
UNIT5_FLD_LNAM_DATA_11  = "ENTL"
UNIT5_FLD_LNAM_DATA_12  = "TURK"
UNIT5_FLD_LNAM_DATA_13  = "TEPS"
UNIT5_FLD_LNAM_DATA_14  = "EVIS"
UNIT5_FLD_LNAM_DATA_15  = "RFV"
UNIT5_FLD_LNAM_DATA_16  = "CUR"
UNIT5_FLD_LNAM_DATA_17  = "ELPT"
UNIT5_FLD_LNAM_DATA_18  = "HUMC"
UNIT5_FLD_LNAM_DATA_19  = "HUMA"
UNIT5_FLD_LNAM_DATA_20  = "HTRC"
UNIT5_FLD_LNAM_DATA_21  = "HVEC"
UNIT5_FLD_NAME_START    = 22
UNIT5_FLD_NAME_DATA_0   = "m"
UNIT5_FLD_NAME_DATA_1   = "m"
UNIT5_FLD_NAME_DATA_2   = "Pa"
UNIT5_FLD_NAME_DATA_3   = "C"
UNIT5_FLD_NAME_DATA_4   = "C"
UNIT5_FLD_NAME_DATA_5   = "C"
UNIT5_FLD_NAME_DATA_6   = "C"
UNIT5_FLD_NAME_DATA_7   = "C"
UNIT5_FLD_NAME_DATA_8   = "m/s"
UNIT5_FLD_NAME_DATA_9   = "m/s"
UNIT5_FLD_NAME_DATA_10  = "kg/m3"
UNIT5_FLD_NAME_DATA_11  = "J/kg"
UNIT5_FLD_NAME_DATA_12  = "m2/s2"
UNIT5_FLD_NAME_DATA_13  = "m2/s3"
UNIT5_FLD_NAME_DATA_14  = "Pa s"
UNIT5_FLD_NAME_DATA_15  = "W/m2"
UNIT5_FLD_NAME_DATA_16  = "A/m2"
UNIT5_FLD_NAME_DATA_17  = "V"
UNIT5_FLD_NAME_DATA_18  = "kg/(m2 s)"
UNIT5_FLD_NAME_DATA_19  = "kg/m2"
UNIT5_FLD_NAME_DATA_20  = "W/(m2 K)"
```

UNIT5_FLD_NAME_DATA_21 = "W/m2"
UNIT5_FLD_SCALE_START = 22
UNIT5_FLD_SCALE_DATA_0 = "1"
UNIT5_FLD_SCALE_DATA_1 = "1"
UNIT5_FLD_SCALE_DATA_2 = "1"
UNIT5_FLD_SCALE_DATA_3 = "1"
UNIT5_FLD_SCALE_DATA_4 = "1"
UNIT5_FLD_SCALE_DATA_5 = "1"
UNIT5_FLD_SCALE_DATA_6 = "1"
UNIT5_FLD_SCALE_DATA_7 = "1"
UNIT5_FLD_SCALE_DATA_8 = "1"
UNIT5_FLD_SCALE_DATA_9 = "1"
UNIT5_FLD_SCALE_DATA_10 = "1"
UNIT5_FLD_SCALE_DATA_11 = "1"
UNIT5_FLD_SCALE_DATA_12 = "1"
UNIT5_FLD_SCALE_DATA_13 = "1"
UNIT5_FLD_SCALE_DATA_14 = "1"
UNIT5_FLD_SCALE_DATA_15 = "1"
UNIT5_FLD_SCALE_DATA_16 = "1"
UNIT5_FLD_SCALE_DATA_17 = "1"
UNIT5_FLD_SCALE_DATA_18 = "1"
UNIT5_FLD_SCALE_DATA_19 = "1"
UNIT5_FLD_SCALE_DATA_20 = "1"
UNIT5_FLD_SCALE_DATA_21 = "1"
UNIT5_FLD_OFS_START = 22
UNIT5_FLD_OFS_DATA_0 = "0"
UNIT5_FLD_OFS_DATA_1 = "0"
UNIT5_FLD_OFS_DATA_2 = "0"
UNIT5_FLD_OFS_DATA_3 = "0"
UNIT5_FLD_OFS_DATA_4 = "0"
UNIT5_FLD_OFS_DATA_5 = "0"
UNIT5_FLD_OFS_DATA_6 = "0"
UNIT5_FLD_OFS_DATA_7 = "0"
UNIT5_FLD_OFS_DATA_8 = "0"
UNIT5_FLD_OFS_DATA_9 = "0"
UNIT5_FLD_OFS_DATA_10 = "0"
UNIT5_FLD_OFS_DATA_11 = "0"
UNIT5_FLD_OFS_DATA_12 = "0"
UNIT5_FLD_OFS_DATA_13 = "0"
UNIT5_FLD_OFS_DATA_14 = "0"
UNIT5_FLD_OFS_DATA_15 = "0"
UNIT5_FLD_OFS_DATA_16 = "0"
UNIT5_FLD_OFS_DATA_17 = "0"
UNIT5_FLD_OFS_DATA_18 = "0"
UNIT5_FLD_OFS_DATA_19 = "0"
UNIT5_FLD_OFS_DATA_20 = "0"

UNIT5_FLD_OFS_DATA_21 = "0"
TRIM_SETTING_DONE = OFF
TRIM_SETTING_SURF = ""
TRIM_SETTING_VOLUME = ""
TRIM_SETTING_MAT = ""
TRIM_SETTING_SCALAR = ""
TRIM_SETTING_VECTOR = ""
TRIM_SETTING_XMIN = -1.0000000000000000e+020
TRIM_SETTING_XMAX = 1.0000000000000000e+020
TRIM_SETTING_YMIN = -1.0000000000000000e+020
TRIM_SETTING_YMAX = 1.0000000000000000e+020
TRIM_SETTING_ZMIN = -1.0000000000000000e+020
TRIM_SETTING_ZMAX = 1.0000000000000000e+020
TIME_DELTA = 0.0000000000000000e+000
DOAFTERREAD_MODE = 0
DOAFTERREAD_REFX = 0.00000000e+000
DOAFTERREAD_REFY = 0.00000000e+000
DOAFTERREAD_REFZ = 1.00000000e+000
DRAW_DISP = 0
LOCK_TO_USE = OFF
LOCK_FROM_USE = OFF
LOCK_REF_USE = ON
LOCK_LRGN = ""
LOCK_FX = 0.00000000e+000
LOCK_FY = 0.00000000e+000
LOCK_FZ = 0.00000000e+000
CHANGE_CYC_LOOP2 = OFF
USE_APX_REDUCE = ON
VAREX_DST_USE = 0
VAREX_DST_LRGN_START = 1
VAREX_DST_LRGN_DATA_0 = "SURFACE*"
VAREX_EIGEN_LVAR3 = ""
VAREX_EIGEN2_LVAR1_XX = ""
VAREX_EIGEN2_LVAR1_XY = ""
VAREX_EIGEN2_LVAR1_XZ = ""
VAREX_EIGEN2_LVAR1_YY = ""
VAREX_EIGEN2_LVAR1_YZ = ""
VAREX_EIGEN2_LVAR1_ZZ = ""
VAREX_DST_MODE = 0
VAREX_DST_LENGTH = 4.40000000e-002
VAREX_DST_DELTA = 2.20000000e-003
VAREX_CSV_USE = 0
VAREX_CSV_FILENAME = ""
VAREX_PMV_USE = 0
VAREX_MSH_USE = 0
VAREX_MVL_USE = 0

VAREX_EIGEN_USE = 0
VAREX_EIGEN2_USE = 0
VAREX_SIS_USE = 0
VAREX_MAT_USE = 0
VAREX_NORMAL_USE = 0
VAREX_SETSTAR_USE = 0
VAREX_FLOWAGE_USE = 0
VAREX_ALLCYC_USE = 0
VAREX_SIS_POSX = 0.00000000e+000
VAREX_SIS_POSY = 0.00000000e+000
VAREX_SIS_POSZ = 0.00000000e+000
VAREX_SIS_LVAR = ""
VAREX_SIS_VAL = 0.00000000e+000
VAREX_SIS_SIDE = -1
FILENAME = fld_name
READONLY_FILESIZE = 0
READONLY_FLDTYPE = 2
READONLY_L2D3D = 3
READONLY_CURCYCID = 1
READONLY_CURCYCID_F = 0.0000000000000000e+000
READONLY_CURCYCLE = 660
READONLY_CURTIME = 0.0000000000000000e+000
READONLY_FLD_SOLVERTYPE = ""
READONLY_FLD_IVER1 = 0
READONLY_FLD_IVER2 = 0
READONLY_FLD_IVER3 = 0
READONLY_USEHASH = ON
READONLY_HASH_XNUM = 87
READONLY_HASH_YNUM = 23
READONLY_HASH_ZNUM = 9
READONLY_SCALE = 2.20000000e+001
READONLY_USEFAZZY = ON
READONLY_ISVF = OFF
READONLY_OLDFLDCYCPOS_NUM = 0
READONLY_CYCLIST_NUM = 2
READONLY_CYCLIST_DATA_0 = 50
READONLY_CYCLIST_DATA_1 = 660
READONLY_TIMELIST_NUM = 2
READONLY_TIMELIST_DATA_0 = 0.00000000e+000
READONLY_TIMELIST_DATA_1 = 0.00000000e+000
READONLY_LRGN_NUM = 10
READONLY_LRGN_DATA_0 = "walls"
READONLY_LRGN_DATA_1 = "face"
READONLY_LRGN_DATA_2 = "curtain"
READONLY_LRGN_DATA_3 = "inlet"
READONLY_LRGN_DATA_4 = "outlet"

READONLY_LRGN_DATA_5 = "@UNDEFINEDMOM"
READONLY_LRGN_DATA_6 = "@UNDEFINEDENTB"
READONLY_LRGN_DATA_7 = "@UNDEFINEDENTF"
READONLY_LRGN_DATA_8 = "@UNDEFINEDENTS"
READONLY_LRGN_DATA_9 = "SURFACE"
READONLY_ISCYL_NUM = 1
READONLY_ISCYL_DATA_0 = 0
READONLY_NGFAX_PER_OV_NUM = 1
READONLY_NGFAX_PER_OV_DATA_0 = 10
READONLY_NELEM_PER_OV_NUM = 1
READONLY_NELEM_PER_OV_DATA_0 = 2521187
READONLY_NELEM = 2521187
READONLY_NESUM = 12445157
READONLY_NNODS_PER_OV_NUM = 1
READONLY_NNODS_PER_OV_DATA_0 = 855974
READONLY_NNODS = 855974
READONLY_NELEMX = 12445157
READONLY_OLDFLD_NGFBX = 0
READONLY_NGFB_PER_OV_NUM = 10
READONLY_NGFB_PER_OV_DATA_0 = 89369
READONLY_NGFB_PER_OV_DATA_1 = 1000
READONLY_NGFB_PER_OV_DATA_2 = 103032
READONLY_NGFB_PER_OV_DATA_3 = 1792
READONLY_NGFB_PER_OV_DATA_4 = 1890
READONLY_NGFB_PER_OV_DATA_5 = 0
READONLY_NGFB_PER_OV_DATA_6 = 90369
READONLY_NGFB_PER_OV_DATA_7 = 103032
READONLY_NGFB_PER_OV_DATA_8 = 0
READONLY_NGFB_PER_OV_DATA_9 = 197083
READONLY_XMIN = 0.00000000e+000
READONLY_XMAX = 2.20000000e+001
READONLY_YMIN = 0.00000000e+000
READONLY_YMAX = 5.71500000e+000
READONLY_ZMIN = 0.00000000e+000
READONLY_ZMAX = 2.21000000e+000
READONLY_LOOPMAX = 2.21000000e+000
READONLY_TMIN = 0.00000000e+000
READONLY_TMAX = 1.57079633e+000
READONLY_VAR1NUM = 14
READONLY_VAR1LNAM_0 = "PRES"
READONLY_VAR1LNAM_1 = "TURK"
READONLY_VAR1LNAM_2 = "TEPS"
READONLY_VAR1LNAM_3 = "EVIS"
READONLY_VAR1LNAM_4 = "YPLS"
READONLY_VAR1LNAM_5 = "USTR"
READONLY_VAR1LNAM_6 = "VELX"

READONLY_VAR1LNAM_7 = "VELY"
READONLY_VAR1LNAM_8 = "VELZ"
READONLY_VAR1LNAM_9 = "VELV"
READONLY_VAR1LNAM_10 = "GX"
READONLY_VAR1LNAM_11 = "GY"
READONLY_VAR1LNAM_12 = "GZ"
READONLY_VAR1LNAM_13 = "GV"
READONLY_VAR1TITLE_0 = "Pressure (PRES)"
READONLY_VAR1TITLE_1 = "Turbulence Energy (TURK)"
READONLY_VAR1TITLE_2 = "Turbulence Dissipation Rate (TEPS)"
READONLY_VAR1TITLE_3 = "Eddy Viscosity Coefficient (EVIS)"
READONLY_VAR1TITLE_4 = "Normalized Wall Distance (YPLS)"
READONLY_VAR1TITLE_5 = "Wall Friction Velocity (USTR)"
READONLY_VAR1TITLE_6 = "Velocity (x-component) (VELX)"
READONLY_VAR1TITLE_7 = "Velocity (y-component) (VELY)"
READONLY_VAR1TITLE_8 = "Velocity (z-component) (VELZ)"
READONLY_VAR1TITLE_9 = "Magnitude of Velocity (VELV)"
READONLY_VAR1TITLE_10 = "x-coordinate (GX)"
READONLY_VAR1TITLE_11 = "y-coordinate (GY)"
READONLY_VAR1TITLE_12 = "z-coordinate (GZ)"
READONLY_VAR1TITLE_13 = "Magnitude of Coordinate (GV)"
READONLY_VAR1MINVAL_0 = -1.01917441e-001
READONLY_VAR1MINVAL_1 = 1.00000000e-009
READONLY_VAR1MINVAL_2 = 1.00000000e-009
READONLY_VAR1MINVAL_3 = 1.02510000e-010
READONLY_VAR1MINVAL_4 = 2.12579242e+000
READONLY_VAR1MINVAL_5 = 6.71869644e-004
READONLY_VAR1MINVAL_6 = -1.95886168e+000
READONLY_VAR1MINVAL_7 = -6.00816109e-001
READONLY_VAR1MINVAL_8 = -4.94657858e-001
READONLY_VAR1MINVAL_9 = 0.00000000e+000
READONLY_VAR1MINVAL_10 = 0.00000000e+000
READONLY_VAR1MINVAL_11 = 0.00000000e+000
READONLY_VAR1MINVAL_12 = 0.00000000e+000
READONLY_VAR1MINVAL_13 = 0.00000000e+000
READONLY_VAR1MINPOS_0 = 132093
READONLY_VAR1MINPOS_1 = 98624
READONLY_VAR1MINPOS_2 = 109073
READONLY_VAR1MINPOS_3 = 120417
READONLY_VAR1MINPOS_4 = 832737
READONLY_VAR1MINPOS_5 = 6757
READONLY_VAR1MINPOS_6 = 212156
READONLY_VAR1MINPOS_7 = 94141
READONLY_VAR1MINPOS_8 = 61427
READONLY_VAR1MINPOS_9 = 0
READONLY_VAR1MINPOS_10 = 419771

READONLY_VAR1MINPOS_11 = 3918
READONLY_VAR1MINPOS_12 = 220
READONLY_VAR1MINPOS_13 = 823869
READONLY_VAR1MAXVAL_0 = 2.22392862e+000
READONLY_VAR1MAXVAL_1 = 7.58132740e-002
READONLY_VAR1MAXVAL_2 = 4.23911864e-001
READONLY_VAR1MAXVAL_3 = 4.68699607e-002
READONLY_VAR1MAXVAL_4 = 3.23851339e+002
READONLY_VAR1MAXVAL_5 = 1.02728940e-001
READONLY_VAR1MAXVAL_6 = 1.77691495e+000
READONLY_VAR1MAXVAL_7 = 1.60017352e+000
READONLY_VAR1MAXVAL_8 = 1.01269128e+000
READONLY_VAR1MAXVAL_9 = 1.96116733e+000
READONLY_VAR1MAXVAL_10 = 2.20000000e+001
READONLY_VAR1MAXVAL_11 = 5.71500000e+000
READONLY_VAR1MAXVAL_12 = 2.21000000e+000
READONLY_VAR1MAXVAL_13 = 2.28373669e+001
READONLY_VAR1MAXPOS_0 = 57846
READONLY_VAR1MAXPOS_1 = 578355
READONLY_VAR1MAXPOS_2 = 746120
READONLY_VAR1MAXPOS_3 = 602845
READONLY_VAR1MAXPOS_4 = 163124
READONLY_VAR1MAXPOS_5 = 830904
READONLY_VAR1MAXPOS_6 = 134268
READONLY_VAR1MAXPOS_7 = 63185
READONLY_VAR1MAXPOS_8 = 60244
READONLY_VAR1MAXPOS_9 = 212156
READONLY_VAR1MAXPOS_10 = 148
READONLY_VAR1MAXPOS_11 = 27442
READONLY_VAR1MAXPOS_12 = 300871
READONLY_VAR1MAXPOS_13 = 209
READONLY_VAR1TYPE_0 = -1
READONLY_VAR1TYPE_1 = -1
READONLY_VAR1TYPE_2 = -1
READONLY_VAR1TYPE_3 = -1
READONLY_VAR1TYPE_4 = -1
READONLY_VAR1TYPE_5 = -1
READONLY_VAR1TYPE_6 = 0
READONLY_VAR1TYPE_7 = 1
READONLY_VAR1TYPE_8 = 2
READONLY_VAR1TYPE_9 = -1
READONLY_VAR1TYPE_10 = 3
READONLY_VAR1TYPE_11 = 4
READONLY_VAR1TYPE_12 = 5
READONLY_VAR1TYPE_13 = 6
READONLY_VAR3NUM = 2

READONLY_VAR3LNAM_0 = "VEL"
READONLY_VAR3LNAM_1 = "G"
READONLY_VAR3TITLE_0 = "Velocity (VEL)"
READONLY_VAR3TITLE_1 = "Coordinate (G)"
READONLY_VAR3MINVAL_0 = 0.00000000e+000
READONLY_VAR3MINVAL_1 = 0.00000000e+000
READONLY_VAR3MINPOS_0 = 0
READONLY_VAR3MINPOS_1 = 823869
READONLY_VAR3MAXVAL_0 = 1.96116733e+000
READONLY_VAR3MAXVAL_1 = 2.28373669e+001
READONLY_VAR3MAXPOS_0 = 212156
READONLY_VAR3MAXPOS_1 = 209
READONLY_VAR3TYPE_0 = -1
READONLY_VAR3TYPE_1 = 0
READONLY_PARTICLE_NUM = 0
READONLY_PARTICLE_VAR1NUM = 0
READONLY_PARTICLE_VAR3NUM = 0
READONLY_INVALIDVALUE = 9.99000000e+019
READONLY_VAR1_ORG_NUM = 6
READONLY_VAR1_NEW_NUM = 0
READONLY_VAR3_ORG_NUM = 1
READONLY_VAR3_NEW_NUM = 0
SOLAR_LOCK = OFF
SOLAR_NX = 0.00000000e+000
SOLAR_NY = 1.00000000e+000
SOLAR_NZ = 0.00000000e+000
SOLAR_VX = 0.00000000e+000
SOLAR_VY = 0.00000000e+000
SOLAR_VZ = 1.00000000e+000
SOLAR_TIME = 0.00000000e+000
SOLAR_STIME = 0.00000000e+000
SOLAR_SUNX = 0.00000000e+000
SOLAR_SUNY = 0.00000000e+000
SOLAR_SUNZ = 0.00000000e+000
SOLAR_ROTN = 0.00000000e+000
SOLAR_ROTD = 0.00000000e+000
SOLAR_ROTE = 0.00000000e+000
SOLAR_ROTF = 0.00000000e+000
SOLAR_ROTL = 0.00000000e+000
SOLAR_STANDL = 0.00000000e+000
SOLAR_JD = 0.00000000e+000
SOLAR_JSKY = 0.00000000e+000
SOLAR_SUNF = 0.00000000e+000
SOLAR_USE_DRAW_SUN = OFF
SOLAR_USE_DRAW_4 = OFF
SOLAR_USE_DRAW_CIRCLE = OFF

SOLAR_USE_DRAW_TIME = OFF
SOLAR_USE_STRCOLOR = ON
SOLAR_COLOR_STR = C255
SOLAR_USE_LINECOLOR = OFF
SOLAR_COLOR_LINE = C0
SOLAR_POSITION = 1
SOLAR_POSITIONX = 0.00000000e+000
SOLAR_POSITIONY = 0.00000000e+000
SOLAR_IS_FROMDIS = 1
SOLAR_DEG = 0
SOLAR_DRAW_BASESIZE = 1.0000000000000000e+000
SOLAR_DRAW_VECSIZE = 1.0000000000000000e+000
SOLAR_DRAW_SUNSIZE = 1.0000000000000000e+000
SOLAR_DRAW_WIDTH = 1.0000000000000000e+000
VIEWPORT_WIDTH = 1
VIEWPORT_COLOR = C8947848
VIEWPORT_SX = 0.0000000000000000e+000
VIEWPORT_SY = 0.0000000000000000e+000
VIEWPORT_EX = 1.0000000000000000e+000
VIEWPORT_EY = 1.0000000000000000e+000
CYCROTATE_AX = 0.0000000000000000e+000
CYCROTATE_AY = 0.0000000000000000e+000
CYCROTATE_AZ = 0.0000000000000000e+000
CYCROTATE_CX = 0.0000000000000000e+000
CYCROTATE_CY = 0.0000000000000000e+000
CYCROTATE_CZ = 0.0000000000000000e+000
CYCROTATE_STATE = -1
DRAW_THIS = ON
ACTIVE_THIS = ON
TITLE_POS = 1
TITLE_ARBITRARYCOORDX = -9.00976290e-001
TITLE_ARBITRARYCOORDY = 8.98454746e-001
TITLE_AUTOCOLOR = ON
TITLE_DRAWFILENAME = ON
TITLE_DRAWFULLPATH = OFF
TITLE_DRAWCYCLE = OFF
TITLE_DRAWTIME = OFF
TITLE_DRAWUNIT = OFF
CYCLEOPERATION_STEP = 1.0000000000000000e+000
CYCLEOPERATION_MODE = 0
TITLE_COLOR = C8947848
TITLE_TIME_USE = OFF
TITLE_TIME_SCALE = 1.0000000000000000e+000
TITLE_TIME_OFFSET = 0.0000000000000000e+000
TITLE_TIME_DIGIT = 3
TITLE_TIME_DIGIT2 = 16

VECTOR_DIGIT = 16
AXIS_DRAW2 = ON
AXIS_TYPE = 1
AXIS_POS = 1
AXIS_ARBITRARYCOORDX = 0.00000000e+000
AXIS_ARBITRARYCOORDY = 0.00000000e+000
AXIS_AUTOPOS = ON
AXIS_COLOR = C16777215
AXIS_ARROW = ON
AXIS_SOLID = OFF
AXIS_MINUS = OFF
AXIS_SCALE = 1.0000000000000000e+000
CYLINDER_SMOOTHMAX = -1
CYLINDER_SMOOTH = OFF
GRID_DRAW = OFF
GRID_AUTOSTEP = ON
GRID_XSTEP = 1.00000000e+000
GRID_YSTEP = 1.00000000e+000
GRID_ZSTEP = 1.00000000e+000
HIST_NUM = 0
PMV_CLO = 7.50000000e-001
PMV_MET = 1.20000000e+000
PMV_RH = 5.00000000e+001
PMV_MRT = 0
PMV_TEMP = 0
PMV_MRT_SMRT = 0
PMV_HUMI_USE = 0
SETSTAR_HUMI_USE = 0
SETSTAR_PRES = 7.60000000e+002
SETSTAR_WEIGHT = 7.00000000e+001
SETSTAR_SURF = 1.80000000e+000
SETSTAR_CLO = 5.00000000e-001
SETSTAR_MET = 8.73000000e+001
SETSTAR_RH = 2.50000000e+001
SETSTAR_MRT = 0
SETSTAR_TEMP = 0
SETSTAR_MRT_SMRT = 0
STRUCT_ANIME_NUM = 12
AUTO_STRUCT_OBJ = OFF
STRUCT_ON_OBJ_START = 0
STRUCT_OFF_OBJ_START = 0
SCALE_MODE = -1
SCALE_CX = 0.00000000e+000
SCALE_CY = 0.00000000e+000
SCALE_CZ = 0.00000000e+000
SCALE0_SX = 1.00000000e+000

SCALE0_SY = 1.20000000e+000
SCALE0_SZ = 3.32727273e+000
SCALE1_NX = 0.00000000e+000
SCALE1_NY = 0.00000000e+000
SCALE1_NZ = 1.00000000e+000
SCALE1_R = 2.51509443e+001
SCALE1_S = 1.00000000e+000
SCALE1_D = 2.51509443e+001
SCALE2_NX = 0.00000000e+000
SCALE2_NY = 0.00000000e+000
SCALE2_NZ = 1.00000000e+000
SCALE2_T = 1.51934603e+001
SCALE2_R = 2.51509443e+001
SCALE2_L = -2.20000000e+000
SCALE2_S = 1.00000000e+000
SCALE2_D = 2.56737193e+001
SCALE3_R = 2.52469800e+001
SCALE3_S = 1.00000000e+000
SCALE3_D = 2.52469800e+001
SCALE4_NX = 0.00000000e+000
SCALE4_NY = 0.00000000e+000
SCALE4_NZ = 1.00000000e+000
SCALE4_RX = 1.00000000e+000
SCALE4_RY = 0.00000000e+000
SCALE4_RZ = 0.00000000e+000
SCALE4_THETASCALE = 6.10000000e+000
SCALE4_AAA = 0.00000000e+000
SCALE4_BBB = 0.00000000e+000
SCALE4_BLADENUM = 0
SCALE4_BLADENAME = ""
BASEVECTOR_USE = OFF
BASEVECTOR_AUTO_COLOR = ON
BASEVECTOR_COLOR = C0
BASEVECTOR_VAR3 = 0
BASESTRUCT_VAR3 = 0
BASEVECTOR_POS = 1
BASEVECTOR_XCOORDINATE = 0.00000000e+000
BASEVECTOR_YCOORDINATE = 0.00000000e+000
BASEVECTOR_MAX_NORMAL = ON
BASESTRUCT_MAX_NORMAL = OFF
BASEVECTOR_AUTO_PARAM = ON
BASEVECTOR_BASELEN_0 = 5.60890435e-001
BASEVECTOR_BASELEN_1 = 4.81666738e-002
BASESTRUCT_BASELEN_0 = 1.00000000e+000
BASESTRUCT_BASELEN_1 = 4.83226112e-002
BASEVECTOR_DRAWLEN_0 = 1.96116733e+000

```
   BASEVECTOR_DRAWLEN_1    = 2.28373669e+001


[FULLSURF]
   LANG_ID              = 1033
   TREE_ORDER_ID         = 3
   DEFAULT_NAME          = ""
   DEFAULT_WITHOUTPOS     = OFF
   SHORT_TITLE           = "FULLSURF"
   LONG_TITLE            = "Surface (1)"
   DISPLAY_TITLE         = "Surface (1)"
   DISPLAY_TITLE_MODIFIED  = OFF
   COL_MATCH_MODE         = 1
   TOPPOS_MODE           = 0
   PLUSMINUS_MODE         = 0
   INTEGRATE1_CALC        = OFF
   INTEGRATE1_SAVE        = OFF
   INTEGRATE1_FN          = ""
   INTEGRATE1_USE_BEEP     = ON
   INTEGRATE1_USE_REDRAW   = ON
   INTEGRATE1_USE_STR      = ON
   INTEGRATE3_CALC        = OFF
   INTEGRATE3_SAVE        = OFF
   INTEGRATE3_FN          = ""
   INTEGRATE3_USE_BEEP     = ON
   INTEGRATE3_USE_REDRAW   = ON
   INTEGRATE3_USE_STR      = ON
   MY_ID                = 3
   PARENT_ID             = 2
   COLORBAR_VECTOR_NAME    = "VEL"
   DRAWABLE              = ON
   TEX_USE              = OFF
   TEX_TYPE              = 0
   TEX_TYPE0_X           = 1.00000000e+000
   TEX_TYPE0_Y           = 1.00000000e+000
   TEX_TYPE0_Z           = 1.00000000e+000
   TEX_TYPE1_NX          = 0.00000000e+000
   TEX_TYPE1_NY          = 0.00000000e+000
   TEX_TYPE1_NZ          = 1.00000000e+000
   TEX_TYPE1_R           = 1.00000000e+000
   TEX_TYPE1_TZ          = 1.00000000e+000
   TEX_TYPE2_NX          = 0.00000000e+000
   TEX_TYPE2_NY          = 0.00000000e+000
   TEX_TYPE2_NZ          = 1.00000000e+000
   TEX_TYPE2_S           = 1.00000000e+000
   TEX_ROTATE0_X         = 0.00000000e+000
```

TEX_ROTATE0_Y = 0.00000000e+000
TEX_ROTATE0_Z = 0.00000000e+000
TEX_ROTATE1_TZ = 0.00000000e+000
TEX_ROTATE1_R = 0.00000000e+000
TEX_ROTATE2_S = 0.00000000e+000
TEX_OFS0_X_X = 0.00000000e+000
TEX_OFS0_X_Y = 0.00000000e+000
TEX_OFS0_Y_X = 0.00000000e+000
TEX_OFS0_Y_Y = 0.00000000e+000
TEX_OFS0_Z_X = 0.00000000e+000
TEX_OFS0_Z_Y = 0.00000000e+000
TEX_OFS1_R_X = 0.00000000e+000
TEX_OFS1_R_Y = 0.00000000e+000
TEX_OFS1_TZ_X = 0.00000000e+000
TEX_OFS1_TZ_Y = 0.00000000e+000
TEX_OFS2_X = 0.00000000e+000
TEX_OFS2_Y = 0.00000000e+000
TEX_USECOLORKEY = OFF
TEX_COLORKEY = C16711680
TEX_UPSIDEDOWN = OFF
TEX_FILENAME = ""
MATRIX_0_0 = -0.1616975998945730
MATRIX_1_0 = 0.1616975998945730
MATRIX_2_0 = 0.0000000000000000
MATRIX_3_0 = 1.8270782278273057
MATRIX_0_1 = -0.0933561528264481
MATRIX_1_1 = -0.0933561528264481
MATRIX_2_1 = 0.1867123056528962
MATRIX_3_1 = 1.5924624958041502
MATRIX_0_2 = 0.1320255374581383
MATRIX_1_2 = 0.1320255374581383
MATRIX_2_2 = 0.1320255374581383
MATRIX_3_2 = -1.9754321042173950
MATRIX_0_3 = 0.0000000000000000
MATRIX_1_3 = 0.0000000000000000
MATRIX_2_3 = 0.0000000000000000
MATRIX_3_3 = 1.0000000000000000
DRAW_ALL = ON
DRAW_LEVEL = 0
SYNCHRONIZE = ON
ACTIVE = OFF
ROTATE_CENTER_X = 0.00000000e+000
ROTATE_CENTER_Y = 0.00000000e+000
ROTATE_CENTER_Z = 0.00000000e+000
VOL2_ISDRAW_START = 1
VOL2_ISDRAW_DATA_0 = ON

VOL2_EMTNAME_START = 1
VOL2_EMTNAME_DATA_0 = "NotRegistered"
VOL2_ORGNAME_START = 1
VOL2_ORGNAME_DATA_0 = "NotRegistered"
VOL2_CHECK = 0
MAT2_ISDRAW_START = 2
MAT2_ISDRAW_DATA_0 = ON
MAT2_ISDRAW_DATA_1 = ON
MAT2_EMTNAME_START = 2
MAT2_EMTNAME_DATA_0 = "MAT0"
MAT2_EMTNAME_DATA_1 = "MAT1"
MAT2_ORGNAME_START = 2
MAT2_ORGNAME_DATA_0 = "MAT0"
MAT2_ORGNAME_DATA_1 = "MAT1"
MAT2_CHECK = 0
ONLY_ONEVAR = ON
CURVAR1_LNAM = "PRES"
SCALAR_DRAW = OFF
USE_VAR1COLOR = OFF
SCALAR_SURFACE_AWAY_DRAW = OFF
SCALAR_SURFACE_COME_DRAW = ON
SCALAR_SURFACE_AWAY_TRANSPARENT = OFF
SCALAR_SURFACE_COME_TRANSPARENT = OFF
SCALAR_EDGE_AWAY_DRAW = OFF
SCALAR_EDGE_COME_DRAW = OFF
SCALAR_EDGE_AWAY_TRANSPARENT = OFF
SCALAR_EDGE_COME_TRANSPARENT = OFF
SCALAR_LINE_AWAY_DRAW = OFF
SCALAR_LINE_COME_DRAW = OFF
SCALAR_LINE_AWAY_TRANSPARENT = OFF
SCALAR_LINE_COME_TRANSPARENT = OFF
SCALAR_SURFACE_LIGHT = ON
SCALAR_SURFACE_WATER = OFF
SCALAR_LINE_STIPPLE = OFF
SCALAR_LINE_NUMBER = ON
SCALAR_LINE_MONOCOLOR = OFF
SCALAR_LINE_WIDTH = 1
SCALAR_LINE_COLOR = C16777215
SCALAR_LINE_NUMBERS_COLOR = C16777215
SCALAR_EDGE_COLOR = C16777215
SCALAR_EDGE_WIDTH = 1
CURVAR3_LNAM = "VEL"
VECTOR_DRAW = ON
VECTOR_DRAW_NODE = OFF
VECTOR_DRAW_CENTER = OFF
VECTOR_NORMALIZE = OFF

VECTOR_MONOCOLOR = OFF
VECTOR_DRAW_EQUAL = OFF
VECTOR_AWAY_DRAW = ON
VECTOR_COME_DRAW = ON
VECTOR_AWAY_TRANSPARENT = OFF
VECTOR_COME_TRANSPARENT = OFF
VECTOR_ARROWTYPE = 4
VECTOR_WIDTH = 1.00000000e+000
VECTOR_COLOR = C16777215
VECTOR_SPACE1 = 1.00000000e+001
VECTOR_SPACE2 = 1.00000000e+000
VECTOR_SPACE3 = 1.00000000e+000
VECTOR_SCALE = 1.00000000e+000
VECTOR_ARROW_1 = 1.00000000e+000
VECTOR_ARROW_2 = 1.00000000e+000
BILLBOARD_ENABLED = 0
DRAWSURF_NUM = 6
DRAWSURF_LRGN_0 = "walls"
DRAWSURF_LRGN_1 = "face"
DRAWSURF_LRGN_2 = "curtain"
DRAWSURF_LRGN_3 = "inlet"
DRAWSURF_LRGN_4 = "outlet"
DRAWSURF_LRGN_5 = "wing"
SURFCUT_NUM = 0
SPREAD_REGINFO_CUR = 0
SPREAD_REGINFO_DATA_START = 0
CUR_OVID = 0
USE_AXISANIME = OFF
AXISANIME_CX = 0.00000000e+000
AXISANIME_CY = 0.00000000e+000
AXISANIME_CZ = 0.00000000e+000
AXISANIME_NX = 0.00000000e+000
AXISANIME_NY = 0.00000000e+000
AXISANIME_NZ = 1.00000000e+000
AXISANIME_THETA = 3.00000000e+001
INTEGRATE1_KAGE_RESULT = 0.0000000000000000e+000
INTEGRATE1_KAGE_MODE = 0
INTEGRATE1_KAGE_CALC = OFF
INTEGRATE1_KAGE_PX = 0.00000000e+000
INTEGRATE1_KAGE_PY = 0.00000000e+000
INTEGRATE1_KAGE_PZ = 0.00000000e+000
INTEGRATE1_KAGE_NX = 0.00000000e+000
INTEGRATE1_KAGE_NY = 0.00000000e+000
INTEGRATE1_KAGE_NZ = 1.00000000e+000
INTEGRATE1_USE_KAGE = OFF
INTEGRATE1_USE_P = ON

INTEGRATE1_USE_N = ON
INTEGRATE1_USE_L = ON
INTEGRATE1_USE_V = ON
INTEGRATE1_USE_VL = ON
INTEGRATE1_USE_CYCTIM = ON
INTEGRATE3_KAGE_MODE = 0
INTEGRATE3_KAGE_PX = 0.00000000e+000
INTEGRATE3_KAGE_PY = 0.00000000e+000
INTEGRATE3_KAGE_PZ = 0.00000000e+000
INTEGRATE3_KAGE_NX = 0.00000000e+000
INTEGRATE3_KAGE_NY = 0.00000000e+000
INTEGRATE3_KAGE_NZ = 1.00000000e+000
INTEGRATE3_USE_P = ON
INTEGRATE3_USE_N = ON
INTEGRATE3_USE_L = ON
INTEGRATE3_USE_VV = ON
INTEGRATE3_USE_VXYZ = ON
INTEGRATE3_USE_VVL = ON
INTEGRATE3_USE_VXYZL = ON
INTEGRATE3_USE_CYCTIM = ON
MESH_EDGE_AWAY_DRAW = OFF
MESH_EDGE_COME_DRAW = OFF
MESH_EDGE_AWAY_TRANSPARENT = ON
MESH_EDGE_COME_TRANSPARENT = ON
MESH_SURF_AWAY_DRAW = OFF
MESH_SURF_COME_DRAW = OFF
MESH_SURF_AWAY_TRANSPARENT = OFF
MESH_SURF_COME_TRANSPARENT = OFF
MESH_SURF_LIGHT = ON
MESH_SURF_WATER = OFF
MESH_EDGE_COLOR = C3355443
MESH_SURF_COLOR = C10584413
MESH_EDGE_WIDTH = 1
MESH_APX_DRAW = ON
MESH_APX_TRANSPARENT = OFF
MESH_APX_COLOR = C16746581
MESH_APX_WIDTH = 1
MESH_APX_AUTO = ON
MODIFY_CUT_XMIN = ON
MODIFY_CUT_XMAX = ON
MODIFY_CUT_YMIN = ON
MODIFY_CUT_YMAX = ON
MODIFY_CUT_ZMIN = ON
MODIFY_CUT_ZMAX = ON
MODIFY_CUT_TMIN = ON
MODIFY_CUT_TMAX = ON

```
   PARENT_TITLE          = ""
   USE_GRAPH             = OFF
   DRAW_NEIGHBOR_VECTOR    = ON
   OIL_USE               = ON
   OIL_AWAY              = OFF
   OIL_COME              = ON
   OIL_TRANSPARENT       = ON
   OIL_NEW               = ON
   OIL_VAR3              = 0
   OIL_WIDTH             = 2.00000000e+000
   OIL_MAXCALC           = 10
   OIL_LENGTH            = 1.00000000e+000
   OIL_MABIKI            = 2.50000000e+001
   VEC_MABIKI            = 1.00000000e+001
   OIL_COLOR             = C8767705
   INTEGRATE_IGNORE_FRONT_BACK = ON
   SMOOTHSHADING         = ON
   PICK_FONT_SIZE        = 100
   PICK_FONT_NAME        = "Arial"
   PICK_COLOR            = C11184810
   PICK_AUTOCOLOR        = ON
   PICK_NO               = ON
   PICK_ALLVAR           = ON
   PICK_USEIJK           = OFF
   PICK_USEVAR1          = OFF
   PICK_USEVAR3          = OFF
   PICKVAR1_LNAM         = "PRES"
   PICKVAR3_LNAM         = "VEL"
   PICK_NUM              = 0
   PICK_PICKGRAPH        = OFF
   APX_MABIKI_NUM        = 5
   APX_MABIKI_USE        = OFF


[PLANE]
   LANG_ID               = 1033
   TREE_ORDER_ID         = 4
   DEFAULT_NAME          = ""
   DEFAULT_WITHOUTPOS    = OFF
   SHORT_TITLE           = "PLANE"
   LONG_TITLE            = "Plane (1)"
   DISPLAY_TITLE         = "Plane (1)"
   DISPLAY_TITLE_MODIFIED  = OFF
   COL_MATCH_MODE        = 1
   TOPPOS_MODE           = 0
   PLUSMINUS_MODE        = 0
```

INTEGRATE1_CALC = OFF
INTEGRATE1_SAVE = OFF
INTEGRATE1_FN = ""
INTEGRATE1_USE_BEEP = ON
INTEGRATE1_USE_REDRAW = ON
INTEGRATE1_USE_STR = ON
INTEGRATE3_CALC = OFF
INTEGRATE3_SAVE = OFF
INTEGRATE3_FN = ""
INTEGRATE3_USE_BEEP = ON
INTEGRATE3_USE_REDRAW = ON
INTEGRATE3_USE_STR = ON
MY_ID = 4
PARENT_ID = 2
COLORBAR_SCALAR_NAME = "VELV"
COLORBAR_VECTOR_NAME = "VEL"
DRAWABLE = ON
TEX_USE = OFF
TEX_TYPE = 0
TEX_TYPE0_X = 1.00000000e+000
TEX_TYPE0_Y = 1.00000000e+000
TEX_TYPE0_Z = 1.00000000e+000
TEX_TYPE1_NX = 0.00000000e+000
TEX_TYPE1_NY = 0.00000000e+000
TEX_TYPE1_NZ = 1.00000000e+000
TEX_TYPE1_R = 1.00000000e+000
TEX_TYPE1_TZ = 1.00000000e+000
TEX_TYPE2_NX = 0.00000000e+000
TEX_TYPE2_NY = 0.00000000e+000
TEX_TYPE2_NZ = 1.00000000e+000
TEX_TYPE2_S = 1.00000000e+000
TEX_ROTATE0_X = 0.00000000e+000
TEX_ROTATE0_Y = 0.00000000e+000
TEX_ROTATE0_Z = 0.00000000e+000
TEX_ROTATE1_TZ = 0.00000000e+000
TEX_ROTATE1_R = 0.00000000e+000
TEX_ROTATE2_S = 0.00000000e+000
TEX_OFS0_X_X = 0.00000000e+000
TEX_OFS0_X_Y = 0.00000000e+000
TEX_OFS0_Y_X = 0.00000000e+000
TEX_OFS0_Y_Y = 0.00000000e+000
TEX_OFS0_Z_X = 0.00000000e+000
TEX_OFS0_Z_Y = 0.00000000e+000
TEX_OFS1_R_X = 0.00000000e+000
TEX_OFS1_R_Y = 0.00000000e+000
TEX_OFS1_TZ_X = 0.00000000e+000

TEX_OFS1_TZ_Y = 0.00000000e+000
TEX_OFS2_X = 0.00000000e+000
TEX_OFS2_Y = 0.00000000e+000
TEX_USECOLORKEY = OFF
TEX_COLORKEY = C16711680
TEX_UPSIDEDOWN = OFF
TEX_FILENAME = ""
MATRIX_0_0 = -0.1616975998945730
MATRIX_1_0 = 0.1616975998945730
MATRIX_2_0 = 0.0000000000000000
MATRIX_3_0 = 1.8270782278273057
MATRIX_0_1 = -0.0933561528264481
MATRIX_1_1 = -0.0933561528264481
MATRIX_2_1 = 0.1867123056528962
MATRIX_3_1 = 1.5924624958041502
MATRIX_0_2 = 0.1320255374581383
MATRIX_1_2 = 0.1320255374581383
MATRIX_2_2 = 0.1320255374581383
MATRIX_3_2 = -1.9754321042173950
MATRIX_0_3 = 0.0000000000000000
MATRIX_1_3 = 0.0000000000000000
MATRIX_2_3 = 0.0000000000000000
MATRIX_3_3 = 1.0000000000000000
DRAW_ALL = OFF
DRAW_LEVEL = 1
SYNCHRONIZE = ON
ACTIVE = OFF
ROTATE_CENTER_X = 0.00000000e+000
ROTATE_CENTER_Y = 0.00000000e+000
ROTATE_CENTER_Z = 0.00000000e+000
VOL2_ISDRAW_START = 1
VOL2_ISDRAW_DATA_0 = ON
VOL2_EMTNAME_START = 1
VOL2_EMTNAME_DATA_0 = "NotRegistered"
VOL2_ORGNAME_START = 1
VOL2_ORGNAME_DATA_0 = "NotRegistered"
VOL2_CHECK = 0
MAT2_ISDRAW_START = 2
MAT2_ISDRAW_DATA_0 = ON
MAT2_ISDRAW_DATA_1 = ON
MAT2_EMTNAME_START = 2
MAT2_EMTNAME_DATA_0 = "MAT0"
MAT2_EMTNAME_DATA_1 = "MAT1"
MAT2_ORGNAME_START = 2
MAT2_ORGNAME_DATA_0 = "MAT0"
MAT2_ORGNAME_DATA_1 = "MAT1"

MAT2_CHECK = 0
ONLY_ONEVAR = OFF
CURVAR1_LNAM = "PRES"
SCALAR_DRAW = OFF
USE_VAR1COLOR = OFF
SCALAR_SURFACE_AWAY_DRAW = ON
SCALAR_SURFACE_COME_DRAW = ON
SCALAR_SURFACE_AWAY_TRANSPARENT = OFF
SCALAR_SURFACE_COME_TRANSPARENT = OFF
SCALAR_EDGE_AWAY_DRAW = OFF
SCALAR_EDGE_COME_DRAW = OFF
SCALAR_EDGE_AWAY_TRANSPARENT = OFF
SCALAR_EDGE_COME_TRANSPARENT = OFF
SCALAR_LINE_AWAY_DRAW = ON
SCALAR_LINE_COME_DRAW = ON
SCALAR_LINE_AWAY_TRANSPARENT = ON
SCALAR_LINE_COME_TRANSPARENT = ON
SCALAR_SURFACE_LIGHT = OFF
SCALAR_SURFACE_WATER = OFF
SCALAR_LINE_STIPPLE = OFF
SCALAR_LINE_NUMBER = ON
SCALAR_LINE_MONOCOLOR = OFF
SCALAR_LINE_WIDTH = 1
SCALAR_LINE_COLOR = C8947848
SCALAR_LINE_NUMBERS_COLOR = C13816530
SCALAR_EDGE_COLOR = C8947848
SCALAR_EDGE_WIDTH = 1
CURVAR3_LNAM = "VEL"
VECTOR_DRAW = ON
VECTOR_DRAW_NODE = OFF
VECTOR_DRAW_CENTER = OFF
VECTOR_NORMALIZE = OFF
VECTOR_MONOCOLOR = OFF
VECTOR_DRAW_EQUAL = ON
VECTOR_AWAY_DRAW = OFF
VECTOR_COME_DRAW = OFF
VECTOR_AWAY_TRANSPARENT = OFF
VECTOR_COME_TRANSPARENT = OFF
VECTOR_ARROWTYPE = 1
VECTOR_WIDTH = 1.00000000e+000
VECTOR_COLOR = C16777215
VECTOR_SPACE1 = 3.00000000e-001
VECTOR_SPACE2 = 3.00000000e-001
VECTOR_SPACE3 = 1.00000000e+000
VECTOR_SCALE = 1.00000000e+000
VECTOR_ARROW_1 = 1.00000000e+000

VECTOR_ARROW_2 = 1.00000000e+000
BILLBOARD_ENABLED = 0
TEST_PICKGRAPH = OFF
GRAPH_START_REF_SP1 = -1
GRAPH_START_REF_SP2 = -1
GRAPH_START_REF_EP1 = -1
GRAPH_START_REF_EP2 = -1
GRAPH_END_REF_SP1 = -1
GRAPH_END_REF_SP2 = -1
GRAPH_END_REF_EP1 = -1
GRAPH_END_REF_EP2 = -1
GRAPH_MU_REF_SP1 = -1
GRAPH_MU_REF_SP2 = -1
GRAPH_MU_REF_EP1 = -1
GRAPH_MU_REF_EP2 = -1
GRAPH_START_REF_X = 1.0000000000000000e+020
GRAPH_START_REF_Y = 1.0000000000000000e+020
GRAPH_START_REF_Z = 1.0000000000000000e+020
GRAPH_END_REF_X = 1.0000000000000000e+020
GRAPH_END_REF_Y = 1.0000000000000000e+020
GRAPH_END_REF_Z = 1.0000000000000000e+020
GRAPH_MU_REF_X = 1.0000000000000000e+020
GRAPH_MU_REF_Y = 1.0000000000000000e+020
GRAPH_MU_REF_Z = 1.0000000000000000e+020
GRAPH_START_REF_SLAVEID = -1
GRAPH_END_REF_SLAVEID = -1
GRAPH_MU_REF_SLAVEID = -1
GRAPH_START_REF_EDGEID = -1
GRAPH_END_REF_EDGEID = -1
GRAPH_MU_REF_EDGEID = -1
VECTOR_EQUAL_LIMIT = 5.0000000000000001e-003
DRAW_BOUNDARY_WITH_PLANE = OFF
DRAW_BOUNDARY_WITH_SURF = ON
DRAW_BOUNDARY_WITH_ISOSURF = OFF
DRAW_BOUNDARY_WITH_HIDENOBJ = ON
INTEGRATE1_USE_P = ON
INTEGRATE1_USE_N = ON
INTEGRATE1_USE_L = ON
INTEGRATE1_USE_V = ON
INTEGRATE1_USE_VL = ON
INTEGRATE1_USE_CYCTIM = ON
INTEGRATE3_USE_P = ON
INTEGRATE3_USE_N = ON
INTEGRATE3_USE_L = ON
INTEGRATE3_USE_VV = ON
INTEGRATE3_USE_VXYZ = ON

INTEGRATE3_USE_VVL = ON
INTEGRATE3_USE_VXYZL = ON
INTEGRATE3_USE_CYCTIM = ON
PLANE_X = 0.00000000e+000
PLANE_Y = 0.00000000e+000
PLANE_Z = 1.00000000e+000
PLANE_C = -1.10000000e+000
BOUNDARY_DRAW = ON
BOUNDARY_TRANSPARENT = OFF
BOUNDARY_STIPPLE = OFF
BOUNDARY_COLOR = C255
BOUNDARY_WIDTH = 1
MESH_EDGE_DRAW = OFF
MESH_SURFACE_DRAW = OFF
MESH_EDGE_TRANSPARENT = OFF
MESH_SURFACE_TRANSPARENT = OFF
MESH_SURFACE_SHADING = ON
MESH_SURFACE_WATER = OFF
MESH_SURFACE_BLOCK = OFF
MESH_EDGE_COLOR = C8947848
MESH_SURFACE_COLOR = C7295493
MESH_EDGE_WIDTH = 1
USE_PROJECTION = OFF
AUTO_APX = ON
DRAW_APX_1 = ON
DRAW_APX_2 = ON
ANIMATION_METHOD = 0
PLANE_ROTATE_PX = 0.00000000e+000
PLANE_ROTATE_PY = 0.00000000e+000
PLANE_ROTATE_PZ = 0.00000000e+000
PLANE_ROTATE_NX = 0.00000000e+000
PLANE_ROTATE_NY = 0.00000000e+000
PLANE_ROTATE_NZ = 1.00000000e+000
PLANE_START_X = 0.00000000e+000
PLANE_START_Y = 0.00000000e+000
PLANE_START_Z = 1.00000000e+000
PLANE_START_C = -0.00000000e+000
PLANE_REFER_X = 0.00000000e+000
PLANE_REFER_Y = 0.00000000e+000
PLANE_REFER_Z = 1.00000000e+000
PLANE_REFER_C = -2.20000000e+000
ANIMATION_OMEGA_DELTA = 9.00000000e+001
ANIMATION_OMEGA_START = 0.00000000e+000
ANIMATION_LOOP = OFF
ANIMATION_GO = OFF
ANIMATION_SCENES = 10

```
   ANIMATION_CURRENT       = 0
   GRAPH2_VAR1             = "PRES"
   PARENT_TITLE            = ""
   USE_GRAPH               = OFF
   OIL_USE                 = ON
   OIL_TRANSPARENT         = ON
   OIL_VAR3                = 0
   OIL_WIDTH               = 1.00000000e+000
   OIL_MAXCALC             = 10
   OIL_LENGTH              = 1.00000000e+000
   OIL_MABIKI1             = 1.00000000e+000
   OIL_MABIKI2             = 1.00000000e+000
   OIL_COLOR               = C8767705
   PICK_FONT_SIZE          = 100
   PICK_FONT_NAME          = "Arial"
   PICK_COLOR              = C11184810
   PICK_AUTOCOLOR          = ON
   PICK_NO                 = ON
   PICK_ALLVAR             = ON
   PICK_USEIJK             = OFF
   PICK_USEVAR1            = OFF
   PICK_USEVAR3            = OFF
   PICKVAR1_LNAM           = "PRES"
   PICKVAR3_LNAM           = "VEL"
   PICK_NUM                = 0
   CLIP_CLIPREGIONLINECOLOR = C16711935
   CLIP_CLIPREGIONPOINTCOLOR = C16711935
   CLIP_CLIPREGIONLINEWIDTH = 1
   CLIP_CLIPREGIONPOINTSIZE = 7
   CLIP_ENABLECLIP         = OFF
   CLIP_NVERTICES_OF_CLIPREGION = 0
   CLIP_MAKECLIPREGIONBYPICK = OFF
   CLIP_SHOWCLIPREGION     = ON


[LIGHT]
   LANG_ID                 = 1033
   TREE_ORDER_ID           = 5
   DEFAULT_NAME            = ""
   DEFAULT_WITHOUTPOS      = OFF
   SHORT_TITLE             = "LIGHT"
   LONG_TITLE              = "Light (1)"
   DISPLAY_TITLE           = "Light (1)"
   DISPLAY_TITLE_MODIFIED  = OFF
   COL_MATCH_MODE          = 1
   TOPPOS_MODE             = 0
```

PLUSMINUS_MODE = 0
INTEGRATE1_CALC = OFF
INTEGRATE1_SAVE = OFF
INTEGRATE1_FN = ""
INTEGRATE1_USE_BEEP = ON
INTEGRATE1_USE_REDRAW = ON
INTEGRATE1_USE_STR = ON
INTEGRATE3_CALC = OFF
INTEGRATE3_SAVE = OFF
INTEGRATE3_FN = ""
INTEGRATE3_USE_BEEP = ON
INTEGRATE3_USE_REDRAW = ON
INTEGRATE3_USE_STR = ON
MY_ID = 5
PARENT_ID = -1
DRAWABLE = ON
TEX_USE = OFF
TEX_TYPE = 0
TEX_TYPE0_X = 1.00000000e+000
TEX_TYPE0_Y = 1.00000000e+000
TEX_TYPE0_Z = 1.00000000e+000
TEX_TYPE1_NX = 0.00000000e+000
TEX_TYPE1_NY = 0.00000000e+000
TEX_TYPE1_NZ = 1.00000000e+000
TEX_TYPE1_R = 1.00000000e+000
TEX_TYPE1_TZ = 1.00000000e+000
TEX_TYPE2_NX = 0.00000000e+000
TEX_TYPE2_NY = 0.00000000e+000
TEX_TYPE2_NZ = 1.00000000e+000
TEX_TYPE2_S = 1.00000000e+000
TEX_ROTATE0_X = 0.00000000e+000
TEX_ROTATE0_Y = 0.00000000e+000
TEX_ROTATE0_Z = 0.00000000e+000
TEX_ROTATE1_TZ = 0.00000000e+000
TEX_ROTATE1_R = 0.00000000e+000
TEX_ROTATE2_S = 0.00000000e+000
TEX_OFS0_X_X = 0.00000000e+000
TEX_OFS0_X_Y = 0.00000000e+000
TEX_OFS0_Y_X = 0.00000000e+000
TEX_OFS0_Y_Y = 0.00000000e+000
TEX_OFS0_Z_X = 0.00000000e+000
TEX_OFS0_Z_Y = 0.00000000e+000
TEX_OFS1_R_X = 0.00000000e+000
TEX_OFS1_R_Y = 0.00000000e+000
TEX_OFS1_TZ_X = 0.00000000e+000
TEX_OFS1_TZ_Y = 0.00000000e+000

TEX_OFS2_X = 0.00000000e+000
TEX_OFS2_Y = 0.00000000e+000
TEX_USECOLORKEY = OFF
TEX_COLORKEY = C16711680
TEX_UPSIDEDOWN = OFF
TEX_FILENAME = ""
MATRIX_0_0 = 1.0000000000000000
MATRIX_1_0 = 0.0000000000000000
MATRIX_2_0 = 0.0000000000000000
MATRIX_3_0 = 0.0000000000000000
MATRIX_0_1 = 0.0000000000000000
MATRIX_1_1 = 1.0000000000000000
MATRIX_2_1 = 0.0000000000000000
MATRIX_3_1 = 0.0000000000000000
MATRIX_0_2 = 0.0000000000000000
MATRIX_1_2 = 0.0000000000000000
MATRIX_2_2 = 1.0000000000000000
MATRIX_3_2 = 0.0000000000000000
MATRIX_0_3 = 0.0000000000000000
MATRIX_1_3 = 0.0000000000000000
MATRIX_2_3 = 0.0000000000000000
MATRIX_3_3 = 1.0000000000000000
DRAW_ALL = OFF
DRAW_LEVEL = 1
SYNCHRONIZE = ON
ACTIVE = OFF
ROTATE_CENTER_X = 0.00000000e+000
ROTATE_CENTER_Y = 0.00000000e+000
ROTATE_CENTER_Z = 0.00000000e+000
ONLY_ONEVAR = ON
BILLBOARD_ENABLED = 0
GL_SPOT_CUTOFF = 1.80000000e+002
GL_AMBIENT_R = 5.00000000e-001
GL_AMBIENT_G = 5.00000000e-001
GL_AMBIENT_B = 5.00000000e-001
GL_DIFFUSE_R = 3.00000012e-001
GL_DIFFUSE_G = 3.00000012e-001
GL_DIFFUSE_B = 3.00000012e-001
GL_SPECULAR_R = 1.00000000e+000
GL_SPECULAR_G = 1.00000000e+000
GL_SPECULAR_B = 1.00000000e+000
GL_POSITION_X = 1.00000001e-001
GL_POSITION_Y = 1.00000001e-001
GL_POSITION_Z = 3.00000000e+000
GL_VECTOR_X = -1.00000001e-001
GL_VECTOR_Y = -1.00000001e-001

GL_VECTOR_Z = -3.00000000e+000
GL_SHINNESS = 2.00000000e+001

[COLORBAR]
LANG_ID = 1033
TREE_ORDER_ID = 6
DEFAULT_NAME = ""
DEFAULT_WITHOUTPOS = OFF
SHORT_TITLE = "COLORBAR"
LONG_TITLE = "ColorBar (1)"
DISPLAY_TITLE = "Colorbar (for Velocity)"
DISPLAY_TITLE_MODIFIED = OFF
COL_MATCH_MODE = 1
TOPPOS_MODE = 1
PLUSMINUS_MODE = 0
INTEGRATE1_CALC = OFF
INTEGRATE1_SAVE = OFF
INTEGRATE1_FN = ""
INTEGRATE1_USE_BEEP = ON
INTEGRATE1_USE_REDRAW = ON
INTEGRATE1_USE_STR = ON
INTEGRATE3_CALC = OFF
INTEGRATE3_SAVE = OFF
INTEGRATE3_FN = ""
INTEGRATE3_USE_BEEP = ON
INTEGRATE3_USE_REDRAW = ON
INTEGRATE3_USE_STR = ON
MY_ID = 6
PARENT_ID = -1
DRAWABLE = ON
TEX_USE = OFF
TEX_TYPE = 0
TEX_TYPE0_X = 1.00000000e+000
TEX_TYPE0_Y = 1.00000000e+000
TEX_TYPE0_Z = 1.00000000e+000
TEX_TYPE1_NX = 0.00000000e+000
TEX_TYPE1_NY = 0.00000000e+000
TEX_TYPE1_NZ = 1.00000000e+000
TEX_TYPE1_R = 1.00000000e+000
TEX_TYPE1_TZ = 1.00000000e+000
TEX_TYPE2_NX = 0.00000000e+000
TEX_TYPE2_NY = 0.00000000e+000
TEX_TYPE2_NZ = 1.00000000e+000
TEX_TYPE2_S = 1.00000000e+000
TEX_ROTATE0_X = 0.00000000e+000

TEX_ROTATE0_Y = 0.00000000e+000
TEX_ROTATE0_Z = 0.00000000e+000
TEX_ROTATE1_TZ = 0.00000000e+000
TEX_ROTATE1_R = 0.00000000e+000
TEX_ROTATE2_S = 0.00000000e+000
TEX_OFS0_X_X = 0.00000000e+000
TEX_OFS0_X_Y = 0.00000000e+000
TEX_OFS0_Y_X = 0.00000000e+000
TEX_OFS0_Y_Y = 0.00000000e+000
TEX_OFS0_Z_X = 0.00000000e+000
TEX_OFS0_Z_Y = 0.00000000e+000
TEX_OFS1_R_X = 0.00000000e+000
TEX_OFS1_R_Y = 0.00000000e+000
TEX_OFS1_TZ_X = 0.00000000e+000
TEX_OFS1_TZ_Y = 0.00000000e+000
TEX_OFS2_X = 0.00000000e+000
TEX_OFS2_Y = 0.00000000e+000
TEX_USECOLORKEY = OFF
TEX_COLORKEY = C16711680
TEX_UPSIDEDOWN = OFF
TEX_FILENAME = ""
MATRIX_0_0 = 0.4319137500954042
MATRIX_1_0 = 0.0000000000000000
MATRIX_2_0 = 0.0000000000000000
MATRIX_3_0 = 1.4057217165149536
MATRIX_0_1 = 0.0000000000000000
MATRIX_1_1 = 0.6478706251431062
MATRIX_2_1 = 0.0000000000000000
MATRIX_3_1 = -1.2522756827048087
MATRIX_0_2 = 0.0000000000000000
MATRIX_1_2 = 0.0000000000000000
MATRIX_2_2 = 6.4787062514310634
MATRIX_3_2 = 0.0000000000000000
MATRIX_0_3 = 0.0000000000000000
MATRIX_1_3 = 0.0000000000000000
MATRIX_2_3 = 0.0000000000000000
MATRIX_3_3 = 0.9999999999999999
DRAW_ALL = ON
DRAW_LEVEL = 0
SYNCHRONIZE = ON
ACTIVE = OFF
ROTATE_CENTER_X = 0.00000000e+000
ROTATE_CENTER_Y = 0.00000000e+000
ROTATE_CENTER_Z = 0.00000000e+000
ONLY_ONEVAR = ON
BILLBOARD_ENABLED = 0

NUM_EXP = OFF
MINMAX_FIX = OFF
INTEGER_NUM = OFF
PRESET_ID = 9
MINMAX_MODE = 1
POSITION_ISHORZ = ON
BACKGROUND = OFF
ADJUST_YELLOW = ON
AUTOCOLOR1 = ON
AUTOCOLOR2 = OFF
AUTOCOLOR3 = ON
OVERFLOW_MODE = 1
LINE_WIDTH = 1
DEG_NUM = 1
NUM_NUM = 8
DEG_MODE = 2
GRA_NODE = 4
GRA_PART = 5
POS_MIN = 2.5000000000000000e-001
POS_MAX = 5.5000000000000004e-001
SIZE_HORZ = 1.00000000e+000
SIZE_VERT = 1.00000000e+000
COLOR1 = C0
COLOR2 = C0
COLOR3 = C15790320
VAR_NAME = "VEL"
VAR_TITLE = "Velocity"
COLORBAR_NUM_SIZE = 1.00000000e+000
COLORBAR_TITLE_SIZE = 1.00000000e+000
COLORBAR_NAME_POS = 0
COLORBAR_NAME_ARBITRARYCOORDX = 0.00000000e+000
COLORBAR_NAME_ARBITRARYCOORDY = 0.00000000e+000
POS_NODE_0 = 2.5000000000000000e-001
POS_NODE_1 = 3.4999999999999998e-001
POS_NODE_2 = 4.5000000000000001e-001
POS_NODE_3 = 5.5000000000000004e-001
VAL_NODE_0 = 0.00000000e+000
VAL_NODE_1 = 3.92233467e-001
VAL_NODE_2 = 7.84466934e-001
VAL_NODE_3 = 1.17670040e+000
VAL_NODE_4 = 1.56893387e+000
VAL_NODE_5 = 1.96116733e+000
COLOR_NODE_0 = C0
COLOR_NODE_1 = C2263074
COLOR_NODE_2 = C2271914
COLOR_NODE_3 = C16777215

```
   COLOR_GRA_0          = C665610
   COLOR_GRA_1          = C1997086
   COLOR_GRA_2          = C2132582
   COLOR_GRA_3          = C3380658
   COLOR_GRA_4          = C11982821
   RANGE_MIN            = 0.0000000000000000e+000
   RANGE_MAX            = 1.9611673347958058e+000
   COLORBAR_DISTANCEBETWEENBARANDVALUE = 0.00000000e+000
   COLORBAR_VALUEPOSITION  = 5.00000000e-001


[COLORBAR]
   LANG_ID              = 1033
   TREE_ORDER_ID        = 7
   DEFAULT_NAME         = ""
   DEFAULT_WITHOUTPOS   = OFF
   SHORT_TITLE          = "COLORBAR"
   LONG_TITLE           = "ColorBar (2)"
   DISPLAY_TITLE        = "Colorbar ( for Magnitude of Velocity )"
   DISPLAY_TITLE_MODIFIED  = OFF
   COL_MATCH_MODE       = 1
   TOPPOS_MODE          = 1
   PLUSMINUS_MODE       = 0
   INTEGRATE1_CALC      = OFF
   INTEGRATE1_SAVE      = OFF
   INTEGRATE1_FN        = ""
   INTEGRATE1_USE_BEEP  = ON
   INTEGRATE1_USE_REDRAW  = ON
   INTEGRATE1_USE_STR   = ON
   INTEGRATE3_CALC      = OFF
   INTEGRATE3_SAVE      = OFF
   INTEGRATE3_FN        = ""
   INTEGRATE3_USE_BEEP  = ON
   INTEGRATE3_USE_REDRAW  = ON
   INTEGRATE3_USE_STR   = ON
   MY_ID                = 7
   PARENT_ID            = -1
   DRAWABLE             = ON
   TEX_USE              = OFF
   TEX_TYPE             = 0
   TEX_TYPE0_X          = 1.00000000e+000
   TEX_TYPE0_Y          = 1.00000000e+000
   TEX_TYPE0_Z          = 1.00000000e+000
   TEX_TYPE1_NX         = 0.00000000e+000
   TEX_TYPE1_NY         = 0.00000000e+000
   TEX_TYPE1_NZ         = 1.00000000e+000
```

TEX_TYPE1_R = 1.00000000e+000
TEX_TYPE1_TZ = 1.00000000e+000
TEX_TYPE2_NX = 0.00000000e+000
TEX_TYPE2_NY = 0.00000000e+000
TEX_TYPE2_NZ = 1.00000000e+000
TEX_TYPE2_S = 1.00000000e+000
TEX_ROTATE0_X = 0.00000000e+000
TEX_ROTATE0_Y = 0.00000000e+000
TEX_ROTATE0_Z = 0.00000000e+000
TEX_ROTATE1_TZ = 0.00000000e+000
TEX_ROTATE1_R = 0.00000000e+000
TEX_ROTATE2_S = 0.00000000e+000
TEX_OFS0_X_X = 0.00000000e+000
TEX_OFS0_X_Y = 0.00000000e+000
TEX_OFS0_Y_X = 0.00000000e+000
TEX_OFS0_Y_Y = 0.00000000e+000
TEX_OFS0_Z_X = 0.00000000e+000
TEX_OFS0_Z_Y = 0.00000000e+000
TEX_OFS1_R_X = 0.00000000e+000
TEX_OFS1_R_Y = 0.00000000e+000
TEX_OFS1_TZ_X = 0.00000000e+000
TEX_OFS1_TZ_Y = 0.00000000e+000
TEX_OFS2_X = 0.00000000e+000
TEX_OFS2_Y = 0.00000000e+000
TEX_USECOLORKEY = OFF
TEX_COLORKEY = C16711680
TEX_UPSIDEDOWN = OFF
TEX_FILENAME = ""
MATRIX_0_0 = 0.4000000000000000
MATRIX_1_0 = 0.0000000000000000
MATRIX_2_0 = 0.0000000000000000
MATRIX_3_0 = -0.7106631989596881
MATRIX_0_1 = 0.0000000000000000
MATRIX_1_1 = 0.6000000000000001
MATRIX_2_1 = 0.0000000000000000
MATRIX_3_1 = -1.2522756827048112
MATRIX_0_2 = 0.0000000000000000
MATRIX_1_2 = 0.0000000000000000
MATRIX_2_2 = 6.0000000000000000
MATRIX_3_2 = 0.0000000000000000
MATRIX_0_3 = 0.0000000000000000
MATRIX_1_3 = 0.0000000000000000
MATRIX_2_3 = 0.0000000000000000
MATRIX_3_3 = 1.0000000000000000
DRAW_ALL = OFF
DRAW_LEVEL = 1

SYNCHRONIZE = ON
ACTIVE = OFF
ROTATE_CENTER_X = 0.00000000e+000
ROTATE_CENTER_Y = 0.00000000e+000
ROTATE_CENTER_Z = 0.00000000e+000
ONLY_ONEVAR = ON
BILLBOARD_ENABLED = 0
NUM_EXP = OFF
MINMAX_FIX = OFF
INTEGER_NUM = OFF
PRESET_ID = 9
MINMAX_MODE = 1
POSITION_ISHORZ = ON
BACKGROUND = OFF
ADJUST_YELLOW = ON
AUTOCOLOR1 = ON
AUTOCOLOR2 = OFF
AUTOCOLOR3 = ON
OVERFLOW_MODE = 1
LINE_WIDTH = 1
DEG_NUM = 1
NUM_NUM = 8
DEG_MODE = 2
GRA_NODE = 4
GRA_PART = 20
POS_MIN = 2.5000000000000000e-001
POS_MAX = 5.5000000000000004e-001
SIZE_HORZ = 1.00000000e+000
SIZE_VERT = 1.00000000e+000
COLOR1 = C0
COLOR2 = C0
COLOR3 = C15790320
VAR_NAME = "VELV"
VAR_TITLE = "Magnitude of Velocity"
COLORBAR_NUM_SIZE = 1.00000000e+000
COLORBAR_TITLE_SIZE = 1.00000000e+000
COLORBAR_NAME_POS = 0
COLORBAR_NAME_ARBITRARYCOORDX = 0.00000000e+000
COLORBAR_NAME_ARBITRARYCOORDY = 0.00000000e+000
POS_NODE_0 = 2.5000000000000000e-001
POS_NODE_1 = 3.4999999999999998e-001
POS_NODE_2 = 4.5000000000000001e-001
POS_NODE_3 = 5.5000000000000004e-001
VAL_NODE_0 = 0.00000000e+000
VAL_NODE_1 = 5.00000000e-002
VAL_NODE_2 = 1.00000000e-001

VAL_NODE_3 = 1.50000000e-001
VAL_NODE_4 = 2.00000000e-001
VAL_NODE_5 = 2.50000000e-001
VAL_NODE_6 = 3.00000000e-001
VAL_NODE_7 = 3.50000000e-001
VAL_NODE_8 = 4.00000000e-001
VAL_NODE_9 = 4.50000000e-001
VAL_NODE_10 = 5.00000000e-001
VAL_NODE_11 = 5.50000000e-001
VAL_NODE_12 = 6.00000000e-001
VAL_NODE_13 = 6.50000000e-001
VAL_NODE_14 = 7.00000000e-001
VAL_NODE_15 = 7.50000000e-001
VAL_NODE_16 = 8.00000000e-001
VAL_NODE_17 = 8.50000000e-001
VAL_NODE_18 = 9.00000000e-001
VAL_NODE_19 = 9.50000000e-001
VAL_NODE_20 = 1.00000000e+000
COLOR_NODE_0 = C0
COLOR_NODE_1 = C2263074
COLOR_NODE_2 = C2271914
COLOR_NODE_3 = C16777215
COLOR_GRA_0 = C133634
COLOR_GRA_1 = C466439
COLOR_GRA_2 = C799244
COLOR_GRA_3 = C1132305
COLOR_GRA_4 = C1465110
COLOR_GRA_5 = C1863708
COLOR_GRA_6 = C2130721
COLOR_GRA_7 = C2197555
COLOR_GRA_8 = C2197831
COLOR_GRA_9 = C2132315
COLOR_GRA_10 = C2132592
COLOR_GRA_11 = C2067076
COLOR_GRA_12 = C2067352
COLOR_GRA_13 = C2330284
COLOR_GRA_14 = C4365496
COLOR_GRA_15 = C6401221
COLOR_GRA_16 = C8568018
COLOR_GRA_17 = C10866399
COLOR_GRA_18 = C13164779
COLOR_GRA_19 = C15529208
RANGE_MIN = 0.0000000000000000e+000
RANGE_MAX = 1.0000000000000000e+000
COLORBAR_DISTANCEBETWEENBARANDVALUE = 0.00000000e+000
COLORBAR_VALUEPOSITION = 5.00000000e-001

```
'=========================================================
End of V-SurfaceMovingVectors
'=========================================================
```

'===

Spray data section in an S file

'===

The following is an example of SPRY data section in an S file describing system of 60 machine mounted sprays. This model was used in a CFD simulation study of methane dilution ability of blowing and exhaust line brattice system.

```
SPRY
  1
              67              68          0.00198
              50          -0.217   -5000
             998          2e-005           0
    0    1    1
            4180              20
         0.00015           0.001          0.0728
          14.227           0.387           1.182
          15.227           1.387           1.182
          15.227           1.387               2
               0              60               0
          14.227            0.45            1.182
              15            0.45            1.182
              15            0.45               2
               0              60               0
          14.227           0.583            1.182
              15           0.583            1.182
              15           0.583               2
               0              60               0
          14.227           0.716            1.182
              15           0.716            1.182
              15           0.716               2
               0              60               0
          14.227           0.849            1.182
              15           0.849            1.182
              15           0.849               2
               0              60               0
/
  1
              67              68          0.00198
              50          -0.3038   -7000
             998          2e-005           0
    0    1    1
            4180              20
         0.00015           0.001          0.0728
          14.227           1.512           1.207
              15           1.512           1.207
```

```
      15        1.512         2
       0         60           0
  14.227         1.595      1.207
      15        1.595      1.207
      15        1.595         2
       0         60           0
  14.227         1.722      1.207
      15        1.722      1.207
      15        1.722         2
       0         60           0
  14.227         1.849      1.207
      15        1.849      1.207
      15        1.849         2
       0         60           0
  14.227         1.976      1.207
      15        1.976      1.207
      15        1.976         2
       0         60           0
  14.227         2.103      1.207
      15        2.103      1.207
      15        2.103         2
       0         60           0
  14.227         2.186      1.207
      15        2.186      1.207
      15        2.186         2
       0         60           0
/
  1
      67         68        0.00198
      50        -0.217   -5000
     998        2e-005          0
   0   1   1
    4180         20
 0.00015       0.001       0.0728
  14.227         2.824      1.182
      15        2.824      1.182
      15        2.824         2
       0         60           0
  14.227         2.957      1.182
      15        2.957      1.182
      15        2.957         2
       0         60           0
  14.227          3.09      1.182
      15         3.09      1.182
      15         3.09         2
       0         60           0
```

```
        14.227          3.223          1.182
          15          3.223          1.182
          15          3.223              2
           0             60              0
        14.227          3.314          1.212
          15              2          1.212
          15              2              2
           0             60              0
/
  1
          67             68        0.00198
          50        -0.1302   -3000
         998          2e-005              0
    0     1     1
        4180             20
     0.00015          0.001         0.0728
       14.082          3.421          0.959
       14.099          3.424          0.958
       14.099          3.424              2
           0             60              0
        14.07          3.421           0.92
       14.087          3.424          0.915
       14.087          3.424              2
           0             60              0
        14.06          3.421          0.881
       14.074          3.424          0.873
       14.074          3.424              2
           0             60              0
/
  1
          67             68        0.00198
          50        -0.1302   -3000
         998          2e-005              0
    0     1     1
        4180             20
     0.00015          0.001         0.0728
       14.082          0.248          0.959
       14.099          0.245          0.958
       14.099          0.245          1.958
           0             60              0
        14.07          0.248           0.92
       14.087          0.245          0.915
       14.087          0.245          1.915
           0             60              0
        14.06          0.248          0.881
       14.074          0.245          0.873
```

14.074 0.245 1.873
0 60 0
/
1
67 68 0.00198
50 -0.217 -5000
998 2e-005 0
0 1 1
4180 20
0.00015 0.001 0.0728
14.061 0.529 0.788
14.066 0.524 0.779
14.066 0.524 2
0 60 0
14.068 0.608 0.776
14.076 0.604 0.763
14.076 0.604 2
0 60 0
14.071 0.671 0.771
14.08 0.671 0.758
14.08 0.671 2
0 60 0
14.068 0.735 0.776
14.08 0.74 0.758
14.08 0.74 2
0 60 0
14.061 0.813 0.788
14.066 0.819 0.779
14.066 0.819 2
0 60 0
/
1
67 68 0.00198
50 -0.217 -5000
998 2e-005 0
0 1 1
4180 20
5e-006 0.001 0.0728
14.059 2.89 0.788
14.067 2.882 0.776
14.067 2.882 2
0 60 0
14.069 2.996 0.773
14.077 2.962 0.76
14.077 2.962 2
0 60 0

14.072 3.029 0.768
14.08 3.029 0.755
14.08 3.029 2
0 60 0
14.069 3.093 0.773
14.077 3.097 0.76
14.077 3.097 2
0 60 0
14.059 3.169 0.788
14.067 3.177 0.776
14.067 3.177 2
0 60 0
/
1
67 68 0.00198
50 -0.1302 -3000
998 2e-005 0
0 1 1
4180 20
5e-006 0.001 0.0728
10.76 0.354 0.931
10.775 0.339 0.936
10.775 0.339 2
0 60 0
10.764 0.35 0.858
10.78 0.334 0.858
10.78 0.334 2
0 60 0
10.76 0.354 0.786
10.775 0.339 0.78
10.775 0.339 2
0 60 0
/
1
67 68 0.00198
50 -0.1302 -3000
998 2e-005 0
0 1 1
4180 20
5e-006 0.001 0.0728
10.021 3.265 0.978
10.036 3.28 0.984
10.036 3.28 2
0 60 0
10.025 3.269 0.906
10.041 3.285 0.906

```
        10.041          3.285           2
          0             60              0
        10.021          3.265           0.834
        10.036          3.28            0.828
        10.036          3.28            2
          0             60              0
/
  1
          67            68          0.00198
          50          -0.1302     -3000
         998          2e-005          0
    0     1     1
        4180            20
        5e-006          0.001           0.0728
        13.12           3.178           1.11
        13.12           3.184           1.088
          15            4           1.088
          0             60              0
        13.121          3.105           1.117
        13.12           3.105           1.104
          15            4           1.104
          0             60              0
        13.121          3.037           1.122
        13.12           3.033           1.11
          15            4           1.11
          0             60              0
/
  1
          67            68          0.00198
          50          -0.1302     -3000
         998          2e-005          0
    0     1     1
        4180            20
        5e-006          0.001           0.0728
        13.121          0.633           1.122
        13.12           0.636           1.11
          15            3           1.11
          0             60              0
        13.121          0.564           1.117
        13.12           0.564           1.104
          15            3           1.104
          0             60              0
        13.12           0.492           1.11
        13.12           0.484           1.088
          15            3           1.088
          0             60              0
```

```
/
  1
              67              68          0.00198
              50          -0.217   -5000
             998          2e-005               0
    0     1     1
            4180              20
          5e-006           0.001          0.0728
          12.823           1.793           0.945
          12.825           1.782           0.926
              15               3           0.926
               0              60               0
          12.825           1.868           0.928
          12.826           1.863           0.907
              15               3           0.907
               0              60               0
          12.825           1.913           0.923
          12.826           1.931           0.901
              15               3           0.901
               0              60               0
          12.825           1.995           0.928
          12.826               2           0.907
              15               3           0.907
               0              60               0
          12.823           2.069           0.945
          12.825            2.08           0.926
              15               3           0.926
               0              60               0
/
/
```

==========

'Example MATLAB code for generation of lognormal distribution plot and histogram:

==========

```
x=(0.0:0.1:5.0)';
m=0.68';
v=0.14';
mu=log((m^2)/sqrt(v+m^2))';
s=sqrt(log(1+v/(m^2)))';
s2=s^2';
y=lognpdf(x,mu,s);
figure
p1=plot(x,y);
set(p1,'Color','red','LineWidth',2)
z= random('Normal',0,1,10000,1)';
xln = exp(mu + s*z)';
figure
hist(xln,50);xlim([0.0 5]);
```

==========

C language function for dust generation and simulation of user defined scrubber efficiency

==========

```
/*************************************
 ***             PARTICLES           ***
 *************************************/
// Attribution of Particles;
fprec PDCoal[5], PDSylica[5], rop_c, ivp, rop_s, ProcSylica;
void usr_pcle1(int isw,int nlines)
{
   //usf_stop("usr_pcle1 is not initialized");
       char line[200], msg[200];
       int i;
       for (i=0; i<5; i++) {
              usf_getline(line,200); sscanf(line,"%lg", &(PDCoal[i]));
sprintf(msg, "usr_pcle1: ddp   PDCoal = %d   %lg\n",i, PDCoal[i]); usf_sout(msg);
       }
       usf_getline(line,200); sscanf(line,"%lg %lg", &rop_c, &ivp); sprintf(msg,
"usr_pcle1: rop_c, ivp = %lg     %lg\n", rop_c, ivp); usf_sout(msg);
       for (i=0; i<5; i++) {
              usf_getline(line,200); sscanf(line,"%lg", &(PDSylica[i]));
sprintf(msg, "usr_pcle1: ddp   PDSylica = %d   %lg\n",i, PDSylica[i]);
usf_sout(msg);
       }
       usf_getline(line,200); sscanf(line,"%lg %lg", &rop_s, &ProcSylica);
sprintf(msg, "usr_pcle1: rop_s   ProcSylica = %lg     %lg\n", rop_s, ProcSylica);
usf_sout(msg);
}
int count_in = 0;
int cpc[5] = {0,0,0,0,0}, spc[5] = {0,0,0,0,0}, cpc_alive=1, spc_alive=1; /*coal
and sylica particle counters*/
int use_pcle1(int isw,int *pidata,fprec *pfdata,int *idata,fprec *fdata,char
*cdata)
{
    //usf_stop("use_pcle1 is not initialized");
//            int i;
              fprec ddp, rop = rop_c, dmax = 0.000005, dmin = 0.0000002, rdp, tmp,
scp, volp, mas, mef;
                     }
              ddp = (fprec)rand()/(RAND_MAX+1)*(dmax-dmin)+dmin;
              rdp  = ddp/2;
              tmp = 20;
              scp = 1;
              volp = (fprec)(4.18879*rdp*rdp*rdp);
              mas = (fprec)(volp*rop);
```

```
                mef = (fprec)(mas*scp);
                pfdata[0] = ddp;
                pfdata[1] = rop;
                pfdata[2] = tmp;
                pfdata[3] = scp;
                pfdata[27] = (-1)*ivp;
                pfdata[28] = 0;
                pfdata[29] = 0;
                count_in++;
                return 0;
}

//Particle Passed through the Scrubber;
int total_passed = 0, cycle_passed=0, scrub_out=0; //See usu_cycle functions
void use_pclget10(int isw, int *pidata,fprec *pfdata,int *idata,fprec *fdata,char
*cdata)
{
        //usf_stop("use_pclget10 is not initialized");

        idata[1] = 0;
        if(strcmp(cdata,"scrub_in") == 0) {
                total_passed++;
                cycle_passed++;
        }

// Particle Start Points;
fprec x_in, rmax, rmin, scrub_ef;
int origin = 0;
int  usr_pcl_typ11(int isw, int nlines)
{
    //usf_stop("usr_pcl_typ11 is not initialized");
        char line[200], msg[200];
        usf_getline(line,200); sscanf(line,"%d", &origin); sprintf(msg,
"usr_pcl_typ11: origin = %d\n", origin);  usf_sout(msg);
        usf_getline(line,200); sscanf(line,"%lg %lg %lg", &x_in, &rmax, &rmin);
sprintf(msg, "usr_pcl_typ11: x_in, rmax, rmin = %lg     %lg     %lg\n", x_in,
rmax, rmin); usf_sout(msg);
        usf_getline(line,200); sscanf(line,"%lg", &scrub_ef); sprintf(msg,
"usr_pcl_typ11: Scrubber Efficiency = %lg\n", scrub_ef); usf_sout(msg);
        return origin*10; /* >0 : The size of arrays X[npcl],Y[npcl] and Z[npcl] */
}

int  use_pcl_typ11(int npcl, fprec *X, fprec *Y, fprec *Z )
{
    int mpcl=0;
        fprec yc, zc, rad=0.1, radmin=0.01, angle=360., anglemin=0.01, rnd_rad = 0,
rnd_angle = 0;
        char msg[200];
    //usf_stop("use_pcl_typ11 is not initialized");
        do {
```

```
                yc=(fprec)rand()/(RAND_MAX+1)*(rmax-rmin)+rmin;
                zc=(fprec)rand()/(RAND_MAX+1)*(rmax-rmin)+rmin;
                X[mpcl] = x_in;
                Y[mpcl] = yc;
                Z[mpcl] = zc;

                if(mpcl >= origin) {
                        yc=0.5;
                        zc=0.5;
                        rnd_rad = (fprec)rand()/(RAND_MAX+1)*(rad-radmin)+radmin;
                        rnd_angle = (fprec)rand()/(RAND_MAX+1)*(6.2832/360.)*(angle-
anglemin)+anglemin;
                        X[mpcl] = 0.39;
                        Y[mpcl] = yc + rnd_rad*cos(rnd_angle);
                        Z[mpcl] = zc + rnd_rad*sin(rnd_angle);
                }
                if(mpcl >= origin + scrub_out) {X[mpcl] = -100.;}
                else { sprintf(msg, "use_pcl_typ11: mpcl, X, Y, Z: %d     %lg
%lg     %lg\n", mpcl, X[mpcl], Y[mpcl], Z[mpcl]); usf_sout(msg);}
                mpcl++;
        } while (mpcl < npcl);
        return mpcl; /* <=npcl : The number of start points(i.e. particles). */
}
```

==========

S file data corresponding to the C language function for dust generation and simulation of user defined scrubber efficiency

==========

The C++ code uses the particle data provided in PCLE and PCLT sections.

```
SDAT
SC/Tetra
  10   0   0
PREI    scrubber.pre
RO      scrubber.r
POST    scrubber
/
   1   1   0

   0   1
CHKF
   1
fan_in
/
CHKL
      1       1       0       1       0
CYCL
      1     500               0.001       0                   0
DES0
   1
EQUA
1101
FANM
%CNAM Fanm_1
   4   0
                  -1                   0                   0                   0
                 0.7
fan
/
/
FLUX
%CNAM Flux_1
  -1   4   0   0   1   0
                  -1                   1                   0                 1.2
               0.0001              0.0001
inlet
/
```

```
%CNAM Flux_2
 -4   0   1   0   0   0
                  0
outlet
/
%CNAM Flux_3
 -4   0   1   0   0   0
                  0
fan_out
/
%CNAM Flux_4
 -1   5   0   0   1   0
                0.7   0
              0.0001                0.0001
scrub_out
/
/
GFIL
 100   0
GRAV
                  0                   0                  -9.8
GWLN
   0
PANL
scrubber
/
PCLB
walls
scrubber
/
PCLC
scrub_in
/
PCLD
LIFE                    1
PASS    10000
STRT                   -1
STRD                   -1
REGN    1
FDIA    1
USEG   10
/
PCLE
 11   1
 12
0.7
```

```
0.1
0.05
0.03
0.02
833    0.5
0.2
0.5
0.1
0.1
0.1
2211    3.5
  1
  3
20
0.9    0.8    0.2
0.85
                -1                -1   0   1   1   0
                833               -1                0                0                1
               -0.5               0                 0
/
PCLT
COUN              -1                -1   0                0
DIAM              0              5e-006   5   0
scrub_in
scrub_out
/
MASS              -1                -1   1                0
DIAM              0              5e-006   5   0
scrub_in
scrub_out
/
/
PROP
%CNAM air(incompressible/20C)
  1   1              1.206          1.83e-005             1007           0.0256   0
/
TBEC
  1   1
/
TBTY
  2
TRAN
  1
WL02
%CNAM Wl02_1
  0   0
```

%CNAM Wl02_2
  0 0
/
  1
walls
/
  2
scrubber
/
/
WLTY
  0
WPUT
  0
ZGWV
  0
GOGO

REFERENCES

1. Belle, B.K., and Clapham, S., 2002, "An improved wet head system prevention of incentive ignition and dust control," E. DeSoza (ed.), Proceedings 9th U.S. Mine ventilation Symposium, Kingston, ON, pp. 479-486.
2. Box, G. E.P., Hunter, William G., and Hunter, J. Stuart, 1978, "Statistics for Experimenters," Jhon Wiley & Sons, New York - Chichester - Brisbane - Toronto, 1978. ISBN 0-471-09315-7.
3. Brunner, D.J., 1995, "Examples of the application of computational fluid dynamics simulations to mine and tunnel ventilation," Proceedings: 7th U.S. Mine Ventilation Simposium, Lexington, KY.
4. Cheng, L., 1973, "Collection of Airborne Dust by Water Sprays," Ind. Eng. Chem. Process Des. Develop., Vol. 12, No. 3, pp. 221-225.
5. Chilton E., Taylor, C.D., Hall, E., and Timko, R.J., 2006, "Effect of Water Sprays on Airflow Movement and Methane Dilution at the Working Face," Proceedings: 11th U.S./North American Mine Ventilation Symposium, June 2006, London, UK: Taylor & Francis Group; pp. 401-406.
6. Chugh, Y.P., Patwardhan, A., Gurley, H., Moharana, A., and Saha, R., 2006, "A field demonstration of the Joy wet head miner technology," Proceedings: 11th U.S./North American Mine ventilation Symposium, The Pennsylvania State University, PA, pp. 233-240.
7. Colinet J.F. and Flesh J.P., 2002, "Exposure to silica dust on continuous miner operation using flooded bed scrubbers," NIOSH Hazard ID.
8. Cooper D.W., 1982, "On the products of lognormal and cumulative lognormal particle size distributions," J. Aerosol Sci., Volume 13, Issue 2 (1982), pp. 111–120
9. Courtney, W.G., 1990, "Frictional ignition with coal mining bits," Bureau of Mines IC 9251.
10. CRADLE, 2009-2014, "Thermofluid Analysis System with Unstructured Mesh Generator SC/Tetra Version 8," User's Guide Solver Reference, Software Cradle Co., Ltd, Japan
11. Creedy, D.P. and Kershaw S., 1988. Firedamp prediction – a pocket calculator solution. The Mining Engineer. Inst of Mining Engineers, Vol. 147, No. 317, Feb., pp.377-379.
12. Dick, W.D., Sachweh, B.A., and McMurry, P.H., 1996, "Distinction of Coal Dust Particles from Liquid Droplets by Variations in Azimuthal Light Scattering," Appl. Occup. Environ. Hyg. Vol. 11, No.7, pp.637-645.
13. Emory, I., Saito K., and Sekimoto, K., 2009, "Scale models in engineering: its theory and application, 3rd edn.," Tokyo, Gihodo.
14. Fields, K.G., Atchison, D.J., and Haney, R.A., 1990, "Evaluation of a combined face ventilation system used with a remotely operated mining machine," Proceedings: 1990 International Symposium on Respirable Dust in the Mineral Industries, pp. 349-353.

15. Fields, K.G., Shultz, M.J., Rude, R.L., Tomko, D.M., Atchinson, D.J., and Gerbec, E.J., 2005, "Respirable Dust Survey Conducted at he Big Ridge Inc., Willow Lake Portal, Saline County, Illinois," US Dept of labor, Mine Safety and Health Technology Center, Dust Division.
16. Frish, U., 1995, "Turbulence - The legacy of A.N. Kolmogorov," Cambridge University Press, Great Britan, ISBN 0 521 45713 5 (hb).
17. Gemci, T., Chigier, N., and Organiscak, A., 2003, "Spray characterisation for coal mine dust removal, " Proceedings: 9th International Conference on Liquid Atomization and Spray Systems, Sorrento, Italy, July 13-18.
18. Gillies, A. D. S., 1982, Studies in improvements to coal face ventilation with mining machine mounted dust scrubber systems," Preprint no. 82–24, SME Annual Meeting, Dallas, TX.
19. Goodman G.V.R., Taylor C.D., Colinet J.F., and Thimons E.D., 1995, "Research by NIOSH for controlling respirable dust and methane gas on continuous miner faces," Proceedings: 7th US Mine Ventilation Symposium, Littleton, CO, June.
20. Goodman, G.V.R., 2000, "Using water sprays to improve performance of a flood-bed dust scrubber," Appl. Occup. Envir. Hyg., Vol. 15, No. 7, pp. 550-560.
21. Goodman, G.V.R., and Listak, J.M. , 1999, "Variation in dust level with continuous miner position," Mining Engineering, Vol. 51, No 2, pp. 53-59.
22. Goodman, G.V.R., Beck, T.W., Pollock, D.E., Colinet, J.E., and Organiscak, J.A., 2006, "Emerging technologies control respirable dust exposures for continuous mining and roof bolting personel," Proceedings: 11th U.S./ North American Mine Ventilation Symposium, The Pennsylvania State University, PA, pp. 211-216.
23. Hall E.E., Taylor C.D., and Chilton J.E., 2007, "Using ultrasonic anemometers to evaluate face ventilation conditions," 2007 SME Annual Meeting and Exhibit, February 25-28, Denver Colorado, preprint 07-096. Littleton, CO February.
24. Huang, P.G., Welsh, D., 2010, "Introduction to CFD in Engineering Design," SC/Tetra Short Course, Mechanical and Materials Engineering Dept., Wright State University, Dayton, OH.
25. Husted, B.P., 2007, "Experimental measurements of water mist system and implication for modeling in CFD," Doctoral Thesis, Department of Fire Safety Engineering, Lund University, Sweden.
26. Jayaraman, N.Y., Jankowski, R.A., and Whitehead, K.L., 1992, "Optimizing continuous miner scrubbers for dust control in high coal seams," Proceedings: 1992 Annual SME Meeting, Phoenix, AZ, Feb. 24-27, pp. 193-205.
27. Jimenez, J., 2004, "Turbulence and vortex dynamics," Notes at the Polytechnique, Madrid and Stanford, 2000-2004, pp. 108.
28. Karacan C.Ö., Schatzel S.J., 2008, "Reservoir Modeling-Based Prediction and Optimization of Ventilation Requirements During Development Mining in Underground Coal Mines," 2008 SME Annual Meeting and Exhibit, February 24-27, Salt Lake City, Utah, preprint 08-010. Littleton, CO.
29. Kentucky Foundation & Kentucky Coal Association, 2011, "Kentucky Coal and Energy Education Project," htp://www.coaleducation.org/technology/Underground/continuous_miners.htm.
30. Kirkpatrick A.T., Kenyon A.E., 1994, "Flow characteristics of Three-Dimensional Wall Jets," ASHRAE Transaction Symposia, SF-98-28-3, pp. 1755-1762.

31. Kissel F.N. and Bielicki R.J., 1975, "Methane Buildup Hazards caused by Dust Scrubber Recirculation at Coal Mine Working Faces, a Preliminary Estimate," U.S. Bureau of Mines, Report of Investigation, RI 8015
32. Kundu, K.P., Cohen, I.M., and Hu, H.H., 2002, "Fluid Mechanics, " Academic Press and Elsevier Science, San Diego, CA, Library of Congress Catalog Card Number: 2001086884, ISBN 0-12-178251-4, pp. 539-554
33. Listak, J.M., Goodman, T.W., and Beck T.W., 2010, "Evaluation of the wet head continuous miner to reduce respirable dust," Mining Engineering, September 2010, pp. 60-64.
34. Lunarzewski, L., 1998, "Gas emission prediction and recovery in underground coal mines," International Journal of Coal Geology 35, pp. 117-145.
35. Luxner, J.V., 1969, "Face Ventilation in Underground Bituminous Coal Mines. Airflow and Methane Distribution Patterns in Immediate Face Area-Line Brattice," report of investigation 7223, United States Department of the Interior, Bureau of Mines.
36. McPherson, Malcolm J., 1993, "Subsurface Ventilation Engineering," Textbook, updated version 2010.
37. Moloney, K. W., Lowndes, I. S., Stokes, M. R., and Hargrave, G., 1997, "Studies on Alternative Methods of Ventilation Using Computational Fluid Dynamics (CFD), Scale and Full Scale Gallery Tests," Proceedings: 6th International Mine Ventilation Congress, Chapter 79 - Auxiliary and Face Ventilation - May 17-22, pp.497-503, ISBN 0-87335-146-0
38. Moloney, K.W., Hargreaves, D.M., Lowndes, L.S., and Pearce, W., 1999, "Validation of Computational Model of Auxilary Ventilation Systems with Experimental Data," Proceedings: 8th US Mine Ventilation Symposium, Rolla, Missouri, June 11-17, 1999, pp. 551-557.
39. Montgomery, Douglas C., "Design and Analysis of Experiments," 7th Edition. Jhon Wiley & Sons, 2009. ISBN 978-470-12866-4
40. NIOSH, 2008, "Work-Related Lung Disease Surveillance Report 2007, Volume 1.," DHHS, NIOSH, Publication No. 2008-143a.
41. Organiscak, J., and Beck, T., 2010, "Continuous miner spray consideration for optimizing scrubber performance in exhaust ventilation system," Mining Engineering, Vol. 62, No.10, pp. 41-46.
42. Petrov T., and Wala A., 2014, "Improvement of blowing curtain face ventilation systems using passive regulator," 2014 SME Annual Meeting, Feb. 23-26, Salt Lake City, UT, Preprint 14-104
43. Petrov T., Wala A.M., and Huang, G., 2013, "Parametric study of airflow separation phenomenon at face area during deep cut continuous mining," Journal of Mining Technology, Maney Publishing, vol. 122, No 4, ISSN: 14749009.
44. Pollock, D. and Organiscak, J., 2007, "Airborne Dust Capture and Induced Airflow of Various Spray Nozzle Designs," Aerosol Science and Technology Journal, 41:711-720.
45. Raabe O.G., 1971, "Particle size analysis using grouped data and the lognormal size distribution," J. Aerosol Sci., 2, pp. 289–303

46. Reed, W.R., and Taylor, C.D., 2007, "Development of coal mine face ventilation systems during the 20th century," Mining Engineering, Vol. 59, No. 8, pp. 40-51, August
47. Rutherford A., 1989, "Vector, Tensors and the basic Equations of Fluid Mechanics," University of Minnesota, Library of Congress, ISBN 0-486-66110-5, Dover Publication Inc New York
48. Sagaut, P., 2002, "Large Eddy Simulation for Incompressible Flows," Third Edition. With a Foreword by Massimo Germano. Library of Congress Control Number: 2005930493, ISSN 1434-8322, ISBN-10 3-540-26344-6 Third Edition Springer Berlin Heidelberg New York.
49. Saito K, Editor, 2008, "Progress in Scale Modeling," Summary of the first International Symposium on Scale Modeling (ISSMI in 1988) and selected papers from Subsequent Symposia (ISSM II in 1997 trough ISSM V in 2006), ISBN: 978-90-481-7951-0, Springer Science, TN USA
50. Schowengerdt, F.D., Brown, J.T., 1976, "Colorado School of Mines tackles control of respirable coal dust," Coal Age, Apr; 81(4), pp. 129-131 .
51. Schultz M.J., Tomko D.M., and Rumbaugh V.E., 2010, "Utilizing Adequate Intake Line Curtain Air quantities to maintain respirable Dust Compliance," 13th US/North American Mine Ventilation Symposium, pp. 109-114
52. Steiner, L., Cornelius, K., Turin F., and Stock, D., 1998, "Work sampling applied to a human factors analysis of mine worker positioning," NIOSH report, Pittsburgh Research Laboratory, Pitsburgh, PA.
53. Suarthana, E., Laney, A.S., Storey, E., Hale, J.M., and Attfield, M.D., 2011, "Coal workers' pneumoconiosis in the United States; regional differences 40 years after implementation of the 1969 Federal Coal Mine Health and Safety Act," Occup Environ Med., Dec;68(12), pp. 908-13. doi: 10.1136/oem.2010.063594.
54. Sullivan, P. and Heerder, J.Van., 1993, "The Simulation of Environmental Conditions in Continuous Miner Developments Using Computational Fluid Dynamics," Journal of the Mine Ventilation Society of South Africa, January 1993, pp.10.
55. Taylor C.D., Rider J., and Thimons E.D., 1996, "Changes in Face Methane Concentrations Using High Capacity Scrubbers with Exhausting and Blowing Ventilation," Proceedings of the SME Annual Meeting, Preprint 96-167, Phoenix, AZ, March, pp. 11-14, 5.
56. Taylor, C.D., Chilton, E.F., Hall, E.E., and Timko, R.J., 2006, "Effect of scrubber on airflow and methane patterns at the mining face," Proceedings: 11th U.S./North American Mine Ventilation Symposium, University Park, PA, June.
57. Taylor, C.D., Karacan C.O., 2010, "Historical Development of Technologies for Controlling Methane in Underground Coal Mines," Conference paper IOSHTIC2 Number: 20037777, Extracting the Science: A Century of Mining Research. Brune JF, ed., Littleton, CO: Society of Mining, Metallurgy, and Exploration, Jan, pp. 478-487
58. Taylor, C.D., Timko, R.J., Thimons, E.D., and Mal, T., 2005, "Using ultrasonic anemometers to evaluate factors affecting face ventilation effectiveness," 2005 SME Annual Meeting, Paper number 05-080, Salt Lake City, UT.

59. Turner D., Wala M.A., and Jacob J.D., 2002, "Particle image velocimetry (PIV) used for mine face ventilation study," Proceedings: 9th U.S./North American Mine Ventilation Symposium, Kingston, Ontario, Canada, June.
60. Volkwein, J.C. and Wellman T.S., 1989, "Impact of Water Sprays on Scrubber Ventilation Effectiveness," U.S. Bureau of Mines Report of Investigation, RI 9259
61. Volkwein, J.C., Halfinger, G.Jr., and Thimons, E.D., 1985, "Machine mounted scrubber helps ventilate face," World Mining Equipment, Vol. 9, No.2, pp.15-16.
62. L.D. Voronina, A.D. Bagrinovskiy, V.S. Nikitin, 1962, " Principles of Mine Ventilation, " National Publishing of Scientific Literature of Mining, Moscow.
63. Wala, A.M., Stoltz, J.R.,Hassan, M.I., 2000, "Scaled modeling of a mine face ventilation system for CFD code validation," Proceedings: Third International Symposium on Scale Modeling, Nagoya, Japan, September
64. Wala, A.M., Stoltz, Jacob, J.D., 2001, "Numerical and experimental study of a mine face ventilation system for CFD code validation," Proceedings: 7th International Mine Ventilation Congress, Krakow, Poland, June.
65. Wala, A.M., Jacob J.D., Turner, D., Rangubhotla, L., 2002, "Experimental study of mine ventilation system for validation of numerical models," Proceedings: 9th U.S./North American Mine ventilation Symposium, Kingston, Ontario, June.
66. Wala, A.M., Jacob, J.D., Huang, P.G., Brown, J.T., 2002, "A new approach to evaluate mine face ventilation," Preprint 02-177: 2002 SME Annual Meeting, Phoenix, AR, February.
67. Wala, A.M., Jacob, J., Brown, J., Huang, G., 2003, "New approaches to mine-face ventilation", Mining Engineering, Vol. 55, No. 3, pp. 25-30, March.
68. Wala, A.M., Jacob J.D., Rangubhotla, L., Watkins, T., 2003, "Evaluation of an Exhaust Face Ventilation System for 20-foot Extended Cut Using Scaled Physical Model," Preprint 03-148: 2003 SME Annual Meeting, Cincinnati, OH, February.
69. Wala, A.M., Jacob J.D., Huang, J., Brown, J., Rangubhotla, L., 2004, "How Scrubbers Help Ventilate the Face During Deep Cut Mining with a Blowing Curtain," Proceedings: 10th U.S./North American Mine ventilation Symposium, Anchorage, AL, May.
70. Wala, A.M., Jacob J.D., Rangubhotla, L., Watkins, T., 2005, "Evaluation of an exhaust face ventilation system for a 6.1-m (20-ft) extended cut using a scaled physical model," Mining Engineering, Vol. 57, No. 10, pp. 33-38,October.
71. Wala, A.M., Vitla S., Taylor C.D., and G. Huang., 2006, "Mine face ventilation: a comparison of CFD results against benchmark experiments for the CFD code validation," Preprint 06-76: 2006 SME Annual Meeting, St. Louis, MO, February.
72. Wala, A.M., Vytla S., Taylor C.D., and G. Huang., 2007, "Mine face ventilation: a comparison of CFD results against benchmark experiments for the CFD code validation,"Mining Engineering, Vol.59, No.10, pp.49-55, October
73. Wala, A.M., Vytla, S., Huang, G., Taylor, C.D., 2008, "Study of the effect of scrubber operation on the face ventilation," Proceedings: 12th U.S./North American Mine ventilation Symposium, Reno, NV, June
74. Walmsley, S.J., 2000., "A computational and experimental study of the sprays produced by fire suppression sprinkler systems., " PhD Thesis, Mech. Eng. Dept.,

University of Manchester Institute Science & Technology (UMIST), Manchester, UK.
75. Walters, D.K. and Cokljat, D., 2008, "A Three-Equation Eddy-Viscosity Model for Reynolds-Averaged Navier-Stokes Simulations of Transitional Flow," ASME Journal of Fluids Engineering, 2008. 130,121401
76. Wang et al., 2013, "Lung Function Impairment Among US Underground Coal Miners, 2005 to 2009"
77. Watzman, B., 2013, "Respirable Coal Mine Dust - The Industry Perspectiveon the Need for New Regulations," 2013 Central Appalachian Regional Work Safety and health Symposium: An interdisciplinary update on miner health and safety, August 22, Lexington KY

VITA

Todor P. Petrov was born in Pazardzik, Bulgaria, Europe, the son of Peter Todorov Petrov and Sofka Atanasova Petrova. He completed his high school education in the Mathematical Gymnasium "K. Velichkov", Pazardzik. He received his M.S. degree in Mining Engineering from the University of Mining and Geology (UMG) "St. Ivan Rilsky", Sofia, Bulgaria. Later, he completed a post-graduate specialization in Computer Technologies, Information and Control System at the same university. Prior to emigrate to U.S.A. in October 2008, he worked as a R&D engineer at the Research Institute of the UMG and later on as Assistant Professor in Mine Ventilation and Safety at the same university. At that time his R&D activities were in: analysis of underground mine fires and early symptoms of SPONCOM; occupational safety and health risk analysis; decision support systems; mine ventilation design; computer modeling; small scale physical models of fan control with a variable frequency drive; and Human Machine Interfaces in automation. In September, 2009 Todor Petrov joined the Mining Engineering Department at the University of Kentucky as a graduate research assistant under the guidance of Dr. Wala. His research project was dedicated to development of industry oriented computational fluid dynamics (CFD) code for analysis/design of face ventilation systems. While in the Mining Department, he became a member of Society for Mining, Metallurgy, and Exploration (SME) and worked as both a research and teaching assistant. He expected to graduate December 2014 with a Philosophy Doctorate in Mining Engineering. Currently Todor Petrov authored or co-authored 2 journal papers, 18 conference papers and 1 innovation.